IFAPA Instituto de Investigación y Formación Agraria y Pesquera

Genetic estimates and immune responses associated with the lymphocystis disease virus (LCDV) in marine fish

TESIS DOCTORAL

Carlos Carballo Pérez

PROGRAMA DE DOCTORADO
BIOLOGÍA CELULAR Y MOLECULAR
2020

Directores:
Manuel Manchado Campaña
Juan José Borrego García

UNIVERSIDAD DE MÁLAGA
Instituto de Investigación y Formación Agraria y Pesquera
CONSEJERÍA DE AGRICULTURA, PESCA Y DESARROLLO RURAL
JUNTA DE ANDALUCIA
GOBIERNO DE ESPAÑA MINISTERIO DE CIENCIA, INNOVACIÓN Y UNIVERSIDADES
INIA Instituto Nacional de Investigación y Tecnología Agraria y Alimentaria
ma UNIVERSIDAD DE MÁLAGA

UNIVERSIDAD
DE MÁLAGA

AUTOR: Carlos Carballo Pérez

http://orcid.org/0000-0001-9047-2930

EDITA: Publicaciones y Divulgación Científica. Universidad de Málaga

UNIVERSIDAD DE MÁLAGA

PROGRAMA DE DOCTORADO EN BIOLOGÍA CELULAR Y MOLECULAR

Genetic estimates and immune response associated with the Lymphocystis Disease Virus (LCDV) in marine fish

TESIS DOCTORAL

CARLOS CARBALLO PÉREZ

2020

UNIVERSIDAD DE MÁLAGA

PROGRAMA DE DOCTORADO EN BIOLOGÍA CELULAR Y MOLECULAR

Genetic estimates and immune response associated with the Lymphocystis Disease Virus (LCDV) in marine fish

Memoria presentada por D. Carlos Carballo Pérez

para optar al grado de:

Doctor en Biología con mención internacional

IFAPA Instituto de Investigación y Formación Agraria y Pesquera

Instituto de Investigación y Formación Agraria y Pesquera
CONSEJERÍA DE AGRICULTURA, PESCA Y DESARROLLO RURAL

Fdo. El doctorando

UNIVERSIDAD DE MÁLAGA

PROGRAMA DE DOCTORADO EN BIOLOGÍA CELULAR Y MOLECULAR

Dr. **JUAN JOSÉ BORREGO GARCÍA,** Catedrático del Departamento de Microbiología de la Universidad de Málaga, como TUTOR dentro del programa de doctorado "BIOLOGIA CELULAR Y MOLECULAR" y DIRECTOR de la presente tesis doctoral realizado por el doctorando.

Dr. **MANUEL MANCHADO CAMPAÑA**, Investigador Principal del Instituto de Investigación y Formación Agraria y Pesquera (IFAPA) y DIRECTOR de la presente tesis doctoral realizado por el doctorando.

INFORMAN:

Que el doctorando D. **CARLOS CARBALLO PÉREZ** ha realizado de forma satisfactoria y bajo nuestra supervisión las actividades de formación dentro del programa de doctorado arriba mencionado, así como el trabajo investigador que se presenta y que lleva por título "Genetic estimates and immune response associated with the Lymphocystis Disease Virus (LCDV) in marine fish".

Este trabajo constituye su proyecto de Tesis para aspirar al Título de Doctor en Biología con mención internacional.

Y para que así conste, y tenga los efectos que correspondan, en cumplimiento de la legislación vigente, extendemos el presente informe en Málaga, a de de 2020.

Fdo. El Tutor: Juan José Borrego García

Fdo. Los directores: Manuel Manchado Campaña Juan José Borrego García

Los estudios realizados en la presente Tesis Doctoral han sido financiados por los siguientes proyectos y becas:

- Proyecto RTA2013–00023-C02-01 Implementación de tecnologías de selección genética y control epigenético en lenguado senegalés (Solea senegalensis) financiado por INIA y EU a través del programa FEDER 2014–2020 "Programa Operativo de Crecimiento Inteligente"

- Proyecto RTA2017-00054-C03-01 "Estudio de los factores genéticos y moleculares que regulan la morfología en lenguado senegalés (*Solea senegalensis*) financiado por MCIU/AEI/FEDER, UE

- Proyecto PP.AVA.AVA201601.9 "Nuevas herramientas genómicas para el análisis genético y evaluación transcriptómica de compuestos funcionales basados en microalgas para impulsar la acuicultura del lenguado (SOLEALGAE)"

- Proyecto de Excelencia de la Junta de Andalucía "Infecciones por linfocistivirus en doradas cultivadas: patogénesis e implicación del sistema inmune en el curso de la infección. Desarrollo de medidas de profilaxis y control" (Ref. P12-RNM-2261).

- Proyecto "Algae for aquaculture and beauty" H2020 Marie Skłodowska-Curie action MSCA-RISE -RISE project 691102,

- Beca predoctoral del Instituto Nacional de Investigación y Tecnología Agraria y Alimentaria. FPI-INIA 2014.

The results derived from this PhD Thesis have been partially published in:

PEER-REVIEWED JOURNALS

Carballo C, Castro D, Borrego JJ, Manchado M. Gene expression profiles associated with lymphocystis disease virus (LCDV) in experimentally infected Senegalese sole (*Solea senegalensis*). Fish Shellfish Immunol. 2017; 66:129-139. doi: 10.1016/j.fsi.2017.04.028. PubMed PMID: 28476672.

Carballo C, Chronopoulou EG, Letsiou S, Maya C, Labrou NE, Infante C, Power DM, Manchado M. Antioxidant capacity and immunomodulatory effects of a chrysolaminarin-enriched extract in Senegalese sole. Fish Shellfish Immunol. 2018; 82:1-8. Epub 2018/08/01. doi: 10.1016/j.fsi.2018.07.052. PubMed PMID: 30064015.

Carballo C, Ortiz-Delgado JB, Berbel C, Castro D, Borrego JJ, Sarasquete C, Manchado M. Feed and immersion challenges with lymphocystis disease virus (LCDV) reveals specific mechanisms for horizontal transmission and immune response in Senegalese sole post-larvae. Fish Shellfish Immunol. 2019; 89:710-718. Epub 2019/04/19. doi: 10.1016/j.fsi.2019.04.049. PubMed PMID: 30999043.

Carballo C, Pinto PIS, Mateus AP, Berbel C, Guerreiro CC, Martinez-Blanch JF, Codoñer F M, Mantecon L, Power DM, Manchado, M. Yeast beta-glucans and microalgal extracts modulate the immune response and gut microbiome in Senegalese sole (*Solea senegalensis*). Fish Shellfish Immunol. 2019; 92:31-39. Epub 2019/05/28. doi: 10.1016/j.fsi.2019.05.044. PubMed PMID: 31128296.

INTERNATIONAL CONFERENCES

Carballo C, Castro D, Borrego JJ, Manchado M. "Pathogenesis of Lymphocystis Disease Virus (LCDV) and associated immune response in Senegalese sole (*Solea senegalensis*)". Poster Presentation. 16th E.A.F.P. International Conference on "Diseases of Fish and Shellfish". Belfast, UK. September 2017.

Pinto P, **Carballo C**, Mateus AM, Martinez-Blanch J, Codoner F, Mantecon L, Manchado M, Power DM. "Microalgal polysaccharide extracts modulate immune response and microbiome in gut of Senegalese sole (*Solea*

senegalensis)". Oral Presentation. 31st Congress of the European Society of Comparative Physiology and Biochemistry. Porto, Portugal. September 2018.

Carballo C. "Microalgae as a source of bioactive compounds to improve the fish health in aquaculture". Oral Presentation. Summer School "Advances in fish aquaculture and microalgae biotechnology" El Puerto de Santa Maria, Cadiz, Spain. September 2018.

Mateus AP, **Carballo C**, Mantecón L, Pinto PIS, Najafpour B, Manchado M, Power DM. Development of immune competence in sole (*Solea senegalensis*) and microalgae as a modulatory factor. Oral Presentation. Public dissemination event of Microalgae4AB project. El Puerto de Santa Maria, Cadiz, Spain. October 2019.

Carballo C, Mateus AP, Mantecón L, Power DM, Manchado M. Microalgal extracts as epigenetic regulators of fish plasticity. Oral Presentation. Public dissemination event of Microalgae4AB project. El Puerto de Santa Maria, Cadiz, Spain. October 2019.

NATIONAL CONFERENCES

Carballo C, Chronopoulou EG, Letsiou S, Maya C, Labrou NE, Infante C, Manchado M. Estudio de las propiedades antioxidantes e inmunomoduladoras de la crisolaminarina. Jornadas de acuicultura en el litoral suratlantico. Cartaya, Huelva, Spain. May 2018.

Carballo C, Shin HS, Borrego JJ, Zamorano MJ, Manchado M. "Caracterización fenotípica de dorada (*Sparus aurata*) infectadas con linfocistivirus para su aplicación en planes de selección genética" Jornadas de acuicultura en el litoral suratlantico. Cartaya, Huelva, Spain. May 2018

ABBREVIATIONS

APCs: antigen presenting cells

BSA: bovine serum albumin

CMC: non-specific cell-mediated cytotoxicity

DE: delayed early genes

DHA: docosahexaenoic acid

DXM: dexamethasone

EPA: eicosapentaenoic acid

FCN: ficolin

FV3: frog virus 3

GALT: gut-associated lymphoid tissue

GIALT: gill-associated lymphoid tissue

IE: immediate early genes

IFN: interferon

Ig: immunglobulin

IL: interleukin

ILT: interbranchial lymphoid

IPNV: Infectious Pancreatic Necrosis Virus

IRF: interferon related factors

ISGs: interferon-stimulated genes

LCD: Lymphocystis disease

LCDV: Lymphocystis Disease Virus

LPS: lipopolysaccharide

LTA: lipoteichoic acid

MAC: membrane-attack complex

MAe: microalgal extract

MALT: mucosa associated lymphoid tissue

MBL: mannose-binding lectin

MCP: major capsid protein

MMCs: melanomacrophage centers

MT: million tonnes

NALT: nasopharynx-associated lymphoid tissue

NCC: non-specific cytotoxic cell

NCCRP 1: NCC receptor protein 1

NCLDV: Nucleocytoplasmic Large DNA Viruses

NK: natural killer

PAMPs: pathogen-associated molecular patterns

PFA: paraformaldehyde

PGN: peptidoglycan

Phdp: *Photobacterium damselae* subsp. *piscicida*

PRP: pattern recognition proteins

PRR: pattern recognition receptors

RAS: recirculation aquaculture systems

ROS: reactive oxygen species

SALT: skin-associated lymphoid tissue

SDDV: Scale Drop Disease Virus

Tc: cytotoxic T-cell

TCR: T-cell receptor

Th: helper T-cell

TLRs: Toll-like receptors

TNF: tumor necrosis factor

Treg: regulatory T-cell

VER: viral encephalopathy and retinopathy

VHSV: Viral Haemorrhagic Septicaemia Virus

VNN: Viral Nervous Necrosis Virus

... Y ya estarán los esteros

rezumando azul de mar.

¡Dejadme ser, salineros,

granito del salinar!

Alberti

Agradecimientos

Desde los versos del portuense Alberti, me gustaría comenzar con los de otro gran andaluz, *Caminante, son tus huellas el camino, y nada más; caminante, no hay camino: se hace camino al andar (Machado).* Y en este camino estoy a punto de llegar a una de las estaciones que tanto había soñado alcanzar a lo largo de mi vida, y que, sin duda alguna, es consecuencia del apoyo, trabajo y la compañía de muchas personas, aquellas que me empujasteis hacia delante cuando perdí ritmo y aquellas que supisteis frenarme en el momento adecuado para llegar a buen puerto.

Y desde el Puerto, en primer lugar, me gustaría agradecer a mis directores, a Juan José Borrego, por toda su ayuda, buenos consejos y todo el tiempo que me ha dedicado y, a Manuel Manchado, del que he aprendido tanto como he podido y al que agradezco enormemente todo lo que me ha enseñado, por estar siempre dispuesto a ponerse las botas y por tantas horas de su vida invertidas en estos últimos años en esta tesis doctoral.

Mi camino hasta aquí comenzó en Málaga, en el departamento de Microbiología. De este periodo agradezco a Esther y a Mari Carmen Alonso, que me dieron mi primera oportunidad y de las que aprendí mucho. A Lola Castro, por tus consejos y por toda tu ayuda en los trabajos de esta tesis.

A mis compañeros y biólogos consortes, a Benjamín, Lorena, Patricia, Alberto, Daniel, Miguel, Estefanía, Pedro, Rocío, Lisandro, Ana y Alejandro, que me hicieron sentir uno mas nada mas conocerme y de los que me enorgullezco llamar amigos, que a pesar de estar todos lejos os siento cerca, y espero impaciente poder hacer una de nuestras quedadas "deportivas". Gracias por vuestra ayuda, por enseñarme todo lo que sabíais y por lo que aprendimos juntos.

Y, caminando, el camino me llevó por tierras gaditanas, donde encontré unos compañeros tan buenos como los que dejé. Mi paso por en el Toruño esta lleno de aprendizaje y buenos recuerdos vividos junto a vosotros. Desde el principio me sentí en casa y me acogisteis como si llevase toda la vida formando parte de este equipo. Gracias a la sección 50plus del *Elite Team*, a Concha y Manolo Aparicio, con los que he compartido y disfrutado tantos muestreos y de los que he aprendido muchísimo. Me llevo las fotos con las doradas, aunque parezca mas un pescador que un científico. A mi compañero Israel, el próximo de la hornada, con el que he compartido muchos buenos momentos trabajando juntos. A todo el personal de cultivos, Moises y Javier y especialmente a Vitorio y Rafael, por todos esos inventos para poder hacer los experimentos y por vuestra disposición, implicación y alegría cada vez que os he necesitado. A Javi, gracias por todas esas horas que dedicaste para enseñarme, quizá con el tiempo y esfuerzo llegue a ser la mitad de bueno y

organizado que tu. A mis compañeros Vicky, María del Mar, Ismael, Anina, Paula, Raúl, Marian, Eugenia, Carmen, Eduardo, Pablo y Paco Sedano, con los que he pasado muy buenos momentos. Y todos los que habéis pasado por el laboratorio en estos años, a Joanna, Evaggelina, María Joao y Pilar. Finalmente, me gustaría agradecer especialmente a Nuria y Aniela, que, a pesar de tantas muestras y muestras, placas y placas, manchas en las batas y experimentos estresantes, siempre me devolvían una sonrisa. Esta tesis tiene tanto de vosotras que no existiría sin vuestra ayuda. Todos me habéis hecho disfrutar de la ciencia y de la vida. No tengo palabras para poder agradecer lo que me habéis dado.

Me gustaría agradecer a todos mis compañeros durante mi estancia en la AUA de Atenas, gracias a Nikolaos Labrou por permitirme realizar mi estancia en su laboratorio y, especialmente a Evi, gracias por tu paciencia, por enseñarme lo que sabes, por todo tu esfuerzo y trabajo invertidos en mi. A los compañeros de Apivita, los que conocí en Atenas y los que han pasado por el Toruño, a Kostas, Sophia Lesiou, Sophia, Vana y Eleni, y su alegría contagiosa, ευχαριστώ.

Agradecer a Carmen Sarasquete y a Juan Bosco del ICMAN CSIC y a todo su equipo por enseñarme y hacerme sentir como en mi propio laboratorio durante mi estancia en su centro. Ha sido un placer trabajar junto a vosotros.

A los compañeros de la UAL de Faro, a Deborah Power y a todo su grupo, a Joao, Liliana, Patricia y Ana Patricia, por toda su ayuda en los experimentos y por vuestra simpatía y cercania. *Muito obrigado*.

A Carlos y Claudia de Fitoplacton y a los compañeros de la universidad de las Palmas, a Juan Manuel Afonso y todo su equipo por su ayuda.

Sin duda, echando la vista atrás, siento que ha sido un camino enriquecedor gracias a la ayuda de todos, pero mis palabras finales van dirigidas a mi familia. A mi hermano, mis primos, y tíos, especialmente a mis tíos Juan y Aurelia, que siempre han estado ahí y a los que aprecio muchísimo. A mi familia gaditana, a Mercedes por hacerme sentir uno mas de sus hijos. A mi perrita Lola y a Mika y Laika, que nos dejaron, pero siempre formaran parte de mí.

A María Jesús, la luz de mi vida, por haberme aguantado todo este tiempo, por comprenderme, por tu apoyo incondicional, por hacerme sonreír siempre, por mirarme como me miras, esta tesis es tan tuya como mía.

A mis padres, Manuel y Carmen, a quienes dedico esta tesis. Gracias por vuestro esfuerzo, por pasar tantas horas trabajando para permitirme llegar aquí, por privaros de tanto para darnos a nosotros, por creer siempre en mi. Me siento orgulloso de tener unos padres como vosotros

INDEX

GENERAL INTRODUCTION

1.1 Aquaculture, a fast-growing economical sector

The rapid growth of global population, expected to be 9.7 billion of persons in 2050, demands an enhanced food supply in the next years. Aquatic products, and fish in particular, are an important source of high quality protein and other valuable nutrients, such as the long-chain omega-3 fatty acids docosahexaenoic acid (DHA) and eicosapentaenoic acid (EPA), vitamins (A, D and B) and minerals (iodine, selenium, zinc, iron, calcium, phosphorus, potassium) (FAO 2016). Nevertheless, in the last 20 years, world capture fisheries reached its sustainable limit, with annual catches around 90 million tonnes (MT), while global demand of marine products still remains increasing progressively. This gap between fisheries offer and market demands is fullfilled by a quick growth of the aquaculture industry worldwide that reached 110.2 MT in 2016, surpassing the production of fisheries (APROMAR 2018; FAO 2018). Currently, China is the main producer accounting for the 57.8% of global aquaculture production that represents 45.4 MT of total aquatic animals, much higher than those of its main competitors (APROMAR 2018; FAO 2018).

Focusing on finfish, the worldwide total production was 54.1 MT in 2016, 47.5 MT from inland aquaculture and 6.6 MT from marine and coastal aquaculture, with Europe producing only 4.3% of total production. Nevertheless, excluding inland aquaculture, percentage for finfish marine and coastal aquaculture were reduced to 56.7% for Asian countries and 27.8% for Europe countries (FAO 2018). European finfish aquaculture is led by Atlantic salmon (*Salmo salar*) followed by rainbow trout (*Onchorynchus mykiss*), gilthead sea bream (*Sparus aurata*) and European sea bass (*Dicentrarchus labrax*). The United Kingdom appears as the main European finfish producer (mainly salmonids total 203,922 tonnes) followed by Greece (main producer of gilthead sea bream and sea bass; 106,165 tonnes) and Spain, in the third position (66,591 tonnes), mainly producing sea bass, rainbow trout and sea bream with a stable production in the last years as will be shown

below (APROMAR 2019).

1.2 Current status of gilthead sea bream (*Sparus aurata*) and Senegalese sole (*Solea senegalensis*) aquaculture

Gilthead sea bream and Senegalese sole are two species of high economic importance in Southern Europe. Although the production of gilthead sea bream is highly extended along the Mediterranean basin, the Senegalese sole is mainly produced in Spain and Portugal. The current status of aquaculture development in both species is completely different in terms of production figures, culture technologies, and current technological challenges and bottlenecks (Manchado *et al.* 2016).

The gilthead sea bream is the main marine fish produced in Europe (95,390 tonnes and 435.1 M€). Total production including Turkey (the main producer in the Mediterranean Sea) increased 10.7% (~246,839 tonnes) in 2018 with respect to 2017 and is expected that continue growing in 2019. While Turkey produced 33.6% of total production in the Mediterranean basin, Spain occupies the fourth position with only 6.0% of total production (APROMAR 2019). Contrary to gilthead sea bream, total production of Senegalese sole is still limited (Dinis *et al.* 1999; Morais *et al.* 2016; APROMAR 2018) in spite of the high market demands and the high prices. The main producer countries of this flatfish are Spain, Iceland, France and Portugal, although all facilities abroad belong to Spanish corporations that did not find suitable areas or did not get authorizations to build the recirculation facilities required for sole production in Spain. Current production figures of this species increased from 200 tonnes at the beginning of this decade to the 1,616 tonnes in 2017 and, although a decrease of a 3.9% was registered in 2018, a fast expansion is expected to accur in 2019 (APROMAR 2018).

Both gilthead sea bream and Senegalese sole are cultivated under different

rearing technologies to fit as much as possible to their biology and swimming behaviour and, hence, provide high standards of welfare that in turn will contribute to enhance growth performance and health (Palstra & Planas 2011; Oca & Masaló 2019). The gilthead sea bream is mainly farmed under intensive conditions in offshore sea cages (Spain, Italy, Cyprus) and secondary in indoors tanks (Greece and Turkey) and under extensive o semi-intensive systems in earth pond in South Spain and Italy (Basurco *et al.* 2011). On the other hand, sole is cultivated almost exclusive under intensive systems in shallow tanks under flow-through or recirculation aquaculture systems (RAS) in which the environment is highly controlled (Morais *et al.* 2016), Also, the flat morphology and its benthic biological behaviour allow for the use of stacked tanks, greatly expanding the cultivation area in a low built surface (Oca & Masaló 2019).

Currently, there is a vast biological knowledge about gilthead sea bream biology and physiology existing well-defined protocols to manipulate broodstock, spawning and larval rearing (Basurco *et al.* 2011). Moreover, this species is considered highly robust and plastic able to adapt to different environments, diet shifts and with a low susceptibility to infections diseases that explain, at least partially, its success in aquaculture (Manchado *et al.* 2016). In the case of Senegalese sole, the industrial production in aquaculture started much later than in sea bream. Although initial attemtps were done in ponds, all of them failed and it was only after 2006 when the RAS were used and the sole production become a reality (Dinis *et al.* 1999; Morais *et al.* 2016; APROMAR 2018). Although the advances in larval rearing and on-growing are important to sustain the sole production (Cerda & Manchado 2013), the lack of control on reproduction success and disease outbreaks still remain as major challenges in this aquaculture (Manchado *et al.* 2016).

Despite the technological progress in both species, there still exist specific and important challenges and bottlenecks in their aquaculture hat need to be solved including new advances in nutrition, genetics, and fish health.

Recent European forums between academia and industry identified the nutrition as a keystone in aquaculture that requires to be optimized to reach best species-specific composition and balance, establishing and defining the nutritional and physiological requirements needed in gilthead sea bream and sole, in each life stage and age, and testing the effects of new raw materials as substitution of fish meal and oil (EATiP 2014; Manchado *et al.* 2016). In addition to formulation and ingredients, a fast evolving field is the use of new additives as functional foods able to improve growth and feed utilization, such as acidifiers or exogenous enzymes, providing enhanced digestibility of the feed materials, or counteracting the negative effects of anti-nutrients or to improve the health and stress resistance of the animals, such as probiotics, prebiotics, phytogenics, and immune-stimulants (Encarnação 2016).

Another important demand of the aquaculture sector is the building of genetic breeding programs for traits such as growth performance, feed conversion efficiency, shape-deformities and disease resistance. Recently, genetics breeding programs were initiated for gilthead sea bream in Europe (Garcia-Celdran *et al.* 2015a; 2015b; 2015c; Lee-Montero *et al.* 2015; 2016), but it is necessary to create a structure that supports these programs in a long-term (EATiP 2014). In sole, despite the first steps of genetic improvement programs (Manchado *et al.* 2019), the aquaculture of this flatfish still has to face up a major control of the reproduction under captivity, since the males are not able to display a proper courtship behaviour required for a successful fertilization (Manchado *et al.* 2016). The intense research efforts on large DNA and RNA genomics, epigenetic regulation and breeding techniques (Cerda *et al.* 2008; Lee-Montero *et al.* 2013; Benzekri *et al.* 2014; Berbel *et al.* 2018; Carballo *et al.* 2018b) are a good starting point to build solid genetic

breeding programs for gilthead sea bream and sole (EATiP 2014; Manchado *et al.* 2016).

A third major challenge for the aquaculture industry is to preserve and enhance fish health minimizing the incidence of infectious diseases and reducing the important associated economic losses. The main disease outbreaks identified in cultured gilthead sea bream and sole were caused by bacteria (FAO 2005-2019b; a). The most common and serious disease is the "vibriosis", that refers to infections caused by different species from *Vibrio* genus, such as *V. anguillarum, V. alginolyticus* or *V. harveyii*, and the photobacteriosis, caused by *Photobacterium damselae* subsp. *piscicida* (Phdp). This latter agent has been recognized as the main important bacterial infection responsible for high economic losses in gilthead sea bream and Senegalese sole in the Mediterranean countries at the end of last century (Toranzo *et al.* 2005; Colorni & Padrós 2011; Morais *et al.* 2016). Finally, flexibacteriosis, and mainly the *Tenacibaculum maritimum* although some other *Tenacibaculum* species were also reported as pathogens in sole, were also identified as responsible for economical losses in this industry (Morais *et al.* 2016). In addition to bacteria, parasites have also emerged as a new problem in gilthead sea bream and Senegalese sole. Main outbreaks in cultured gilhead sea bream were associated with *Amyloodinium spp.*, *Cryptocarion spp.*, *Ichthyobodo spp.*, *Trichodina spp.* and *Enteromyxum leei* (Paperna & Baudin-Laurencin 1979; Estensoro *et al.* 2010; Bahri 2012; Borrego *et al.* 2017a). In the case of Senegalese sole, the protozoa *Endolimax piscium* was recently identified as the causing agent of an amoebic disease in sole that provoke tumorous hepatic and muscle lesions and an important delay in weight gain (Constenla *et al.* 2014; 2018).

Within the infectious diseases, the viral infections are a special group due to economic impact but also for the tight regulation in law that can become a limiting factor for the expansion of aquaculture. Additionally to the direct losses of fish production, overcosts derived from reduced productivity, the removal of animal

carcasses and the restrictions of export markets convert them in a real barrier for fish production (Whittington & Chong 2007; Rigos & Katharios 2010). Main viral diseases in gilthead sea bream and Senegalese sole will be reviewed below.

1.3 Viral infections in gilthead sea bream and Senegalese sole

Gilthead sea bream and Senegalese sole have been reported to be infected by different viruses including betanodavirus (Viral Nervous Necrosis Virus, VNNV), Infectious Pancreatic Necrosis Virus (IPNV), and the Lymphocystis Disease Virus (LCDV). Experimental infections using the Haemorrhagic Septicaemia Virus (VHSV) were also reported (Lopez-Vazquez *et al.* 2011; 2017).

The VNNV is the aetiological agent of the viral encephalopathy and retinopathy (VER). Senegalese sole has been shown to be highly susceptible to betanodavirus infection with important mortality episodes, mainly in larvae and juveniles sole (Padros *et al.* 2019), whereas gilthead sea bream appears to be resistant with some mortality episodes in larvae (Cherif *et al.* 2009). Although two main genotypes RGNNV and SJNNV appeared to be pathogenic in sole, the reassortant RGNNV/SJNNV that has the RG RNA1 and SJ RNA2 genomes are reported as the most virulent to this species (Souto *et al.* 2018).

Also, IPNV and VHSV can produce mortality in Senegalese sole, but not in gilthead sea bream to date. An IPNV associated with a high mortality episode on a farm in south-west Spain was reported in sole (Rodriguez *et al.* 1997). Moreover, experimental infections using the rhabdovirus VHSV produced important mortalities and typical signs as shown in experimental infection (Rodriguez *et al.* 1997; Lopez-Vazquez *et al.* 2011; 2017), but no natural outbreaks have been reported to date (Padros *et al.* 2019). Furthermore, an aquareovirus was detected in gilthead sea bream in a natural outbreak episode in larvae, but only provoked moderate mortality (Bandin *et al.* 1995).

The LCDV is considered the most important viral infection in gilthead sea bream (Borrego *et al.* 2017b) and secondarily in Senegalese sole (Alonso *et al.* 2005; Cano *et al.* 2010). In the former species, LCDV is frequently detected as *polyomavirus* and *papillomavirus* co-infections although the implications of this co-occurrence is still unknown (Labella *et al.* 2019). Due to the importance of LCDV in gilthead sea bream aquaculture and the wide range of species that invades including sole (Borrego *et al.* 2017b), this virus was used as a model for the current PhD Thesis.

1.4 Lymphocystis disease virus (LCDV)

1.4.1 LCDV Classification

LCDV is the causative agent of Lymphocystis disease (LCD). This virus belongs to *Iridoviridae* family that is included within the Nucleocytoplasmic Large DNA Viruses (NCLDV) together with *Poxviridae, Asfarviridae, Ascoviridae, Mimiviridae* and *Phycodnaviridae* families (Jancovich *et al.* 2015). The members of the family *Iridoviridae* comprise a diverse collection of viruses with linear, double-stranded DNA genomes enclosed within an icosahedral capsid (Jancovich *et al.* 2012).

The major capsid protein gene (*mcp*) is relatively conserved in *Iridoviridae* family, and it is recognized as a suitable target for phylogenetic studies (Tidona *et al.* 1998). According to *mcp* phylogeny, *Lymphocistivirus* genus has been classified into nine different genotypes (Borrego *et al.* 2017b):

- Genotype I, that included the isolate LCDV-1 from European flounder.
- Genotype II, the isolate LCDV-C from Japanese flounder.
- Genotype III, the isolate LCDV-RF from black rockfish.
- Genotype IV, that included the two isolates, LCDV-RC and LCDV-SB, from cobia (*Rachycentron canadum*) and Japanese seabass (*Lateolabrax japonicus*) respectively.
- Genotype V, the isolate the LCDV-CB from painted glass fish (*Parambassis*

baculis).

- Genotype VI, the isolate LCDV-TL from gourami (*Trichopodus leerii* and *T. trichopterus*).
- Genotype VII, the isolate LCDV-SA from gilthead sea bream and Senegalese sole.
- Genotype VIII, isolated from largemouth bass (*Micropterus salmoides*).
- Genotype IX, isolated from American yellow perch (*Perca flavescens*).

From these nine genotypes, only three have been recognized as different species up to date: the LCDV-1 (genotype I), LCDV-C (genotype II) and LCDV-Sa (genotype VII) isolated from gilthead sea bream and studied in this PhD thesis. Some of the other viral isolates were proposed as a new species, however, their taxonomic position remains still unclear and they were not recognized (Chinchar *et al.* 2017a).

1.4.2 LCDV structure

LCDV virions are naked (Fig. 1a) and they contain an external bilaminar capsid with an icosahedral symmetry and a helicoidal core. Also, LCDV displays hair-like fibrils on the capsid surface of unknown function (Devauchelle 1985; Flugel 1985; Liu *et al.* 2016b).

LCDV genome is a linear dsDNA molecule that are circularly permuted and terminally redundant (Goorha & Murti 1982). Genome size is highly variable within the family and ranges from 140 to 303 kilobases (Kb). Due to the redundancy found in the genome, the unit-length genome sizes (the sum of the size of only the unique genes) range from 105 to 212 kb (Jancovich *et al.* 2012) and it contains 183 putative open reading frames (ORFs) with a conserved core of 26 genes that encode proteins larger than 30 amino acids (Eaton *et al.* 2007), including those genes for viral structural proteins such as the major capsid protein (*mcp*), and the proteins involved in the regulation of gene expression, virus replication, and virulence (Jancovich *et al.* 2015). Recently, the complete genome of LCDV isolate from gilthead sea bream

(LCDV-Sa) was sequenced comprising 208.5 kb in length, significantly longer than those of the two lymphocystiviruses previously sequenced (LCDV-C and LCDV-1, with 186 kb and 103 kb, respectively) and a 33% of GC content, slightly higher than the others LCDV species (27.2% in LCDV-C and 29.1% in LCDV-1). Also, this genome encodes a set of at least eight genes with a high homology with genes from the Scale Drop Disease Virus (SDDV) not found in other LCDV species (Lopez-Bueno *et al.* 2016).

1.4.3 LCDV multiplication

The viral replication of LCDV has been poorly studied up to now. Instead, the frog virus 3 (FV3) was used as the model for replication of *Iridoviridae* family, as a recently reviewed in Chinchar *et al.* (2017b) and depicted in Fig. 1b. Firstly, the non-enveloped virions of this family initiate the infection cycle by binding the cell membrane with subsequent entry of the viral core into the cytoplasm, entering the viral DNA into the nucleus and start the expression of viral genes in a coordinated temporal cascade: (i) expression of early genes [immediate early (IE) and delayed early (DE)] by the host RNA polymerase II; (ii) expression of a viral DNA polymerase and DNA replication in the nucleus (first stage of viral DNA replication); (iii) transport of DNA to cytoplasm and methylation to avoid degradation or prevent recognition of viral DNA by the immune system; (iv) DNA synthesis in large concatemers in the cytoplasm (second stage of viral DNA replication); and (v) expression of late viral genes using a virus-encoded RNA polymerase II and linked to DNA synthesis.

The mechanism of virion assembly in iridovirus are proposed by analogy with others NCLDVs viruses (Mutsafi *et al.* 2014; Suarez *et al.* 2015). The virion assembly occurs in the cytoplasm, probably derivates from the endoplasmic reticulum for the deposition of viral capsid and other viral proteins. Viral assembly sites are closely related to mitochondria to supply energy need. The capsid proteins

assemble creating icosahedral capsids after which the viral DNA enters, incorporating a full-length genome plus extra segment creating virions with linear, circularly permuted and terminally redundant genomes, Finally, mature virions are cumulated in paracrystalline arrays.

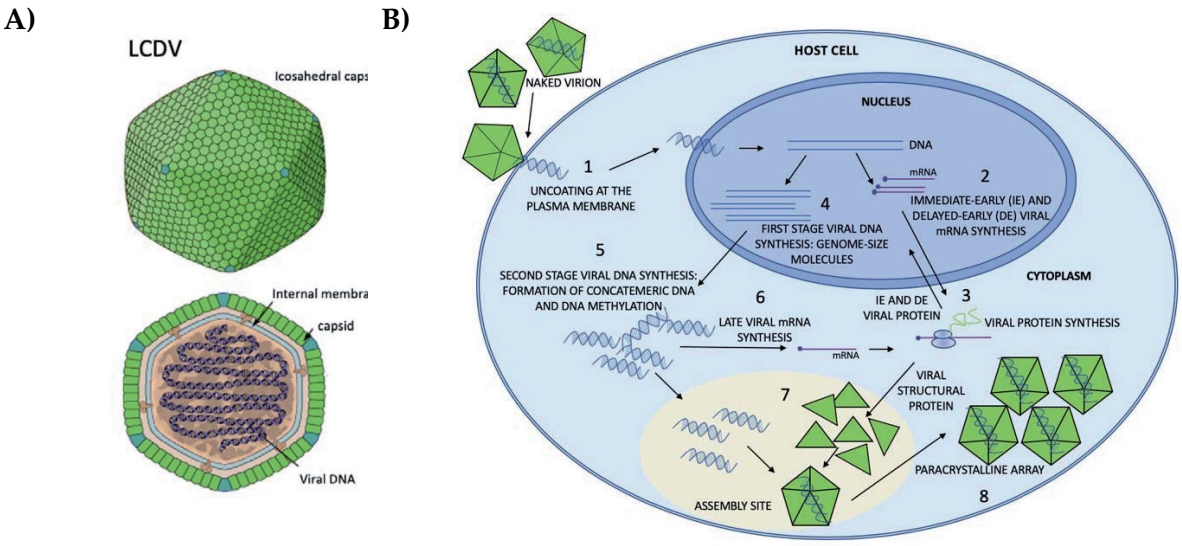

Figure 1. Lymphocystis disease virus. A). Virion and internal structure representation (modified from ViralZone, Swiss Institute of Bioinformatics). B). Scheme of iridovirus replication: The viral DNA penetrates into the cell (1) and goes to the nucleous, starting the expression of immediate-early (IE) and delayed-early (DE) genes (2), those include viral DNA polymerase, that initiates the replication in the nucleus, copiying a genome-size molecule (4) and continuing in the cytoplasm with the syntesis of concatemeric DNA (5), from which started the expression of late genes (6). The virion assembly takes place in the assembly site (7), acumulating the virions on paracrystaline arrays on the cytoplasm until breaks cell (8). [modified with permission fom (Chinchar *et al.* 2017b)]

1.4.4 Lymphocystis disease

The lymphocystis disease (LCD) refers to the clinical signs caused by LCDV and it is usually observed as a chronic and self-limiting process highly dependent on the host health status and environmental conditions (Williams 1996). Using experimental infections, the average time to observe the skin lesion spans for at least three weeks after LCDV injection (Bovo & Florio 2008; Kvitt *et al.* 2008; Hossain *et al.* 2009; Borrego *et al.* 2017b).

The main clinical lesion in the LCD is the lymphocyst that is a proliferative lesion of hypertrophied fibroblastic cells in the dermis connective tissue (Paperna *et al.* 1982; Samalecos 1986). This tumor-like lesions spread through the fish skin and fins, and they are whitish-grayish to pinkish colored (Sarasquete *et al.* 1998; Borrego *et al.* 2017b) (Fig. 2). Although LCDV is typically dermatotrophic (Colorni & Padrós 2011), the virus can also be detected in several internal organs, such as intestine, liver, spleen, kidney and brain, being the virus capable to infect the fibroblast, hepatocytes and cells of the mononuclear phagocyte system to set a systemic infection (Valverde *et al.* 2017a).

Figure 2. Gilthead sea bream showing tipical lymphocysts (blue circle) of a LCDV infection (photograph supplied by M. Manchado)

LCD normally does not cause significant mortalities although under some circumtances severely infected fish may die, usually limited to those individuals whose swimming, breathing, or feeding is severely impaired by particularly large and cumbersome lymphocysts, specially in younger fish (Colorni & Padrós 2011). Moreover, LCD infected animals may be more susceptible to secondary bacterial infections, parasitic infestations or cannibalism episodes by healthy animals, that may increase mortality rates (Williams *et al.* 2005; Colorni & Padrós 2011; Dezfuli *et al.* 2012; Haddad-Boubaker *et al.* 2013). Although mortality remains usually very

low, the morbidity is close to 100% and it is associated with an important delay in growth rates and a reduced marketability that have a profound impact on economic costs in the hatcheries (Nishida *et al.* 1998; Iwamoto *et al.* 2002).

LCDV spreads when the lymphocystis cells break and the virus progeny content is released. Hence, the horizontal transmission is assumed to occur through the skin and gills by direct contact or by waterborne exposure with infected animals (Wolf 1988; Bowser *et al.* 1999; Kvitt *et al.* 2008). Nevertheless, the transmission routes are not completely elucidated since horizontal transmission through contaminated feed was also demonstrated in gilthead sea bream larvae supplied LCDV-positive rotifers (Cano *et al.* 2013). A better understanding of the spreading and transmission mechanisms, particularly in LCDV infections in sole, is required to implement control strategies to limit this virus in the aquaculture facilities is required.

1.5 Immune system in fish

The study of the host defences against microbial diseases has become an essential tool to keep high standards of immunocompetent fish in intensive farming. The immune system in fish is associated with different organs and tissues that can be classified into the non-mucosal lymphoid organs and the mucosa associated lymphoid tissue (MALT) (Fig. 3). The major lymphoid organs are the thymus, head kidney and spleen. The thymus, located near the gill cavity, is the organ in which the T cell lineages maturate and differentiate (Uribe *et al.* 2011). Head kidney or pronephros is the organ for haematopoiesis in fish until adulthood and B-cell proliferation (Zapata *et al.* 2006; Tian *et al.* 2009). The spleen is the secondary immune organ in fish. Both head kidney and spleen contain the macrophages, which aggregate in melanomacrophage centers (MMCs), and lymphoid cells (Press *et al.* 1994; Zapata *et al.* 2006; Uribe *et al.* 2011). In addition to these major immune organs, fish also contain the MALTs, that although more

diffuse than in mammals (Rombout *et al.* 2011), they also play a key role in fish continously exposed to several microbes in surrounded water (Salinas 2015).

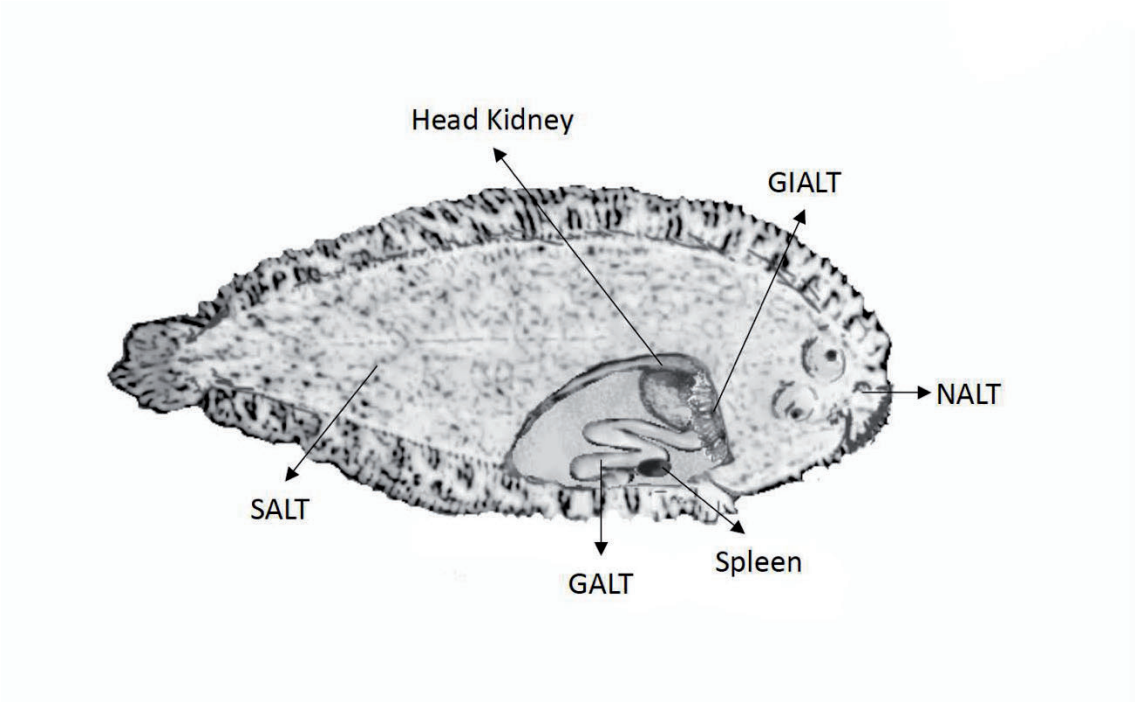

Figure 3. Scheme of the distribution of MALTs and the position of the main immunological organs head kidney and spleen in Senegalese sole. Gut-associated lymphoid tissue (GALT), skin-associated lymphoid tissue (SALT), gill-associated lymphoid tissue (GIALT) and nasopharynx-associated lymphoid tissue (NALT)

The immune system in fish is complete, as in mammals, and comprises both an innate and adaptive or acquired immune defence systems (Magnadottir 2006; Secombes & Wang 2012). Both systems are highly interconnected and, in general, the innate response precedes the adaptive response, activating and canalyzing the nature of the adaptive response and co-operating in the maintenance of homeostasis (Fearon & Locksley 1996). In early larval stages these systems remain immature and they are highly dependent upon the maternally- transferred immune factors (lysozyme, hormones and immunoglobulin, among others) (Zhang *et al.* 2013). Nevertheless, these maternal transferred factors only persist for a limited

time and larvae progressive acquire their own defenses, first the innate followed by the adaptive system (Vadstein *et al.* 2013). Both immune systems are revised below.

1.5.1 Innate immune system

The innate immune system is considered as the first barrier to cope with pathogen invasion. This system recognizes conserved motifs in the pathogen surfaces called pathogen-associated molecular patterns (PAMPs) such as bacterial cell wall, lipopolysaccharide (LPS) and peptidoglycan (PGN), nucleic acids present in virus and bacterial including the double-stranded viral RNA, and several complex polysaccharides, such as β-glucans or mannans (Medzhitov & Janeway 2002). These PAMPs bind to different proteins or receptors present in the immune cells, called patterns recognition receptors (PRRs) that are reponsible for the initiation of the immune response. Some of these receptors are toll-like receptors (TLRs), RIG-I-like receptors (RLRs), cytosolic DNA sensors (CDSs), and class A scavenger receptors (SR-As) (Poynter *et al.* 2015). This innate immune system is commonly divided into three main components: the epithelial/mucosal barrier, the cellular components and the humoral parameters (Magnadottir 2010).

1.5.1.1 Epithelial and mucosal barriers

The epithelial and mucosal barriers of the skin, gill and alimentary tract are extremely important to cope with diseases providing a physical and mechanical protection against microbial attacks (Magnadottir 2006). Particularly important is the mucus layer, a complex viscous mixture of immunogenic compounds containing several immune defence humoral parameters, including antiviral components such as mucins, immunoglobins, lysozyme, antimicrobial peptides, and defensins that contribute to both innate and adaptive immunity (Magnadottir 2010; Raj *et al.* 2011; Gomez *et al.* 2013; Merrifield & Rodiles 2015).

Strongly related to these physical barriers we can find the MALTs. They are

classified depending on their location in the gut-associated lymphoid tissue (GALT), skin-associated lymphoid tissue (SALT), the gill-associated lymphoid tissue (GIALT) and the recently discovered nasopharynx-associated lymphoid tissue (NALT) (Salinas 2015). This immune tissue has abundant leukocytes in gill filaments (Haugarvoll *et al.* 2008) and in lamina propria and intestinal epithelium of gut (Fuglem *et al.* 2010) that contribute to innate and adaptive responses and produce molecules that work together to maintain mucosa homeostasis (Salinas 2015).

Another third barrier essential for fish health is the microbiome. These mucous-associated microbial communities contain beneficial microorganisms in a ''normobiosis'' state. Nevertheless, any perturbation on the normal composition facilitate the harmful microbes proliferation given arisen to the called ''dysbiosis' that could enhance susceptibility to disease (Llewellyn *et al.* 2014; Talwar *et al.* 2018). Microbiome composition are influenced by a) environmental factors, such as temperature, pH, oxygen, water quality or microbial community composition in the environment (Larsen *et al.* 2013; Bierlich *et al.* 2018); b) host-associated factors such as the genetic background, the developmental stage or physiological status (Talwar *et al.* 2018; Pinto *et al.* 2019); and, c) diet-associated factors, such as the source of nutrients used in the diet or the addition of probiotic and prebiotics (Parma *et al.* 2016; Rimoldi *et al.* 2018; Talwar *et al.* 2018; Tapia-Paniagua *et al.* 2019). Recently, Pinto *et al.* (2019) described the microbiomes in the skin and gut in normal pigmented and pseudo-albino Senegalese sole juveniles, indicating that microbial populations in the gut but not in gills were dependent on the melanin levels.

1.5.1.2 Cellular components

The main cellular components of the innate immune system are the phagocytic cells (monocytes and macrophages), granulocytes (neutrophils) and the non-specific cytotoxic cells (NCC and NK-like cells) (Secombes & Wang 2012). The mononuclear phagocytic system (monocytes and macrophages) plays important roles in host protection and homeostasis. The macrophages recognize the PAMPs by binding to a wide set of PRRs, such as Toll Like Receptors (TLRs) and complement receptors, triggering a defensive response through the the production and releasing of pro-inflammatory cytokines, such as tumor necrosis factor α (TNFα), interleukin 1β (IL1β) and interleukin 6 (IL6), nitric oxide production and respiratory burst activity (Hodgkinson *et al.* 2015; Grayfer *et al.* 2018).

Neutrophils and mast cells are also key components of the inflammatory immune response against a wide variety of pathogens. Neutrophils are essential to the acute inflammatory response producing a robust respiratory burst response, releasing inflammation-associated leukotriene B4, and inducing macrophages to trigger reactive oxygen species (ROS) production; and also have an important role in the recovery of basal level in pro-resolving phase (Havixbeck *et al.* 2016). The mast cells, also known as eosinophilic granular cells, play an important role in the inflammatory response in teleosts by degranulation and release of mediators of inflammation (Sfacteria *et al.* 2015).

In fish, the non-specific cytotoxic cell (NCC), homologues to NK cell in mammals, are involved in non-specific cell-mediated cytotoxicity (CMC) (Shen *et al.* 2002; Nakanishi *et al.* 2011). Also, other non-specific cytotoxic cells have been described in channel catfish, the NK-like cells that do not express any of the markers of non-specific cells or T-cells (Shen *et al.* 2004). NCCs are small agranular lymphocytes, characterized by the expression of the NNC receptor protein 1 (NCCRP-1). These cells recognize the presence of bacterial and viral molecules

(Evans & Jaso-Friedmann 1992; Yoshida *et al.* 1995; Hogan *et al.* 1996), initiating a signalling cascade that leads to the production of cytokines and chemokines and the release of cytolytic granules, killing infected cells (Evans & Jaso-Friedmann 1992; Yoder & Litman 2011).

1.5.1.3 Humoral parameters

The humoral parameters of the innate immune system comprise soluble components that include the transferrin, TLRs, hydrolases such as lysozyme, protease inhibitors, the complement system, agglutinins and precipitins such as lectins and pentaxins and cytokines such TNF, IL1β, chemokines and interferon (IFN) (Magnadottir 2006; 2010; Zhu *et al.* 2013).

Transferrin is an evolutionary conserved protein that acts as an iron chelator inhibiting the growth inhibitor of invading pathogens, mainly bacteria, although it also has a role as an immune regulator during acute inflammation (Trites & Barreda 2017).

The TLRs are one group of well-known PRRs. These PRRs recognize bacteria by binding LPS (TLR4), PGN and lipoteichoic acid (LTA) in the bacterial cell wall (TLR1/TLR2) and bacteria flagellin (TLR5). Also, the TLRs recognize some DNA and CpG motifs in bacterial and viral DNA (TLR9), dsRNA (TLR3) and ssRNA (TLR7 and TLR8) (Pietretti & Wiegertjes 2014).

The lysozyme is another key molecule of the innate immune system. In fish, there are two main types: the c-type lysozyme (the chicken-type lysozyme) and the g-type lysozyme (goose-type lysozyme). These lytic enzymes have antibacterial activity mainly in Gram-positive. In addition, it acts as immunomodulator and opsonin, activating the complement system and phagocytes (Saurabh & Sahoo 2008; Mai & Wang 2010; Chen *et al.* 2018). Both, c- and g-type lysozyme have been

characterized in Senegalese sole. The g-type transcription was modulated by fish density and feed ration (Salas-Leiton *et al.* 2010), glucocorticoids (Salas-Leiton *et al.* 2012) and hormones (Ponce *et al.* 2011). Moreover, expression of both lysozymes was triggered in response to different microbial components and bacteria (Ponce *et al.* 2011; Nunez-Diaz *et al.* 2016) demonstrating the important of these molecules in host defence.

Protease inhibitors are present in serum and other body fluids in fish to block bacterial proteases, restricting the ability of bacteria to invade and infect the host (Ellis 1990b; 2001; Magnadottir 2006). The total antiprotease enzymatic activity increases in the mucus of sole after a challenge with *T. maritimum* (Guardiola *et al.* 2019). Moreover, this activity dropped in gilthead sea bream fed with a diet with a high substitution of fish meal with soy protein made them more susceptible to *Edwardsiella tarda* (Khosravi *et al.* 2015). These results also indicate that this activity is a good marker as lysozymes to predict the immunocompetence in fish.

The complement system is another relevant component of the innate immunity highly conserved in fish and mammals (Secombes & Wang 2012). This system is activated by three main ways: the alternative complement pathway (ACP), the classical complement pathway (CCP) (Rauta *et al.* 2012) or the lectin pathway (Walport 2001; Nakao *et al.* 2011; Zhang & Cui 2014). Regardless the pathway that triggered the complement response, all of them activate the C3 factor, the major acute-phase protein upon bacterial, viral and parasite infection (Nakao *et al.* 2000). The gilthead sea bream has different isoforms of C3 factor that would increase the capacity of this fish to recognize a broader spectrum of potential pathogens and reinforce a specific immune response (Sunyer *et al.* 1997). This gene is up-regulated in response to bacterial (Phdp) and VNNV infection but decreases under stress condition (Mauri *et al.* 2011). In sole, C3 factor is also activated in response to LPS (Prieto-Alamo *et al.* 2009) or Phdp (Nunez-Diaz *et al.* 2016)

demonstrating its defensive role in this species.

The lectins comprise a highly diverse group of sugar-binding proteins, such as galectins, C-type lectin, pentraxins, among others, that can specifically bind to glycoproteins and glycolipids present in the pathogens membranes (Magnadottir 2006; da Silva Lino *et al.* 2014). These molecules act inducing the phagocytosis, initiating complement system and enhancing the NK cell activity (Arason 1996; Osorio & Reis e Sousa 2011). These lectins play a key role in the recognition of β-glucans acting as mediators of the prebiotic activity associated with these molecules.

Cytokines are a family of molecules secreted by activated immune-related cells in response to pathogens, including viruses (Salazar-Mather & Hokeness 2006). These molecules can be divided into TNFs, ILs, chemokines and IFNs (Zhu *et al.* 2013), and the activity of these molecules have been extensively revised in fish (Goetz *et al.* 2004; Laing & Secombes 2004; Zou & Secombes 2016). In the context of this PhD thesis, we will focus on the IFNs that are the most important antiviral cytokines of humoral innate immune system. They are expressed in response to viruses that in turn induce a large number of interferon-stimulated genes (ISGs), which possess diverse effector and regulatory functions. In teleosts, two groups of IFNs were described based on the number of cysteine bridges and sequence similarity (Zou *et al.* 2007), type I and type II, having both IFNs antiviral activity in the fish model *Danio rerio* (Lopez-Munoz *et al.* 2009). IFN type I are the main cytokines in the antiviral response, through induction of ISGs, although the IFN type II, also knows as IFNγ, probably is the most important cytokine orchestrating the immune response, activating macrophages, increasing the respiratory burst, nitric oxide production and inflammatory response with the expression of pro-inflammatory cytokines (*TNFa, IL1b*) and chemokines (*CXC10*, *CXC13*) genes, and antiviral genes (*MX, ISG15,* interferon related factors *(IRF)* genes)(Pereiro *et al.*

2019). In gilthead sea bream, it has been described three different Mx isoforms (Fernandez-Trujillo *et al.* 2011) with antiviral activity against different viruses, such as IPNV, VHSV and LCDV. The isoforms Mx1 and Mx2 presented *in vitro* antiviral activity against LCDV (Fernandez-Trujillo *et al.* 2013). In Senegalese sole, the Mx had antiviral activity against IPNV and VHSV *in vitro* (Alvarez-Torres *et al.* 2013) and is positively activated in response to IPNV and VNNV challenge (Fernandez-Trujillo *et al.* 2008; Labella *et al.* 2018).

1.5.2 Adaptive immune system

Fish are considered the most primitive vertebrate with an adaptive immune system able to respond to a wide range of antigens enhancing the defensive capabilities against recurrent infections through cellular and humoral mechanisms (Scapigliati *et al.* 2018; Diaz-Rosales *et al.* 2019).

1.5.2.1 Cellular components

The cellular components of adaptive immunity are the B and T lymphocytes. The B lymphocytes express in their cell membrane three different heavy immunglobulin (Ig) chain classes, the IgM, IgT/Z and IgD. Based on these surface Ig, three major B cell populations are described in teleosts: the IgM+/IgD+ B cells, that are the most abundant population in systemic lymphoid organs such as head kidney or spleen, and represent also the majority of B cells in blood and the peritoneal cavity; the IgT/Z+ B cells, that express surface IgT/Z, are the main population of B lymphocytes in MALTs; and IgM-/IgD+ B cells have also been described, but only in channel catfish and European rainbow trout (Parra *et al.* 2016; Scapigliati *et al.* 2018).

The T lymphocytes are characterized by expressing the T-cell receptor (TCR) in their surface (Secombes & Wang 2012). In teleost fish, as in mammals, there are two classes of T cells, those expressing $\alpha\beta$- and $\gamma\delta$-TCR in their surface. Also,

together with TCR, T cells exhibit co-receptors and they are classified as cytotoxic (Tc; CD8), helper (Th; CD4) and and a subset of pro-inflammatory T helper cells known as regulatory (Treg, Th17) (Nakanishi *et al.* 2011; Takizawa *et al.* 2016; Kasheta *et al.* 2017). The Tc cells recognize viral peptides presented by the mayor histocompatibility complex (MHC) class I to kill virus-infected cells (Fischer *et al.* 2006; Laing & Hansen 2011). By other side, the Th cells recognize the MHC class II, present only in the "professional" antigen presenting cells (APCs) (Laing & Hansen 2011). The primary differentiation of T cell in fish, as in mammals, occurs in the thymus, from where mature T cells migrate to other lymphoid organs and MALTs (Hansen & Zapata 1998; Tacchi *et al.* 2014; Tafalla *et al.* 2016; Scapigliati *et al.* 2018), considering the gut as the main lymphoid tissue for T cells in adult fish (Boschi *et al.* 2011).

1.5.2.2 Humoral parameters

The main humoral parameters of adaptive immunity are the Ig, the MHC and co-stimulatory molecules, and some relevant cytokines (Zhu *et al.* 2013). The Igs neutralize pathogens, facilitate phagocytosis of pathogens through opsonization, and activate classical complement (Rauta *et al.* 2012). In fish, three Ig isotypes were identified: IgM, IgD and IgT (also called IgZ in zebrafish). IgM and IgT isotypes are compartmentalized, a systemic distribution for IgM and in mucosa for IgT. IgD has an unclear function and only was found as a serum Ig in catfish (Edholm *et al.* 2011; Zhang *et al.* 2011; Ramirez-Gomez *et al.* 2012).

The MHC molecules are responsible for antigen presentation, which in turn initiate the adaptive immunity response to pathogens. MHC is divided into two groups: MHC class I and MHC class II. MHC class I is present in all host cells and consists of a heterodimer of α and the β-2 microglobulin subunits. The MHC class II contains two subunits α and β (Wilson 2017), is only expressed by APC and activates the Th CD4+ cells

Cytokines also play an important role in adaptive immunity, such as the γ-chain (γc) cytokines family members, the transforming growth factor-β (TGF-β) and other ILs, all of them described in fish (Wang & Secombes 2013; Zhu *et al.* 2013). Some of the γc cytokines family members include the IL-2, IL-4, IL-7, IL-15, and IL-21, all the members found in mammals except IL-9. The γc cytokines have a wide range of activities in adaptive immunity, such as the activation and regulation of Th cells, NK cells and B cells, among others. Although the function of these cytokines is based on mammals, it is believed that similar roles are played in fish (Wang & Secombes 2013).

1.6 Strategies for disease control in aquaculture

The evolution of aquaculture production toward sustainable models needs to be accompanied by advances in disease control and prevention measures to reduce the risks of disease outbreak and minimize the use of chemicals. To control viral outbreaks in the hatcheries and particularly LCDV, and due to absence of efficient commercial vaccines, three main strategies are highlighted: (a) monitoring and removal of asymptomatic carriers; (b) enhancement of immune system by the use immunostimulants supplied through the diet; and (c) genetic selective breeding for resistance lineages. These three points will be developed below.

1.6.1 Monitoring and removal of asymptomatic carriers

Monitoring of asymptomatic carriers is considered the first control step in a biosecurity program to prevent the introduction of any pathogen in the aquaculture facilities. Hence, broodstocks are routinely monitored for targeted pathogens, mainly those with a high impact on fish mortality (Smith 1998). Athough this strategy does not prevent horizontal transmission, it still remains useful to prevent vertical transmission in spite of requiring a continuous monitoring of broodstocks.

In the case of LCDV, the asymptomatic carriers are considered one of the

main causes for the persistent infections in the aquaculture facilities (Wolf 1988). To control LCDV asymptomatic carriers, several sensitive diagnostic methods were developed in the last years including a PCR-hybridization assay (Cano *et al.* 2007), a loop-mediated isothermal amplification technique (Valverde *et al.* 2017b) and a real-time quantitative PCR (qPCR) assay (Valverde *et al.* 2016b). Although the PCR-hybridization is highly sensitive (Cano *et al.* 2007), it requires several days to deliver the results. On the other hand, the loop-mediated isothermal amplification is a rapid method although the sensitivity (ten copies of viral DNA per reaction) is a bit lower than qPCR assay (Valverde *et al.* 2017b). Finally, the qPCR assay detects up to two copies of viral DNA genome per reaction, becoming suitable for detection of LCDV carriers. Using this protocol, the LCD prevalence in asymptomatic gilthead sea breams was estimated between 30 and 100% in aquaculture farms (Valverde *et al.* 2016b; 2017a). Moreover, although target tissue for viral detection was the caudal fin, LCDV could be detected in several internal organs, such as intestine, liver, spleen, kidney and brain in diseased and asymptomaic gilthead sea breams, indicating that this virus can establish a systemic infection in subclinical fish (Valverde *et al.* 2017a).

1.6.2 Enhancement of immune system by immunostimulant feed supplements

Another strategy for a sustainable disease control includes the oral supply of immunostimulants, such as the use of plant, fungi and algae extracts with prebiotic actions and probiotics. Both of them are the frequently used as feed supplements in aquaculture due to their ability to enhance health and prevent disease outbreaks with a great potential benefit for animal health (Douxfils *et al.* 2017). However, the restrictions and difficulties associated with the use of living microorganisms in the feeds have extended the use of prebiotics and particularly functional saccharides, also called immunosaccharides, such as the β-glucans that directly stimulate the innate immune system instead of byproducts of probiotics (Song *et al.* 2014; Akhter

et al. 2015).

Prebiotics are normally non-digestible molecules that selectively modulate the intestinal microbiome by promoting indigenous microbial populations and preventing pathogen proliferation (Dimitroglou *et al.* 2011; Akhter *et al.* 2015). The enhancement of immune system by the use of probiotics or prebiotics have been reported as suitable to increase disease resistance to LCDV in *P. olivaceus* (Harikrishnan *et al.* 2010a; 2010b). However, no information exists in Senegalese sole or gilthead sea bream. Carbohydrates (poly- and oligosaccharides) such as mannan-, fructo- and galacto-oligosaccharides, inulin or β-glucans are widely recognized for their prebiotic activity. In this PhD thesis, the β-glucans will be used to modulate the immune system in sole and the protective actions of new microalgal immunostimulant extracts on the defence response to LCDV invasion will be studied.

1.6.3 β-glucans characteristics

The β-glucans are prebiotics that modulate microbiomes and act as immunosaccharides binding to PRRs to trigger an innate immune response (Meena *et al.* 2013; Song *et al.* 2014). β-glucans are structurally an heterogeneous group of polysaccharides, that are part of the cell wall or used as energy storage in bacteria, fungi, algae, and plants. The basic repetitive structure consists of D-glucose monomers linked by a β-glycosidic (1,3)-β, (1,4)-β, or (1,6)-β bonds, with branching linked by β -(1,4) or β -(1,6). β-glucans have different solubility, molecular mass, tertiary structure, degree of branching, polymer charge and solution conformation (triple or single helix or random coil) depending on the source and preparation (Brown & Gordon 2005). The binding of β-glucans to their receptors induces a cascade of innate and adaptive immune response such as phagocytosis, oxidative burst, and the production of cytokines and chemokines in DC and macrophages (Brown *et al.* 2003).

β-glucans are considered of high biotechnological and biomedical interest, due to their antitumoral, anti-inflammatory, anti-obesity, anti-allergic, anti-osteoporotic, and immunomodulating activities (Bashir & Choi 2017). These have been proposed as a supplement in feed pellets, to enrich live food for fish (artemia and rotifers) (Ringø *et al.* 2012) and, can also act as adjuvant of vaccines (Jin *et al.* 2018). In aquaculture, β-glucans are mainly used as immunostimulants and prebiotics to enhance fish growth, survival and the immune response and also improve resistance to several different pathogens (Ringø *et al.* 2012; Meena *et al.* 2013). In teleost, the immune-modulating effects of these polysaccharides, such as anti-inflammatory or antimicrobial abilities, have been widely studied (Stier *et al.* 2014). Moreover, recent reports demonstrate the role of β-glucans on trained immunity by epigenetic reprogramming of myeloid cells in fish (Saeed *et al.* 2014; Netea *et al.* 2016; Petit & Wiegertjes 2016; Petit *et al.* 2019b).

In aquaculture, the most common source of β-glucans is spent brewers' yeast (*Saccharomyces cerevisiae*) and to a lesser extent β-glucans from seaweeds (laminarin) or from cereal grains (Ringø *et al.* 2012; Meena *et al.* 2013). The commercial MacroGard® is an insoluble preparation of β-1,3/1,6-glucans that contains a minimum of 60% β-glucans plus lipids, protein, ash and moisture and no nucleotides (Miest *et al.* 2016). The production Yestimun® is also insoluble but highly purified glucan (Stier *et al.* 2014). In recent years there has been an increased interest in the production of microalgae biomass due to its biosynthetic capacity and high growth rates and it is regarded as a valuable resource for source diversification (Bozarth *et al.* 2009; Daboussi *et al.* 2014). β-glucans from microalgae, also called chrysolaminarin, is a short (20-30 linear residues with low degree of branching), soluble polysaccharide synthetized for energy storage by several marine microalgae including haptophyte and stramenopiles (such as diatoms and *Nannochloropsis*) (Sadovskaya *et al.* 2014; Gugi *et al.* 2015; Rojo-Cebreros *et al.* 2017)

and, although several species of microalgae are used as a feed source in fish hatcheries (Hemaiswarya *et al.* 2011), no information about the bioactivity of chrysolaminarin exists in fish.

The diatom *Phaeodactylum tricornutum* has become a target for biorefinery feedstock and for high value-added bioactive compounds mainly fucoxanthin, chrysolaminarin and eicosapentaenoic acid (Zhang *et al.* 2018b). This microalga has between 4.9-17.1% of β-glucans of total dry mass and its isolation can be coupled with the purification of other bioproducts such as pigments and lipids (Gugi *et al.* 2015; Caballero *et al.* 2016; Gao *et al.* 2017; Zhang *et al.* 2018b). The biosynthesis of chrisolaminarin is highly dynamic relying on light and nutrient levels and also shows growth-phase dependency (Myklestad & Granum 2009; Xia *et al.* 2014; Caballero *et al.* 2016; Gao *et al.* 2017). Previous studies indicated that this microalga, administrated as a dietary supplement, enhanced immune parameters in gilthead sea bream (Cerezuela *et al.* 2012). The microalgae, as microorganism rich in valuable chemical compounds, could have bioactive compounds in these complex extracts that potentially have immunomodulatory effects in fish in order to be used in aquaculture industry. In the present PhD thesis, the effect of microalgae extracts as immunomodulator was evaluated in Senegalese sole.

1.6.4 Genetic evaluation of the resistance against LCDV

Selecting breeding programs are generally focused in evaluating growth, morphology, feed conversion efficiency traits and selection for resistance to bacterial and viral infections, being this way the most sustainable strategy to reduce and minimize the impact of viral infection in aquaculture although it requires evaluation of genetic variation in species-specific populations (EATiP 2014).

In gilthead sea bream, most of genetic programs that are now ongoing in Europe are mostly focused on the improvement of growth, morphology and carcass

quality (Garcia-Celdran *et al.* 2015b; Lee-Montero *et al.* 2015; Navarro *et al.* 2016), and genetic estimates for disease resistance were only reported for the bacterial pathogen Phdp (Antonello *et al.* 2009; Palaiokostas *et al.* 2016).

If we focus on the breeding genetic programs for viral infection resistance, genetic estimates for VNNV in Asian seabass (Liu *et al.* 2016a), IPNV in Atlantic salmon (Houston *et al.* 2008; 2010; Moen *et al.* 2015) Infectious Hematopoietic Necrosis Virus (IHNV) in rainbow trout and steelhead (*Oncorhynchus mykiss*), were reported. Moreover, a major locus associated with resistance against LCDV genotype II was identified in *Paralichthys olivaceus* (Fuji *et al.* 2006) and used for the design of marker-assisted breeding programs and the building of LCDV-resistant broodstocks (Fuji *et al.* 2007). As indicated above, the gilthead sea bream is recurrently infected and LCDV outbreaks are observed every year, occasionally, associated with high mortalities (Kvitt *et al.* 2008; Haddad-Boubaker *et al.* 2013). However, the genetic variation controlling susceptibility to LCDV in gilthead sea bream remains still unexplored.

OBJECTIVES

The general objective of this PhD Thesis is the study of new strategies to control and mitigate the impact of LCD in the Mediterranean hatcheries cultivating Senegalese sole and gilthead sea bream, two fish species with different susceptibility to LCDV. To achieve this objective, the defensive responses triggered in Senegalese sole postlarvae and juveniles after a LCDV challenge and the dissemination routes in the host were studied. Moreover, the use of polysaccharides and microalgal extracts as inmunomodulators and reprogramming effectors as optimal approaches to control the LCDV infections in Senegalese sole were evaluated. In these studies, new microalgal extracts were obtained and tested by means of a wide approach using biochemical assays, microbiome and genomics analysis using post-larvae and juvenile soles. Finally, the genetic estimates to LCDV susceptiblity was investigated in gilthead sea bream, a species with high susceptiblity and evident clinical signs for phenotype quantification.

The specific objectives of this PhD thesis are:

1. Study of LCDV infection course in Senegalese sole post-larvae. Determination of target organs for dissemination and persistence of LCDV in sole post-larvae and identification of expression patterns associated with LCDV infection. This objective is developed in chapter entitled "Feed and immersion challenges with Lymphocystis Disease Virus (LCDV) reveals specific mechanisms for horizontal transmission and immune response in Senegalese sole post-larvae"

2. Study of LCDV infection course in Senegalese juvenile soles. Determination of target organs for dissemination and persistence of LCDV in juvenile soles and identification of expression patterns associated with LCDV infection. This objective is developed in chapter "Gene expression profiles associated with Lymphocystis Disease Virus (LCDV) in experimentally infected Senegalese sole (*Solea senegalensis*)"

3. Evaluation of the effects of bioactive compounds to modulate the defensive response against LCDV in Senegalese sole: Characterization of *in vivo* responses induced by bioactive compounds in sole post-larvae and juveniles. The study in postlarvae is described in the chapter entitled "Microalgal extracts induce a trained immune that modifies the responses to bioactive compounds and after a challenge with LCDV". The study in juveniles is described in chapters entitled "Antioxidant capacity and immunomodulatory effects of a chrysolaminarin-enriched extract in Senegalese sole"and "Yeast β-glucans and microalgal extracts modulate the immune response and gut microbiome in Senegalese sole (*Solea senegalensis*)"

4. Genetic evaluation of the resistance against LCDV infection in gilthead sea bream. This objective is developed in chapter entitled "Heritability estimates and genetic correlation for growth traits and LCDV susceptibility in the gilthead sea bream (*Sparus aurata*)".

Feed and immersion challenges with Lymphocystis Disease Virus (LCDV) reveals specific mechanisms for horizontal transmission and immune response in Senegalese sole post-larvae

The results of this chapter were published in: Carballo C., Ortiz-Delgado J.B, Berbel C., Castro D., Borrego J.J., Sarasquete C., Manchado M. Feed and immersion challenges with lymphocystis disease virus (LCDV) reveals specific mechanisms for horizontal transmission and immune response in senegalese sole post-larvae. 2019. Fish Shellfish Immunol. 89:710-718. doi: 10.1016/j.fsi.2019.04.049.

3.1 Introduction

LCD is a viral pathology that affects more than one hundred fish species worldwide both in freshwater and marine environments [reviewed in (Borrego *et al.* 2017b)]. The causative agent is the LCDV that belongs to the genus *Lymphocystivirus*, family *Iridoviridae*, and exhibits a marked tropism towards dermal fibroblasts. The typical lesions, known as lymphocysts, have a nodular aspect that in massive infections can spread and cover most of the skin body surface including fins (Smail & Munro 2001). In the Mediterranean basin and European South Atlantic coasts, LCDV infections are mainly identified in hatcheries producing gilthead sea bream (*Sparus aurata*) appearing as self-limiting episodes with a high morbidity and low mortality, unless secondary infections or exacerbated cannibalism occur (Colorni & Padrós 2011). The integumentary lesions fully disappear in a few weeks, depending on the environmental temperature, and the recovered animals remain as asymptomatic carriers that convert the LCD in a chronic and recurrent problem in aquaculture hatcheries. Although LCDV has been detected in a wide range of fish species including the Senegalese sole (*Solea senegalensis*), the reported outbreaks of LCD in this species are still scarce (Alonso *et al.* 2005; Cano *et al.* 2010).

The high rates of LCDV prevalence have been associated with both vertical and horizontal viral transmission (Cano *et al.* 2013). Embryos from infected brooders were demonstrated to carry the LCDV on the egg surface (Cano *et al.* 2013). However, the horizontal transmission by direct contact with infected animals or through contaminated water after breaking lymphocysts and the subsequent releasing of viral content has been hypothesized as the main mechanism that explains the high morbidity in highly susceptible species such as sea bream, although no experimental evidences of waterborne viral transmission were still provided. Only the horizontal transmission through the supply of LCDV-infected live preys to the larvae during early developmental stages was demonstrated,

representing an efficient way to deliver LCDV particles and to establish a systemic infection (Cano *et al.* 2009b; 2013). In Senegalese sole, there is no information about LCDV transmission routes. In the chapter 4 of the present PhD thesis, we demonstrated that after intraperitoneal (i.p.) injection LCDV spreads rapidly through the bloodstream to invade several internal organs. The intense defensive response triggered in the host reduced progressively the number of viral particles but the LCDV could be detected 15 days after the experimental infection (Carballo *et al.* 2017). Although i.p. injection represents an adequate experimental approach to investigate the defensive mechanisms of fish against LCDV, further studies are necessary to establish the viral pathogenesis, the subsequent pathological alterations, and the defensive responses in the host.

Sole has been proposed as a model to study larval ontogeny, hormone regulation, epigenetic mechanisms or nutritional requirements in marine fish larvae due to its robustness to handling and the short larval rearing period (Benzekri *et al.* 2014). Sole post-larvae (~20-30 days post-hatch) have a well-developed immune system highly responsive to environmental stimuli and pathogens (Ponce *et al.* 2011; Salas-Leiton *et al.* 2012; Ferraresso *et al.* 2016; De Swaef *et al.* 2017; 2018). This chapter of the present PhD thesis aimed to determine the LCDV pathogenesis and defensive responses triggered in Senegalese sole post-larvae challenged using two transmission routes, by immersion in contaminated water or through feeding with LCDV-positive live artemia. Viral loads, tissue distribution and associated histopathological changes were determined. The time-course of the host defensive response was also analyzed using a panel of 22 immune genes. The data obtained provide new evidences of horizontal transmission for LCDV revealing significant differences in the histopathology, tissue distribution and host responses depending on the transmission route. The information generated is relevant to understand the mechanism of LCDV infection in marine fish and provide new clues for the control

of this disease in aquaculture.

3.2 Material and methods

3.2.1 Virus collection, culture conditions

LCDV genotype VII was isolated from lymphocystis-diseased gilthead sea bream specimens from a local farm (Southern Spain) as previously described in Carballo *et al.* (2017). The virus infectious titer was calculated using the $TCID_{50}$ assay as previously described (Alonso *et al.* 2005).

3.2.2 Experimental design

All procedures were authorized by the Bioethics and Animal Welfare Committee of IFAPA and given the registration number 10-06-2016-102 by the National authorities for regulation of animal care and experimentation.

Senegalese sole post-larvae (30 days post-hatch, dph) were supplied by Cupimar S.A. (San Fernando, Cadiz, Spain) and transported to IFAPA Centro El Toruño (El Puerto de Santa Maria, Cadiz, Spain). At arrival, the fish were distributed into 12 plastic trays (375 cm^2, 300 larvae per tray) containing 1l final volume of autoclaved seawater (salinity 35 ppt, 8 ppm oxygen). The trays were located in a temperature-controlled room and water temperature was maintained constant at 20 ºC. Daily, water was manually renewed (~90%) and larvae were fed with artemia (~3,000 metanauplii/tray). The animals were kept in these conditions for two days before starting the experiment. No mortality was registered in this period.

To carry out the immersion challenge, post-larvae from six trays were carefully transferred to 140 mm petri dishes containing 50 ml of sterile seawater. Three Petri dishes were added a LCDV suspension (10^5 $TCID_{50}$/ml final

concentration), whereas the remaining three plates received the same volume of phosphate buffer saline (PBS) and they were considered as the negative control group. After two hours, post-larvae were collected using a 150 μm mesh, washed with sterile seawater and transferred back to the plastic trays. Thereafter, the animals were fed and handled as described above and disease signs monitored for 1 week. Post-larvae (n=100) were sampled at 1, 2, and 7 days post-infection (dpi). They were euthanized using overdose of tricaine methane sulfonate (MS-222), fixed in RNA-later (Invitrogen) and stored at -80°C until use for viral detection and gene expression analysis. For histological analyses, larvae were fixed in paraformaldehyde (PFA) 4% as previously described (Roman-Padilla *et al.* 2016a; 2016b) and stored at -20ºC until use.

For the feed challenge, artemia metanauplii were enriched for 1 h using a LCDV suspension at 10^5 $TCID_{50}$/ml. Then, artemia were filtered, washed and resuspended in sterile seawater before supplying to the sole post-larvae. As indicated above, three plastic trays (n=300) were used as negative controls and they were fed 3,000 non-infected artemia (10 metanauplii/post-larva). The other three plastic trays were provided with the same quantity of LCDV-enriched live preys. After 1 h, no artemia was observed and the water was fully renewed using sterile seawater. The fish were maintained for 1 week and they were fed, sampled and monitored as indicated above for the immersion challenge.

3.2.3 Histological and *in situ* hybridization analyses

Fixed samples were washed in PTW (1% PBS, 0.1% Tween 20) three times for 30 min each and then they were transferred to 10% EDTA/2% formaldehyde solution at 4ºC for 7 days. After fixation and decalcification, samples were washed three times in PTW as described above, embedded in paraffin and serially sectioned at 5-6 μm thickness as previously described (Ortiz-Delgado *et al.* 2005). The haematoxylin-eosin technique (Ortiz-Delgado *et al.* 2014) was used for histological

studies.

In order to detect the presence of viral DNA in larvae tissues, histological sections of non-infected (control) and infected post-larvae from immersion and oral challenges at 1, 2 and 7 dpi were analyzed by *in situ* hybridization as previously described (Alonso *et al.* 2004; Cano *et al.* 2009a). A fragment of the LCDV *mcp* gene was amplified using specific primers (RT-LCDV-F and RT-LCDV-R2) (Valverde *et al.* 2016a) and the following PCR program: 95ºC for 2 min, followed by 35 cycles of 1 min at 95ºC, 1 min at 53ºC and 10 min at 72ºC. The fragment was cloned into the TOPO-TA vector (Invitrogen) and the probe synthetized using the PCR DIG Probe Synthesis Kit (Roche). Deparaffinised and rehydrated sections were permeabilised with Triton X-100, and then treated with proteinase-K (100 μg/ml in 0.1 M Tris buffer, pH 8) for 30 min at 37 °C. Target DNA in tissue sections and probe were simultaneously denatured at 95 °C for 5 min, and hybridization performed overnight at 55 °C. The slides were washed in saline sodium citrate buffer with 6 M urea and 0.2% (w/v) bovine serum albumin (BSA) for 10 min at hybridization temperature. Tissue sections were blocked with blocking reagent, and incubated with an anti-DIG monoclonal antibody (Roche Applied Science) conjugated to alkaline phosphatase for 1 h. The colorimetric detection of the hybridization signal was carried out with NBT/BCIP. Staining controls were performed in tissue sections by omitting the DNA probe.

3.2.4 Quantification of viral DNA copies

Three pools of artemia metanauplii (40 mg) were taken and analysed after LCDV enrichment. In post-larvae, a total of 8 individual randomly sampled from triplicate trays at each time point (1, 2 and 7 dpi) were processed. Total DNA of artemia and whole post-larvae was isolated using Isolate II Genomic DNA Kit (Bioline). DNA samples were treated with RNase A (Bioline) following the manufacture's protocol. DNA was quantified spectrophotometrically using the

Nanodrop ND-8000. Absolute quantification of viral DNA copies was carried out according to the protocol specified by Valverde *et al.* (2016b) using a CFX96™ Real-Time System (Bio-Rad) in a 20 µl final volume containing 200 ng of DNA, 300 nM each of specific forward and reverse primers, and 10 µl of iQ™ SYBR® Green Supermix (Bio-Rad). The amplification protocol used was as follows: initial 7 min denaturation and enzyme activation at 95 ºC, 40 cycles of 30 s at 95 ºC and 1 min at 59 ºC.

3.2.5 RNA isolation and gene expression analysis

Post-larvae were dissected, selecting the anterior portion containing the head and the abdominal cavity and discarding the caudal region. The anterior portion of larvae (n=3) were suspended in 1 ml of TRI-Reagent (Sigma-Aldrich) and homogenized in the Fast-prep FG120 instrument (Bio101) using Lysing Matrix D (Q-Bio-Gene) for 60 s at speed setting 6. The aqueous phase was transferred to a column of Isolate II RNA Mini Kit (Bioline) and total RNA was treated twice with DNase I using Isolate II RNA Mini Kit (Bioline) for 30 min following the manufacture's protocols.

To determine *mcp* gene expression, cDNA synthesis and qPCR assays were carried out as previously described in Carballo *et al.* (2017). The reference gene used was 18S rRNA (Infante *et al.* 2008).

To quantify host gene expression after LCDV challenge, the cDNA synthesis was carried out using the i*Script*™ cDNA Synthesis Kit (Bio-Rad) and the qPCR assays were carried out on a CFX96™ Real-Time System (Bio-Rad) using a 10-µl volume containing cDNA generated from 200 ng of original RNA template, 300 nM each of specific forward and reverse primers, and 5 µl of SYBR Premix Ex Taq (Takara, Clontech). Most of the primers were published elsewhere and they were sole-specific: *il1b, tnfa, clec, cxc10, ifn1, irf7, irf8, irf9* (Carballo et al. 2018a), *irf1, irf3*

(Carballo et al. 2017), *hsp90a* (Manchado *et al.* 2008), *lysg* (Ponce *et al.* 2011), *mx* (Fernandez-Trujillo *et al.* 2008) and *c3* (Benzekri *et al.* 2014). Primers for *irf2, irf4, irf5, irf10, ifna3, cox2 cd4 and cd8a* were designed in this chapter (Table 1). The amplification protocol used was as follows: initial 7 min denaturation and enzyme activation at 95 ºC, 40 cycles of 30 s at 95ºC, 15 s at 68ºC and 30 s at 72ºC. Each PCR assay was done in duplicate. The ubiquitin (*ub52*) and glyceraldehyde-3-phosphate dehydrogenase (*gadph2*) genes were used as reference genes, and the sample from control group at 1 dpi was used as calibrator (Infante *et al.* 2008; Armesto *et al.* 2014). Relative mRNA expression was determined using the comparative method $2^{-(\Delta\Delta Ct)}$. Clustering analysis was carried out by PermutMatrix (Caraux & Pinloche 2005) using log2 transformation of fold-change with parameters set as following: Dissimilarity: Euclidean distance, Hierarchical: Complete Linkage Method, Seriation: Multiple-fragment heuristic (MF).

3.2.6 Statistical analysis

The qPCR data were log-transformed in order to comply with normality and homogeneity of variance. A two-way ANOVA was used to test the changes in gene expression after the viral challenge using treatments and time as fixed factors. When a significant effect of virus was determined, single ANOVAs were carried out. Statistical analyses were performed using SPSS v21 software (IBM).

Table 1: Primers designed in this study. Target gene, amplicon size and unigene code in SoleaDB [9] are indicated.

Target	Primer	Sequence (5′→3′)	Amplicon (bp)	Code
irf2	F	GCTCCTCCCACTCGTACCCGCTCCA	120	unigene45267
	R	TGTAGTTCCGCCTCCAGCCTGCACCAAC		
irf4	F	CCATCACTTTTCCGTTCCCGTACCCCGAG	102	unigene135376
	R	CGTCCGGCATCATCCACAAACGCACCC		
irf5	F	CGACCCTGCGAAGTGGAAAGCGAACCT	96	unigene37530
	R	TGCACCGGCGTCTCTTTGGTTCCGT		

irf10	F	AAGCCATGAACTGCCTGTTGTGTCACCTCG	119	unigene282743
	R	GGCCATCGGACCGCTCCAGTACACCC		
ifna3	F	ACTTGACTCATCGCTTCCTGATCGACACCA	84	unigene48491
	R	TGTCTGCTTGCTTCTGCATCGACACACAGG		
cox2	F	GTTTATCCCGGACCCGCAGGGCACCA	112	unigene535312
	R	AGCCGCGGTGAATGCAGGTCCTTTCT		
cd4	F	ACATCTATGCCCGTCACCATCCCCTGC	119	unigene10638_
	R	ACGCCTGAAGACTGCCGAGGGAAGAATTGC		split_1
cd8a	F	CCCAGACGAAGCCCCCCACGACCAC	105	unigene59609
	R	CCGGGCCCAGAATGAGCGGAGAGCA		

3.3 Results

3.3.1 Quantification of viral DNA in LCDV-infected post-larvae

To demonstrate the horizontal transmission of LCDV in Senegalese sole post-larvae (30 dph), two different infection routes were assayed: water immersion (10^5 $TCID_{50}$/ml final concentration) and through feeding using artemia metanauplii. The viral concentration in the enrichment medium for artemia was the same used in the immersion challenge, and resulted in a viral load of (9.7±1.4) $x10^6$ viral DNA copies/metanauplius. During the trial (7 days), no mortality or signs of disease were observed.

Viral DNA was detected in 100% of LCDV-infected post-larvae at 1 dpi. The infection percentage dropped to 75.0-87.5% at 2 dpi and 62.5% at 7 dpi. Post-larvae from the negative control groups were PCR-negative at all time points analyzed.

The absolute quantification of viral DNA (Fig. 4) showed a higher viral load in immersion-infected post-larvae at 1 dpi (371±150 viral DNA copies/µg total DNA) than at 2 and 7 dpi (47±7 and 51±5 viral DNA copies/µg total DNA, respectively). In contrast, the number of DNA copies remained low and constant in feeding-infected post-larvae (66±9, 38±5 and 40±4 viral DNA copies/µg total DNA at 1, 2 and 7 dpi, respectively). No expression of *mcp* was detected through the trial.

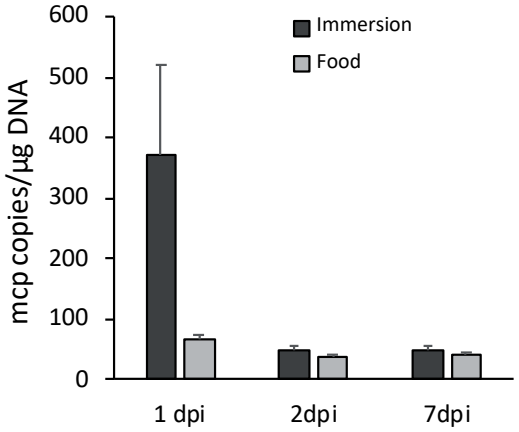

Figure 4. LCDV DNA quantification in infected Senegalese sole post-larvae at 1, 2 and 7 dpi. Dark bars, water immersion challenge; light bars, feed (artemia metanauplii) challenge. Data were expressed as mean ± SEM.

3.3.2 Histological analysis

To identify specific lesions associated with the LCDV infection route, a comparative histological analysis between negative controls and infected fish was carried out. Histological sections of Senegalese sole post-larvae challenged by immersion at 2 dpi (Fig. 5A-H) showed hypertrophied epidermal mucous cells in the skin and a moderate shrinkage of muscular fibers from myotomes and a disorganization of collagen myosepts (Fig. 5B). In the gills, a moderate hyperplasia of interlamellar epithelium conducting to a lamellar obliteration and fusion of adjacent lamellae and the disorganization of gill filaments were found (Fig. 5D). At 7 dpi, severe lamellar fusions were identified in the gills of LCDV-infected soles (Fig. 5E) not observable in the controls (Fig. 5F). No signs of histopathological disorders were detected in the gut, neither in the mucosa, the *lamina propria* or the muscle layers (Fig. 5G-H). In the post-larvae infected through feeding (Fig. 5I-L), mucous cells also appeared hypertrophied in the anterior intestine at 2 dpi (Fig. 5J). In contrast, at 7 dpi, just a moderate atrophy of the mucosa layer and an apparent

size-reduction of mucous cells were observed (Fig. 5L).

3.3.3 *In situ* hybridization of viral DNA

Tissue localization of viral DNA in infected post-larvae revealed a clear route-specific distribution pattern (Fig. 6). Viral genome was detected only at 1 dpi in both viral transmission routes. LCDV was mainly detected in epithelial cells of dorsal fin, buco-pharyngeal cavity and intestine, in Malpighi cells of the epidermic layer and around the mucous cells in the skin, surrounding vasculature in trunk muscle and in head kidney when post-larvae were infected by immersion (Fig. 6C-H). Nevertheless, post-larvae infected through feeding only showed positive hybridization signals in the hepatic parenchyma and the *lamina propria*, with no signal in the intestinal epithelium (Fig. 6I-J). All negative controls failed to show any positive signal for viral DNA hybridization.

3.3.4 Gene expression analysis

To evaluate the defensive response triggered by post-larvae in response to both types of LCDV challenge, a set of 22 transcripts were analyzed comprising antiviral defenses [antiviral Mx protein, interferon 1 (*ifn1*), *ifna3* and nine interferon-related factors (IRFs) (*irf1*, *irf2*, *irf3*, *irf4*, *irf5*, *irf7*, *irf8*, *irf9*, *irf10*)], *il1b*, chemokines *tnfa* and *cxc10*, complement factor *c3*, PAMP receptor *clec*, the antigen differentiation *cd4* and *cd8a*, g-type lysozyme (*lysg*), the cyclooxygenase *cox2* and heat shock protein *hsp90aa*.

The clustering analysis clearly separated negative controls from LCDV-infected groups (Fig. 7, blue vs red and yellow squares) although with time- and infection route-specific branches. The LCDV-feeding infected group had the most intense and well-differentiated response at 1 and 2 dpi. In contrast, post-larvae infected by immersion had a moderate up-regulation of these genes with main transcriptional response later at 2 dpi.

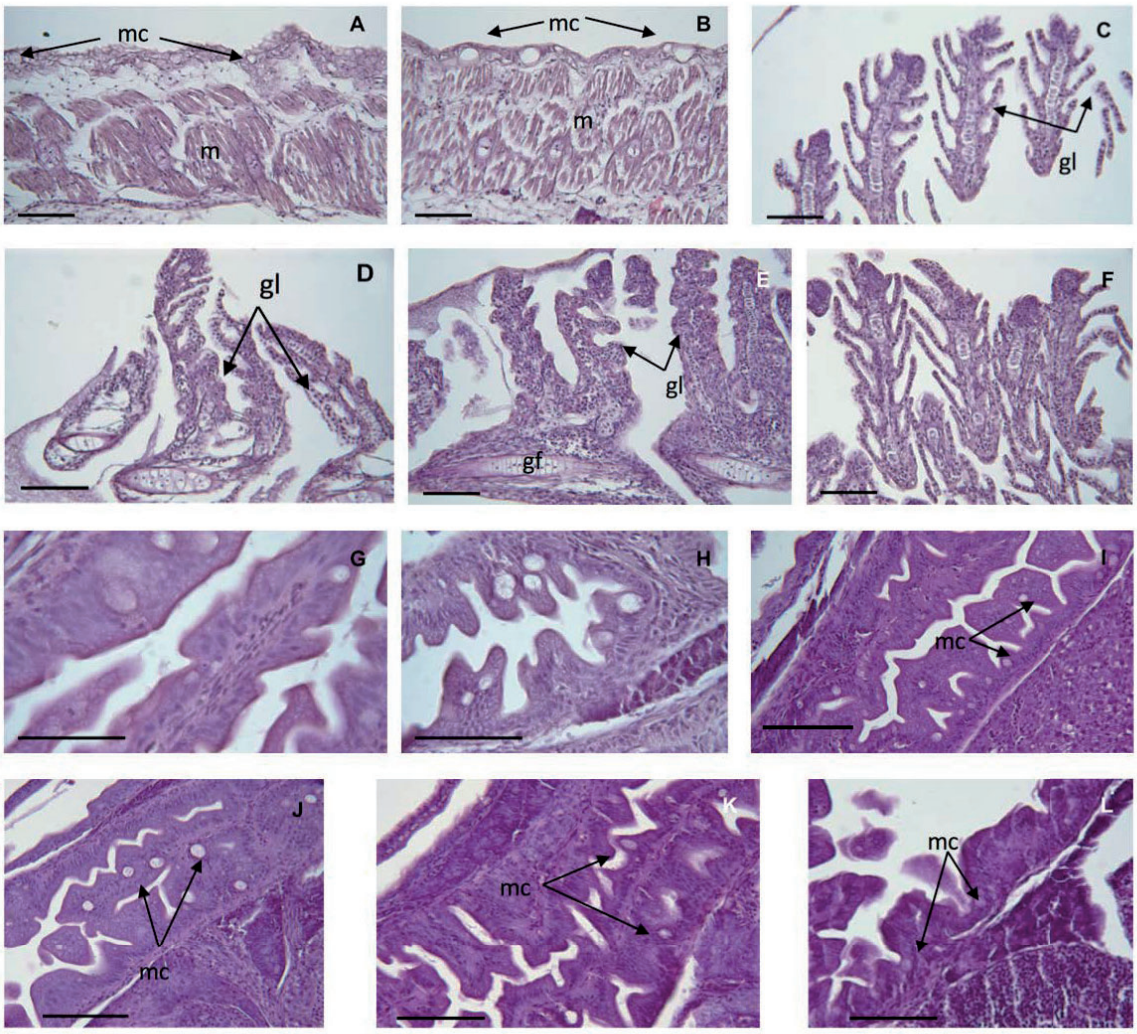

Figure 5. Histopathology of LCDV infection in sole post-larvae. Immersion challenge: **(A)** Transversal section of the skin layer and subjacent musculature in one specimen from the negative control group. Note muscle fibers packed in blocks (myotomes) between sheets of collagen (myosepts); **(B)** epidermal mucous cells hypertrophy, shrinkage of muscular fibers and myosept disorganization in LCDV-infected sole; **(C,F)** histological sections of gills in negative controls; **(D)** moderate hyperplasia of interlamellar epithelium and lamellar obliteration and fusion in LCDV-infected sole at 2 dpi; **(E)** severe lamellar fusion in gills in LCDV-infected sole at 7 dpi; longitudinal sections of intestine from LCDV-infected **(G)** and negative control **(H)** post-larvae at 7 dpi. No signs of pathological disorders were detected. Feed challenge: **(I)** transversal section of anterior intestine in negative control at 2 dpi; **(J)** mucous cell hypertrophy in LCDV-infected sole at 2 dpi; transversal section of anterior intestine in negative control **(K)** and LCDV-infected **(L)** post-larvae at 7 dpi. Note a moderate atrophy of mucosa layer and an apparent size-reduction of mucous cells in infected specimens **(l)**. Scale bars represent 50 μm. gf: gill filament; gl: gill lamellae; mc: mucous cells; m: trunk muscle.

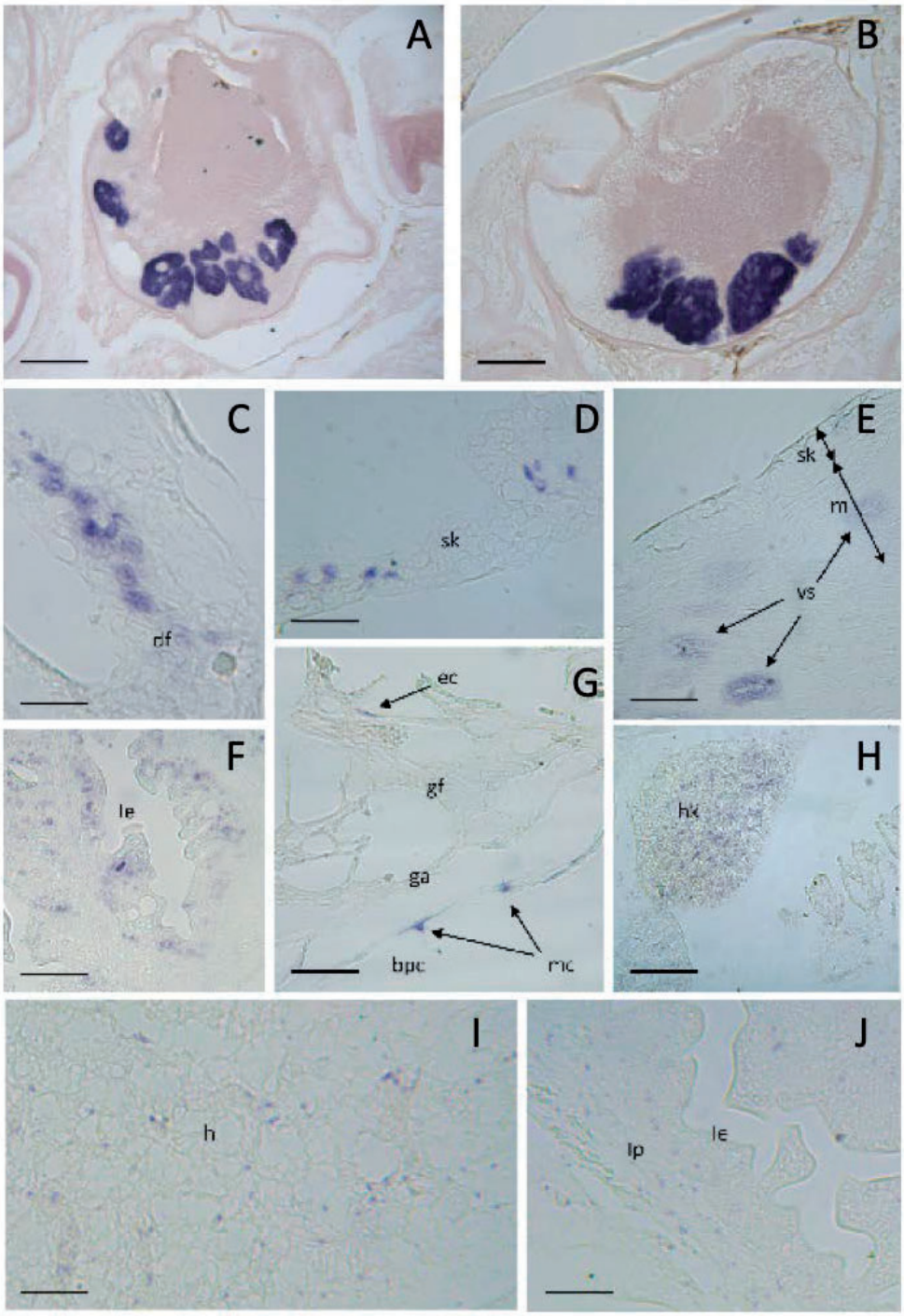

Figure 6. Detection of LCDV by *in situ* hybridization. **(A)** and **(B)** Positive control of LCDV particles within lymphocysts in a naturally infected *S. aurata* specimen. In sole post-larvae infected by immersion at 1 dpi, hybridization signals (dark blue staining) can be observed in epithelial cells from dorsal fin **(C)**, Malpighi cells in the epidermic layer of the skin **(D)**, periphery of vasculature in trunk muscle **(E)**, epithelial cells from intestine **(F)**, mucous and epithelial cells from the buco-pharyngeal cavity **(G),** and in head kidney **(H)**. Post-larvae infected by feeding: hepatic parenchyma **(I)** and the *lamina propria*/submucosa **(J)**. Note absence of viral DNA in the intestinal epithelium. Scale bars represent 50 μm. bpc: buco-pharyngeal cavity; df: dorsal fin; ec epithelial cells; gf: gill filament; ga: gill arch; h: hepatocytes; hk: head kidney; ie: intestinal epithelium; lp: *lamina propria*/submucosal layer; m: trunk muscle; mc mucous cells; sk: skin; vs: vascular system.

A detailed gene-specific analysis is depicted in Table 2. Expression profiles in post-larvae exposed to LCDV by immersion indicated a fast and statistically significant induction of proinflammatory cytokines *il1b* and *tnfa, cxc10* and *irf7* at 1 dpi. However, most antiviral defense genes (*ifn1*, *ifna3*, *mx*, *irf2*, *irf3*, *irf4*, *irf5*, *irf8*, and *irf9*), the complement factor *c3*, *cox2* and *hsp90aa* were activated later at 2 dpi. The *tnfa* and *irf 7* also remained activated at 2 dpi. When compared with post-larvae infected through feeding, most antiviral defense genes (*ifn1*, *ifna3*, *mx*, *irf4*, *irf7*, *irf9*, and *irf10*) were activated faster, including the proinflammatory cytokines *il1b* and *tnfa*, the complement *c3*, *lysg*, *cxc10* and T-cell markers *cd4* and *cd8a*. Most of them remained up-regulated at 2 dpi but also a statistically significant increase in *irf2*, *irf3*, *irf5 cox2*, *clec* and *hsp90aa* expression was observed.

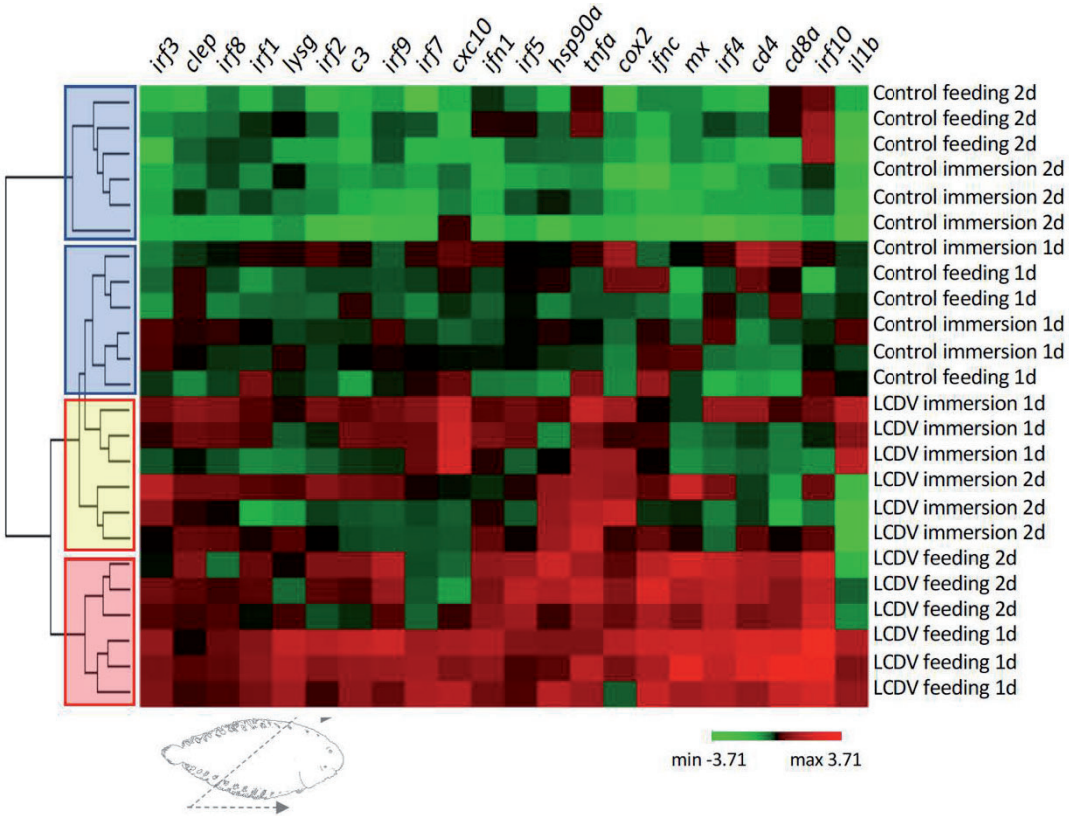

Figure 7. Hierarchical clustering analysis based on differentially transcribed genes. Data were expressed as log2 of fold change. Green and red colors indicate low and high expression values according to the scale shown. The samples are identified on the right and included control and LCDV-infected post-larvae and transmission route (immersion or feed) at 1 and 2 dpi. The main clusters grouping the samples appear on the left [control (blue), infected by immersion (yellow) and feeding-infected (red)]. The cut section of Senegalese sole post-larva used for gene expression analysis is indicated below.

Table 2: Gene expression fold changes (F-C) at 1 and 2 days after LCDV challenge by immersion or feeding. Two-way ANOVA are indicated for infection (i), time (t) and interaction (t*i) are indicated (*P<0.05; ** P<0.01). When infection was significant, one-way ANOVA was carried out for each time (F-C_1 or F-C_2). Significance at P<0.05 is indicated (*). ns, not significant

Gene name	Gene description	Feed				
		F-C1	F-C2	i	t	t*i
il1b	Interleukin 1β	2.0±0.3*	1.6±0.3	**	**	*
tnfa	Tumor necrosis factor α	2.2±0.4*	4.2±0.8*	**	ns	**
hsp90aa	Heat shock protein 90a	1.9±0.5	6.4±2.0*	**	ns	ns
clec	c-type lectin	1.1±0.1	3.1±0.4*	**	ns	ns
lysg	g-type lysozyme	2.7±0.3*	1.1±0.1	**	**	ns
cxc10	Chemokine cxc10	2.2±0.3*	1.3±0.3	**	**	ns
cox2	Cyclooxygenase 2	1.7±0.6	4.4±0.3*	**	ns	ns
c3	Complement factor 3	2.4±0.4*	4.0±0.6*	**	**	ns
ifn1	Interferon type 1	3.2±0.4*	6.5±1.3*	**	ns	*
ifna3	Interferon type a3	2.0±0.3*	2.1±0.1*	**	ns	*
mx	GTP binding protein mx	4.1±1.2*	4.4±1.2*	**	ns	*
irf1	Interferon regulatory factor 1	1.7±0.1*	2.0±0.2	*	ns	ns
irf2	Interferon regulatory factor 2	1.8±0.4	3.1±0.6*	*	*	ns
irf3	Interferon regulatory factor 3	1.7±0.1	4.1±0.5*	**	*	ns
irf4	Interferon regulatory factor 4	3.1±0.4*	6.8±0.5*	**	ns	**
irf5	Interferon regulatory factor 5	1.4±0.2	2.8±0.4*	**	ns	**
irf7	Interferon regulatory factor 7	2.2±0.1*	3.0±0.1	*	**	ns
irf8	Interferon regulatory factor 8	1.3±0.1	1.6±0.2	ns	ns	ns
irf9	Interferon regulatory factor 9	2.4±0.7*	3.4±0.7*	**	ns	*
irf10	Interferon regulatory factor 10	7.8±2.7*	3.7±0.3*	**	ns	**
cd4	cluster of differentiation 4	3.8±1.0*	8.0±1.1*	**	**	**
cd8a	cluster of differentiation 8a	4.9±1.1*	3.6±0.3	**	**	**
		Immersion				
		F-C1	F-C2	i	t	t*i
il1b	Interleukin 1β	2.5±0.4*	1.0±0.2	*	**	**
tnfa	Tumor necrosis factor α	2.3±0.5*	5.1±0.9*	**	ns	ns
hsp90aa	Heat shock protein 90a	1.0±0.2	4.5±0.2*	*	ns	ns
clec	c-type lectin	1.4±0.2	1.9±0.2	ns	ns	ns
lysg	g-type lysozyme	0.8±0.1	1.5±0.4	ns	ns	ns
cxc10	Chemokine cxc10	3.8±0.2*	0.9±0.1	**	**	**
cox2	Cyclooxygenase 2	1.7±0.3	7.3±2.9*	**	ns	ns

c3	Complement factor 3	1.2±0.2	3.0±0.7*	**	**	ns
ifn1	Interferon type 1	1.1±0.0	3.7±0.1*	**	ns	**
ifna3	Interferon type a3	1.3±0.2	2.9±0.4*	**	**	*
mx	GTP binding protein mx	0.7±0.1	5.9±3.2*	*	ns	*
irf1	Interferon regulatory factor 1	1.0±0.2	1.7±0.6	ns	ns	ns
irf2	Interferon regulatory factor 2	1.1±0.2	2.7±0.7*	*	ns	ns
irf3	Interferon regulatory factor 3	1.1±0.2	4.3±1.6*	**	ns	ns
irf4	Interferon regulatory factor 4	1.2±0.4	3.9±1.3*	*	*	*
irf5	Interferon regulatory factor 5	1.2±0.2	1.7±0.2*	*	*	ns
irf7	Interferon regulatory factor 7	1.5±0.1*	2.8±0.2*	**	**	**
irf8	Interferon regulatory factor 8	1.3±0.2	2.1±0.3*	*	ns	ns
irf9	Interferon regulatory factor 9	1.3±0.2	2.8±0.7*	**	**	*
irf10	Interferon regulatory factor 10	1.0±0.2	2.3±0.5	ns	ns	ns
cd4	cluster of differentiation 4	1.2±0.4	3.0±0.5	ns	ns	ns
cd8a	cluster of differentiation 8a	0.8±0.2	1.5±0.5	ns	*	*

Gene expression profiles associated with Lymphocystis Disease Virus (LCDV) in experimentally infected Senegalese sole (*Solea senegalensis*)

The results of this chapter were published in: Carballo C., Castro D., Borrego J.J., Manchado M. Gene expression profiles associated with Lymphocystis Disease Virus (LCDV) in experimentally infected Senegalese sole (*Solea senegalensis*). 2017. Fish Shellfish Immunol. 66:129-139. doi: 10.1016/j.fsi.2017.04.028.

4.1 Introduction

Fish farming requires adequate management and control measures to cope with disease outbreaks specially for those of viral aetiology due to the lack of effective therapies (Terlizzi *et al.* 2012). The LCD is a worldwide disease reported in several fish species both in wild and cultured populations (Borrego *et al.* 2017b). In the Mediterranean aquaculture, LCD is mainly observed in gilthead sea bream (*Sparus aurata*) and secondary in other species such as Senegalese sole (*Solea senegalensis*) (Alonso *et al.* 2005; Cano *et al.* 2010). The typical sign of LCD is the presence of small pearl-like nodules (known as lymphocysts) on the skin and fins, which may occur singly or more generally grouped in raspberry-like clusters of tumorous appearance (Smail & Munro 2001). Mortality rates are normally low and the recovered fish remain as asymptomatic hosts without clinical signs that could shed viral particles into the environment to infect new fish (Alonso *et al.* 2005; Cano *et al.* 2010). In spite of this low mortality, the LCD imposes important economic losses to the aquaculture industry since animals with the typical lesions appear unsightly and cannot be commercialized (Borrego *et al.* 2017b). Moreover, LCD outbreaks increase the susceptibility to secondary bacterial infections, cannibalism and/or parasitic infestations that negatively influence fish performance and indirectly mortality (Colorni & Padrós 2011).

LCDV belongs to genus *Lymphocystivirus*, family *Iridoviridae*. According to the polymorphisms in the gene encoding for the major capsid protein (MCP), the LCDV isolates are classified into nine different genotypes, from which the genotype VII is routinely found in gilthead sea bream and Senegalese sole (Cano *et al.* 2010; Borrego *et al.* 2017b). Previous studies have demonstrated that this virus, after contacting the host, spreads rapidly to several internal organs through the leukocytes to replicate in fibroblasts, hepatocytes and macrophages (Sheng *et al.* 2007; Cano *et al.* 2009a). This rapid viral dissemination activates a systemic

defensive response that comprises some interferon regulatory factors (IRFs) (including *irf3*, *irf5*, *irf7*, *irf8* and *irf9*) and *mx* (Hu *et al.* 2010; 2011; 2012; 2013; 2014), the signal transducer and activator of transcription (STAT) 2 and STAT3, and the hepcidin (Wang *et al.* 2011; 2013). This early response seems essential to cope with virus infection as demonstrated by *in vitro* studies with clonal populations of transfected CHSE-214 cells that stably express Mx proteins (Fernandez-Trujillo *et al.* 2013). Once the virus bypasses these defence mechanisms, the number of viral copies increases and the typical lymphocystis lesion arises (Iwakiri *et al.* 2014). In Japanese flounder, the lymphocyst formation implies changes in the expression of genes related to apoptosis inhibition, cell cycle arrest and alterations of collagen fibres with the proliferation of macrophages, granulocytes and epithelioid cells in the dermis (Sheng *et al.* 2007; Dezfuli *et al.* 2012; Iwakiri *et al.* 2014). However, further research is necessary to understand the course of LCDV infection and to characterize the defensive immune response triggered by the host to establish efficient control measures.

The Senegalese sole is a valuable species in Southern Europe aquaculture that can be infected by LCDV (Alonso *et al.* 2005; Cano *et al.* 2010). Currently, information available about the course of infection, pathogenesis and the defensive immune response triggered by LCDV in this species is limited. The aims of chapter 4 of the present PhD thesis were: a) to evaluate the time-course and tissue distribution of LCDV after experimental infection in Senegalese sole juveniles; and b) to analyse the host defensive response in kidney and intestine by quantifying the expression of 56 genes related to the innate immune system including interferon-related genes, interleukins and their receptors, chemokines, lysozymes, and antimicrobial peptides among others. The results will be useful for a better understanding of LCD pathogenesis and the identification of the defensive mechanisms activated by sole to fight against this viral infection.

4.2 Material and methods

4.2.1 Virus and culture conditions

LCDV genotype VII was recovered from diseased gilthead sea bream specimens from a local farm (South of Spain). Skin and fin lesions were scrapped and suspended (20% w/v) in Leibovitz L-15 medium (Gibco). The cell suspension was homogenized by using Ultra-Turrax® T10 basic (IKA®), centrifuged twice (7500x*g*, 15 min, 4ºC), and the supernatant collected and incubated with 10% penicillin-streptomycin overnight at 4ºC. Virus suspension was stored at -80ºC until use. Virus titre was calculated using the 50% tissue culture infectious dose ($TCID_{50}$) endpoint dilution assay as previously described (Alonso *et al.* 2005).

4.2.2 Fish trial and experimental design

A total of 72 Senegalese sole specimens (4.1±1.2 g) were transported from IFAPA centre El Toruño (El Puerto de Santa María, Spain) to the University of Malaga (Spain). Animals were distributed into 6 tanks (volume 150 l) attached to two independent recirculation systems. All specimens were tagged individually using Visible Implant Elastomer (Northwest Marine Technology) and a piece of caudal fin was taken and frozen at -80ºC to check for the presence of LCDV genome using the PCR-hybridization assay described in Cano *et al.* (2007). This procedure was carried out to discard asymptomatic carriers. All specimens used in the trial were negative for the detection of LCDV DNA.

The animals were acclimated in the tanks for a week prior to virus injection and no death or signs of disease were observed. To carry out the infection, soles were anesthetised using phenoxyethanol (100 ppm) and injected intraperitoneally (*i.p.*) with a LCDV suspension (100 µl; 10^5 $TCID_{50}$/fish). The control group was injected with Leibovitz L-15 medium and both groups were kept in separate

recirculation systems. During the experiment, the water temperature was 20.0±0.5 ºC, salinity 35-37 ppt, and oxygen 6 ppm under natural photoperiod. Animals were manually fed once a day in the morning (1% total weight) with commercial pellets (Skretting). Two animals of each tank (6 animals per condition) were sampled at 1, 2, 3, 5, 7, and 15 dpi. Soles were euthanized with an overdose of phenoxyethanol (300 ppm) and rapidly dissected to take individually samples of kidney, intestine, skin, fin, liver, brain and spleen. All samples were immediately frozen in liquid nitrogen and stored at -80ºC until use. Moreover, blood samples were taken by tail bleeding. All procedures were authorized by the Bioethics and Animal Welfare Committee of IFAPA and given the registration number 10-06-2016-102 by the National authorities for regulation of animal care and experimentation.

4.2.3 DNA isolation and quantification of viral copies

Total DNA from blood, kidney, gut, skin-fin pool, liver, brain and spleen samples (~20-50 mg) was isolated using the NucleoSpin® Tissue DNA extraction Kit (Macherey-Nagel). DNA samples were treated with RNaseA (Macherey-Nagel) following the manufacturer's protocols. DNA was quantified spectrophotometrically using the Nanodrop ND-8000.

Absolute quantification of viral DNA copies was carried out according to the protocol described by Valverde *et al.* (2016b). Three specimens were analysed for each time and tissue, except for blood at 1 and 2 dpi in which six individuals were processed. Real-time assays were carried out on a CFX96™ Real-Time System (Bio-Rad) in a 20-µl final volume containing 200 ng of DNA, 300 nM each of specific forward and reverse primers, and 10 µl of iQ™ SYBR® Green Supermix (Bio-Rad). The amplification protocol used was as follows: initial 7 min denaturation and enzyme activation at 95ºC, 40 cycles of 30s at 95ºC and 1 min at 60 °C. Melting curve analyses were carried out in order to check amplification specificity.

4.2.4 RNA isolation and gene expression analysis

Total RNAs from kidney, gut, skin-fin, liver, brain and spleen (n = 3) were isolated using TRI-Reagent (Sigma-Aldrich). Homogenization (30-50 mg of each organ) was carried out in the Fast-prep FG120 instrument (Bio101) using Lysing Matrix D (Q-Bio-Gene) for 60 s at speed setting 6. The aqueous phases were transferred to columns of the RNeasy Mini Kit (Qiagen) and RNA isolation procedures were carried out in accordance with the manufacturer's protocol. In all cases, total RNA was treated twice with DNase I using the RNase-Free DNase kit (Qiagen) for 30 min. RNA sample quality was checked on an agarose gel, and quantification was determined spectrophotometrically using the Nanodrop ND-8000. Total RNA (2 μg) from each sample was reverse-transcribed using High Capacity cDNA Reverse Transcription kit (Applied Biosystems) according to the manufacturer's protocol.

To quantify *mcp* gene expression, qPCR assays were carried out on a CFX96™ Real-Time System (Bio-Rad) using specific primers (Valverde *et al.* 2016b). Real-time reactions were carried out in a 10-μl volume containing cDNA generated from 200 ng of original RNA template, 300 nM each of specific forward and reverse primers, and 5 μl of SYBR Premix Ex Taq (Takara, Clontech). The amplification protocol used was as follows: initial 7 min denaturation and enzyme activation at 95ºC, 40 cycles of 30s at 95ºC, 15 s at 60°C and 30 s at 72°C. Each PCR assay was performed in duplicate. The reference gene used was 18S rDNA (Infante *et al.* 2008).

To evaluate gene expression patterns associated with LCDV infection, intestine and kidney samples were processed as described above. Single qPCR assays were carried out on a CFX96™ Real-Time System (Bio-Rad) using Senegalese sole specific primers for *irf1* (F: 5'-CCAACTTCCGCTGTGCCCTGAACTCG-3' and R: 5'-GCCTGGTGGCCTTTGTTGACGCTCT-3') and *irf3* (F: 5'-TTTCCGACTGG-

TCTACAGCCCTGGTGTCA-3' and R:5'-CCATCGCCCAGCTTGTCCAGGATG-TGT-3') transcripts. Real-time reactions were done in a 10-µl volume containing cDNA generated from 10 ng of original RNA template, 300 nM each of specific forward and reverse primers, and 5 µl of SYBR Premix Ex Taq (Takara, Clontech). The amplification protocol used was as follows: initial 7 min denaturation and enzyme activation at 95ºC, 40 cycles of 30 s at 95ºC, 15 s at 68 °C and 30 s at 72 °C. Each PCR assay was performed in duplicate. To estimate efficiency, a standard curve was generated for each primer pair based on 10-fold serial dilutions corresponding to cDNA transcribed from 100 to 0.01 ng of total RNA. Calibration curves exhibited a correlation coefficient higher than 0.99, and the corresponding real-time PCR efficiencies (E) were 1.09 and 1.10 for *irf1* and *irf3*, respectively. The ubiquitin gene (*ub52*) was used as reference gene, and the sample from control group at 1 dpi was used as calibrator. Relative mRNA expression was determined using the comparative method $2^{-(\Delta\Delta Ct)}$.

For chip-based RT-qPCR analyses, the OpenArray® Real-Time PCR platform (Life Technologies) was used. Total RNA (2 µg) from each sample was reverse-transcribed using the High Capacity cDNA Reverse Transcription Kit (Life Technologies) and qPCR reactions were performed using the TaqMan® OpenArray® Real-Time PCR Master Mix. All cDNA Taqman amplification procedures were carried out in accordance with the manufacturer's protocol. To run the Taqman assays, an OpenArray® Real-Time PCR Instrument (Life Technologies) was used. Samples were loaded into the OpenArray plates with the OpenArray® AccuFill™ System according to the manufacturer's protocols. The OpenArray chips were designed in the format 56x48, containing probes for 53 transcripts related to innate immune system and three reference genes. Full gene names, primers and probes for each gene, amplicon size and main gene function were described in Montero *et al.* (2015). Each subarray was loaded with 5 µl of master mix containing specific cDNA

and the qPCR mixture. All sequences were obtained from SoleaDB (Benzekri *et al.* 2014). For data analysis, the raw data were imported into the Datassist *v*3.01 software and Cq values exported and analysed using the $2^{-(\Delta\Delta Ct)}$ method. Those data with no consistency across biological replicates or with Cq values higher than 30 were excluded from the analyses (*clys1* and *cc25* in kidney, and *clys1, clys2, tlr5s*, *cox1a*, *il6*, *ifnc*, *cc25*, *cxc13*, *c1qlprotein4*, *c3*, *c5*, *c9* and *factor* h in intestine). The ubiquitin (*ub52*) was also used as the reference gene for normalization, and control group at 1 dpi as calibrator. PermutMatrix (Caraux & Pinloche 2005) was used to conduct a cluster analysis with the different experimental conditions analysed using log 2 of fold change with parameters set as following: Dissimilarity: Euclidean distance, Hierarchical: Complete Linkage Method, Seriation: Multiple-fragment heuristic (MF).

4.2.5 Statistical analysis

The qPCR data were log-transformed in order to comply with normality and homogeneity of variance. A two-way ANOVA was used to test the differences in viral DNA copies using the tissue and time as fixed factors and one-way ANOVA for *mcp* expression analysis in tissues. A two-way ANOVA (SYBR qPCRs) or MANOVA (chip-based qPCRs) were used to test the changes in gene expression after the viral challenge using treatments and time as fixed factors. When a significant effect of virus was determined, single ANOVAs were carried out. Statistical analyses were performed using SPSS v21 software (IBM) and Statistix 9 (Analytical Software).

4.3 Results

4.3.1 Viral DNA quantification and gene expression

No mortality or signs of disease were registered during the trial (from 1-15 dpi). In animals from the control group, no PCR products of viral copies were amplified in any of the tissues analysed. In infected fish, viral DNA was detected in blood at 1 dpi (83% of specimens) and 2 dpi (33% of specimens) and no DNA amplification (except in one specimen) was obtained from 5-15 dpi. In contrast, positive amplifications were obtained in the liver, kidney, and intestine from 1-15 dpi (average 85.7, 78.6 and 78.6% of specimens, respectively). No amplification was obtained in brain, skin and caudal fin samples at any time except for 1 specimen at 15 dpi in caudal fin. The absolute quantification of viral DNA showed the highest number of genome copies in kidney with a significantly reduction as the infection progressed from 1-2 to 5-7 dpi (Fig. 8A).

To check if the virus was able to replicate in the host cells, the relative abundance of the *mcp* mRNA was quantified. Viral mRNAs were not detected in any organ analysed (kidney, intestine, skin-fin, liver, brain, and spleen) at 1 and 2 dpi. However, at 5 and 7 dpi, *mcp* transcripts were detected in kidney, intestine, skin-fin and liver, and at 15 dpi only in skin-caudal fin pools. Quantification of transcripts in positive samples from 5 to 15 dpi (n=3-5 specimens for each tissue) showed the highest levels in kidney and the lowest in liver, although these differences were not statistically significant due to the high variation observed between individuals (Fig. 8B).

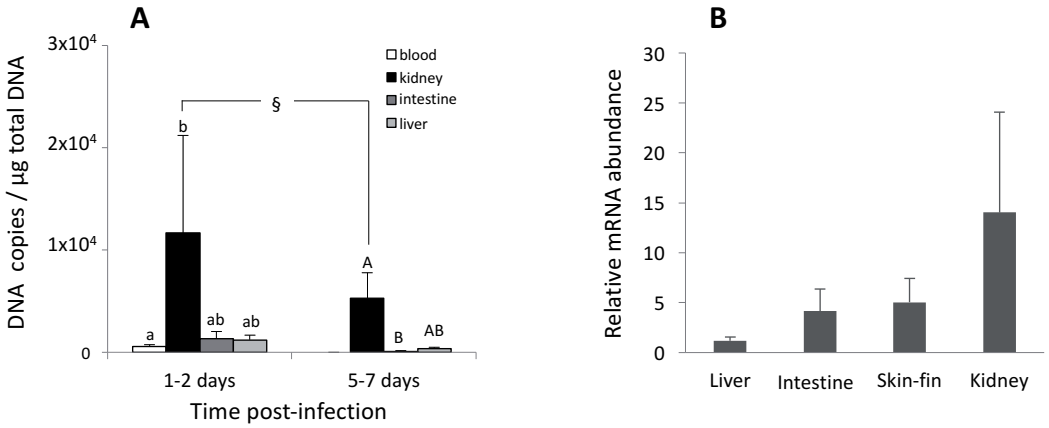

Figure 8. LCDV detection in infected soles. A: Number of DNA copies per µg of total DNA at 1-2 and 5-7 days in blood, kidney, intestine and liver. The "§" indicates significant differences between sampling points. Different letters denote significant differences between organs (in lowercase in uppercase at 1-2 and 5-7 dpi, respectively); B: Number of *mcp* mRNA transcripts in liver, intestine, skin-fin pools and kidney. Data were expressed as mean ± SEM.

4.3.2 Expression profiles in kidney after virus injection

To evaluate the immune response against LCDV, firstly the relative expression levels of *irf1* and *irf3* in control and infected soles were determined by using SYBR-based qPCR analyses. Results showed a clear transcriptional activation of both genes in kidney and intestine at 1 dpi (8.1- and 6.5-fold in kidney and 5.8 and 2.2-fold in intestine, respectively), and at 2 dpi (3.8 and 6.7-fold in kidney and 5.2- and 8.8-fold in intestine, respectively) (Fig. 9). Later, at 5 dpi, no significant differences between both experimental groups were detected indicating a fast response of IRFs to LCDV infection. Thus, samples taken at 1 and 2 dpi were selected for chip-based qPCR analysis.

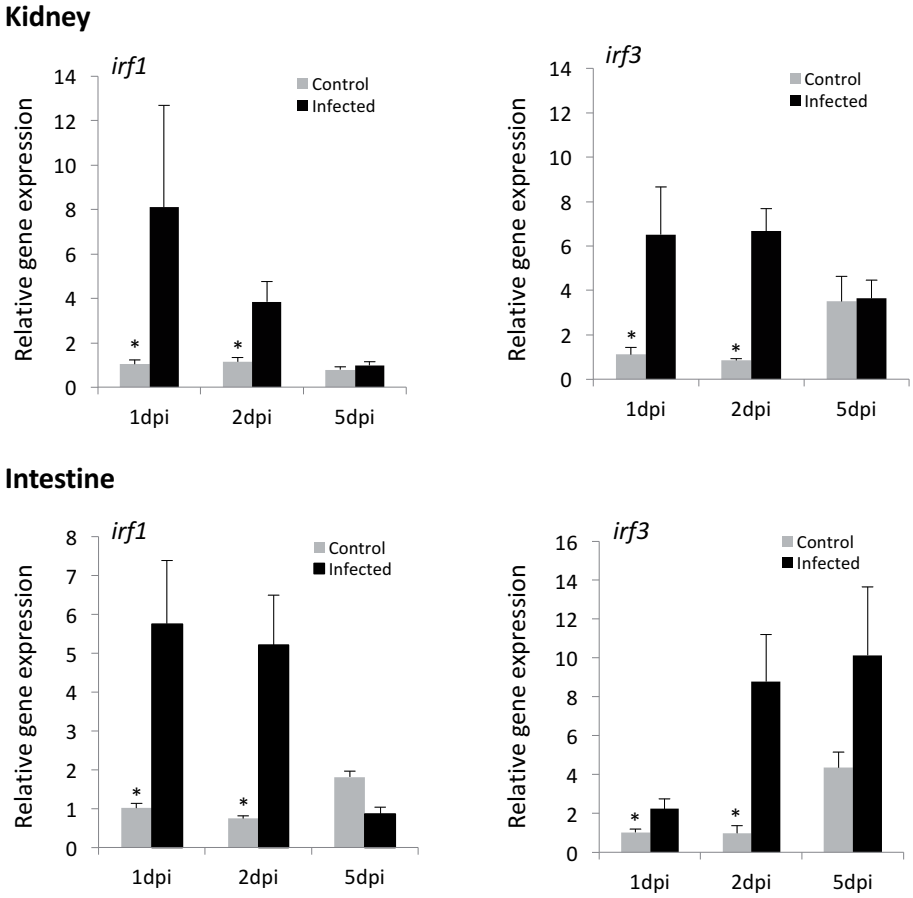

Figure 9. Relative expression levels of the *irf1* and *irf3* in kidney and intestine at 1, 2 and 5 dpi by using SYBR qPCR. Data were expressed as the mean fold change (mean + SEM, n = 3) from the calibrator (control group 1 dpi). Asterisks denote significant differences between control (grey) and infected (black) for each day ($P < 0.05$) after determining that treatment factor in two-way ANOVA was significant.

A total of 31 transcripts were differentially expressed in kidney after the viral infection (Fig. 10). This set of transcripts included the antiviral Mx protein and seven interferon-related factors (IRFs) (*irf1*, *irf2*, *irf3*, *irf7*, *irf8*, *irf9*, *irf10*). Moreover, seven ILs (*il1b*, *il6*, *il8-II*, *il8-III*, *il11a*, *il12b*, *il15*), five chemokines, (*tnfa*, *cc-ck3*, *cxc10*, *cxc13*, *cc19*), three IL receptors (*il8r*, *il10r*, *il15ra*), three paralogs of g-type lysozyme (*glys1*, *glys2* and *glys3*), the complement fractions *c4-1* and *c4-2*, the antigen differentiation *cd4*, the toll-like receptor *tlr5s*, and the metabolic gene *gapdh2* were also differentially expressed. The clustering analysis using differentially expressed transcripts clearly identified the response to virus (control vs infection), as well as a time-dependent response at 1 and 2 dpi (Fig. 10).

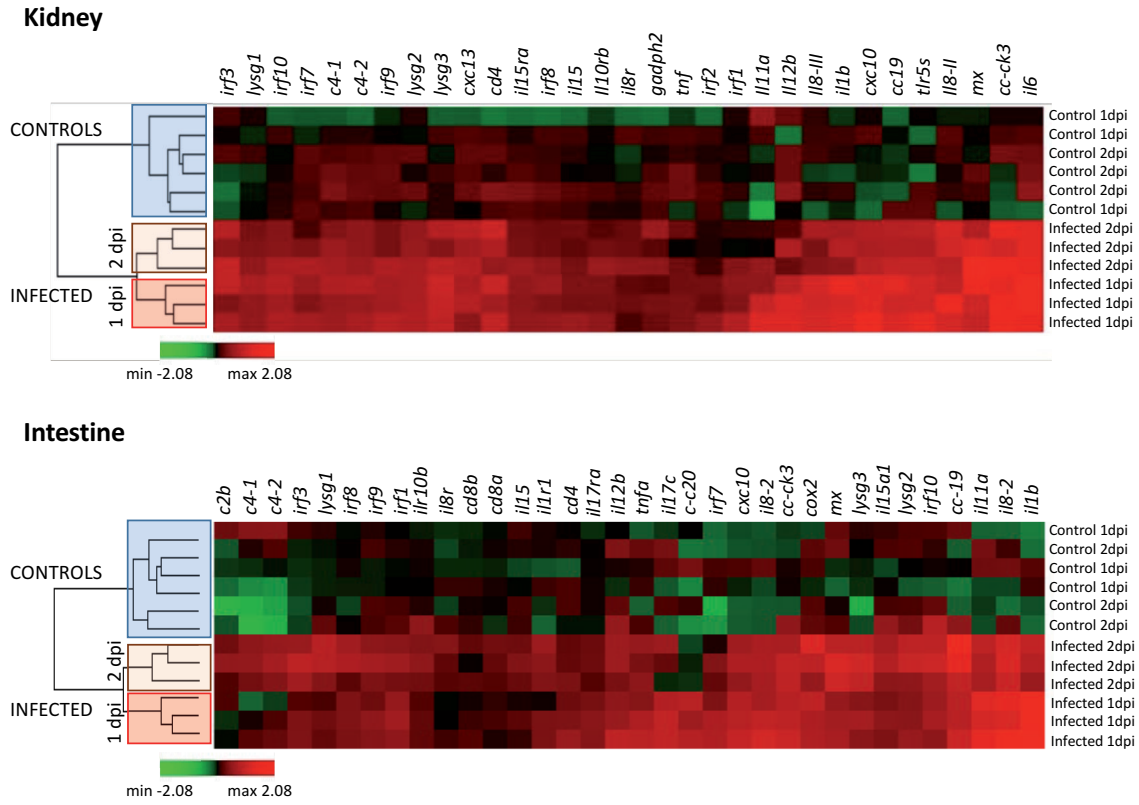

Figure 10. Hierarchical clustering analysis based on set of differentially expressed transcripts identified in kidney and intestine as determined by chip-based qPCR. Data were expressed as log 2 of fold-change. Green and red colours indicate low and high expression values according to the scale shown. The samples are identified on the right (control and infected at 1 and 2 dpi) and the main clusters grouping the samples on the left (control or infected at 1 or 2 dpi). Full-names for the transcripts indicated on the top can be found in Montero et al. 2015

The abundance of the seven IRF-encoding transcripts increased at 1 dpi (ranging from 2.5 to 5.5-fold) and reduced at 2 dpi, although transcript levels remained still higher than the control (except for *irf2*; Fig. 11). For *irf3*, transcript abundance was reduced later at 5 dpi (Fig. 9). A similar activation profile for the three *lysg*-encoding transcripts (ranging from 4.0- to 10-fold change for *lysg1* and *lysg3*, respectively, at 1 dpi; Fig. 11) and the IL-encoding mRNAs (between 2.3- and 92.7-fold for *il10* and *il6*, respectively, at 1 dpi; Fig. 12) was observed. Regarding IL receptors, *il10rb* and *il15ra* expression was activated at 1 dpi whereas *il8r*

transcription increased significantly at 2 dpi (Fig. 12). In the case of chemokines, *cc-ck3*, *cxc10* and *cc19* mRNA levels highly increased at 1 dpi (between 18.5- and 44.4-fold for *cc19* and *cc-ck3*, respectively) and dropped at 2 dpi, while a moderate *cxc13* induction was observed (only 4.9-fold at 1 dpi; Fig. 13). The *mx* mRNA levels highly increased 22.3- and 40.8-fold at 1 and 2 dpi, respectively, whereas the cytokine *tnfa* expression was only activated 2.3-fold at 1 dpi (Fig. 13). The c*4-1*, *c4-2* and *tlr5s* also showed higher mRNA levels at 1 than 2 dpi. Finally, the *cd4* mRNA levels increased significantly in a similar magnitude at both sampling times.

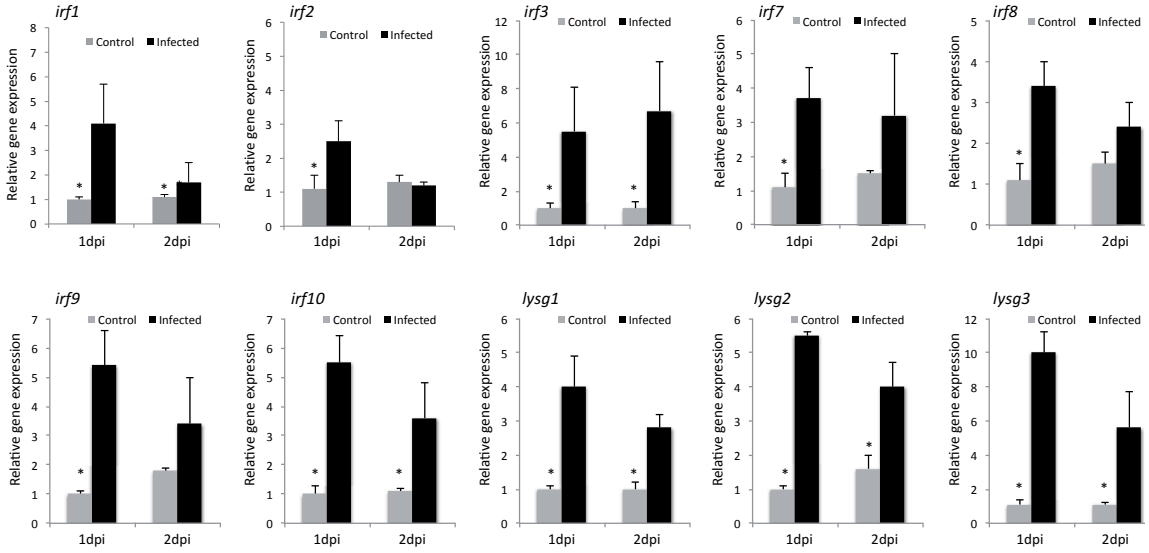

Figure 11. Relative expression levels of the IRFs (*irf1*, *irf2*, *irf3*, *irf7*, *irf8*, *irf9* and *irf10*) and three g-type lysozymes (*lysg1*, *lysg2* and *lysg3*) in kidney at 1 and 2 dpi as determined by chip-based qPCR. Data were expressed as the mean fold change (mean + SEM, n = 3) from the calibrator (control group 1 dpi). Asterisks denote significant differences between control (grey) and infected (black) for each day ($P< 0.05$) after determining that treatment factor in two-way MANOVA was significant.

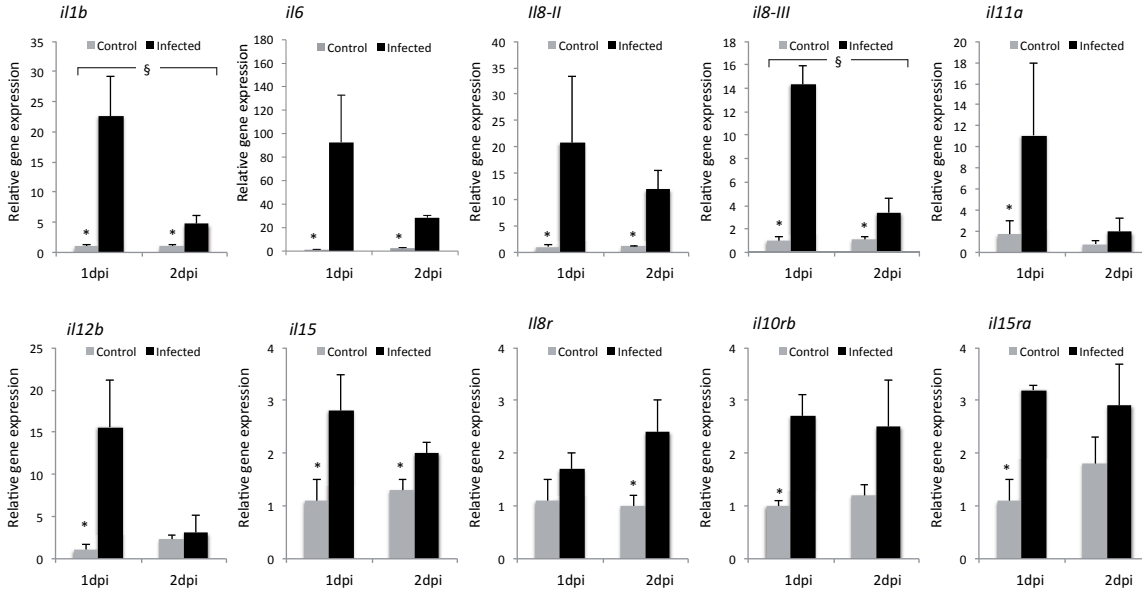

Figure 12. Relative expression levels of the ILs (*il1b, il6, il8-II, il8-III, il11a, il12b* and *il15*) and their receptors (*il8r, il10rb* and *il15ra*) in kidney at 1 and 2 dpi as determined by chip-based qPCR. Data were expressed as the mean fold change (mean + SEM, n = 3) from the calibrator (control group 1 dpi). Asterisks denote significant differences between control (grey) and infected (black) for each day ($P< 0.05$) after determining that treatment factor in two-way MANOVA was significant. § indicate significant differences between sampling points.

4.3.3 Expression profiles after virus injection in intestine

As previously observed in kidney, SYBR-based qPCR assays indicated that *irf1* and *irf3* transcripts increased significantly at 1 and 2 dpi and no significant differences were observed at 5 dpi (Fig. 9).

Differentially expressed transcripts in the intestine were quite consistent with those observed in kidney (65.8 % in common), and included the antiviral Mx protein and six IRFs (*irf1*, *irf3*, *irf7*, *irf8*, *irf9*, *irf10*), seven interleukins (*il1b*, *il8-II*, *il8-III*, *il11a*, *il12b*, *il15, il17c*), five chemokines (*tnfa*, *cc-ck3*, *cxc10*, *cc19*, *cc20*), five IL receptors (*il1r*, *il8r*, *il10r*, *il15ra*, *il17r*), three paralogs of g-type lysozyme (*lysg1*, *lysg2* and *lysg3*), the complement fractions *c2*, *c4-1* and *c4-2*, the antigen differentiation factors *cd4*, *cd8a* and *cd8b*, and the prostaglandin-related gene *cox2*. The clustering analysis also differentiated control from infected fish and identified a transient

response to LCDV at 1 and 2 dpi (Fig. 10).

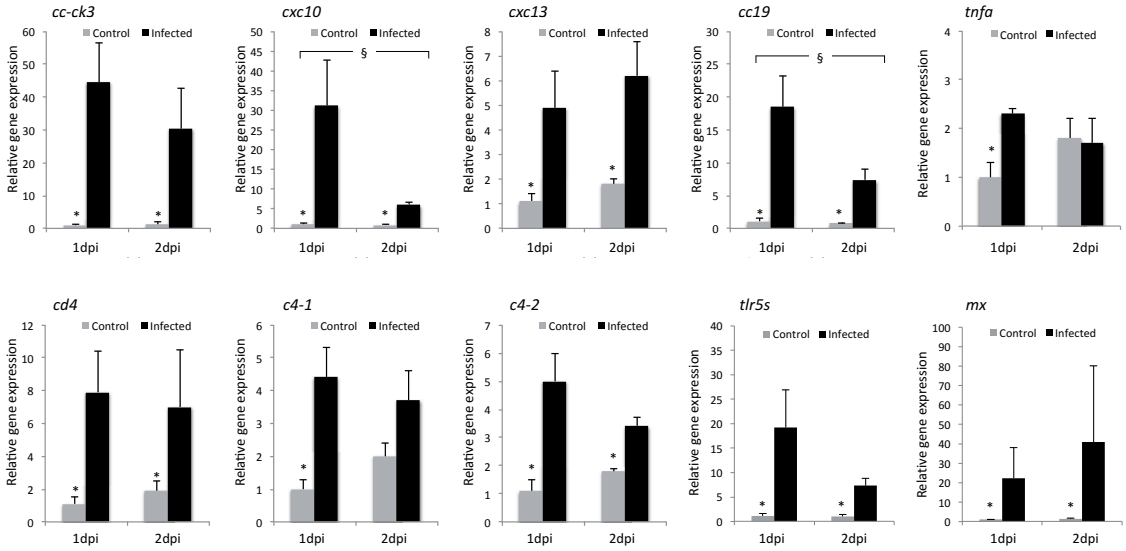

Figure 13. Relative expression levels of the chemokines (*cc-ck3*, *cxc10*, *cxc13*, *cc19*), *tnfa*, the complement factors *c4a* and *c4b* and the transcripts *cd4*, *mx* w *tlr5s* in kidney at 1 and 2 dpi as determined by chip-based qPCR. Data were expressed as the mean fold change (mean + SEM, n = 3) from the calibrator (control group 1 dpi). Asterisks denote significant differences between control (grey) and infected (black) for each day ($P< 0.05$) after determining that treatment factor in two-way MANOVA was significant. § indicate significant differences between sampling points.

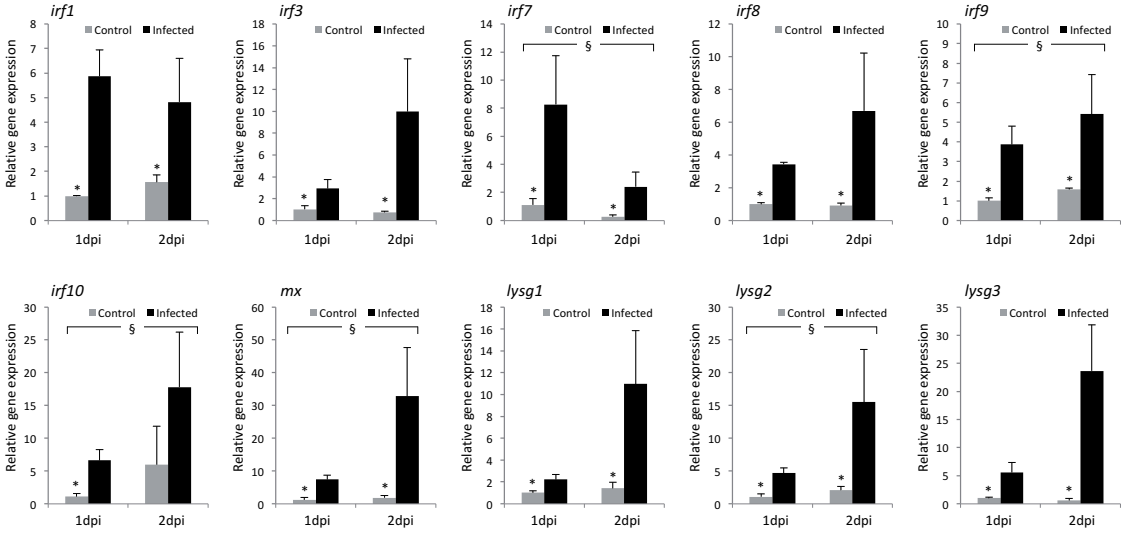

Figure 14. Relative expression levels of the IRFs (*irf1*, *irf3*, *irf7*, *irf8*, *irf9* and *irf10*), *mx*, and three g-type lysozymes (*lysg1*, *lysg2* and *lysg3*) in intestine at 1 and 2 dpi as determined by chip-based qPCR. Data were expressed as the mean fold change (mean + SEM, n = 3) from the calibrator (control group 1 dpi). Asterisks denote significant differences between control (grey) and infected (black) for each day ($P< 0.05$) after determining that treatment factor in two-way MANOVA was significant. § indicate significant differences between sampling points.

The magnitude of induction for the IRF-encoding transcripts was similar in the intestine and the kidney (ranging between 2.9 and 8.8-fold) although the induction peak was delayed in the former organ (Fig. 14). Moreover, the transcription of *mx* and the three g-type lysozyme paralogs was also highly activated at 2 dpi (between 7.4- and 38.6-fold for *lysg2* and *lysg3*, respectively).

Six out of seven differentially expressed IL-encoding transcripts (except *il15*), *tnfa*, three chemokines (*cc-ck3*, *cxc10*, *cc20*) and *cd4* exhibited a significantly higher induction at 1 than 2 dpi (Figs. 15 and 16). The magnitude of activation for most of the IL-encoding transcripts was significantly higher in this tissue than in kidney (between 9.7- and 372-fold for *i112b* and *il1b*, respectively). In contrast, the induction of IL receptors (ranging from 2.3- to 5.9-fold for *il17ra* and *il1r*, respectively), *cc19* (64.9-fold) (Fig. 16) and *cox2* (13.1-fold) was higher at 2 than 1 dpi (Fig. 17). Expression of *cd8a* and *cd8b* antigens and the complement fractions *c2*, *c4-1* and *c4-2* increased significantly only at 2 dpi (Fig. 16).

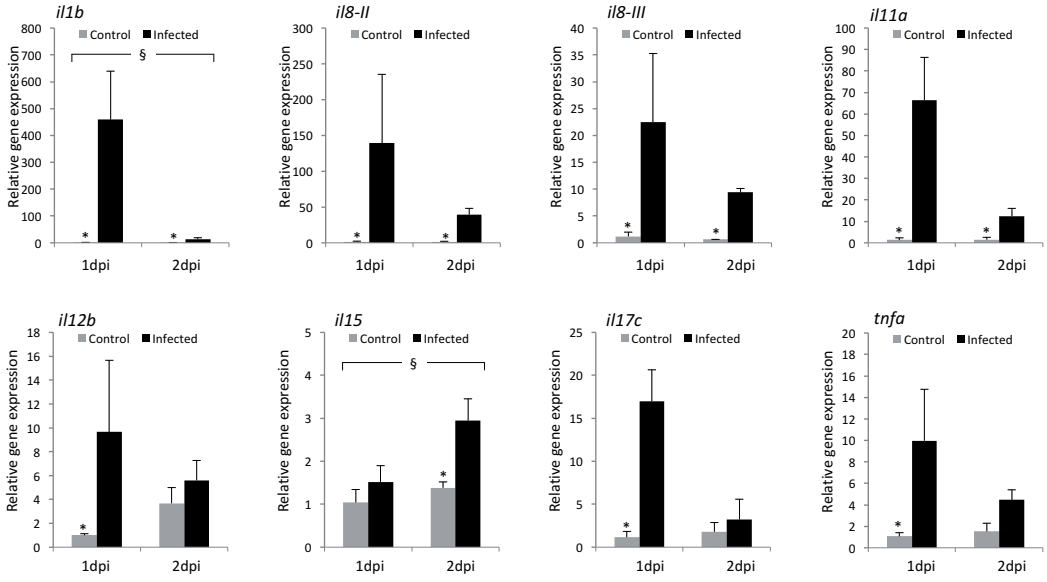

Figure 15. Relative expression levels of the ILs (*il1b, il8-II, il8-III, il11a, il12b, il15 and il17c*) and *tnfa* in intestine at 1 and 2 dpi as determined by chip-based qPCR. Data were expressed as the mean fold change (mean + SEM, n = 3) from the calibrator (control group 1 dpi). Asterisks denote significant differences between control (grey) and infected (black) for each day ($P < 0.05$) after determining that treatment factor in two-way MANOVA was significant. § indicate significant differences between sampling points.

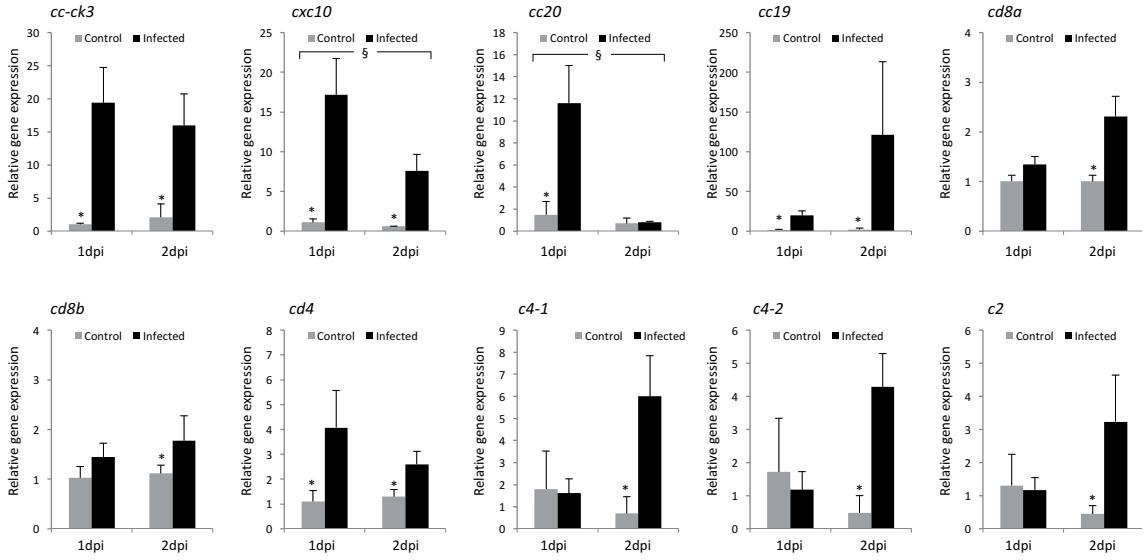

Figure 16. Relative expression levels of the chemokines (*cc-ck3*, *cxc10*, *cc19* and *cc20*), *cd8a, cd8b and cd4* and complement factors *c2, c4a* and *c4b* in intestine at 1 and 2 dpi as determined by chip-based qPCR. Data were expressed as the mean fold change (mean + SEM, n = 3) from the calibrator (control group 1 dpi). Asterisks denote significant differences between control (grey) and infected (black) for each day ($P< 0.05$) after determining that treatment factor in two-way MANOVA was significant. § indicate significant differences between sampling points.

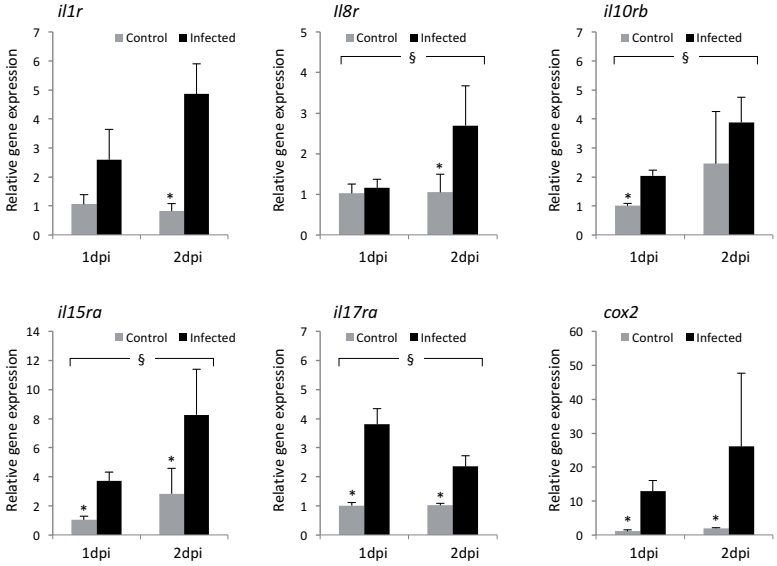

Figure 17. Relative expression levels of the IL receptors (*il1r*, *il8r*, *il10rb*, *il15ra* and *il17ra* and *cox-2* in intestine at 1 and 2 dpi as determined by chip-based qPCR. Data were expressed as the mean fold change (mean + SEM, n = 3) from the calibrator (control group 1 dpi). Asterisks denote significant differences between control (grey) and infected (black) for each day ($P < 0.05$) after determining that treatment factor in two-way MANOVA was significant. § indicate significant differences between sampling points.

Microalgal extracts induce a trained immune that modifies the responses to bioactive compounds and after a challenge with LCDV

Manuscript in preparation

5.1 Introduction

Viral infections represent one of the most important threats to intensive fish farming due to the important losses associated with mortalities, reduced productivity, restrictions to fish commercialization and extra investments in disease management and prevention (Borrego *et al.* 2017b). The most important strategies to fight against viruses in aquaculture are the development of pathogen-specific vaccines, the design of breeding genetic selection schemes and the use of feed additives that can act as immunostimulants able to enhance the adaptive and innate immune responses and the protection against viral pathogens in the host (Akhter *et al.* 2015; Charoonnart *et al.* 2018; Leiva-Rebollo 2019). Probiotics and prebiotics are the most used feed supplements in aquaculture to strength immune system. However, the restrictions and difficulties associated with the use of living microorganisms in the feeds have extended the use of prebiotics and particularly functional saccharides also referred to as immunosaccharides such as the β-glucans that directly stimulate the innate immune system instead of byproducts of probiotics (Song *et al.* 2014; Akhter *et al.* 2015).

The β-glucans are potent immunosaccharides found from bacteria to plants and with capacity to enhance immune response and prevent disease outbreaks when supplied orally or injected (Meena *et al.* 2013; Song *et al.* 2014; Akhter *et al.* 2015). The β-glucans share a basic structure of glucose residues linked with β-D-glycosidic bonds but they differ in their chemical and specific bioactive properties depending on the position and distribution of glycosidic bonds, degree of branching, molecular size and type and solubility characteristics (Barsanti *et al.* 2011; Meena *et al.* 2013; Noss *et al.* 2013). The branched 1,3/1,6 β-glucan variants from yeast and algae are the most used as a feed ingredient in aquaculture (Meena *et al.* 2013; Vetvicka *et al.* 2013). Recently, a new function of β-glucans, and particularly the soluble β-glucan laminarin, to epigenetically reprogram myeloid cells in fish has been demonstrated (Petit *et al.* 2019b). This cell priming promotes

an innate immune memory that implies metabolic reprogramming and enhanced immune response to the stimuli and can be applied in early larval stages to improve larval rearing and survival (van der Heijden *et al.* 2018; Petit *et al.* 2019b; Zhang *et al.* 2019). Recently, several studies have demonstrated that the Senegalese sole larvae at hatch could be reprogrammed by thermal treatments to modify growth performance in juveniles (Firmino *et al.* 2017; Carballo *et al.* 2018b). However, the use of epigenetic reprograming of early life stages to modulate immune system is still poorly explored.

LCDV is the causative agent of the LCD, a highly contagious process reported in more than a hundred of species and responsible for high economic losses in the aquaculture industry worldwide (Borrego *et al.* 2017b). Genetic analysis identified a major locus associated with resistance against the genotype II of this virus was identified in *Paralichthys olivaceus* (Fuji *et al.* 2006). However, in absence of resistance animal lineages, the oral supply of immunostimulants is the most important control strategy to block or reduce the viral replication. Both probiotics and herbal extracts enhanced the innate immune and disease resistance to LCDV in *P. olivaceus* (Harikrishnan *et al.* 2010a; 2010b). However, no information is available about the action of β-glucans. Previous studies demonstrated that injection of glucans activated the *mx* expression and heighten the defensive response triggered by polyI:C (Kim *et al.* 2009; Falco *et al.* 2012). Moreover, β-glucans improved the survival rates after Grass Carp Hemorrhage Virus (GCHV) infection in grass carp (*Ctenopharyngodon idella*) associated to a prolonged induction of antiviral *mx* gene (Kim *et al.* 2009). However, this effect is not fully conserved since intraperitoneal injection of β-glucans did not protect against Viral Haemorrhagic Septicemia Virus (VHSV) infection in turbot (Libran-Perez *et al.* 2018). Recently, the different immunomodulatory actions of particulate yeast β-glucans and a microalgal extract enriched in polysaccharides was established in Senegalese sole (Carballo *et al.* 2018a; 2019b). Moreover, expression profiles after

LCDV infection after immersion and by feeding were reported in Senegalese sole post-larvae (Carballo *et al.* 2019a). However, the potential use of these immunostimulants and trained immunity to modulate the responses to LCDV has not been still investigated.

The microalgae *Nannochloropsis gaditana* is routinely used aquaculture due to its nutritional value for larval rearing (Ferreira *et al.* 2018). However, this microalga is rich in valuable chemical compounds such as polyunsaturated fatty acids and carotenoids pigments and its extracts exhibit a potent antioxidant cytoprotective effects to dermal fibroblasts under oxidative stress (Mitra *et al.* 2015; Letsiou *et al.* 2017). In this study, the potential activity to reprogram larvae in early stages and priming immune system using a crude extract of *N. gaditana* was investigated. For this purpose, a two-part trial was carried out using sole post-larvae, that display complete immune responses in absence in adaptive immunity. Firstly, the response to yeast β-glucans and a microalgal extract supplied through live preys was evaluated. Secondly, the pretreated post-larvae were challenged with LCDV. The results obtained provide new evidences of trained immunity in early larvae and bring new applications of microalgae that could benefit the sole aquaculture industry.

5.2 Material and methods

5.2.1 Microalgae extract and yeast β-glucan sources

All microalgae in this study were supplied by Fitoplancton Marino S.A. For the larval reprogramming trial, *N. gaditana* (Nanno) was initially grown indoors using autoclaved seawater (salinity 33 ppt) enriched with filter-sterilized f/2 nutrients in 50 ml flasks bubbled filter-sterilized CO_2-enriched air (2%) under standard conditions indicated in Carballo *et al.* (2018a). Microalgae were inoculated in the outdoor photobioreactors (PBRs) and cultivated under seasonal

environmental conditions. After harvesting by continuous-flow centrifugation 4 h after sunrise, microalgae were frozen at -20 ºC, freeze-dried and broken by high-pressure before use. To prepare the crude extract, microalgae broken cells were suspended in sterilized seawater added dimethyl sulfoxide (0.01% final concentration) at a concentration 1:10 w/v. After thoroughly vortexing, the solution was kept at 4ºC for 24h. Before use, the crude extract was centrifuged at 10,000xg for 15 min and 4ºC and the soluble fraction collected in a clean tube and maintained at 4ºC until use.

For the feeding trial, a microalgal extract (MAe) from the microalgae *Phaeodactylum tricornutum* previously obtained by us (Carballo *et al.* 2018a; 2019b) was tested. Pure Yeast β-glucan was purchased from Quimivita (Barcelona, Spain).

5.2.2 Virus collection and culture conditions

The LCDV genotype VII was recovered from diseased animals (gilthead sea bream specimens) as previously described (Carballo *et al.* 2017; 2019a). The viral titer was calculated by the $TCID_{50}$ assay and later confirmed by qPCR as previously reported (Alonso *et al.* 2005; Valverde *et al.* 2016b).

5.2.3 Fish trials

All procedures were authorized by the Bioethics and Animal Welfare Committee of IFAPA and given the registration number 26–11–15-374 by the National authorities for regulation of animal care and experimentation.

To reprogram larvae by using microalgal extracts, eggs from two wild broodstocks belonging to IFAPA Centro El Toruño (El Puerto de Santa Maria, Cadiz, Spain) and CUPIMAR (San Fernando, Spain) were used. The eggs were mixed, viable eggs separated by buoyancy (total 120,000 eggs) and later incubated in a 500-l cylindroconical incubator at 20ºC in open circuit. After 24h, hatched larvae were collected and distributed into two buckets (40,000 larvae each one) setting a final volume of 4 l with slight aeration to facilitate larval dispersion. Temperature

water was 20ºC, oxygen 6.5 ppm and salinity 37 ppt. One bucket was added the *N. gaditana* crude extract (Nanno group) at 0.2 mg dry mass equivalent/ml final concentration. The second bucket was used as a control group that was added the same volume of sea water and handled in parallel with Nanno group. After 2h, larvae from each group was concentrated using a mesh and rinsed using clean seawater and then distributed in 400-l tanks in triplicate and cultivated following standard hatchery protocols until 32 days post-hatch (dph) as described in Fernández-Díaz *et al.* (2001). Larvae were sampled at the end of metamorphosis (21 dph) to determine dry weight and length were determined from each tank. Samples of each tank (20-25 larvae) were distributed in slides in duplicate for each tank, photographed to determine total length using ImageJ v1.47 software and oven dried (24 h, 60 °C) to estimate mean dry weight. Before the trial at 32 dph, wet weigh was also measured (n=20 specimens/treatment).

To test the biological and immunological effects of the microalgal extract (MAe) from the *P. tricornutum* and yeast β-glucan (Y) on Nanno-trained and control fish, a two-part trial was designed as depicted in Fig. 18. Firstly, the 32-dph post-larvae were orally supplied both bioactive compounds through live preys and later they were challenged by LCDV. A total 720 post-larvae (age 32 dph) of the reprogrammed and control groups (Control and Nanno) were distributed into 18 plastic trays (360 cm^2, 80 larvae per tray) containing 1l final volume of filtered-sterile seawater (salinity 35 ppt, 6 ppm oxygen). The trays were located in a temperature-controlled room to keep water temperature at 20º C. The animals were kept in these conditions one day before starting the experiment. In this period, water remained stagnant for 24h and renewed (~90%) with hyperoxygenated (300% saturation) before treatments. Larvae were fed with artemia (~1200 metanauplii/tray; 15 art/post-larvae). No mortality was registered in this period.

In the first part of the trial the MAe and Y compounds were orally administrated through the live preys. The artemia metanauplii (200 art/ml) were

enriched for 30 min using a final concentration of 2 mg/ml of both Mae and Y. A negative control for artemia enrichment (SW group) was also carried out in parallel. After 30 min, the artemia was filtered throught mesh and suspended in clean seawater and supplied to sole post-larvae (~1200 metanauplii/tray; 15 art/fish). After 1 h, no artemia was observed and a second dose was supplied 4h later using enriched artemia as indicated above. The water remained stagnant and were fully replaced by oxygenated (300% saturated) sea water at 6 h and 24h, after sampling. The animals were kept in the trays for additional 48 h and mortality was also daily recorded. In this period, post-larvae were fed artemia once a day and water manually in the morning (Fig. 18a).

Post-larvae (n=4/group) were sampled at 6 and 24 h after first supply of enriched live preys. They were euthanized using overdose of tricaine methane sulfonate (MS-222), fixed in RNA-later (Invitrogen) and stored at -80 °C until use for gene expression analysis. Also, some post-larvae (n=6/group) were also sampled for enzymatic analysis at 6, 24 and 48 h. They were euthanized as described above, immediately freezing in dry ice and stored at -20ºC until use.

After 48h of supplying the bioactive compounds, the sole post-larvae of SW and Y treatments (MAe was discarded due to the high mortality) were pooled and redistributed in 8 new plastic trays (180 cm^2, 30 fish/tray). After 24h, they were challenged with LCDV supplied through the live preys as described in Carballo *et al.* (2019a) (Fig. 18b). Briefly, artemia metanauplii were enriched for 30 min using a LCDV suspension containing $5x10^4$ $TCID_{50}$/ml final concentration. Then, artemia was filtered, washed and resuspended in clean seawater before supplying a total of 450 infected artemia (15 metanauplii/post-larvae) to each tray containing the control or Nanno-trained post-larvae. Two negative controls for each experimental group using non-infected artemia (SWC) was also carried out. All the trial was carried out in duplicate trays. After 1 h, no artemia was observed and the water fully renewed using clean sterile seawater. The animals were maintained for 24 hours. Sole post-

larvae were sampled at 3, 6 and 24 h for quantification of LCDV DNA copies and gene expression analysis. Samples (n=6) were managed and fixed as describe above and kept at -80ºC until use.

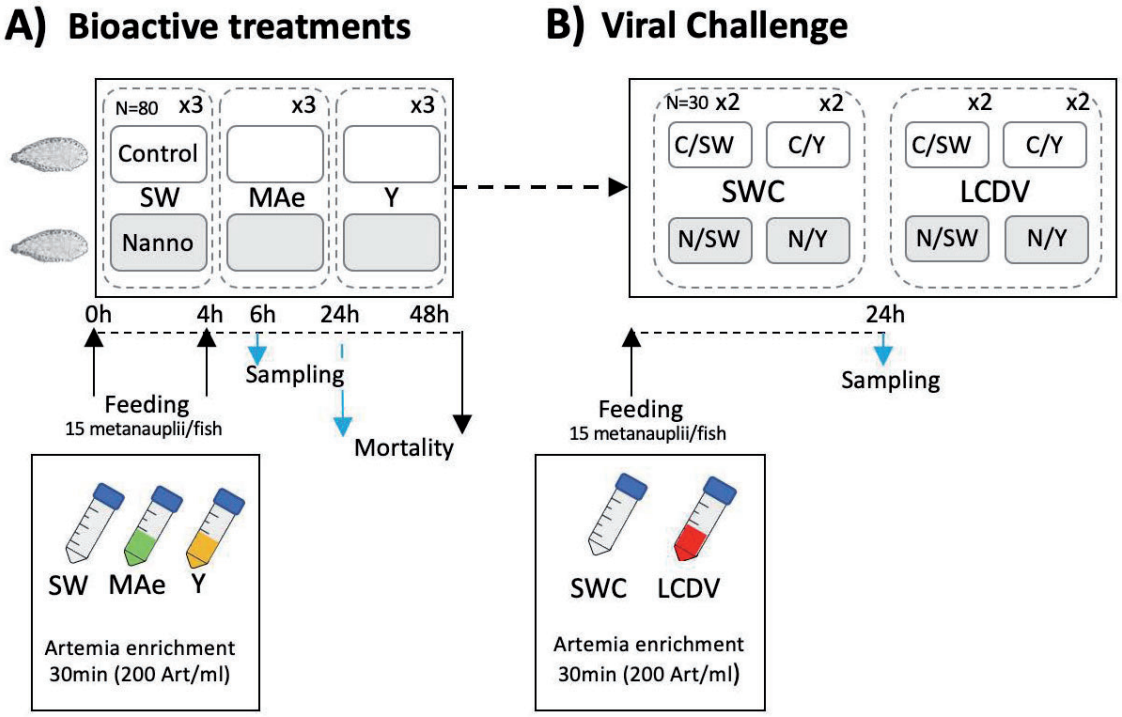

Figure 18. Experimental design A) Bioactive treatment. Nanno-trained (N) and non-trained sole post-larvae (C) were distributed in trays (n=80) and administrated artemia enriched for 30 min with bioactive treatments (Microalgal extract (MAe) and yeast β-glucans (Y)) and seawater (SW) as a control group in triplicate (x3). A second dose was also supplied at 4h after the onset of the trial and the post-larvae were sampled at 6 and 24 h (in blue). B) Viral challenge. After 48 h, post-larvae from SW and Y groups (fom the Control and Nanno-trained groups) were redistributed in new trays (n=30) in duplicated (x2) and 24 h later was challenged with artemia infected with the virus (LCDV). Post-larvae fed artemia enriched with clean seawater (SWC) was used as a control. Samplings were carried out at 24 h after feeding with LCDV. Mortality was monitored for 72h.

5.2.4 RNA isolation and gene expression analysis

In the first part of the experiment, total RNA from post-larvae (n=4) sampled at 6 and 24 h after oral administration of bioactive compounds were extracted using the II RNA Mini Kit (Bioline). Individual larvae were homogenized in the Fast-prep FG120 instrument (Bio101) using Lysing Matrix D (Q-Bio-Gene) for 60 s at speed setting 6 and total RNA was treated twice with DNase I using Isolate II RNA Mini Kit (Bioline) the for 30 min following the manufacturer's protocols. RNA quantity

was checked spectrophotometrically using the Nanodrop ND-8000 (Thermo Scientific) and quality in agarose gel.

In the second part of the trial, total RNA from post-larvae (n=4) sampled at 24 h after LCDV challenge was purified using TRI-Reagent (Sigma-Aldrich) as described in Carballo *et al.* (2019a) Briefly, whole larvae were homogenized in the Fast-prep FG120 instrument (Bio101) using Lysing Matrix D (Q-Bio-Gene) containing TRI-Reagent for 60 s at speed setting 6. After adding chloroform and centrifugation, the aqueous phase was transferred to a column of Isolate II RNA Mini Kit (Bioline) and processed as described above.

RNA was reverse-transcribed using the *iScript*™ cDNA Synthesis Kit (Bio-Rad) and the qPCR assays were carried out on a CFX96™ Real-Time System (Bio-Rad) using a 10-µl volume containing cDNA generated from 200 ng of original RNA template, 300 nM each of specific forward and reverse primers, and 5 µl of SsoAdvanced™ Universal SYBR® Green Supermix (Bio-Rad). Primers used in this study were previously published: *il1b, tnfa, clec, cxc10, irf7* (Carballo *et al.* 2018a), *irf3* (Carballo *et al.* 2017), *mx* (Fernandez-Trujillo *et al.* 2008) *cd4 and cd8a* (Carballo *et al.* 2019a). The amplification protocol used was as follows: initial 7 min denaturation and enzyme activation at 95ºC,40 cycles of 30 s at 95ºC and 30s at 60 ºC. Each PCR assay was performed in duplicate. The ubiquitin (*ub52*) and β-actin (*actb2*) genes were used as reference genes (Infante *et al.* 2008). Relative mRNA expression was determined using the comparative method $2^{-(\Delta\Delta Ct)}$. Clustering analysis was carried out using PermutMatrix (Caraux & Pinloche 2005).

5.2.5 Enzymatic assays

Frozen post-larvae were weighed and homogenized individually in 500 µL of extraction buffer, according to the methodology previosly described in Sych *et al.* (2013). Supernatants were stored in -80ºC until analysis.

Total protein of sole post-larva homogenates at 6, 24 and 48 hours after

exposure with dietary treatment (n=6/group) was measured by the Bradford method, using Bio-Rad protein assay dye reagent concentrate colorimetric assay (BioRad) and measured at 595 nm using a microplate reader (BioTek Synergy 4, BioTek Instruments, Inc.). Total protein was normalized by the wet weight of larva and expressed as mg/mg.

Lysozyme and total anti-protease activity were also measured in larval homogenates (n=6/group, at 6, 24 and 48h) using the turbidimetric assays previously described by Ellis, (1990a; 1990b) and modified by Hanif *et al.* (2004). Data obtained were normalized by the total protein content in each mg of larval wet weight and expressed as U/mg for lysozyme specific activity and as the percentage of trypsin activity calculated regarding the positive control with 100% trypsin activity (% of trypsin activity/mg protein). All the measures were performed using a microplate reader (BioTek Synergy 4, BioTek Instruments, Inc.).

5.2.6 Quantification of viral DNA copies

Total DNA of whole larvae, six independent post-larvae from each treatment and time, and artemia was isolated used Isolate II Genomic DNA Kit (Bioline). In the case of 24h LCDV challenge samples, also DNA was isolated from organic phase of Trizol used for RNA isolation, following the manufacturer's protocols. In both cases, DNA samples were treated with RNase A (Bioline) following the manufacture's protocols. DNA was quantified spectrophotometrically using the Nanodrop ND-8000. Absolute quantification of viral DNA copies was carried out according the protocol specified by Valverde *et al.* (2016b) using a CFX96™ Real-Time System (Bio-Rad) in a 10 µl final volume containing 200 ng of DNA, 300 nM each of specific forward and reverse primers, and 5 µl of SsoAdvanced™ Universal SYBR® Green Supermix (Bio-Rad). The amplification protocol used was as follows: initial 7 min denaturation and enzyme activation at 95 ºC, 40 cycles of 30 s at 95 ºC and 1 min at 59ºC.

5.2.7 Statistical analysis

Mortality curves after the administration of bioactive compounds and reprograming treatments were analysed using a Log Rank test. The qPCR data were log-transformed in order to comply with normality and homogeneity of variance.

A General Linear Model (GLM) analysis was used to test statistically significant changes in gene expression and enzymatic analysis using as fixed factors the bioactive compound treatments, larval reprogramming and time in the first part of the trial and the bioactive compounds treatments, larval reprogramming and infection in the second part of the trial. When a significant interaction between factors was detected, a two-way or one-way ANOVA were carried out followed by a LSD post-hoc for the bioactive compounds treatments.

For viral quantification, a two-way ANOVA was carried out using the time and bioactive compound or reprogramming treatments as fixed factors followed by a LSD post-hoc when necessary.

The Principal Components Analysis (PCA) was conducted using FactoMineR (Lê *et al.* 2008). Statistical analyses were performed using SPSS v21 software (IBM) with statistical significance set at $P<0.05$ and data are presented as mean ± standard error of the mean (SEM).

5.3 Results

5.3.1 Effects of larval reprogramming on growth and post-larvae survival after oral administration of bioactive compounds

To monitor the effects of reprogrammed larvae on growth using *N. gaditana* extracts, larvae were sampled at the end of metamorphosis (21 dph). Larvae from the Nanno-trained group were statistically significant higher than those of control group as determined by dry weight (1.58±0.21 vs 1.16±0.08 mg) and standard length (0.84±0.01 vs 0.70±0.03 mm, respectively (P<0.05).

At the beginning of the trial for administration of bioactive compounds (MAe and Y), the animals (32 dph) were randomly distributed in the trays with an average wet weight 12.73±0.95 mg and 13.28±0.34 mg for control and Nanno-trained groups (P>0.05), respectively.

Survival after the administration of bioactive compounds was monitored for 72h (Fig. 18). One hundred percent survival (no mortality) was observed in all experimental groups at 6 h after the supply of enriched (MAe and Y) and non-enriched (SW) live preys. However, significant differences (P<0.05) in mortality between the bioactive compounds treatments (SW<Y<MAe) and the reprogrammed groups (Control<Nanno) could be observed later at 24, 48 and 72h. Cumulative mortality in the SW group at 72h was 7.1±12.4% and 1.9±1.6% for the control and Nanno-trained groups, respectively (Fig. 19). In Y treated group, only a slight mortality at 24h was recorded in the Nanno-trained group (2.7±3.2%). The cumulative mortality at 72h was 5.4±3.5% and 35.8±8.7% for Control and Nanno-trained groups, respectively (Fig. 19). The highest mortality rates were observed in larvae supplied MAe. At 24h, mortality was 18.6±16.3% for the control and 96.6±2.6% for Nanno groups. Cumulative mortality at the end of the trial reached 69.6±17.0% and 100% in the control and Nanno-trained groups, respectively.

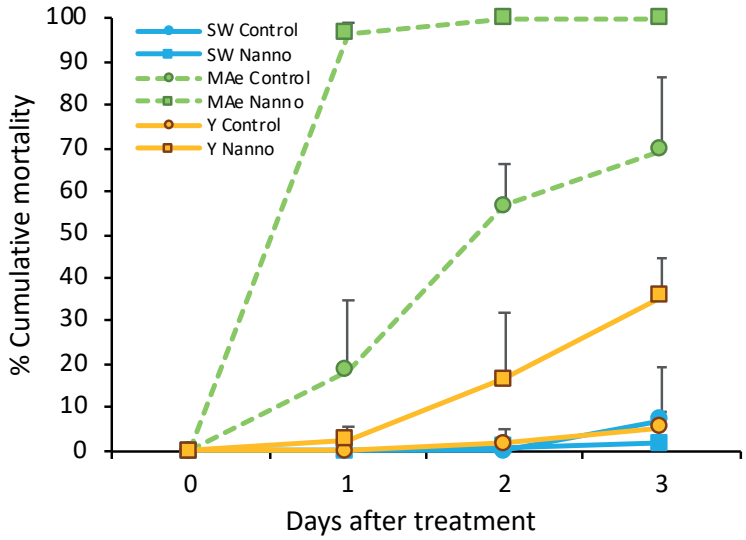

Figure 19. Cumulative mortality (%) of non-trained (Control) and Nanno-trained (Nanno) post-larvae administrated the bioactive compounds treatments (MAe and Y). Control group is indicated with circle markers and Nanno-trained post-larvae in square markers. Seawater control (SW) group is represented in blue line, MAe in dashed green line and Y in orange line. Mortality were recorded at 24h, 48h and 72h after the onset of the trial.

5.3.2 Enzymatic activity associated with larval reprogramming and the administration of bioactive compounds in post-larvae

Lysozyme and total anti-protease activities were measured in the whole post-larvae at 6 and 24h after the onset of the experiment. Due to the high mortality in the MAe group at 24h, the enzymatic activities could not be determined. Both the lysozyme (Fig. 20A) and total anti-protease activities (Fig. 20B) showed statistically significant differences along time, both for the reprogramming and for the bioactive compound treatments (P<0.05). Both enzymatic activities decreased with the time, being higher in Nanno-trained post-larvae compared to the Control group. Regarding to the bioactive compounds, only MAe increased the lysozyme and antiprotease activity compared to the SW control, although the later only in the Control group.

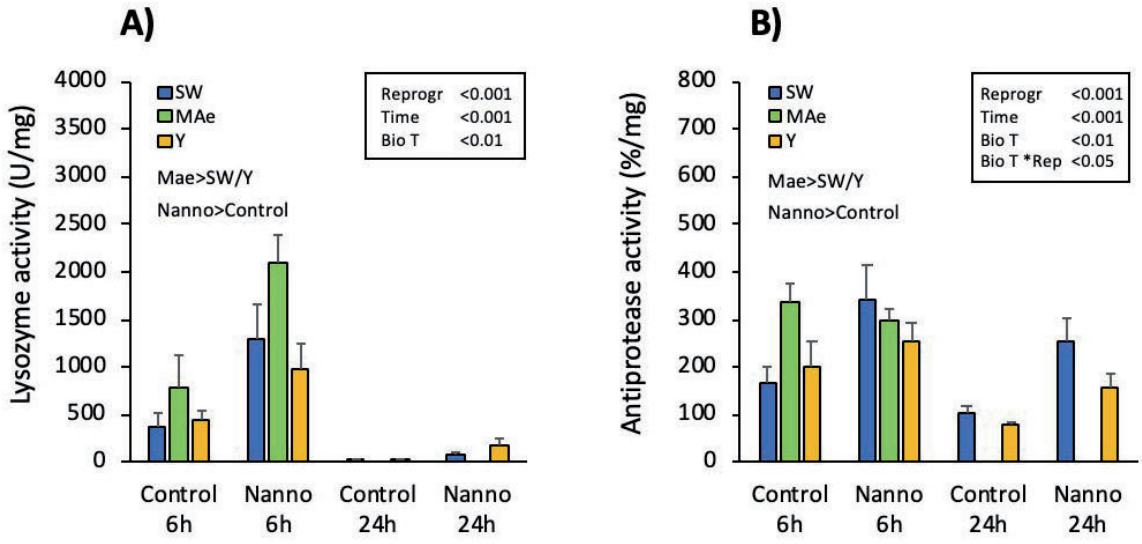

Figure 20. Lysozyme (A) and antiprotease (B) enzymatic activities of non-trained (Control) and Nanno-trained (Nanno) post-larvae administrated the bioactive compounds treatments (MAe and Y). Activities were measured in whole post-larvae homogenates sampled at 6 and 24h after the onset of the trial. The mean ± SEM are represented and expressed as U/mg for lysozyme (A) and %/mg for anti-protease activity (B). Statistical significances for reprogramming (Reprogr), bioactive treatments (Bio T) and time are indicated. Interactions are shown only when significant.

5.3.3 Expression profiles associated with larval reprogramming and the administration of bioactive compounds in post-larvae

In order to evaluate the effects of orally administrated MAe and Y bioactive compounds on the immune system, the expression levels of nine genes were quantified: the pro-inflammatory genes *il1b* and *tnfa*, receptor lectin type-c (*clec)*, chemokine *cxc10*, antiviral genes *irf3*, *irf7* and *mx* and lymphocytes markers *cd4* and *cd8a* (Fig. 21).

All genes, except *il1b* and *cxc10,* showed significant differences in expression levels associated with the sampling times (6 and 24h). Moreover, *cxc10* and *mx* showed statistically significant differences (P<0.05) in the steady-state gene expression levels due to the reprogramming treatments. For these genes, Nanno-trained larvae showed 2.0- and 1.5-fold higher mRNA levels than the control for *cxc10* and *mx*, respectively (Fig. 21). Moreover, a significant interaction time*reprogramming was observed for *il1b*, with higher mRNA levels in the control

than in the Nanno group at 24h.

Regarding to the bioactive compounds, a clear effect on *il1b*, *irf7* and *mx* gene expression was observed. The *il1b* mRNA levels were higher in the MAe group than in SW. These differences were the highest at 24h (average 2.3-fold higher than the SW). In the case of irf7 and *mx*, a significant interaction time*bioactive treatment was detected with an up-regulation of mRNA levels in MAe at 6h and a down-regulation in MAe and Y with respect to the SW at 24 h.

A significant interaction time*bioactive treatment for *tnfa*, *cxc10*, *irf3* and *cd4* was also determined. At 6h, mRNA levels were higher for MAe and Y for *tnfa*. At 24h, mRNA amounts decreased significantly for *tnfa*, *irf3* and *cd4* in the MAe and Y groups, the *cxc10* in the MAe group and the *clec* in the Y treatment with respect to the SW group.

5.3.4 Viral loads of post-larvae challenged with LCDV

Sole reprogrammed post-larvae from the SW and Y groups were further challenged with LCDV. The viral final concentration in the seawater used to enrich the artemia was $5x10^4$ $TCID_{50}$/ml, resulting in $5.3\pm3.0x10^5$ *mcp* copies μg/metanauplii.

Post-larvae from the SWC group did not amplify any PCR products of viral copies at any time. However, the viral *mcp* DNA was detected in all post-larvae exposed to LCDV-infected artemia at 4 and 6 h post-challenge (pch). However, the rates of LCDV positive animals at 24 h pch decreased to 57.1% and 87.5% in the SW and Y groups, respectively. When the reprogramming treatment was considered, LCDV was equally detected in Control and Nanno (66.7%).

No differences in the amounts of viral DNA copies between Control and Nanno-trained groups and between SW and Y groups were found ($P>0.05$). However, significant differences along time were detected ($P<0.05$). The number of DNA copies was higher at 4 h pch (40±6 *mcp* copies/μg DNA in SW and 35±5 mcp

copies µg/DNA in Y groups) than at 6 h pch (14±2 and 20±3 *mcp* copies/µg DNA) and 24 h pch (25±8 and 30±9 *mcp* copies/µg DNA) (Fig. 22A). Similar results were obtained when reprogramming groups were compared (Fig. 22B).

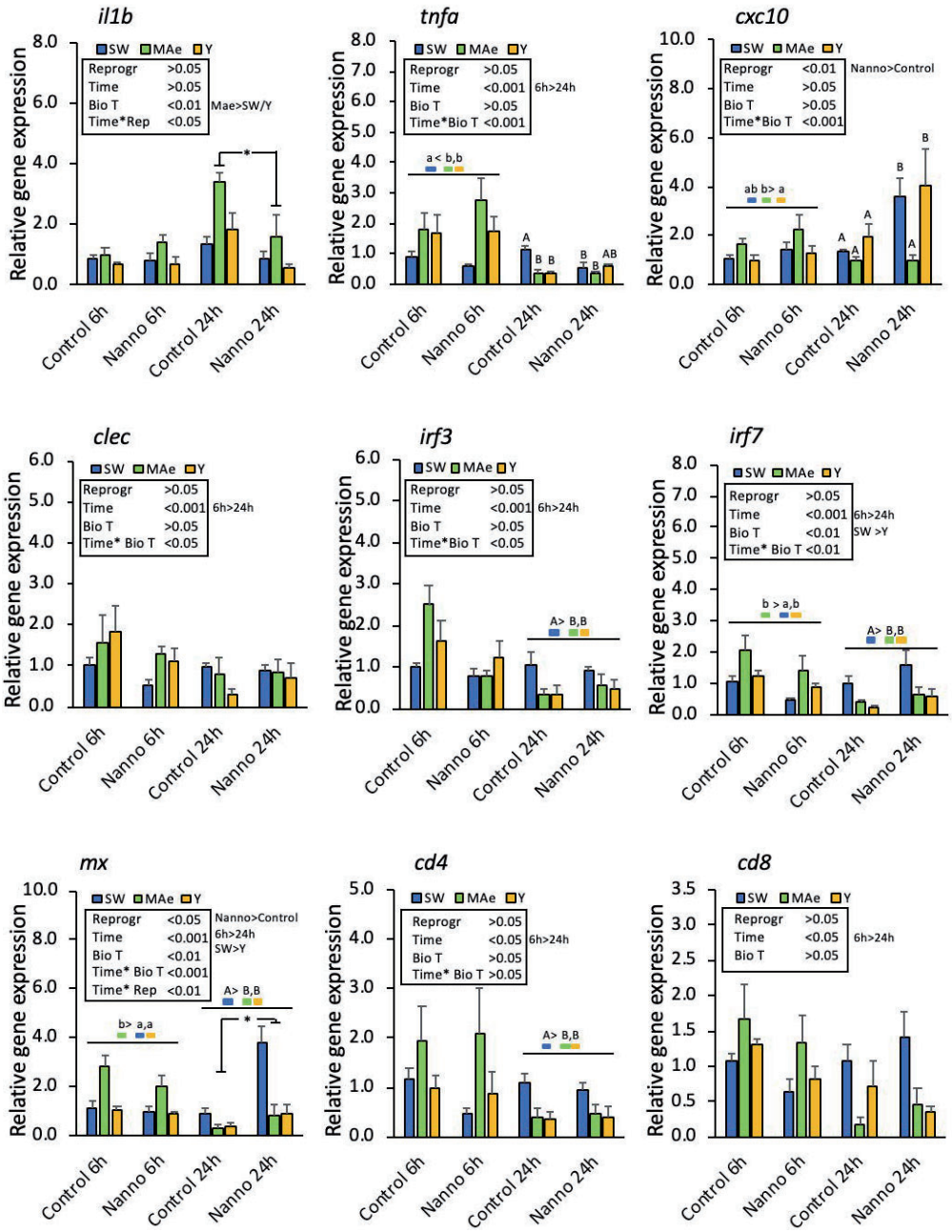

Figure 21. Relative gene expression levels of non-trained (Control) and Nanno-trained (Nanno) post-larvae supplied the bioactive compounds treatments (MAe and Y). Expression levels were determined at 6 and 24 h after the onset of the trial. Control group (SW) is indicated in blue bars, MAe in green bars and Y in orange bars. Data are expressed as mean ± SEM, n = 4 from the calibrator group (SW control 6h). Statistical significances for reprogramming (Reprogr), bioactive treatments (Bio T) and time factors and post-hoc comparisons are shown. When interaction is significant, a two-way anova is carried out. In thise case, letters denote significant differences between bioactive compound treatments at a specific time point (6h in lowercase and 24h in uppercase). Asterisks indicate significant differences between reprograming treatments at a specific time point. Significant differences were set at P<0.05.

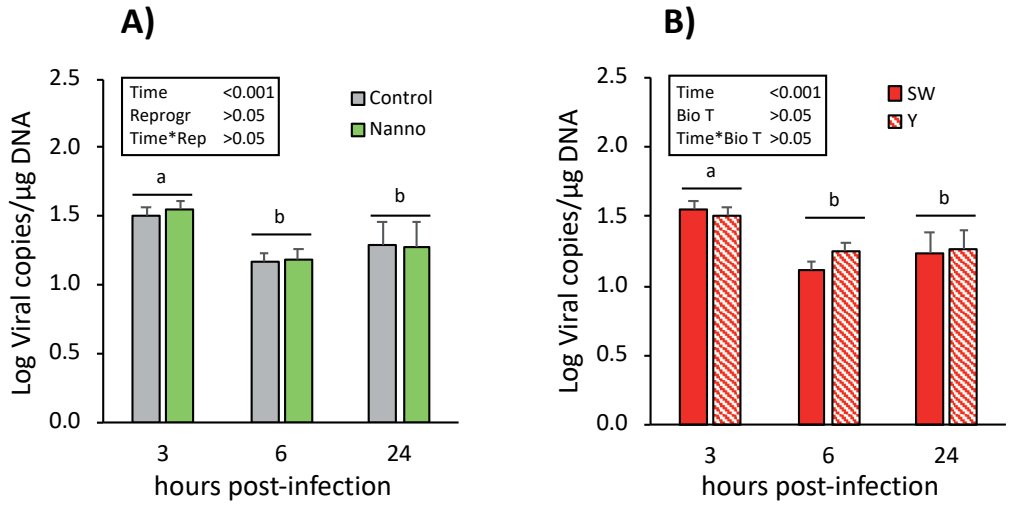

Figure 22. LCDV DNA quantification in infected Senegalese sole post-larvae at 3h, 6h and 24h post challenge. A) LCDV DNA copies non-trained (grey) and Nanno-trained (green); B) LCDV DNA copies in the SW (red) and Y (red and white) groups, Data were expressed as mean logarithm of viral DNA copies per µg of total DNA ± SEM. Letters indicate the significant differences between sampling points (P<0.05).

5.3.5 Gene expression profiles after LCDV challenge of reprogrammed larvae and after the administration of bioactive compounds

In order to evaluate the immune response associated with the LCDV challenge, the expression pattern of same gene panel indicated above was analyzed. A clustering analysis clearly separated the LCDV-challenged from the SW group (Fig. 23A). Moreover, a specific branch for Nanno_SW in the infected group was also identified. In non-infected fish (SWC), two major branches separating from SW and Y were identified. A PCA analysis clearly separated the LCDV-challenged from the SW group (Fig 23B and C) and the SW and Y specimens appeared slightly separated within them. No clear association between reprogramming treatments within the challenged groups were observed.

A detailed analysis of gene expression profiles (Figs. 24 and 25) indicated that all genes except *cxc10* responded to the viral challenge although modulated by reprogramming and bioactive compound administration differentiating the antiviral genes *irf7*, *irf3* and *mx* response from that observed for pro-inflammatory cytokine *il1b* and lymphocytes markers *cd4* and *cd8a*.

The LCDV activated differentially the expression *irf7*, *irf3* and *mx* depending on the reprogramming and bioactive compound treatments. In the SW group, the activation of the three antiviral genes after the LCDV challenge was higher in the Nanno-trained than control group (Fig. 24). In contrast, the response induced by the virus in the Y group was higher in the non-trained control group. Unlike the antiviral genes, the pro-inflammatory cytokine *il1b* only activated the expression after the LCDV challenge in the control but not in the Nanno-trained group in the SW treatment. In contrast, post-larvae fed Y highly induced the expression of both genes and equally in Nanno and control groups. The *cd4*, *cd8* and *clec* did not responded to the LCDV infection in the SW but they were highly induced in the Y treatment.

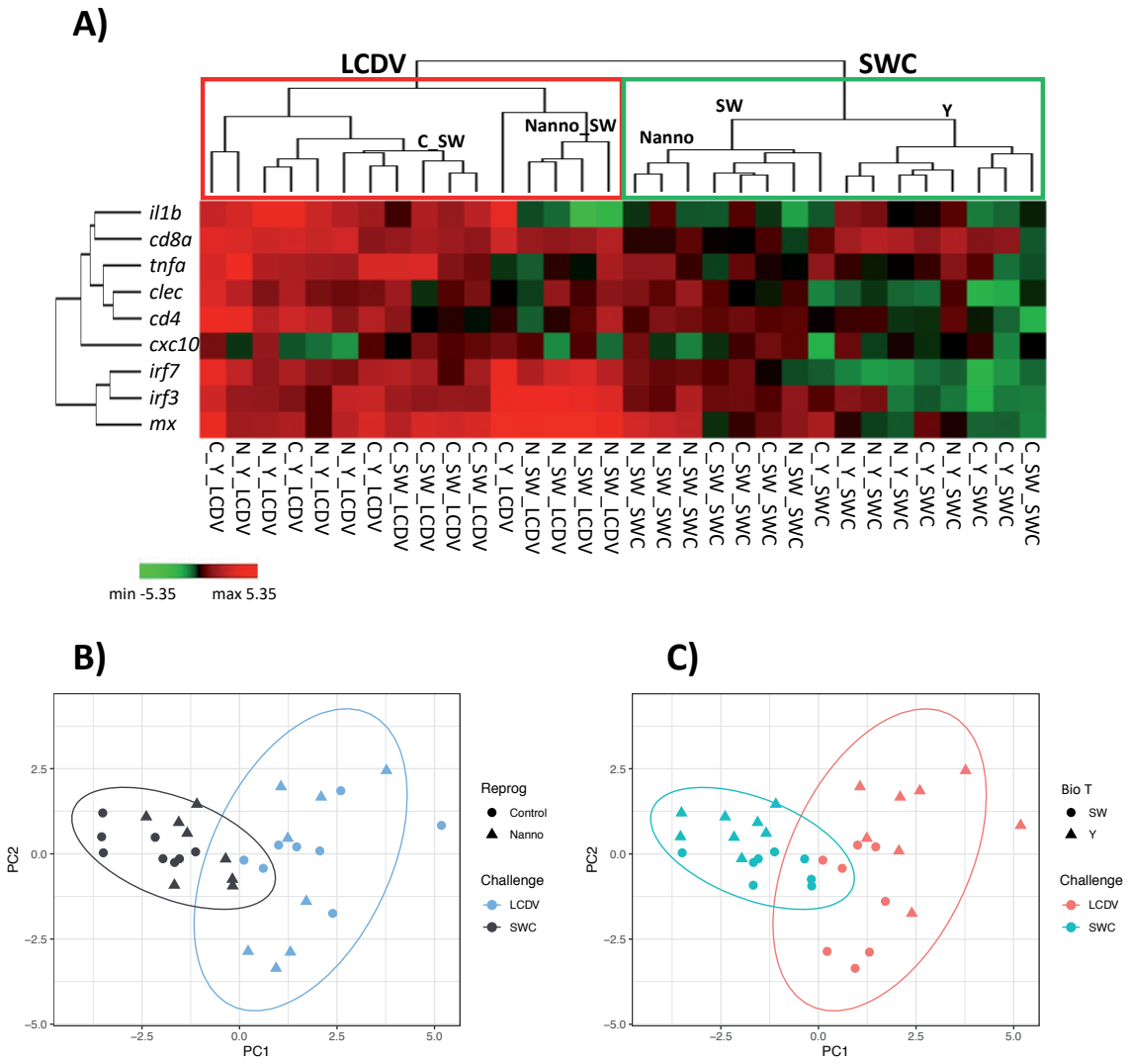

Figure 23. Principal components analysis (PCA) and hierarchical heat map cluster of all genes analyzed in the LCDV challenge trial. A) Hierarchical heat map using normalized log2 of fold-change. Green and red colors indicate low and high expression values according to the scale shown. Sample codes are as follows: first part of the name indicates non-trained control (C) and Nanno-trained (N); second part indicates if post-larvae were administrated microalgal extracts (MAe), yeast β-glucans (Y) or negative control (SW); the third part if post larvae were challenge with LCDV (LCDV) or negative control (SWC). The main clusters grouping the LCDV (red) and control (SWC) as well as other subclusters grouping similar samples are indicated. Gene names are shown on the left. B) and C) Principal Component Analysis (PCA) plot based on the complete set of genes analysed representing the samples (n=4) for reprogramming (B) or bioactive compound (C) treatments. The confidence ellipses (95%) for LCDV challenge groups are indicates. The dimension 1 explained the 48.6% and the dimension 2 the 20.5%.

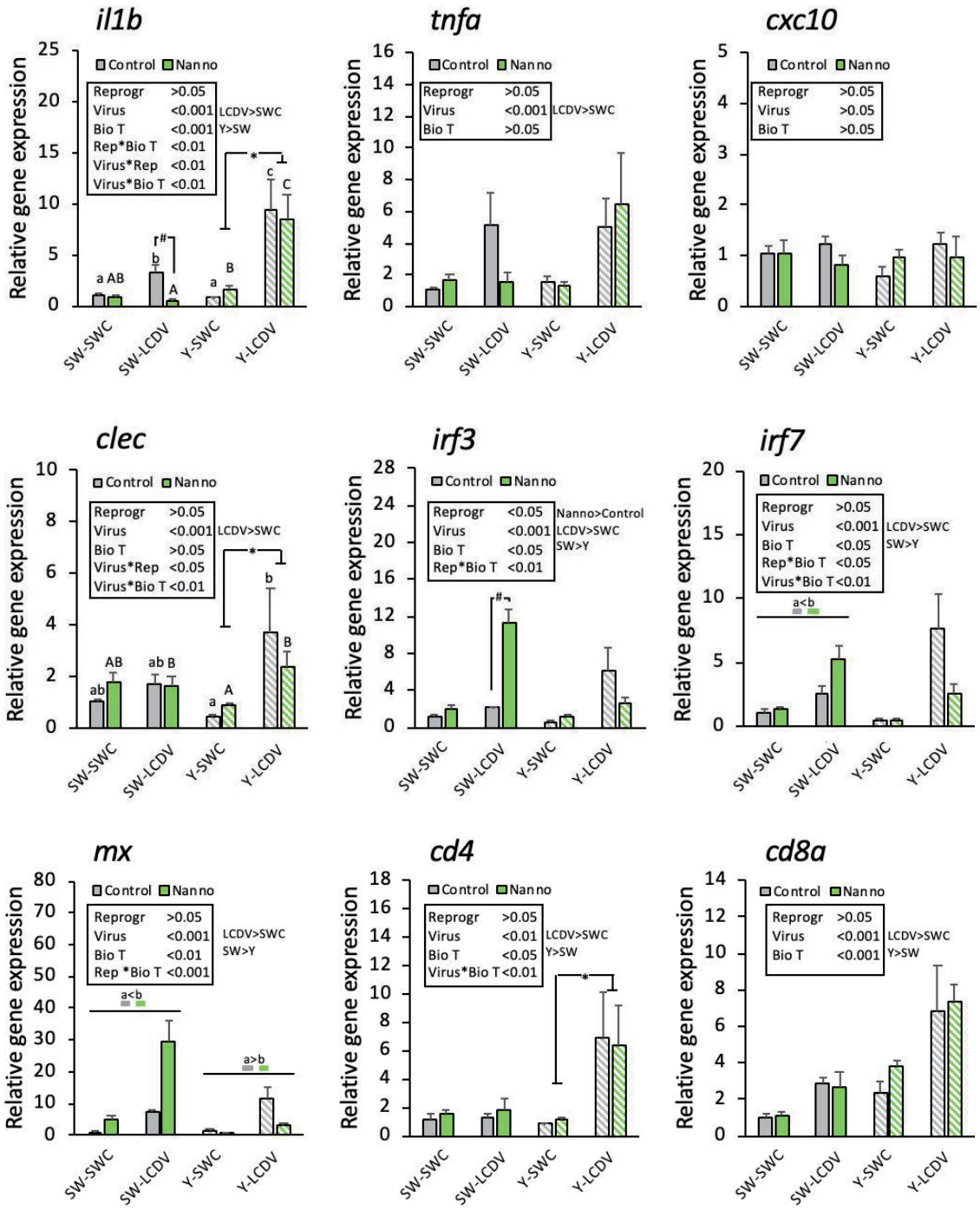

Figure 24. Relative gene expression levels of non-trained (Control) and Nanno-trained (Nanno) post-larvae supplied Y or the control SW and later challenged by LCDV. The SWC indicates a non-infected group. Expression levels were determined at 24 h after the challenge. Data are expressed as the mean ± SEM, n = 4 from the calibrator group (non-trained Control SW-SWC group). Statistical significances for reprogramming (Reprogr), bioactive treatments (Bio T) and LCDV infection (Virus) and post-hoc comparisons are shown. When interaction is significant, a two-way anova is carried out. In thise case, letters indicate significant differences between reprograming group for each bioactive treatment. Asterisks denote significant differences between viral treatments for each bioactive treatment. Letters above the color squares and hash sign denote significant differences between between groups. Significant differences were set at P<0.05.

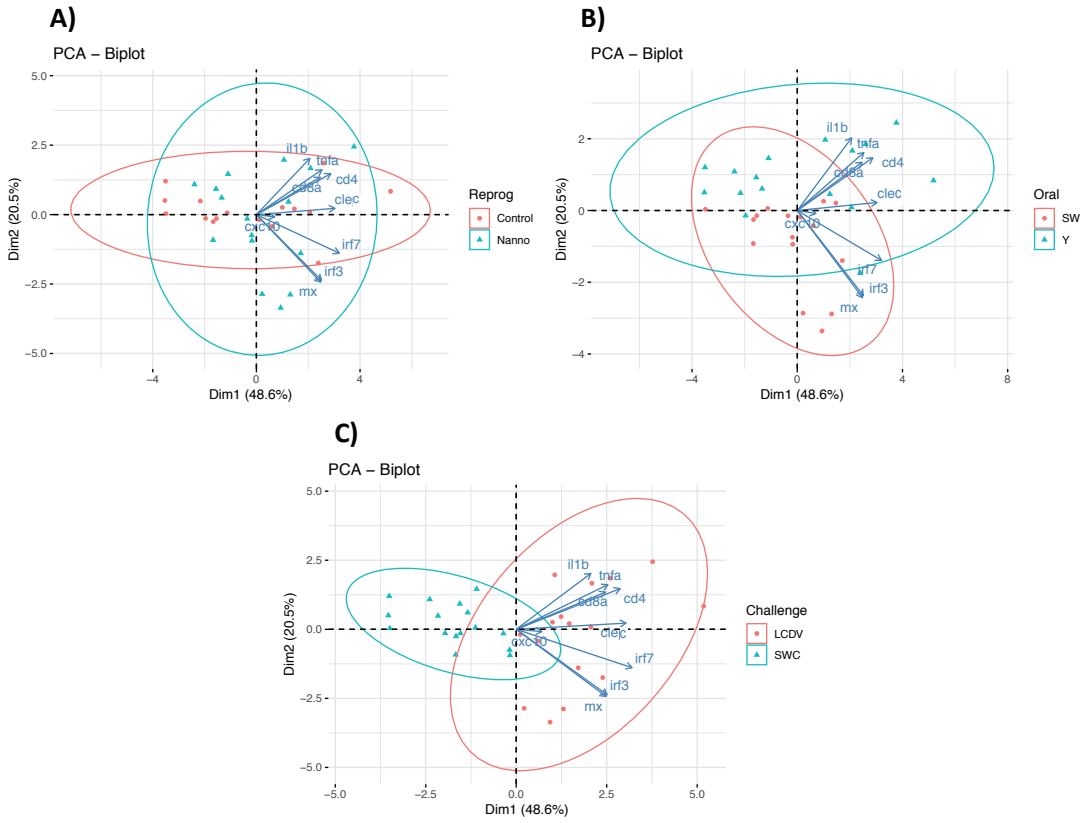

Figure 25. The principal component analysis (PCA) biplot of the set of genes analysed for reprogramming (A), bioactive compounds (B) and virus challenged (C) samples. The name of the genes are indicated in the arrows. The confidence ellipses (95%) for each experimental group are shown.

Antioxidant capacity and immunomodulatory effects of a chrysolaminarin-enriched extract in Senegalese sole

The results of this chapter were published in: Carballo C., Chronopoulou E.G., Letsiou S., Maya C., Labrou N.E., Infante C., Power D.M., Manchado M. Antioxidant capacity and immunomodulatory effects of a chrysolaminarin-enriched extract in Senegalese sole. Fish Shellfish Immunol. 2018 Nov; 82:1-8. doi: 10.1016/j.fsi.2018.07.052.

6.1 Introduction

The β-glucans are considered as potent immunosaccharides able to enhance the immune response and prevent disease outbreaks (Meena *et al.* 2013; Song *et al.* 2014). These bioactive molecules activate the production of pro- and anti-inflammatory cytokines, which in turn modulate humoral and cellular immunity through different pathways conferring antimicrobial, antitumoral and anti-proliferative properties (Stier *et al.* 2014; Du *et al.* 2015; Bashir & Choi 2017). Moreover, β-glucans exhibit antioxidant, anti-diabetic, and anti-obesity effects (Vannucci *et al.* 2013; Bashir & Choi 2017) and the broad spectrum of applications in biotechnology and biomedicine fields makes them of high biotechnological and biomedical interest. In aquaculture, β-glucans are mainly used as immunostimulants and prebiotics and are administered by injection or as a dietary supplement able to enhance fish growth, survival and the immune response and also improve resistance to several different pathogens (Ringø *et al.* 2012; Meena *et al.* 2013). Moreover, recent findings that reported a role of β-glucans on trained immunity by epigenetic reprogramming of monocyte-to-macrophage differentiation (Saeed *et al.* 2014; Netea *et al.* 2016; Petit & Wiegertjes 2016) have even increased the interest on these polysaccharides.

The β-glucans are widely distributed in the nature and can be obtained from different sources such as bacteria, algae, fungi and plants. They share a common basic structure and are composed of glucose homopolymers bound together by glycoside bonds. The position and distribution of the glycoside bonds, molecular size and type, solubility and degree of branching, gives each β-glucan a unique structure and specific bioactive properties (Barsanti *et al.* 2011; Meena *et al.* 2013; Noss *et al.* 2013; Synytsya & Novak 2014). The antioxidant and anti-proliferative properties of β-glucans from fungi and plants have been extensively studied for food and clinical uses (Kofuji *et al.* 2012; Vannucci *et al.* 2013; Gugi *et al.* 2015; Fortin *et al.* 2018). In a similar way, β-(1,3;1,6)-glucans from yeast are the most used in

aquaculture as immunostimulants and to a lesser extent β-(1,3;1,6) from seaweeds (laminarin) or β-(1,3;1,4) from cereal grains (Ringø *et al.* 2012; Meena *et al.* 2013). However, little information is available about the antioxidative properties and immunomodulatory actions of β-glucans from microalgae, the chrysolaminarin (also known as leucosin).

Chrysolaminarin is a soluble β-glucan synthetized for energy storage by several marine microalgae including haptophyte and stramenopiles (such as diatoms and *Nannochloropsis*) (Sadovskaya *et al.* 2014; Gugi *et al.* 2015; Rojo-Cebreros *et al.* 2017). The biosynthesis of this polysaccharide is highly dynamic relying on light and nutrient levels and also shows growth-phase dependency (Myklestad & Granum 2009; Xia *et al.* 2014; Caballero *et al.* 2016; Gao *et al.* 2017). Unlike glucans from fungi and plants, chrysolaminarin is low molecular weight (1-40 kDa) and contains only 20-30 linear residues with a low degree of branching (Gugi *et al.* 2015; Rojo-Cebreros *et al.* 2017). The interest in recent years in the production of biomass from the diatom *Phaeodactylum tricornutum* has rapidly grown due to its biosynthetic capacity and high growth rates and it is regarded as a valuable resource for novel food supplements, cosmeceuticals and several other industrial applications (Bozarth *et al.* 2009; Daboussi *et al.* 2014). The chrysolaminarin cell content in this diatom ranges between 4.9-17.1% of the dry mass and its isolation can be combined with the purification of other bioproducts such as pigments and lipids (Gugi *et al.* 2015; Caballero *et al.* 2016; Gao *et al.* 2017; Zhang *et al.* 2018b). Although several species of microalgae are used as a feed source in fish hatcheries (Hemaiswarya *et al.* 2011), no information about the bioactivity of chrysolaminarin exists in fish.

The aquaculture production of the flatfish Senegalese sole is rapidly growing in Europe with large investments in advanced recirculation facilities to transform production into a highly intensive model (Manchado *et al.* 2016). However, this development needs to be accompanied by disease control and prevention measures

so as to reduce the risks of disease outbreaks and minimize the use of chemicals. Currently the aquaculture of this species is mainly threated by bacterial diseases such as Vibriosis, *Photobacterium damselae* subsp. *piscicida* (Phdp) and *Tenacibaculum* spp. (Morais *et al.* 2016) and several prevention strategies such as inactivated vaccines (Arijo *et al.* 2005) or phage therapy (Silva *et al.* 2016) are under investigation. The use of immunostimulants such as β-glucans suitable to be incorporated as vaccine adjuvants or feed supplements is another strategy successfully used for several other species (Ringø *et al.* 2012; Meena *et al.* 2013; Song *et al.* 2014; Vallejos-Vidal *et al.* 2016). The aims of the chapter 6 were: (i) characterize the antioxidant properties of a chrysolaminarin-enriched extract from *P. tricornutum*; (ii) study its *in vivo* and *in vitro* toxicity; and (iii) evaluate the transcriptional response after intraperitoneal injection in juveniles. The results obtained demonstrate the antioxidant and immunomodulatory actions of this microalgal extract enriched in this unexplored β-glucan, still relatively little exploited by the aquaculture industry.

6.2 Materials and methods

6.2.1 Microalgae cell culture and *β*-glucan sources

The *P. tricornutum* strain used in this study was obtained from the Microalgae Culture Collection of Fitoplancton Marino, S.L. (CCFM). Microalgae were initially grown indoors using autoclaved seawater (salinity 33 ppt) enriched with filter-sterilized f/2 nutrients in 50 ml flasks bubbled filter-sterilized CO_2-enriched air (2%). Microalgal cultures were carried out in a temperature-controlled room (22ºC) under continuous illuminating conditions using artificial daylight fluorescent light (150 μmol/μEm^2 s). Once the cultures reached the early stationary phase they were used to inoculate in 1 l culture flasks. This process of scaling up in volume was repeated until reach 50 l cultures, which were then used to inoculate in the outdoor photobioreactors (PBRs). Light-dark cycles and ambient temperature

were influenced by seasonal environmental conditions (10-11 h of light, temperatures ranging from 10-22 ºC) and pH was controlled by CO_2 injection when necessary. Cells were harvested by continuous-flow centrifugation 4 h after sunrise, frozen at -20 ºC and freeze-dried for further use.

The chrysolaminarin-enriched crude extract was prepared at Fitoplancton Marino using the warm-water extraction method (Chiovitti *et al.* 2004) with slight modifications. Freeze-dried microalgae were heated under alkaline pH conditions and the proteins were later precipitated by a pH-shift approach after removing cell debris. The supernatant containing the polysaccharides was precipitated by adding absolute ethanol (1 v:v) for 24h at 4ºC. After collecting the precipitates by centrifugation, they were frozen at -80ºC and preserved by freeze-drying. This chrysolaminarin-enriched crude extract was characterized by the phenol-sulfuric acid method (Dubois *et al.* 1956) indicating a 47.3% reducing sugar with ~5% of total protein as determined by the Bradford assay. The particulate (1,3)-(1,6)-β-glucan (Yestimun®) from brewers' yeast was purchased from Quimivita (Barcelona, Spain).

6.2.2 Total Antioxidant Capacity Assays

The total antioxidant capacity (TAC) of the yeast β-glucan and the chrysolaminarin-enriched extract (1% w/v) were measured using three methods: oxygen radical absorbance capacity (ORAC) assay, ferric reducing antioxidant power (FRAP) and the 2,2-diphenyl-1-picrylhydrazyl (DPPH) free radical scavenging assay. The ORAC assay was carried out using fluorescein as the probe as described by Gillespie *et al.* (2007). ORAC values were calculated by subtracting the area under the blank curve from the area under the sample curve (Net AUC) and expressed as Trolox equivalents (μmol Trolox/g). FRAP assays were carried out according to Benzie & Strain, (1996) method and the results were expressed as μg ascorbic acid/mg of β-glucan dry mass. DPPH assays were performed according to Molyneux, (2004). DPPH activities were expressed as % free radical scavenging and the IC_{50} values (the amounts of β-glucan (mg) required to scavenge 50% DPPH

radicals) were also estimated.

6.2.3 Human skin cell culture and cytoxicity tests

Primary Normal Human Dermal Fibroblasts (NHDF) isolated from normal human adult skin were purchased from Lonza Clonetics™ (Lonza Walkersville) and cultured as previously described (Letsiou *et al.* 2017). The cell proliferation test was assessed by using an MTT kit (Vybrant MTT cell proliferation assay kit, Thermo Fisher Scientific) according to the manufacturer's protocol. The MTT assay is based on the reduction of the tetrazolium salt, MTT [3-(4,5-dimethylthiazol-2-yl)-2,5-diphenyltetrazolium bromide] by actively growing cells to produce blue formazan product. NHDF were incubated with different β-glucan concentrations (ranging 0.001-1% w/v in a final volume of 100 μL) for 24h and optical density measured at 570 nm.

6.2.4 Fish trials

All procedures were authorized by the Bioethics and Animal Welfare Committee of IFAPA and given the registration number 26–11–15-374 by the National authorities for regulation of animal care and experimentation.

The chrysolaminarin-enriched extract was intraperitoneally (i.p.) injected using coconut oil (Renuka Agri Organics LTD) as a vehicle for a slow and prolonged release of the polysaccharide. The freeze-dried extract was firstly suspended in PBS, then added the same volume (1:1) of coconut oil and vortexed to generate an emulsion. A control solution mix using the same 1:1 (PBS: coconut oil proportion but without extract) was also prepared and used for injection to the sham control. The experimental design is depicted in Fig. 26. A total of 70 specimens of sole (average weight 19.3±3.3g) were supplied by Cupimar S.A. (San Fernando, Cádiz). The animals were distributed into eight cylindrical tanks (1 m^2 surface) in an open flow-through circuit. The animals were kept for one week before starting the experiment and fed with commercial diets (Skretting; 1% biomass). Before

manipulating the animals, they were sedated with phenoxyethanol (100 ppm final concentration). Four tanks (10 specimens each) were given intraperitoneal (i.p) injections of 100 μL of the chrysolaminarin-containing solution (1 mg/fish). This dose of chrysolaminarin by i.p. injection was selected based on a previous study (Selvaraj *et al.* 2005). Moreover, three tanks (10 specimens each) were injected with the control solution (sham control group). Mortality was monitored daily and six animals per treatment (two specimens from each tank remaining the fourth tank in chrysolaminarin-injected fish untouched) were sampled at 2 and 5 days post injection (dpi) and organs collected. Animals were euthanized using an overdose of phenoxyethanol (250 ppm final concentration) and the kidney, spleen and intestine dissected out. Samples for gene expression analysis were fixed in RNA-later (Invitrogen) and stored at -80°C until use. In the trial, a temperature of 22.3ºC±0.6, dissolved oxygen of 6.5±0.5 ppm, and salinity of 40.2±1 ppt were recorded. At 7 dpi, 27 surviving specimens were given a second i.p. injection of chrysolaminarin-enriched extract (1 mg/fish, 14 specimens; group Chr_Chr) or the control solution (13 specimens; group Chr_C) and distributed into four tanks. All fish from sham control group were again injected only with the control solution (30 specimens; group C_C) and distributed into three tanks. In the trial, a temperature of 20.8ºC±0.7, dissolved oxygen of 6.0±0.7 ppm, and salinity of 38.5±0.6 ppt were recorded. Mortality was monitored daily and two animals per tank were sampled at 2 dpi. Fish were euthanized and samples collected as indicated above.

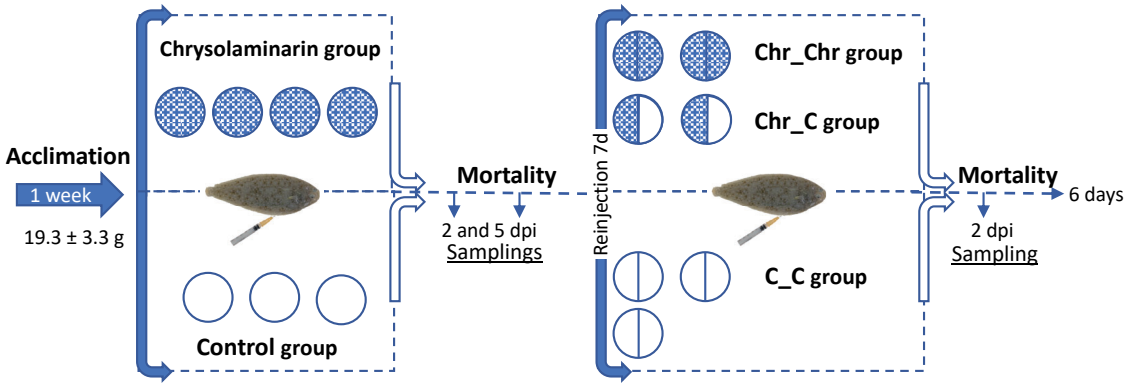

Figure 26. Experimental design. Soles (19.3±3.3 g) were acclimated for 1 week before i.p. injection. Chrysolaminarin-enriched extract was suspended in a coconut oil and PBS emulsion (1:1) and injected 1mg/fish (Chrysolaminarin group) and the sham control group just with the emulsion. At 7 dpi (dash line), the chrysolaminarin-injected fish were reinjected with chrysolaminarin (Chr_Chr group) or the emulsion (Chr_C group) whereas the sham control group was reinjected only with the emulsion (C_C group) Mortality was monitored for 13 days and samplings were carried out at 2 and 5 dpi and 2 days after reinjection.

6.2.5 RNA isolation and RT-qPCR analysis

Total RNAs from the intestine (~40-50 mg) and spleen (~15 mg) was isolated using the NucleoSpin RNA isolation Kit (Macherey-Nagel) following the manufacturer's protocol. Samples were homogenized in the Fast-prep FG120 instrument (Bio101) using Lysing Matrix D (Q-Bio-Gene) for 60 s at speed setting 6. In the case of kidney (~10-15 mg), tissue homogenization was carried out as indicated above using 1 ml of TRI-Reagent (Sigma-Aldrich). After adding chloroform (0.2 ml) and centrifugation, the aqueous phase was transferred to columns of the NucleoSpin RNA isolation Kit (Macherey-Nagel) to complete the RNA purification in a similar way to intestine and spleen. Isolated RNA samples were treated twice on-column with DNase I using a NucleoSpin RNA isolation Kit (Macherey-Nagel) for 30 min. RNA sample quality was checked by agarose gel electrophoresis and quantification was determined spectrophotometrically using the Nanodrop ND-8000 (Thermo Scientific). One µg of total RNA was reverse-transcribed using the iScript™ cDNA Synthesis kit (Bio-Rad) according to the manufacturer's protocol.

To evaluate the immunomodulatory effects of chrysolaminarin-enriched extract the following gene panel was selected: pro-inflammatory cytokines: *il1b* and *tnfa*; cellular stress: heat shock protein 90 alpha (*hsp90aa*); antimicrobial peptide: hepcidin (*hamp1*); bacterial defence: g-type lyzozyme (*lysg*); chemokine: *cxc10*; complement factor (*c3*); antiviral defence: interferon 1 (*ifn1*), interferon-induced Mx protein (*mx*), interferon-related factors (*irf1*, *irf3*, *irf7*, *irf8* and *irf9*); glucan receptor c-type lectin (*clec*). Primers for amplification of *hsp90aa*, *hamp1*, *mx*, *irf1* and *irf3* and the reference genes *ubi* and *actb1* were previously published (Fernandez-Trujillo *et al.* 2008; Infante *et al.* 2008; Manchado *et al.* 2008; Salas-Leiton *et al.* 2010; Carballo *et al.* 2017). Primers used for amplification of *il1b*, *tnfa*, *c3*, *clec*, *cxc10*, *ifn1*, *irf7*, *irf8* and *irf9* (Table 3) were designed using the Oligo v7 software using specific sequences from SoleaDB (Benzekri *et al.* 2014). The c-lectin receptor was identified by blasting the salmon glucan receptor sequences for *sclrc* genes (Kiron *et al.* 2016).

Real-time analysis was carried out on a CFX96™ Real-Time System (Bio-Rad). Real-time reactions were performed in a 10 µl volume containing cDNA generated from 10 ng of original RNA template, 300 nM each of specific forward and reverse primers, and 5 µL of SYBR Premix Ex Taq (Takara, Clontech). The amplification protocol used was as follows: initial 7 min denaturation and enzyme activation at 95ºC, 40 cycles of 30 s at 95ºC, 15 s at 68°C and 30 s at 72°C. Each PCR assay was performed in duplicate. The PCR protocol to amplify the *mx* gene was described in Fernandez-Trujillo *et al.* (2008). Data were normalized using the geometric mean of ubiquitin (*ubi*) and β-actin (*actb1*) (Infante *et al.* 2008) and relative mRNA expression calculated using the comparative Cq method (Schmittgen & Livak 2008). PermutMatrix (Caraux & Pinloche 2005) was used to conduct a cluster analysis with the different experimental conditions analysed using $\log_{10}$ of fold change with parameters set as following: Dissimilarity: Euclidean distance, Hierarchical: Complete Linkage Method, Seriation: Multiple-fragment heuristic (MF).

Table 3. Primers used for RT-qPCR. Gene names, primer sequences, amplicon size and the target unigene from SoleaDB (Benzekri et al. 2014) are indicated.

Target	Primer	Sequence (5′→3′)	Amplicon (bp)	source
il1b	F	GCACCCTCATGTCTGCCCGCTTCCCT	105	unigene346347
	R	AGGTTCTGTAGCGTTGGGCCATCTCTGT		
tnfa	F	CCAAGCGTTTGCTCAGGGCGGCTTC	116	unigene26860
	R	GGCCTTCGCTGCAGGAGACTCTGAACGAC		
clec	F	CCCCCATCGTCTGCCCTCTGAACTGG	90	unigene416724
	R	ACTGACTCTCGTCCCACTCTCTGAAGACCC		
cxc10	F	CGCGCTCGACAACAGCCAGTCAAAGCAAC	121	unigene30191
	R	ACAGTGACAGTGCTGGTGAGGAACTCCTT		
irf7	F	GGCAAAATCAGCGAGTTCCCCAACGACA	93	unigene68007
	R	CACCATCTTGAAGCGCACGGACAGGTT		
irf8	F	AGCCTGCGACATGGAAGACAAGACTCCG	86	unigene17110
	R	GTCCAGCTGCGACCGTTCTCTCACCTCC		
irf9	F	TCACCGTGCAGACCGAGGAGCCCGTT	79	unigene2689_split_1
	R	TCCAGTCTGATCTCGTCCACCGCGTCTCT		
ifn1	F	AGCACAAGGAAAGCGCTGCCTGTGGT	94	unigene638812
	R	AAGCAGTTGTGGTGTTTGTGCAGGACGAT		

6.2.6 Statistical analysis

All data were checked for normal distribution with the Kolmogorov–Smirnov test as well as for homogeneity of variance with the Levene's test and when necessary a log transformation was applied. Survival rates were assessed by using one-way ANOVA test. To test the existence of significant differences in gene expression in the injection trial, a two-way ANOVA was performed using treatment and time as fixed factors and in case of significance a Student's t-test was performed. For reinjection trial, a one-way ANOVA followed by an LSD post hoc test was carried out. Differences with $p < 0.05$ were considered to be statistically significant. Analyses were performed using SPSS v21 software (IBM Corp., Armonk) and Statistix 9 (Analytical Software, Tallahassee).

6.3 Results

6.3.1 Antioxidant activities

The total antioxidant capacity (TAC) as determined by ORAC, FRAP and DPPH is depicted in Figure 27. The chrysolaminarin-enriched extract had 14.2-folds higher TAC as determined by ORAC than particulate yeast β-glucan (29.8±7.3 vs 2.1±0.7 μmol Trolox/g). In a similar way, chrysolaminarin-enriched extract also showed higher reducing antioxidant power than yeast β-glucan (1.0±0.01 vs 0.2±0.03 μg ascorbic acid/mg at concentration of 10 mg/ml). In contrast, DPPH radical scavenging activity was higher in the yeast β-glucan (estimated IC_{50} values were 1,896±144 and 353±28 μg/ml for the chrysolaminarin-enriched extract and yeast β-glucan, respectively).

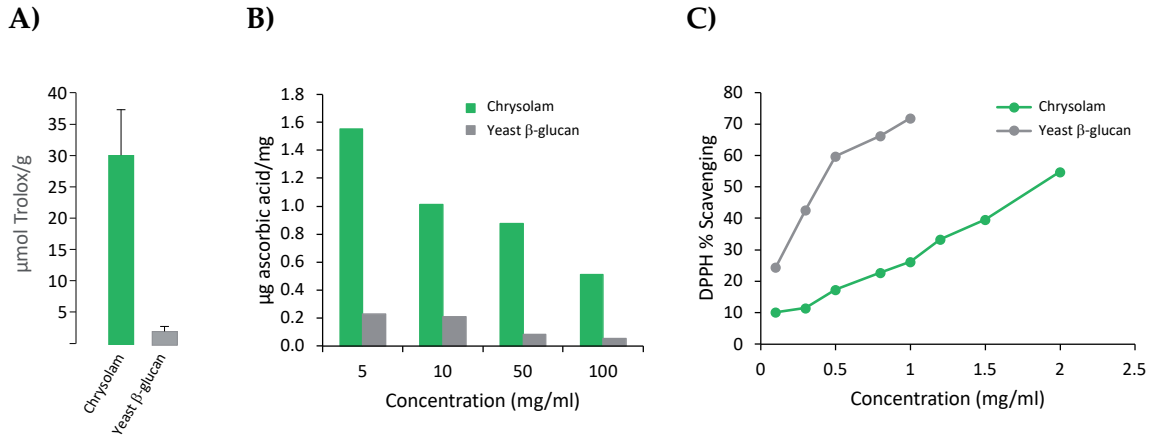

Figure 27. Total antioxidant capacity (TAC) of chrysolaminarin and yeast β-glucan. **(A)** the oxygen radical absorbance capacity (ORAC) assay. **(B)** ferric reducing antioxidant power (FRAP). **(C)** the 2,2-diphenyl-1-picrylhydrazyl (DPPH) free radical scavenging assay. ORAC values were expressed as Trolox equivalents (μmol Trolox/g), FRAP as μg ascorbic acid/mg and DPPH as percentage of scavenging of free radical.

6.3.2 Cell toxicity and fish survival

The cytotoxic activity of the chrysolaminarin-enriched extract and yeast β-

glucan (ranging from 0.001 to 1% w/v final concentration) was assayed in the primary dermal cell cultures NHDF using the MTT assay (Fig. 28A). Cell survival with the microalgal crude extract was slightly higher (100%) than with yeast β-glucan (89.6%) at the lowest concentration (0.001%) and impaired cell viability was observed at 0.01%. Mortality was concentration-dependent in both β-glucans (only 39% survival at the highest concentration 1%).

In vivo experiments using 0.005% w/w of chrysolaminarin-enriched extract resulted in 29.4% cumulated mortality at 6 dpi (Fig. 28B). No mortality was detected in the sham control group (C_C). Moreover, reinjection of the chrysolaminarin-enriched extract or control solution at 7 dpi to the fish previously injected with the extract (Chr_Chr or Chr_C groups) did not provoke any additional mortality (Fig. 28B).

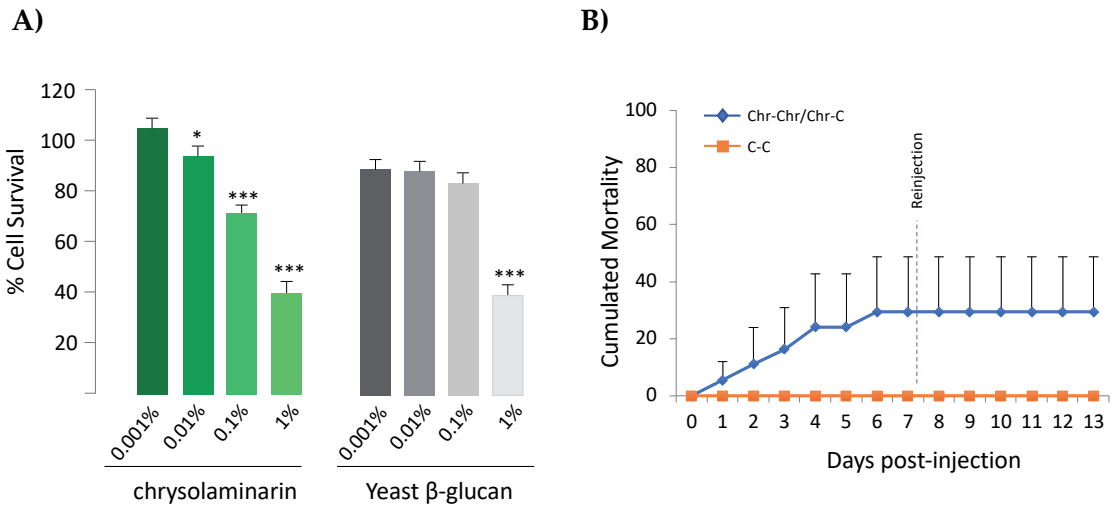

Figure 28. (A) Toxicity of chrysolaminarin-enriched extract and yeast glucan in human fibroblast cells as determined by MTT. Asterisks indicate significant differences with respect to the lower concentration. *p<0.05; ** p<0.01; *** p<0.001. **(B)** *In vivo* cumulative mortality in sole intraperitoneally injected with chrysolaminarin-enriched extract. The experimental groups Chr_Chr, Chr_C and C_C are indicated.

6.3.2 Expression profiles in immunological organs

To evaluate the immunomodulatory activity of the chrysolaminarin-enriched extract, transcript abundance of genes related to the inflammatory response, cellular stress, carbohydrate binding receptors and defence against bacteria and viruses was quantified in three immunological organs: kidney, spleen and intestine. A cluster analysis clearly separated the expression response observed in chrysolaminarin-injected soles from the sham control at 2 dpi in the three organs studied (Fig. 29) while it was hardly observable at 5 dpi (only in kidney appeared separated both experimental groups). The injection of the microalgal extract rapidly (2 dpi) up-regulated the expression of *il1b*, *hsp90aa* and *hamp1* (5.6-, 12.5- and 4.9-folds, respectively) and down-regulated that of *clec* and *ifn1* in the kidney with respect to the sham control. Later at 5 dpi, the antiviral defence genes *irf1*, *irf3*, *irf8*, *irf9* and *mx* significantly decreased their expression levels ($p < 0.05$) (Fig. 30). The reinjection of the chrysolaminarin-enriched extract at 7 days (Chr_Chr group) only reduced significantly the expression of *hsp90aa* and *irf3* with respect to both groups reinjected with the control solution (C_C and Chr_C groups). No change in gene expression was detected for *il1b*, *tnfa*, *c3*, *hamp1*, *clec*, *ifnc*, *irf7* or *mx* (data not shown).

In intestine and spleen, a subset of ten genes was selected to evaluate the immune response (indicated in Fig. 29). In intestine, the mRNA levels of *il1b*, *hamp1* and *irf3* were up-regulated 16.6-, 43.7- and 10.5-folds, respectively at 2 dpi and the *c3* mRNA abundance significantly increased 4.4-fold at 5 dpi (Fig. 31). In the spleen, expression of *il1b*, *hsp90aa*, *c3* and *hamp1* increased 12.6-, 5.8, 5.4- and 10.0-folds, respectively at 2 dpi while *cxc10* and *irf3* mRNA levels significantly decreased (3.9- and 3.2-folds, respectively) at 5 dpi (Fig. 31). No change in gene expression was detected for *tnfa*, *clec*, *irf7* and *g-lys* in intestine and spleen and for *hsp90aa* and *cxc10* in intestine (data not shown).

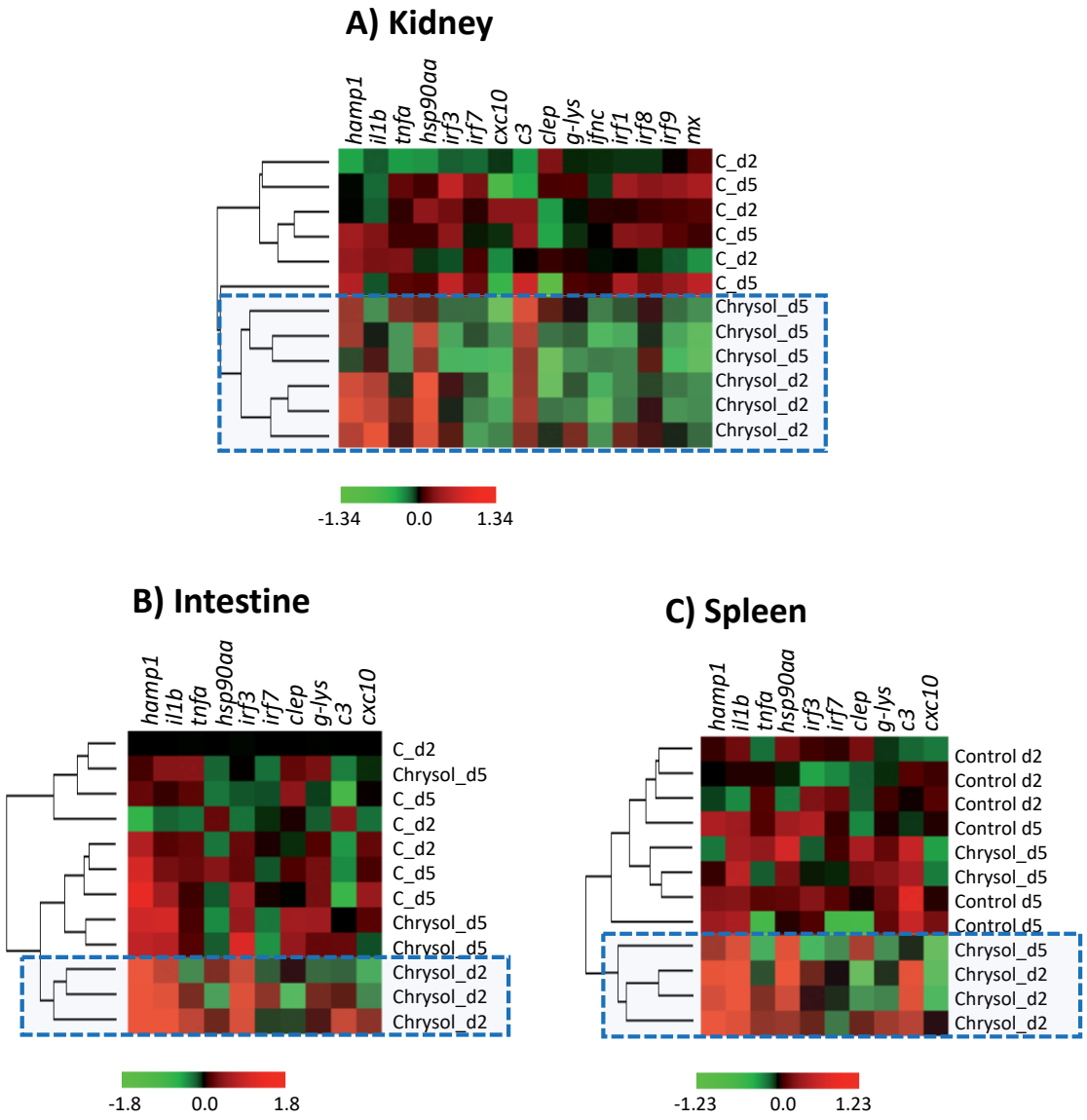

Figure 29. Hierarchical clustering analysis based on set of expressed transcripts in kidney **(A)**, intestine **(B)** and spleen **(C)** as determined by qPCR. Data were normalized and expressed as log10 of fold change. Green and red colours indicate low and high expression values according to the scale shown. The samples are identified on the right (control and chrysolaminarin-enriched extract at 2 and 5 dpi) and the main clusters grouping separating both experimental group samples are boxed in blue. Full-names for the transcripts shown on the top are indicated in M&M.

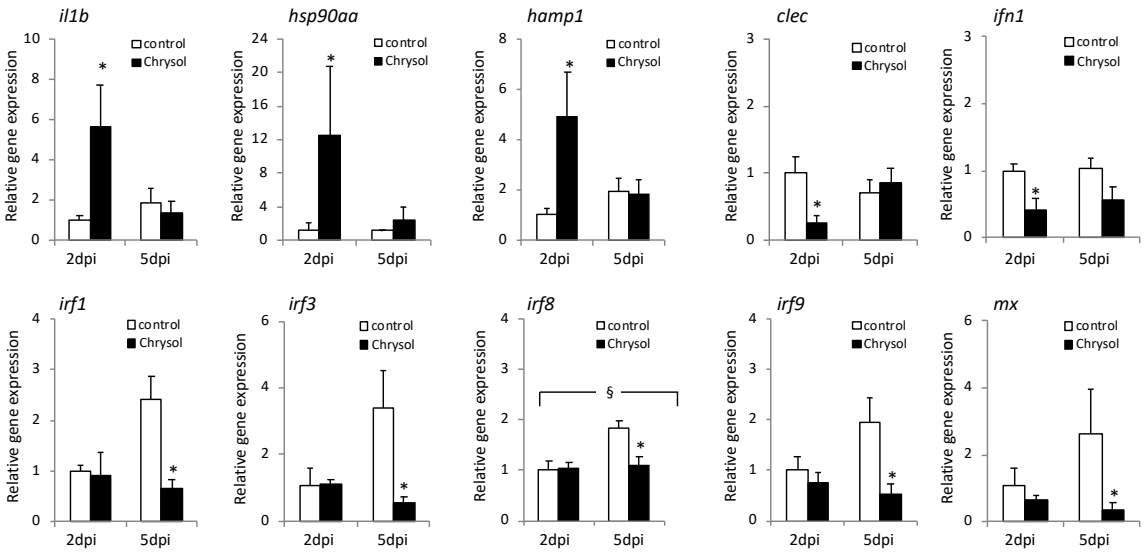

Figure 30. Differentially expressed genes in kidney after i.p. injection of the chrysolaminarin-enriched extract. Data were expressed as the mean fold change (mean + SEM, n = 3) from the calibrator (control 2 dpi). A two-way ANOVA was used to determine statistical differences. Asterisks denote significant differences between control (white) and chrysolaminarin-enriched extract (black) injected fish. § indicates significant differences due to time.

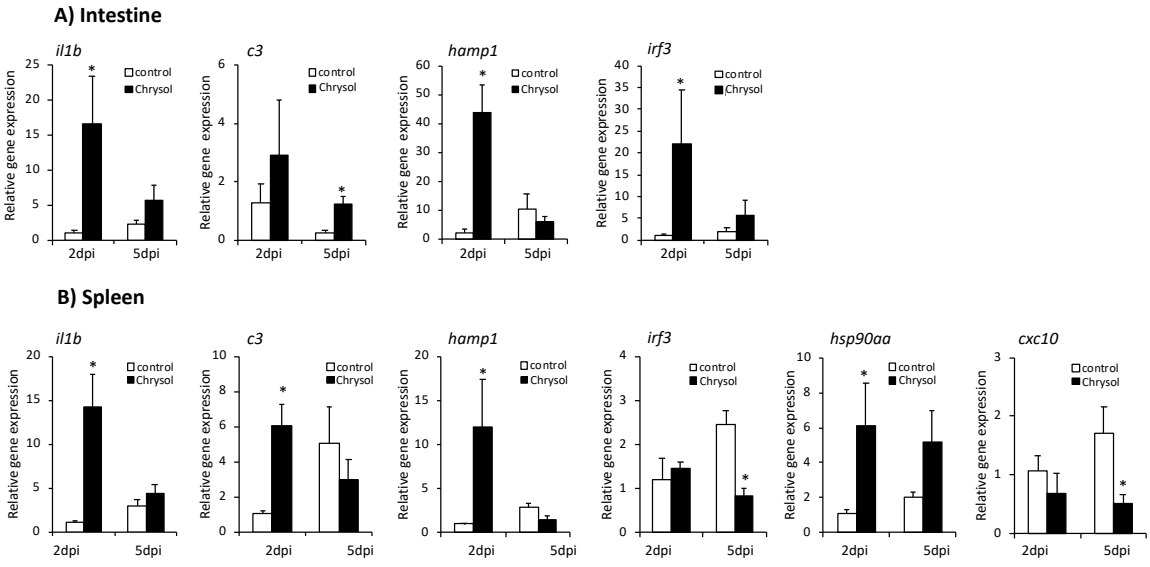

Figure 31. Differentially expressed genes in intestine **(A)** and spleen **(B)** after i.p. injection of the chrysolaminarin-enriched extract. Data were expressed as the mean fold change (mean + SEM, n = 3) from the calibrator (control 2 dpi). A two-way ANOVA was used to determine statistical differences. Asterisks denote significant differences between control (white) and chrysolaminarin-enriched extract (black) injected fish.

Yeast β-glucans and microalgal extracts modulate the immune response and gut microbiome in Senegalese sole (*Solea senegalensis*)

The results of this chapter were published in: Carballo C., Pinto P.I.S., Mateus A.P., Berbel C., Guerreiro C.C., Martinez-Blanch J.F., Codoñer F.M., Mantecon L., Power D.M., Manchado M. Yeast β-glucans and microalgal extracts modulate the immune response and gut microbiome in Senegalese sole (*Solea senegalensis*). Fish Shellfish Immunol. 2019. 92:31-39. doi: 10.1016/j.fsi.2019.05.044.

7.1 Introduction

Prebiotics are important feed supplements in aquaculture due to their capacity to enhance health and prevent disease outbreaks. These ingredients are normally non-digestible molecules that selectively modulate the intestinal microbiome by promoting indigenous microbial populations and preventing pathogen proliferation (Dimitroglou *et al.* 2011; Akhter *et al.* 2015). Carbohydrates (poly- and oligosaccharides) such as mannan-, fructo- and galacto-oligosaccharides, inulin or β-glucans are widely recognized for their prebiotic activity. All these non-digestible sugars are fermented in the gut resulting in the enhanced production of short chain fatty acids (SCFA), mainly formate, acetate, propionate and butyrate (Morrison & Preston 2016; McLoughlin *et al.* 2017). These secondary metabolites modulate the production and release of cytokines and chemokines and leukocyte recruitment producing beneficial effects on diabetes, colon cancer, obesity and systemic inflammation in mammals (Vinolo *et al.* 2011; McLoughlin *et al.* 2017). In spite of the potential benefits of prebiotics for animal health, their use in aquaculture is still limited and their actions are far from understood (Dimitroglou *et al.* 2011).

The β-glucans are a chemically heterogeneous family of polysaccharides commonly utilized as prebiotics and vaccine adjuvants in aquaculture (Meena *et al.* 2013; Song *et al.* 2014). These molecules are composed of a glucose backbone of varying lengths linked by either β-(1,3)-, β-(1,4) or β-(1,6) glycoside bonds and side chains linked by β-(1,4) or β-(1,6) (Myklestad & Granum 2009; Barsanti *et al.* 2011). β-glucans are ubiquitous in bacteria, algae, protozoans, chromistans and plants and act as bacterial aggregators, virulence factors, energy storage compounds or structural components of cell walls (McIntosh *et al.* 2005; Myklestad & Granum 2009). However, only β-(1,3;1,6)-glucans from fungi and algae have been used as prebiotics due to their action as microbiome modulators and immunosaccharides

that bind to specific pathogen associated molecular pattern (PAMP) receptors to trigger an innate immune response (Meena *et al.* 2013; Song *et al.* 2014). The β-glucans have a wide spectrum of molecular sizes, solubility and degree of branching and polymerization, which explains their unique tertiary structures, physicochemical properties and specific bioactivity (Zekovic *et al.* 2005; Novak & Vetvicka 2008; Vetvicka & Vetvickova 2010; Noss *et al.* 2013). In human whole blood cultures, a specific cytokine response is stimulated by β-glucans with different chemical characteristics (Noss *et al.* 2013). For this reason, the activity of each β-glucan as an immune modulator needs to be evaluated.

Yestimun® and chrysolaminarin are two different β-(1,3;1,6)-glucans obtained from brewers' yeast and microalgae, respectively. The former is particulate and insoluble with a branch-on-branch structure, high molecular weight (>200 kDa) and high degree of polymerization (Barsanti *et al.* 2011; Stier *et al.* 2014). In contrast, chrysolaminarin is a soluble, side-chain branched glucan of small size (1-40 kDa) containing between 20–30 linear residues and a low degree of branching (Gugi *et al.* 2015). Both types of β-glucans exhibit different antioxidant and antiproliferative capacities (Carballo *et al.* 2018a). Studies in mammals indicate that particulate β-glucans interact with a C-type lectin receptor to activate the dectin-1 pathway whereas the soluble β-glucans act via the CR3 receptor to activate the complement pathway (Qi *et al.* 2011). In aquaculture, the action of particulate β-glucans has been studied and they enhance non-specific and specific immune markers regardless of the route of administration (Meena *et al.* 2013; Vetvicka *et al.* 2013). However, the immunomodulatory action of chrysolaminarin-enriched extracts is still poorly characterized although we have shown that they trigger a transient acute inflammatory response when injected intraperitoneally (Carballo *et al.* 2018a).

A major threat to sustainable fish aquaculture is disease and for this reason there is high interest in prebiotics that can stimulate a robust immune response and

improved disease resistance (Ringø *et al.* 2010). The rapid expansion of the microalgae industry has led to the development of new valuable biotechnological products (de Jesus Raposo *et al.* 2015; Hamed 2016). The status and scale of biomass production for the diatom *Phaeodactylum tricornutum* has made this species a target for biorefinery feedstock and for high value-added bioactive compounds mainly fucoxanthin, chrysolaminarin and eicosapentaenoic acid (Zhang *et al.* 2018b). A previous study in gilthead seabream using this microalga as a dietary supplement indicated they had enhanced immune parameters (Cerezuela *et al.* 2012). However, the use of whole microalgal cells or their extracts as feed supplements to modulate microbiota and the immune response still remains poorly explored and new studies are required to explore their biological actions and beneficial properties. The present study aimed to evaluate short- and medium-term effects of particulate yeast β-glucans and soluble microalgal extracts enriched in polysaccharides, when applied by oral intubation to Senegalese sole (*Solea senegalensis*). The outcome of the treatments was evaluated by assessing immune plasma activities, transcript expression in the intestine and spleen and the intestinal microbiota composition. The results provide insight into the immunomodulatory action of yeast β-glucans and chrysolaminarin on *Vibrio* communities and gut health and their potential as prebiotics for sole aquaculture.

7.2 Material and methods

7.2.1 Yeast β-glucan and microalgal sources

An insoluble (1,3)-(1,6)-β-glucan, 85% pure from brewers' yeast (Yestimun® pure) was purchased from Quimivita (Barcelona). Microalgal polysaccharide-enriched extract (MAe) was supplied by Fitoplancton Marino, S.L. using the microalgae, *Phaeodactylum tricornutum* from the Microalgae Culture Collection (CCFM). Microalgae culture conditions and the preparation of the extracts is

detailed in Carballo *et al.* (2018a). In brief, microalgae were produced in outdoor seawater photobioreactors under natural environmental conditions for spring in Cadiz (Spain). The microalgae were harvested after sunrise, frozen at -20 ºC and freeze-dried. The MAe was prepared using a warm-water extraction method (Chiovitti *et al.* 2004) followed by protein precipitation using a pH-shift and then polysaccharides precipitation using ethanol. The final extract was estimated to contain 47.3% reducing sugar (Carballo *et al.* 2018a). Whole-cells of *P. tricornutum* were supplied in freeze-dried packages.

7.2.2 Fish trial

All procedures were authorized by the Bioethics and Animal Welfare Committee of IFAPA and given the registration number 26–11–15-374 by the National authorities for the regulation of animal care and experimentation.

To test the effects of yeast β-glucans and MAe on the Senegalese sole, solutions were directly delivered to the intestine using an oral intubation method. To optimize this methodology and establish the timeframe of uptake, some preliminary trials were carried out. Intubation was performed using a flexible polypropylene catheter 1.3 mm in diameter, attached to a 1 ml syringe that was introduced into the mouth from the blind side of the sole. All the procedures were carried out using anesthetized fish (150 ppm phenoxythanol). To monitor the timeframe of uptake and dispersal after intra-intestinal delivery, phosphate-buffered saline (PBS) containing a blue food colouring (1.25% v:v) was used as a tracker. Once the intubation methodology was established, one hundred and twenty juvenile sole (19.2±4.3 g, mean ± standard deviation) were randomly distributed between twelve rectangular tanks (500 l) in an open circuit at 21±1°C, oxygen saturation >90% and salinity 42 ppt. Animals were adapted for one week to the experimental tanks and fed commercial pellets (2% biomass; Skretting) using belt-feeders. Before the intubation experiments sole were fasted for two days to avoid uncontrolled effects of the intestinal contents. Four groups were established

in randomly chosen tanks (n=10 fish/tank, three replicate tanks per group): "Control" (C), fish were intubated and provided with PBS (vehicle); "Yeast" (Y), fish were supplied with yeast β-glucans (1 mg/fish in PBS); "MAe", fish were supplied with microalgal extracts (1 mg/fish in PBS); and "MA", fish received a suspension of rehydrated microalgae *P. tricornutum* (10 mg/fish in PBS). The doses used for the Y and MAe groups were selected using the results of a previous study that revealed a pro-inflammatory response after the intraperitoneal injection of the microalgal extract (Carballo *et al.* 2018a). The dose used for freeze-dried microalgae was estimated based on the 6.9-21.2% dry weight fraction of chrysolaminarin reported for *P. tricornutum* (Caballero *et al.* 2016; Gao *et al.* 2017).

To investigate short-time responses fish were sampled at 3 h (n=5 fish/group), 24 h (n=8 fish/group) and 48 h (n=5 fish/group) and for medium-term responses fish were sampled 7 days after oral intubation (n=12/group). For sampling, fish were anesthetized (200 ppm phenoxyethanol) and blood was collected by puncture of the caudal vein. The anterior intestine and spleen were collected into RNA-later (Sigma-Aldrich) and a portion of the middle intestine was fixed in ice-cold 4% PFA, pH 7.4. Blood samples were left to clot at room temperature for 3 h and then centrifuged at 2,000g for 10 min at 4ºC and the supernatant (serum) removed and stored at -20ºC until determination of the total protein content and enzymatic activities. Samples for RNA extraction (anterior intestine, and spleen) were fixed in RNA-later (Sigma-Aldrich), kept overnight at 4ºC and then stored at -80ºC. Samples for histology (middle intestine) were collected into ice-cold 4% PFA, pH 7.4. Fixation was carried out at 4 °C with agitation, samples were washed three times with PBS and once with sterile water and then stored in methanol at -20 °C, until processing for histology. At day 7th after intubation samples from the mid-gut were collected for microbiome analysis. Sample collection was carried out in a laminar flow cabinet, using sterilized dissection material, and tissue was transferred to RNA-later, incubated at 4ºC for

24 h and then stored at -20ºC until DNA extraction for the microbiome analysis.

7.2.3 Blood serum activity assays and histology

Serum samples were kept at -20ºC and used for immunoassays within 1 month of collection. Immune parameters were measured in serum collected from sole at 24 and 48 h and 7 days after oral intubation (n=5/group). Total serum protein (mg/ml) was determined using the Bradford method and diluted serum samples (1:40) with a Bio-Rad protein assay dye reagent concentrate colorimetric assay (BioRad) and measured at 595 nm using a microplate reader (BioTek Synergy 4, BioTek Instruments, Inc.). The total anti-protease activity was measured using the method reported by Ellis, (1990b) and modified by Hanif *et al.* (2004). Total anti-protease activity was expressed based on the percentage of trypsin activity (calculated by comparison with the positive control) and normalized using the protein content of the serum (% of trypsin activity/mg protein). The lysozyme activity was carried out using the turbidimetric assay reported by Ellis, (1990a). The specific activity of serum lysozyme was expressed as U/mg protein and determined using a standard curve made with hen egg white lysozyme (HEWL, Sigma-Aldrich). One unit of lysozyme activity gave a reduction in absorbance of 0.001 per min.

Histology of the middle intestine was performed to evaluate possible inflammatory effects of the treatments. Paraffin embedded tissue blocks were prepared by dehydration of tissue through a graded ethanol series (70 - 100%), followed by saturation in xylene and inclusion in low melting point paraffin wax. Serial transverse sections (5 μm) of the embedded middle intestine were prepared using a rotary microtome (Leica RM 2135). Sections were mounted on poly-L-lysine (Sigma-Aldrich) coated slides and dried overnight in an oven at 37ºC. Dewaxed and rehydrated sections were stained using haematoxylin and eosin and were mounted in DPX (Fluka). Slides were examined with a Leica DM2000 microscope and images were captured with a digital camera (Leica DFC480) coupled to a computer.

7.2.4 RNA isolation and RT-qPCR analysis

Samples from the anterior intestine (n=3; ~50 mg) and spleen (n=3-5; ~15 mg) were suspended in 1 ml of TRI-Reagent (Sigma-Aldrich) and homogenized in a Fast-prep FG120 instrument (Bio101) using Lysing Matrix D (Q-Bio-Gene) for 60 s at speed setting 6. After adding chloroform (0.2 ml) and centrifuging at 14.000 rpm for 15 min, the aqueous phase was recovered and transferred to a column of the Isolate II RNA Mini Kit (Bioline). Contaminating genomic DNA was removed from total RNAs by treating twice for 30 min with DNase I following the manufacturer's protocols. Total RNA quality was checked by agarose gel electrophoresis and a Nanodrop ND-8000 (Thermo Scientific) was used to determine the concentration. Total RNA (1 μg) was reverse transcribed using an iScript™ cDNA Synthesis kit (Bio-Rad) according to the manufacturer's protocol.

Real-time PCR analysis (qPCR) was carried out for samples taken at 3h, 24h, 48h and 7 days after oral intubation. The number of specimens analysed ranged between 3 and 5 for each sampling time. All qPCR assays were run in duplicate on a CFX96™ Real-Time System (Bio-Rad). The final reaction volume was 10 μl and it contained cDNA generated from 10 ng of the original RNA template, 300 nM each of the specific forward and reverse primers, and 10 μl of SsoAdvanced™ Universal SYBR® Green Supermix (Bio-Rad). The genes for the pro-inflammatory cytokines, *il1b* and *tnfa* and the chemokine *cxc10*, interferon-related factors *irf3* and *irf7*, glucan receptor c-type lectin (*clec*), g-type lysozyme (*lysg*), antimicrobial peptide hepcidin (*hamp1*) and cell surface markers of T lymphocytes (T helper *cd4* and T cytotoxic *cd8*) (Carballo *et al.* 2019a)) were analysed. Primers for Senegalese sole *il1b, tnfa, clec, cxc10, irf3, irf7, hamp1* and *lysg* have previously been published (Salas-Leiton *et al.* 2010; Ponce *et al.* 2011; Carballo *et al.* 2017; 2018a). The qPCR amplification protocol was as follows: 7 min for denaturation and enzyme activation at 95 ºC followed by 40 cycles of 30 s at 95 ºC and 1 min at 60 ºC. Data were normalized using the geometric mean of ubiquitin (*ubi*) and β-actin (*actb2*) (Infante *et al.* 2008) and the

relative mRNA expression was calculated using the comparative Cq method (Livak & Schmittgen 2001).

7.2.5 DNA isolation, microbiome analysis and *Vibrio* quantification

DNA was extracted from 20-35 mg of middle intestine collected 7 days after intubation (n=5 individuals/treatment) using a DNeasy Blood & Tissue Kit (Qiagen). Tissue was subjected to mechanical disruption with 0.1 mm zirconia/silica beads (Biospec) and by applying three cycles of 20 s at 6,800 rpm in a Bertin Precellys 24 homogenizer. DNA extraction followed the manufacturer's instructions and included pre-digestion with 20 mg/ml lysozyme (BioChemica, PanReact, AppliChem) and RNase treatment (0.3 mg/ml, Thermo Fisher). The concentration, quality and integrity of DNA was analyzed by agarose gel electrophoresis and spectroscopy (Nanodrop ND-8000). Amounts of 50 ng of DNA was generated per treatment group by pooling an equal concentration of DNA/fish (n=5) and four microbiome libraries, C, Y, MAe and MA, were generated. A 16S Metagenomic Sequencing Library Preparation protocol for Illumina MiSeq was used for library production using primers targeting the hypervariable V3 and V4 regions of the 16S rRNA gene (Klindworth *et al.* 2013). Libraries were sequenced at Lifesequencing S.L.-ADM (Valencia) on an Illumina MiSeq instrument. Bioinformatics analyses were carried out using a pipeline developed by Lifesequencing S.L.-ADM, as previously described (Codoner *et al.* 2018). These analyses included adaptor trimming, cleaning and merging of the reads (with a minimum of Q20 and final quality of 36.6), chimera removal, identification and classification of operational taxonomic units (OTU) by comparison with the NCBI 16S rRNA database (using a minimum identity of 97%) and hierarchical clustering based on microbial composition. The Chao1 index was determined as a measure of species richness and the Shannon index as an indicator of species diversity.

To obtain further insight into *Vibrio* and *Mycoplasma* in the collected samples, qPCR using optimized genus-specific primers targeting the 16S rRNA gene (Botes *et al.* 2005; Tall *et al.* 2012) was performed using as the template the individual DNAs used to generate the pools for treatment-specific library construction. Duplicate qPCR reactions were carried out as previously described (Pinto *et al.* 2018) in a 10 µl volume containing 20-50 ng DNA, 300 nM of each primer and the Sso Fast EvaGreen Supermix (Bio-Rad). The calculated copy number of *Vibrio* or *Mycoplasma* bacteria was normalized in relation to the micrograms of total DNA extracted from the mid-gut.

7.2.6 Statistical analysis

Prior to statistical analyses, all data were checked for normality using a Kolmogorov-Smirnov test and homogeneity of variance using a Bartlett's test and, when necessary, they were log-transformed. To assess statistical differences in serum activities and the short-term transcriptional response in the intestine, a two-way analysis of variance (two-way ANOVA) using treatment and time as fixed factors was carried out. A Duncan's post-hoc test was carried out when the factor, treatment, was significant. For the short-term transcriptional response in the spleen and medium-term expression profiles in the intestine and spleen, a one-way ANOVA was performed. Differences in *Vibrio* and *Mycoplasma* abundance in each treatment with respect to the control were assessed with a student's t-test. Data are presented as mean ± standard error of the mean (SEM). Statistical analyses were carried out using SPSS v21 software (IBM) with statistical significance set at $P<0.05$.

7.3 Results

7.3.1 Blood serum activities and histology

Short-term responses after Y, MAe and MA treatments revealed significant

differences in the lysozyme activity and total serum proteins (P<0.05; Fig.32). For lysozyme, the MAe group had a significantly lower activity than the C group 48h after intubation (P<0.05), while no significant differences were observed with respect to the Y or MA groups. The antiprotease activity did not differ between groups but differed significantly along time (P<0.05). Fish from the MAe group had significantly reduced levels of total serum proteins compared to the C, Y and MA groups at 48h (P<0.05; Fig. 32). No significant differences in total serum proteins or enzyme activities was observed between any of the groups in the medium-term response after 7 days. Histological analysis of the middle-gut at 24h and 7d after treatments did not reveal any notable changes in the morphology of the middle intestine of the treated and control fish (Fig. 33).

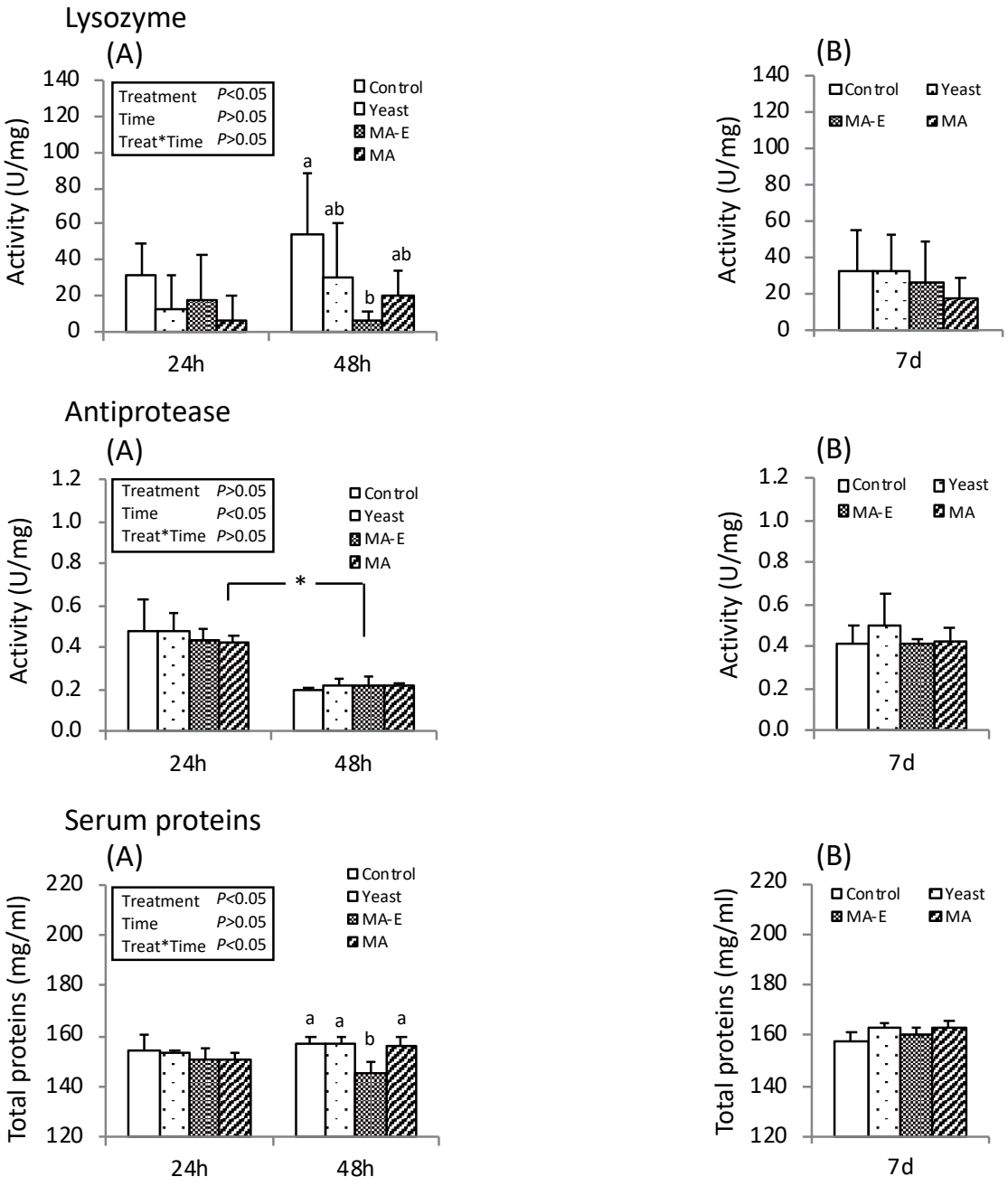

Figure 32: Plasma activities and protein levels. Samples of fish from the control group (control), treated with insoluble yeast β-glucans (Y), microalgal extracts (MAe) and whole-cell microalgae (MA) were sampled at 24 and 48h **(A)** or 7 days **(B)** after oral intubation. The results are shown as the mean ± SEM and expressed as U/mg for lysozyme and anti-protease activity and as mg/ml for total proteins. Different letters indicate significant differences between oral intubation treatments at a specific time point. Asterisks indicate significant differences between samples at different times post-intubation in the short-term response. Significant differences were set at $P<0.05$ (Two-way ANOVA).

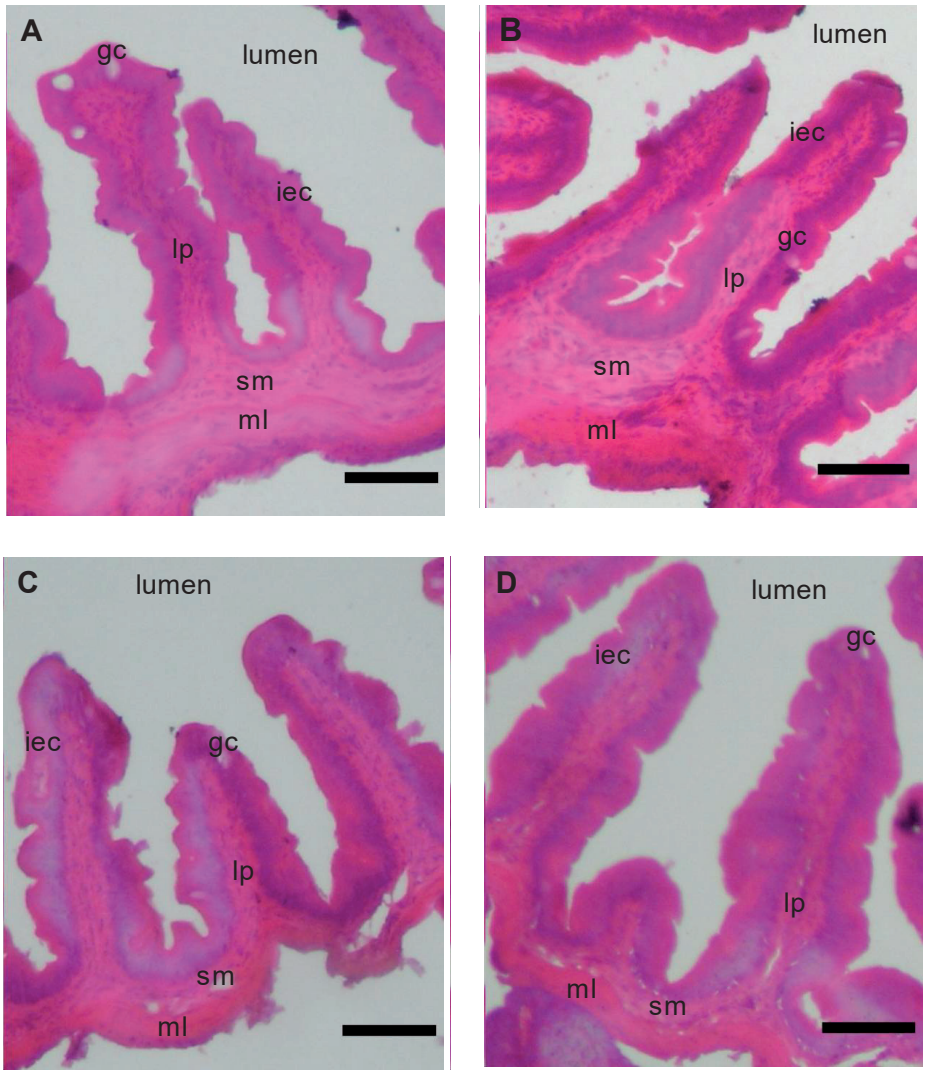

Figure 33. Histology of middle intestine: (A) control (C), (B) yeast β-glucans (Yeast), (C) microalgal extracts (MAe) and (D) whole-cell microalgae (MA); 24h after oral intubation. Intestinal transverse sections (5 μm) were stained with Hematoxylin and Eosin. Intestinal folds are lined by simple columnar epithelium constituted by absorptive intestine epithelial cells (iec) with unstained scattered goblet cells (gc). Submucosa (sm); Muscular layer (ml); lamina propria (lp). Scale bar: 50 μm.

7.3.2 Short-term expression profiles in the intestine and spleen

The short-term response to the treatments included a significant (P<0.05, Two-way ANOVA) change in *il1b*, *tnfa*, *cxc10*, *irf3* and *irf7* expression levels. The *il1b* mRNAs were up-regulated in fish from the Y group compared to the C, MAe and MA groups (P<0.05; Fig. 34). Moreover, *irf7* transcripts were increased in the Y group compared to the C and MAe groups. In contrast, *tnfa* and *cxc10* appeared significantly down-regulated (P<0.05) in fish from the MAe group compared to the

other three groups. The most pronounced change in expression was observed at 3 and 24 h after intubation. The *irf3* mRNAs showed a clear interaction between factors, and were down-regulated in Y, MAe and MA groups with respect to the C group after 3 h and an inverse response was obtained at 48 h (Fig. 34). An effect of time was observed for *tnfa*, *cxc*, *irf3*, *irf7* and *clec*. No significant changes in gene expression of *lysg* and *hamp1* were observed (data not shown).

In the spleen, expression levels were only analyzed 24h after the intubation treatments (Fig. 35). A down-regulation of *il1b*, *tnfa*, *cxc10*, *lysg*, *irf3* and *cd4* mRNA levels occurred in the MAe group and *tnfa*, *irf3* and *cd4* were down-regulated in the Y group relative to the C group. Moreover, *il1b* was up-regulated in the spleen of fish from MA group compared to the other three groups.

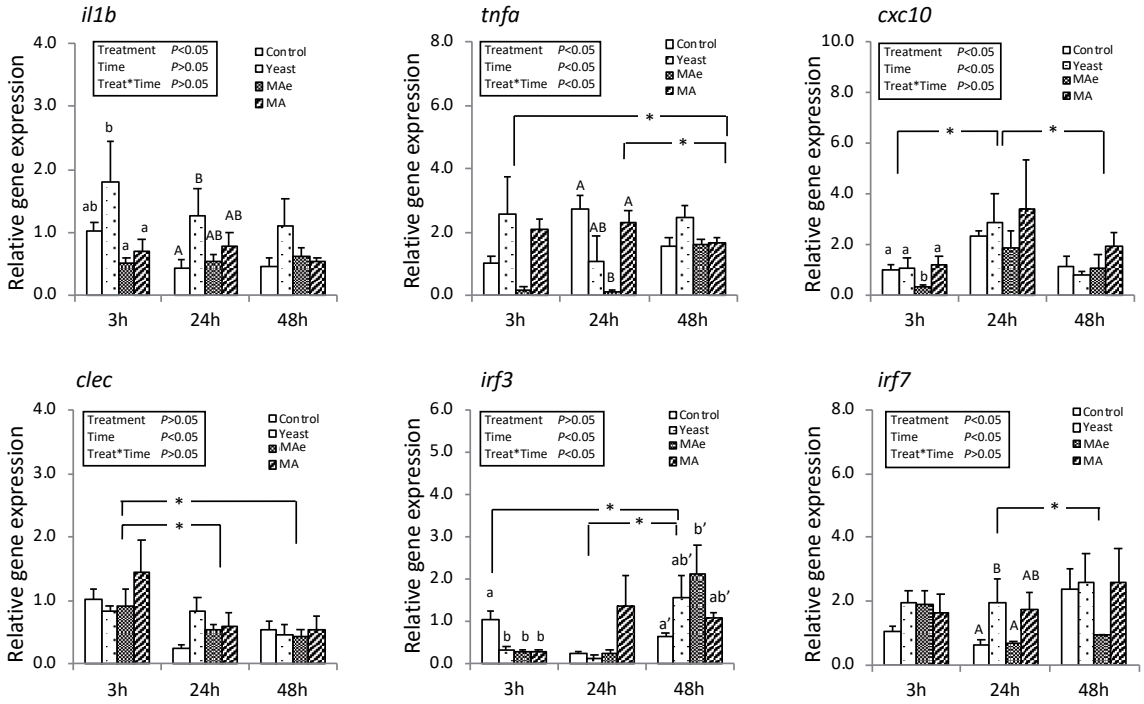

Figure 34: Relative gene expression levels in the intestine at 3, 24, and 48h after oral intubation. Four experimental groups are indicated: control, treated with insoluble yeast β-glucans (Yeast), microalgal extracts (MAe) and whole-cell microalgae (MA). Data were expressed as the mean fold change (mean ± SEM, n = 3) from the calibrator (control 3h after oral intubation). A two-way ANOVA was used to determine statistical differences. Different letters indicate significant differences between oral intubation treatments for a specific time point. Asterisks denote significant differences between samples at different times post-intubation. Significant differences were set at $P<0.05$ (Two-way ANOVA).

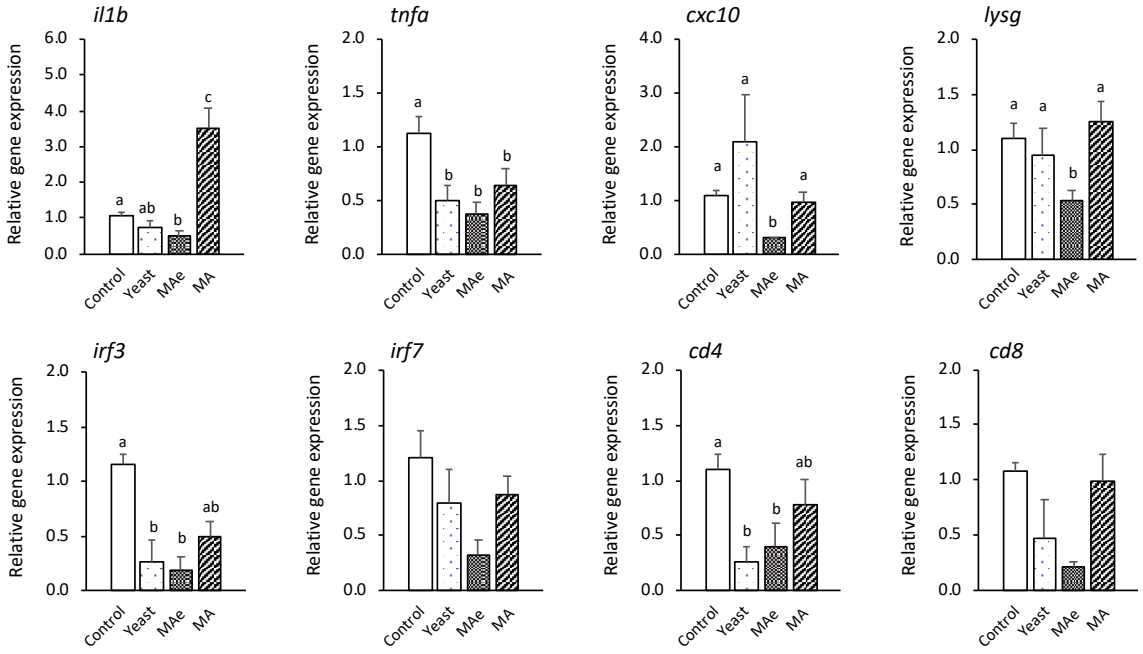

Figure 35: Relative gene expression levels in the spleen 24h after oral intubation. Four experimental groups are indicated: control, treated with insoluble yeast β-glucans (Yeast), microalgal extracts (MAe) and whole-cell microalgae (MA). Data were expressed as the mean fold change (mean ± SEM, n = 3) from the calibrator (control 3h after oral intubation). Different letters indicate significant differences between oral intubation treatments. Significant differences were set at P<0.05 (one-way ANOVA).

7.3.3 Medium-term expression profiles in the intestine and spleen

The gene expression profiles in the intestine 7 days after intubation revealed an up-regulation of *clec* and *irf7* in the Y, MAe and MA groups relative to the C group. In the spleen, only *il1b* was significantly up-regulated in the MA group compared to the C group (Table 4).

Table 4: Relative expression levels at 7 days after oral intubation. The fold-changes between the control (Ctrl) group with respect to yeast β-glucans (Yeast), microalgal polysaccharide-enriched extract (MAe) and whole-cell microalgae (MA) are indicated. A one-way ANOVA was carried out followed by Tukey's posthoc test (significance at $P<0.05$ is indicated by "*"; ns, not significant).

Gene name	Gene description	Intestine					
		Ctrl vs Y		Ctrl vs MAe		Ctrl vs MA	
il1b	Interleukin 1b	0.60±0.11	ns	0.80±0.17	ns	1.17±0.2	ns
tnfa	Tumor necrosis factor α	1.41±0.11	ns	1.90±0.56	ns	1.90±0.4	ns
lysg	g-type lysozyme	1.17±0.06	ns	1.11±0.33	ns	1.18±0.1	ns
cxc10	Chemokine cxc10	1.19±0.11	ns	1.45±0.91	ns	3.46±1.2	ns
irf3	Interferon regulatory	1.07±0.37	ns	1.34±0.69	ns	2.88±1.6	ns
irf7	Interferon regulatory	2.81±0.80	*	4.36±1.37	*	4.74±1.6	*
hamp1	hepcidin	0.82±0.06	ns	0.82±0.09	ns	1.04±0.2	ns
clec	c-type lectin	1.85±0.27	*	1.87±0.39	*	2.97±0.1	*
		spleen					
		Ctrl vs Y		Ctrl vs MAe		Ctrl vs MA	
il1b	Interleukin 1b	2.13±1.05	ns	2.17±0.69	ns	3.23±0.5	*
tnfa	Tumor necrosis factor α	0.98±0.35	ns	0.58±0.09	ns	0.46±0.1	ns
lysg	g-type lysozyme	1.74±0.25	ns	1.84±0.35	ns	1.90±0.5	ns
cxc10	Chemokine cxc10	1.24±0.21	ns	1.92±0.59	ns	3.27±1.0	ns
irf3	Interferon regulatory	1.01±0.21	ns	0.60±0.23	ns	0.60±0.1	ns
irf7	Interferon regulatory	1.02±0.14	ns	0.93±0.33	ns	1.10±0.2	ns
cd4	Cluster differenciation 4	1.04±0.33	ns	0.48±0.16	ns	1.30±0.3	ns
cd8a	Cluster differentiation 8a	0.91±0.13	ns	1.65±0.25	ns	0.85±0.1	ns

7.3.3 Microbiome modulation

To evaluate the effect of treatments on microbiome composition, more than 200,000 reads for the amplified 16S rRNA gene, which yielded an average of 23,457 good-quality reads per library (Table 5), were analysed. Rarefaction analysis (Fig. 36) confirmed that most libraries were close to saturation at the sequencing depth utilised and indicated that most of the bacterial diversity was covered. The results indicated that the intestinal microbiome had low complexity, with around 150 OTU genera detected in the C group and a lower number of OTUs in the treatment groups. A Chao1 index of 313 for the C group, 191 for the MAe, 155 for the Y and 265 for the MA groups also indicated that treatments decreased the microbiome species richness. The Shannon diversity indexes were 1.7 for the C group, 1.9 for

MA, 1.3 for MAe and 1.1 for Y, and reinforced the notion of reduced bacterial diversity in the sole gut for MAe and Y treatments.

Table 5. Sequencing statistics from 16S rRNA gene microbiome analyses. Number of raw, paired-end and filtered reads and the final average lenght, total data (in Megabases) and average quality are shown for each microbiome library from the middle intestine of Senegalese sole, 7 days after oral intubation with the 4 treatments: control (C), yeast β-glucans (Yeast), microalgal extracts (MAe) and whole-cell microalgae (MA).

Library	Raw reads	Paired-end reads	Filtered reads	Av. Length	Total Mb	Av. Qual.
C	63134	30765	26611	420.7	11.2	36.7
Yeast	45542	21801	19163	419.4	8.0	36.7
Mae	54494	26222	22520	418.3	9.4	36.6
MA	60038	29399	25535	421.6	10.8	36.6
Total	223208	108187	93829		39.4	
Average	55802	27047	23457	420.0	9.9	36.6

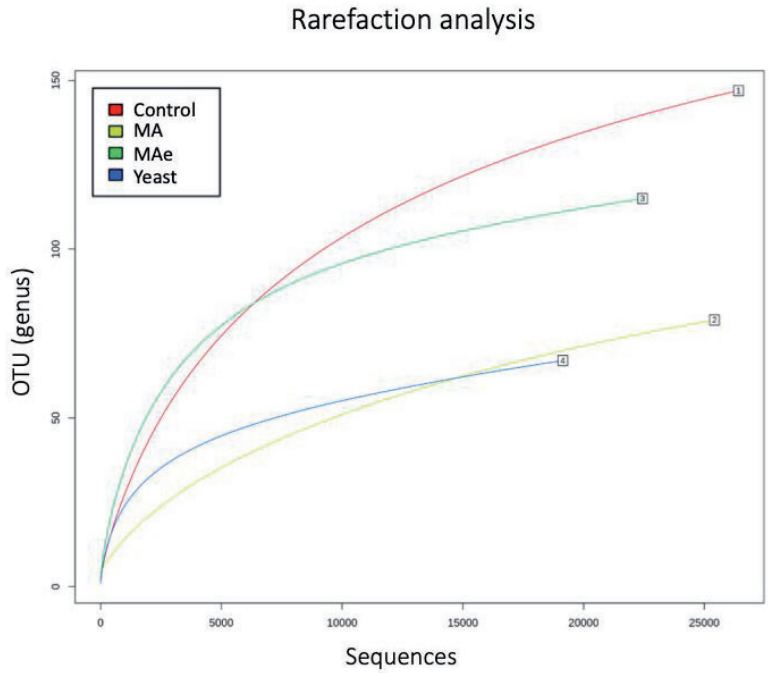

Figure 36. **Rarefaction curves**. Control (C), yeast β-glucans (Yeast), microalgal extracts (MAe) and whole-cell microalgae (MA).

A total of 243 different genera were identified but only five genera were present at more than 1% in the intestinal microbiome (not shown). The dominant bacterial genera in the intestine of the C group or in treated sole was *Vibrio*, which accounted for 93% of the control microbiome. Lower proportions of *Vibrio* were detected in the Y and MAe groups (86% and 88% *Vibrio*, respectively) followed by the MA group with 73% *Vibrio* (Fig. 37A). At the species level, a non-pathogenic *Vibrio scophthalmi* cluster, was the most abundant species and accounted for 56-74% of the annotated bacterial reads across the treatments (not shown). The second most abundant bacterial genus in the microbiome was *Catenococcus*, present at 0.6% of the C group but increased to 6.7, 2.5 and 17.4% in the Y, MAe and MA groups, respectively. Finally, the genera *Brevinema*, *Shewanella* and *Mycoplasma* comprised up to 5.7% of the intestine microbiomes but varied relatively little between the treatment groups (Fig.37A). Hierarchal clustering analysis separated the polysaccharide treatments (Y and MAe) from the C group. The MA treatment had the most divergent microbiome composition relative to the other groups (Fig. 37A). The significant decrease ($P<0.05$) in the load of bacteria from the *Vibrio* genus in the intestine of juvenile sole from the MAe and Y groups compared to the C group was confirmed by qPCR (Fig. 37B). No significant differences were detected in the load of *Mycoplasma* bacteria between the treatment groups and C group (not shown).

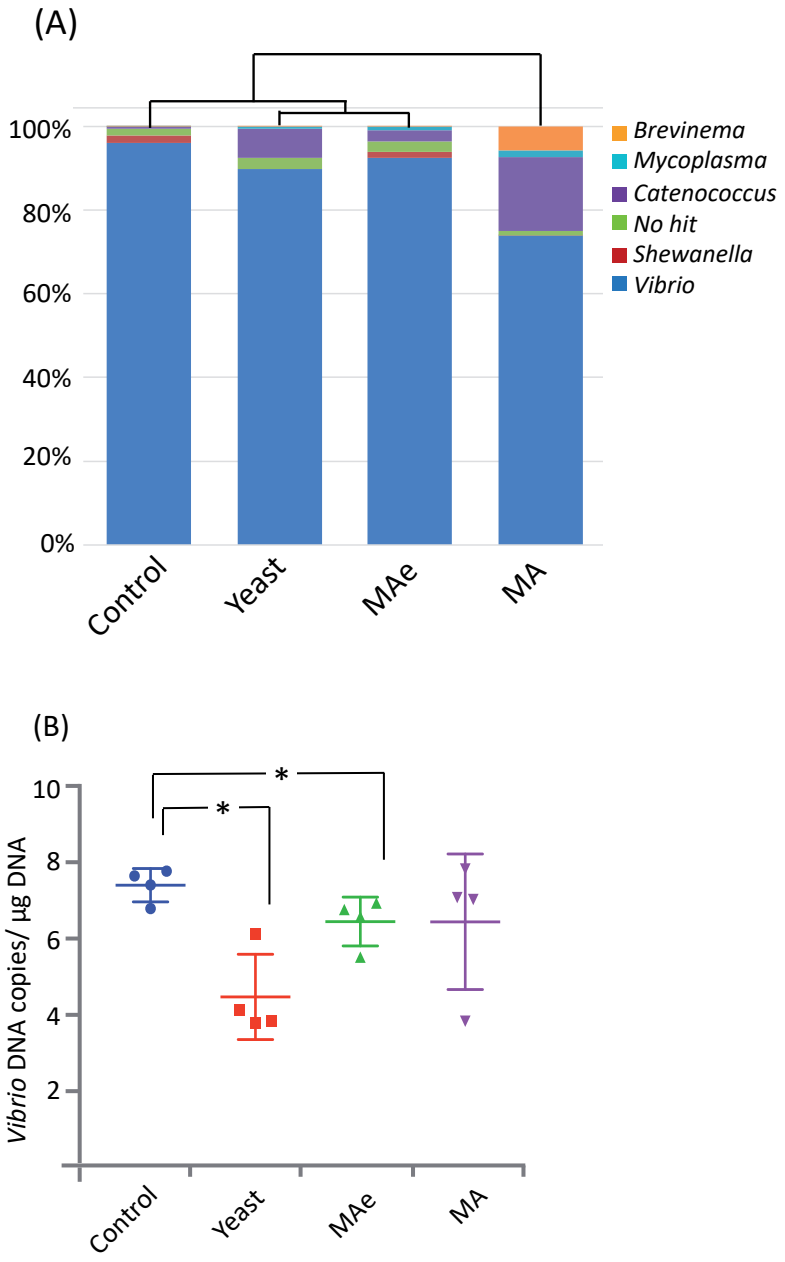

Figure 37: A- Microbiome gut composition (in percentage) for the main bacterial genera, present at >1% representation. The scheme represents the hierarchal clustering of the main bacterial genera in the gut of the four experimental groups: control, treated with insoluble yeast β-glucans (Yeast), microalgal extracts (MAe) and whole-cell microalgae (MA). B- Quantification by qPCR using genera-specific primers for *Vibrio* DNA in each group (bars represent the mean ± SEM of n=5 fish gut DNA/group, normalized using µg of DNA used in each PCR). * indicate significant differences compared to the control with P<0.01(Student's t-test).

Heritability estimates and genetic correlation for growth traits and LCDV susceptibility in the gilthead sea bream (*Sparus aurata*)

Manuscript in preparation

8.1 Introduction

The lymphocystis disease (LCD) is a highly contagious viral infection responsible for high economic losses in the aquaculture industry worldwide (Borrego *et al.* 2017b). The causative agent is the lymphocystis disease virus (LCDV) that belongs to the genus *Lymphocystivirus*, family *Iridoviridae.* This virus is hosted in the infected fish for long periods causing no clinical signs (known as asymptomatic carriers) until host immunocompetence decreases due to different factors such as temperature shifts, grading operations, transport or high tank densities. Then, the virus actively multiplies in host cells giving arise to the typical lesions (named as lymphocysts) consisting of irregularly shaped, randomly distributed white masses in the integumentary surfaces that in severe infections aggregate in nodular structures (Paperna *et al.* 1982). Experimental challenges have demonstrated that at least three weeks after LCDV injection are required for the observation of clinical signs (Kvitt *et al.* 2008; Hossain *et al.* 2009; Borrego *et al.* 2017b). Once the lesions appear, the disease spans for approximately 20 days, the time required for the hypertrophic dermal cells mature and break resulting in high morbidity but low mortality rates unless secondary infections occur (Paperna *et al.* 1982; Smail & Munro 2001; Kvitt *et al.* 2008; Colorni & Padrós 2011). In spite of being a self-limiting benign process (Kvitt *et al.* 2008), LCDV infection has a high economic impact in the hatcheries due to the important delay in fish growth, reducing feed conversion rates and making fish unavailable for commercialization due to external lesions and the lack of acceptance by the consumers.

Several approaches have been established to control LCDV outbreaks in the hatcheries in the absence of efficient commercial vaccines. The most extended approach is the monitoring and removal of asymptomatic carriers by using highly sensitive diagnostic methods (Valverde *et al.* 2016b; 2017a). This strategy has been successfully applied to prevent vertical transmission but it requires a continuous evaluation of broodstocks and does not prevent horizontal transmission. A second

approach is the use immunostimulants supplied through the diet to enhance immune response and block virus replication (Harikrishnan *et al.* 2010a; Sun *et al.* 2013). This strategy is especially useful when stressful operations in the hatcheries are planned and preventive measures can be implemented. A third approach is genetic selective breeding for resistance lineages. In *Paralichthys olivaceus*, a major locus associated with resistance against LCDV genotype II was identified (Fuji *et al.* 2006) and used for the design of marker-assisted breeding programs and LCDV-resistant broodstocks (Fuji *et al.* 2007). This latter strategy has revealed as one the most sustainable strategy to reduce and minimize the impact of LCDV outbreaks in aquaculture although it requires evaluation of genetic variation in species-specific populations.

The gilthead sea bream (*Sparus aurata*) is one the most cultured fish species in the Mediterranean basin. This species is infected by genotype VII that it is frequently observed in other Mediterranean species such as Senegalese sole (Cano *et al.* 2010; Carballo *et al.* 2017). LCDV outbreaks are recurrently observed every year and, occasionally, associated with high mortalities (Kvitt *et al.* 2008; Haddad-Boubaker *et al.* 2013). Currently, most of genetic programs ongoing for this species are mostly focused on the improvement of growth, morphology and carcass quality (Garcia-Celdran *et al.* 2015a; 2015b; Lee-Montero *et al.* 2015; Navarro *et al.* 2016). Genetic estimates for disease resistance were only reported for the bacterial pathogen *Photobacterium damselae* subsp. *piscicida* (Antonello *et al.* 2009; Palaiokostas *et al.* 2016). However, the genetic variation controlling susceptibility to LCDV in sea bream remains still unexplored. This study aimed to estimate genetic parameters (heritabilities and genetic correlations) for LCDV susceptibility (as evaluated by the number of DNA viral copies and the severity of lesions as function of surface covered and intensity) and growth (weight and length) in gilthead sea bream. The results are the first step to create new genetically-improved broodstocks with a

lower susceptibility to this disease that can enhance the sustainable production of this important aquacultured species.

8.2 Materials and methods

8.2.1 Animals

Three broodstocks hosted at center IFAPA El Toruño (El Puerto de Santa María, Spain) belonging to the Spanish genetic breeding program PROGENSA® were used for family production: a) Non-selected animals or control broodstock (52 breeders, 4 years old); b) F1+F2 Broodstock that included animals of two 1st (females) and 2nd (males) generations selected for growth (30 breeders; 7 years old in the case of females and 4 years old for males); c) F2 broodstock that included only animals selected for growth of the 2nd generation (57 breeders; 4 years old). The female:male ratio was approximately 2:1 in the tanks. The three broodstocks were under a controlled photoperiod (8L:16D) to synchronize maturation and egg release that was initiated at the beginning of December 2016. During this period, animals were fed ad libitum Vitalis Cal (Skretting) and egg production was daily monitored. When total egg production became stable, two egg batches were established: one at the end of February and another in early April 2017. In both cases, eggs from the three broodstocks were collected and pooled for 4 consecutive days to maximize family production according to the 4DL model (Elalfy *et al*., unpublished). Incubation was carried out in cylinder conical tanks (1,000 l) at a density of 500-1000 larvae/l. Water conditions were as follows: temperature 19.0°C, salinity 34 ppt and dissolved oxygen 6.4 mg/l. All spawns were checked by PCR to confirm the absence of LCDV infections as a previously reported (Valverde *et al.* 2016b). As the LCD is very difficult to experimentally reproduce in the lab due to the highly dependence on environmental factors, viable non-hatched eggs and hatched larvae were transported to an industrial hatchery in Huelva (Spain) in which LCDV outbreaks were previously observed. Both larval batches were reared at an initial density of

100 larvae/l in 5 m^3 tanks. Rearing protocols were those used in the hatchery at commercial scale and these two batches were always managed as experimental units not graded until sampling.

The LCDV outbreak occurred in June 2017 with temperature 26ºC and salinity 36 ppt. At the moment of the sampling, clear lesions compatible with LCDV infections were evident in the animals. As our animals were cultivated under industrial conditions and all tanks were managed in the same way, no negative tanks were available. LCDV infection was confirmed by qPCR and the degree of lesion intensities were determined image analysis. A total of 500 animals were randomly sampled from each batch and *in situ* sacrificed in slurring ice to preserve external lesions and thereafter transported to center IFAPA "El Toruño" for phenotyping and samplings. The two batches were named as batch1 (eggs from April; age ~80 days post-hatch (dph)) with a high number of typical lymphocysts and batch2 (eggs from February: ~140 dph) with less prominent lesions but all characteristic of LCDV infection.

8.2.2 Data collection and image analysis

All animals were handled under strict biosecurity measures to avoid virus propagation in the facilities. All animals were photographed individually using a Canon Eos1300D camera following the methodology previously established in PROGENSA® (Navarro *et al.* 2016). Then, animals were weighted and individually frozen at -20ºC for later tissue sampling. All procedures were authorized by the Bioethics and Animal Welfare Committee of IFAPA.

Image analysis was carried out using the Fiji 2.0.0-rc-69/1.52i (Schindelin *et al.* 2012). All fish specimens were measured for furcal length and later evaluated for the extent of surface covered by lesions and their intensity by dividing the specimens in three corporal regions (Table 6; Fig.41): region1 (R1) that spanned from caudal part of the operculum to the end of pectoral fin; region (R2) that spanned from the end of pectoral fin to the base of caudal fin; region3 (R3), caudal

fin. Each region was ranked as 1 if lesions were covering less than 30% surface, 2 if between 30 and 70% and 3 if more than 70% (Table 6). Head was not considered due to the difficulty to clearly visualize the lesions. Moreover, lesion intensities were established for each region as 1 if they were not prominent, 2 if slightly prominent and 3 when lymphocysts were evident (Table 6). All animals were independently evaluated by two researchers for phenotypic traits (surface and intensity) and both evaluations were used to build a consensus rating for each animal. Moreover, the severity index from surface (S) covered by lesions and their intensity (I) was calculated as follows: SI= S*I using the mean of the three regions for S and I. Such index oscillates between 1 and 9 and was used to define 4 categories for genetic analysis: weak, moderate, severe or very severe (Table 6).

Table 6. Rates (R) for LCDV lesions according to surface covered and intensity. Categories for severity index are also shown

Surface		Intensity		Severity index	
R	%	R	Type	R	Category
1	<30	1	White layer but not prominent	1-2	weak
2	30-70	2	Slightly prominent	2-4	moderate
3	>70	3	lymphocysts	4-8	severe
				8-9	very severe

8.2.3 Quantification of viral DNA

Although the skin is the organ with the highest number of viral DNA copies, LCDV also replicates in the liver (Kvitt *et al.* 2008; Valverde *et al.* 2017a). This organ was selected as the target organ to quantify the viral DNA copies in each specimen since it provides enough biomass for the nucleic acid isolation minimizing the risk of cross-contamination between individuals. Livers were aseptically dissected, individually separated in eppendorf tubes and kept frozen at -20ºC until processing. All materials were cleaned with ethanol and distilled water between animals. In the case of *batch1*, total DNA was isolated using Isolate II Genomic DNA Kit (Bioline) and in the case of *batch2*, DNA samples were purified using

phenol:chloroform:isoamyl alcohol (Sigma) following the manufacturer's instructions. DNA samples were treated with RNase A (Bioline) and quantified spectrophotometrically using the Nanodrop ND-8000. Absolute quantification of viral DNA copies was carried out according to the protocol specified by Valverde *et al.* (2016b) based on the quantification of the major capsid protein (*mcp*). Assays were run in a CFX96™ Real-Time System (Bio-Rad) in a 10 µl final volume containing 200 ng of DNA, 300 nM each of specific forward and reverse primers, and 10 µl of iQ™ SYBR® Green Supermix (Bio-Rad). The amplification protocol used was as follows: initial 7 min denaturation and enzyme activation at 95 ºC, 40 cycles of 30 s at 95 ºC and 1 min at 59 ºC.

8.2.4 Genotyping and parentage assignment

DNA for offspring parentage assignment was isolated from liver as previously reported in section 2.3. Breeders were sampled before the spawning season and blood (~0.5 ml) was taken by puncturing in the caudal vein using a heparinized syringe, added heparin (100mU) and kept at -20ºC until use. DNA from breeders was extracted from blood using the Isolate II Genomic DNA Kit and treated with RNase A (Bioline) following the manufacturer's instructions.

Genotyping was carried out using multiplex PCR SMsa-1 and SMsa-2 (Lee-Montero *et al.* 2013). PCRs were run in the ABI3130 Genetic Analyzer (Applied Biosystems) and data analyzed using the Genemapper v3.8. Parentage assignment was determined using the exclusion method using Vitassign v8.2.1 (Vandeputte *et al.* 2006). The breeder gender was considered as unknown.

8.2.5 Statistical analysis

Comparison of rates for surface covered by lesions and their intensity was carried out by nonparametric tests Wilcoxon test or Kruskal-Wallis. Data for weight and number of LCDV DNA copies were log-transformed to achieve adjustment to normality. Statistical analysis to test phenotype differences were carried out using

Prism8 (Graphpad). Variance components associated with the susceptibility to LCDV were estimated separately for *batch1* and *batch2* based on bivariate linear mixed models fitted by restricted maximum likelihood (REML) in Wombat (Meyer, 2007): $y = X\beta + Zu + e$, where y is the observed trait, β, is the vector for fixed factor (broodstock origin), u is the vector for animal random factor and e is the error. Heritability and the phenotypic and genotypic correlations were calculated for four traits: weight, length, number of LCDV DNA copies and LCDV susceptibility as defined by SI in binary scale: 0=weak/moderate and 1=severe/very severe. Some runs using the weight as covariate for SI were also carried but no effect on genetic estimates was determined and hence not included in the analyses.

Heritability estimates for binary LCDV susceptibility in the observed scale were later transformed to the underlying liability scale according to Dempster & Lerner, (1950) using the formula $h^2 = [p(1-p)/z^2] \times h^2_{obs}$, where h^2_{obs}, is the heritability on the observed scale (binary trait), h^2 is the heritability on the liability scale, p is the proportion of affected individuals and z is the density of a standard normal distribution at the pth quantile. In addition, heritability estimates for binary LCDV susceptibility were also calculated using a Bayesian framework under the threshold model as implemented in the MCMCglmm R package (Hadfield 2010). A χ^2 distribution with one degree of freedom as the prior distribution and we applied a probit scale and fixed the value of the residual variance to 1 was used. MCMC run for 1 million iterations with a thinning interval of 100 after a burn-in of 100 000 (de Villemereuil et al. 2013). Binary trait heritability was estimated as $h^2 = Va/(Va+1+1)$ as described in the course notes for the program MCMCglmm (Hadfield 2010).

8.3 Results

8.3.1 Biometric data

Two fish experimental batches (*batch1* and *batch2*) were evaluated for LCDV-susceptibility after a disease outbreak in a commercial hatchery. These fish batches were built by collecting the eggs during four consecutive days (4DL model) for family production from three sea bream broodstocks and they were always managed as a single unit under the same culture conditions from larval stages until disease outbreak and sampling. At the moment of disease outbreak, average weight was 1.3±0.5 g for *batch1* (~80 dph) and 3.8±1.1 g for *batch2* (~140 dph) (P<0.05; Fig. 38A). Average length was 3.8±0.4 cm for *batch1* and 5.3±0.4 cm for *batch2* (P<0.05; Fig. 38B).

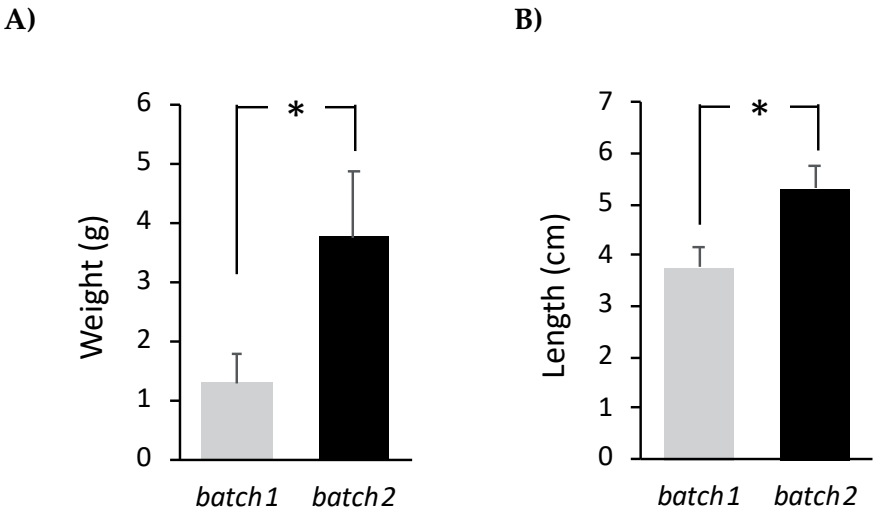

Figure 38. Weight and length for batch1 and batch2. The mean ± standard deviation is indicated (total n=498 for each batch). Asterisk denotes significant differences between batches

8.3.2 Disease phenotyping

All sampled animals had external skin lesions compatible with the LCDV infection (100% morbidity). To quantify the percentage of surface covered by lesions and their intensity, each animal was photographed and later analyzed by

image analysis for three regions (R1-R3). (see M&M section; Table 6 and Fig. 41). Phenotype data for surface and intensity traits are depicted in Fig. 39. Wilcoxon test showed that surface covered in *batch2* was significantly lower than *batch1* ($P<0.05$; average 2.55 and 2.49 for *batch1* and *batch2*, respectively). Analysis of the body region revealed that the surface of regions 1 and 2 was more affected (2.73±0.47 and 2.66±0.55) than region 3 (2.27±0.77) ($P<0.05$) in *batch1* (Fig. 39). In contrast, a gradient from region 1 (2.86±0.35) to region 3 (1.92±0.83) ($P<0.05$) was detected in *batch2*. Lesion intensities were also significantly ($P<0.05$) higher in *batch1* than *batch2* (average 1.9±0.7 vs 1.5±0.6) (Fig. 39). No differences in intensity among regions were observed (1.79-1.93 for *batch1* and 1.4-1.6 for *batch2*).

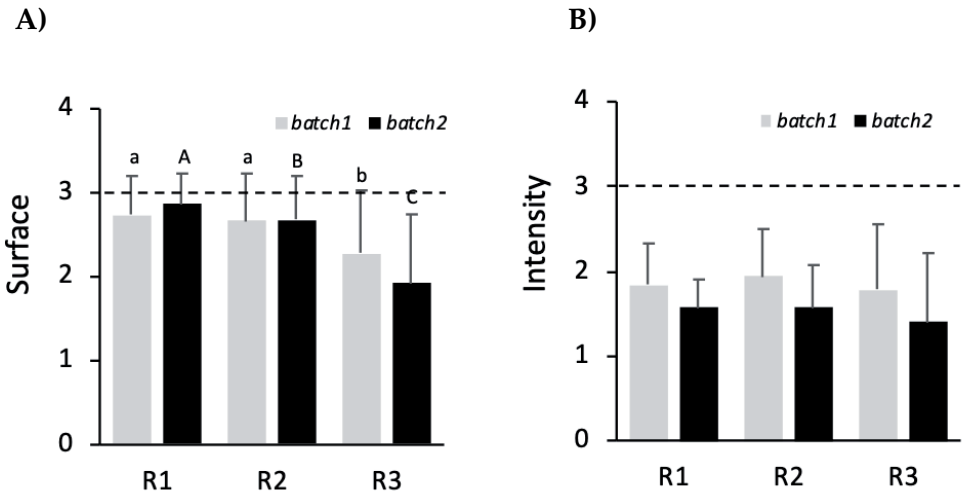

Figure 39. Rates of surface covered (a) and lesion intensity (b) for regions (R) 1, 2 and 3 in *batch1* and *batch2*. The dashed line indicates the maximum rate value. Letters indicate significant differences between regions for batch1 (lowercase) or *batch2* (uppercase). Mean ± standard deviation is indicated.

To better characterize the genetic variation and the correlations between productive traits, the severity index (SI) was used to classify the animals into four categories: weak, moderate, severe or very severe (Fig. 40). The average SI was 5.0±2.6 and 3.9±2.2 for *batch1* and *batch2*, respectively. In *batch1*, 60% of fish was considered as severe or very severe infected and this percentage dropped to 40% in *batch2* (Fig. 40).

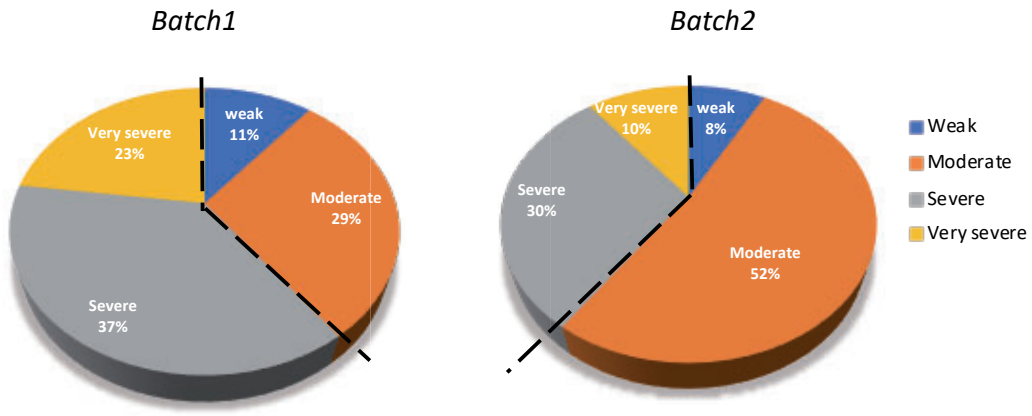

Figure 40. Representation of SI categories in *batch1* and *batch2*. The percentages for the four categories are indicated. The dashed line indicates the binary classifaction as low (weak and moderate) and high (severe and very severe) susceptible fish

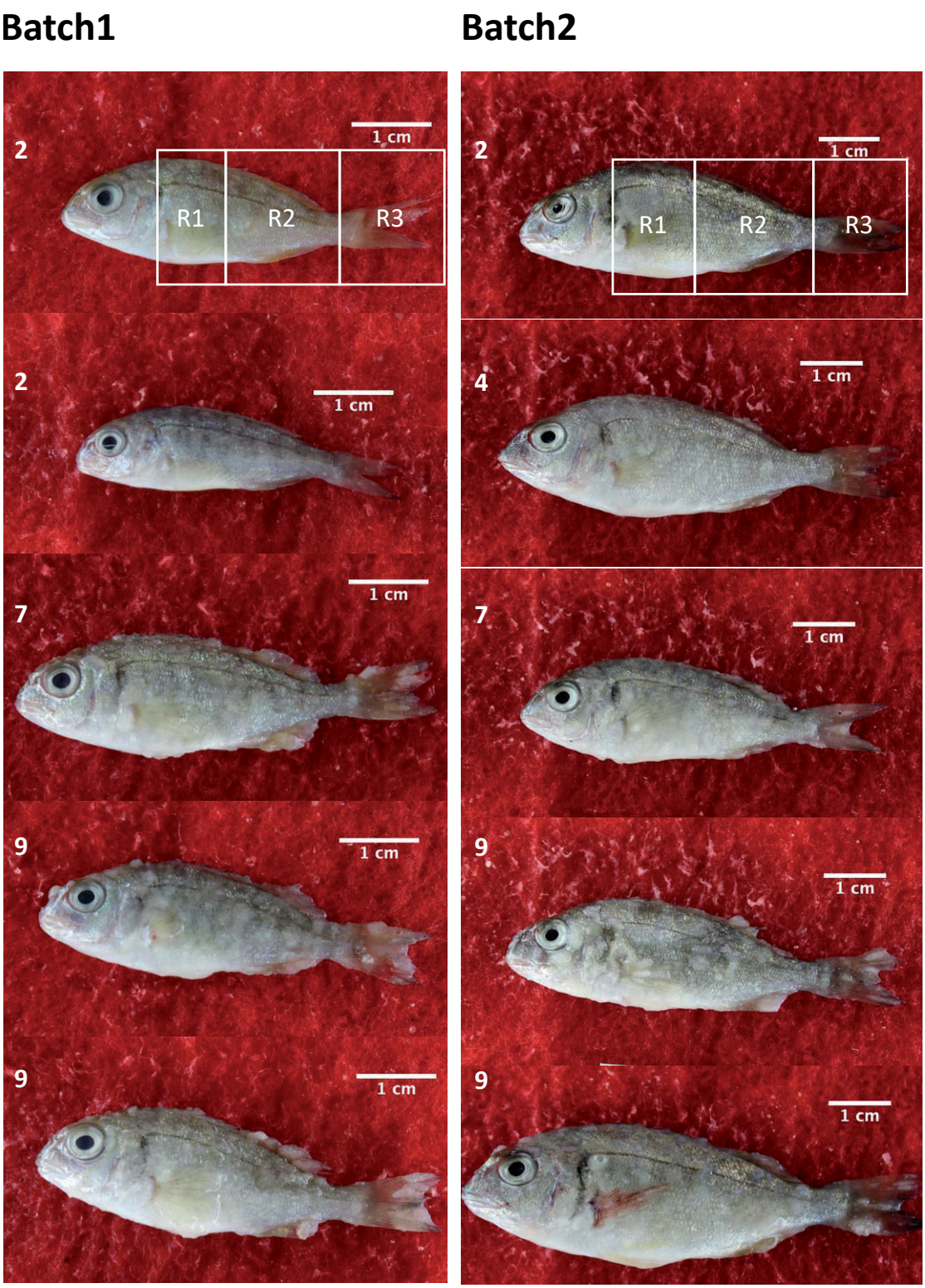

Figure 41. Images of evaluated fish for *batch1* adnd *batch2*. Length scale is indicated. Regions 1, 2 and 3 and the SI for each animal are indicated.

8.3.3 Quantification of viral DNA copies.

Viral DNA copies were quantified in the liver of fish from *batch1* and *batch2* (Fig. 42). The average number of LCDV copies was $9.2x10^{7}\pm7.2x10^{8}$ µg total/DNA in *batch1* and $6.3x10^{5}\pm5.9x10^{6}$ µg total/DNA in *batch2*. Interestingly, a high and positive correlation between the average number of viral DNA particles in liver and the SI categories (r^2=0.90-0.94) was determined (Fig. 42).

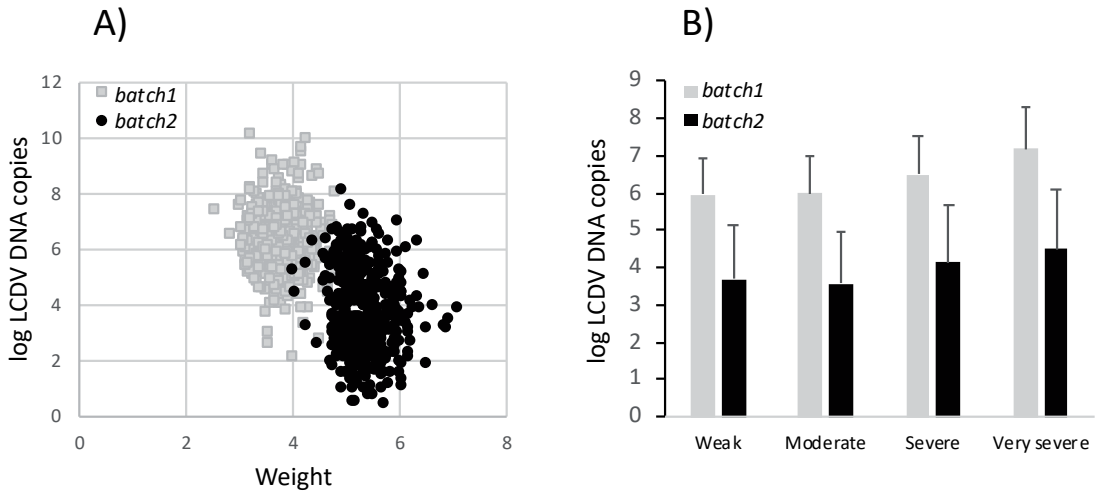

Figure 42. LCDV DNA copies in logaritmic scale for *batch1* and *batch2*. A) DNA copies as function of weight; B) DNA copies as function of four SI categories.

8.3.4 Parental contribution and genetic estimates

The 95.9% of the progeny in *batch1* were assigned to one breeder and 86% to a unique parent pair. These figures were 93.4 and 84.0% in *batch2*. The total number of families were 150 and 128 for *batch1* and *batch2*, respectively with the 87% offspring assigned F2 broodstock, 9.7% to broodstock F1+F2 and 3.3% to the non-selected control broodstock. A total of 54 out of the 82 breeders contributed offspring although with a high bias in contribution percentages (Fig. 43). The reconstructed breeder sex ratio contributing offspring was 1M:2.8F and 1M:1.6F for *batch1* and *batch2*, respectively. Males showed a higher bias (P<0.05) in offspring contribution per breeder than in females with maximal percentages ranging

between 31 and 51% for *batch1* and *batch2*, respectively (9 and 16%, respectively in female). The analysis of SI and the number of LCDV DNA copies by family indicated a large variation that was even more evident in *batch2* (Fig. 44). The SI ranged from 1.7 to 9 in both batches and the log number of viral DNA copies between 4.6-7.9 (in logarithmic scale) in *batch1* and 1.8-6.2 in the *batch2*.

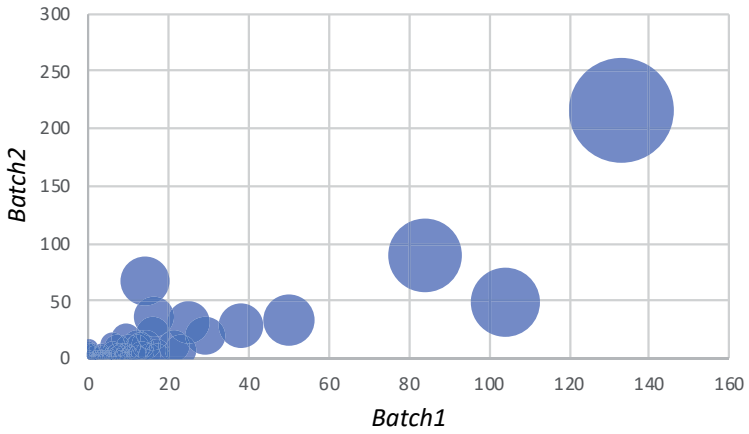

Figure 43. Parental offspring contributions in *batch1* and *batch2*. The circle size is proportional to the offspring family sizes.

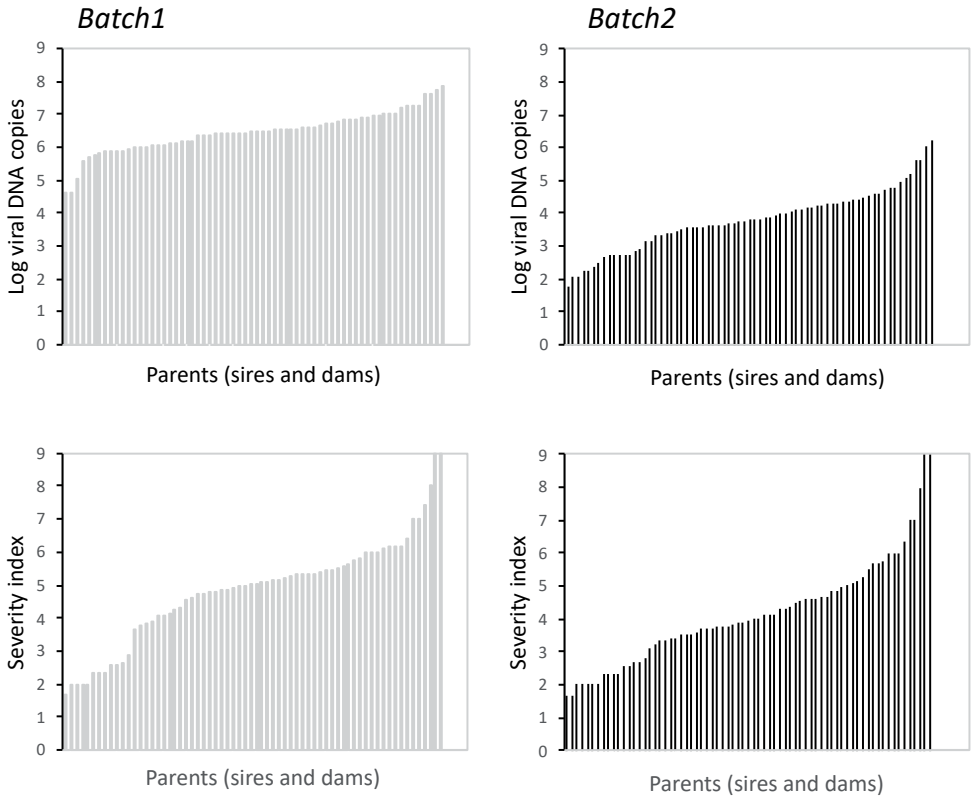

Figure 44. Variation in LCDV DNA copies in logaritmic scale and SI of sire and dam families for *batch1* and *batch2*.

The heritability and genetic correlation estimates for weight, length, LCDV DNA copies and SI in binary scale (SI) are presented in Table 7. Heritabilities for weight and length were 0.18 and 0.14 in *batch1*, respectively and they decreased to 0.06 and 0.05 in *batch2*. Heritability for the number of viral DNA copies was low in both batches (0.04 and 0.08 for *batch1* and *batch2*, respectively).

Table 7. Heritabilities (in bold) and the phenotypic (below the diagonal) and genetic correlations (above the diagonal). Means ± standard deviations (SD) are indicated for body weight, fork length, LCDV DNA copies and SI in binary scale (SI).

Batch1	weight	length	DNA copies	SI
weight	**0.18±0.10**	0.98±0.03	0.50±0.68	0.67±0.30
length	0.93±0.01	**0.14±0.09**	0.34±0.65	0.44±0.39
DNA copies	-0.04±0.05	-0.04±0.05	**0.04±0.05**	0.99±0.35
SI	0.10±0.05	0.03±0.05	0.32±0.05	**0.20±0.10**§
				0.32±0.16‡
Batch2	weight	length	DNA copies	SI
weight	**0.06±0.07**	0.94±0.12	-0.90±0.64	-0.79±0.65
length	0.89±0.01	**0.05±0.08**	-1.00±0.72	-0.80*
DNA copies	-0.12±0.05	-0.16±0.05	**0.08±0.08**	0.99±0.43
SIs	-0.25±0.05	-0.24±0.05	0.20±0.05	**0.14±0.08**§
				0.21±0.09‡

(*) No SD was retrieved after convergence.
(§) heritability for binary SI in the observed scale
(‡) heritability for binary SI in the liability scale

To estimate the genetic susceptibility to LCDV infection under the threshold model, animals were binary coded according to SI: weak/moderate vs severe/very severe. In the observed scale, the heritability for the binary SI was 0.20±0.10 and 0.14±0.08 for *batch1* and *batch2*, respectively. When heritabilities were transformed to the liability scale, the values increased to 0.32 and 0.21, respectively. A Bayesian linear mixed model was also carried out to estimate heritability using the binary-coded LCDV susceptibility data. The Bayesian narrow-sense heritability estimate was 0.33 and 0.24 for *batch1* and *batch2*, respectively, with a 95% Bayesian credibility interval for the additive genetic component of 0.12–0.67 and 0.01-0.53 (Fig. 45).

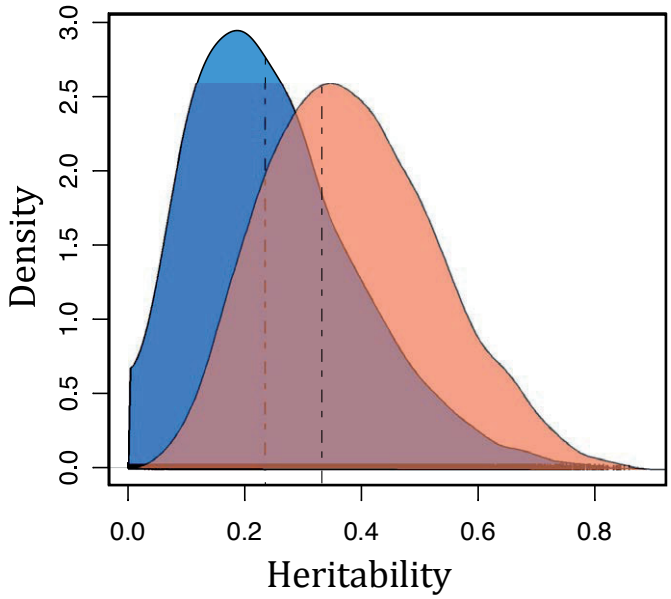

Figure 45. Posterior distributions of the heritability estimates for *LCDV* susceptibility in batch1 (red) and batch2 (blue) generated from Bayesian MCMCglmm models. Dashed lines correspond to distribution modes.

The genetic and phenotypic correlations between the weight, length, LCDV DNA copies and SI are given in Table 7. Genetic correlations were very high and positive between growth traits (weight and length) and between disease traits (number of LCDV DNA copies and SI) in both batches. However, when growth and disease traits were compared, the genetic correlations were positive and moderate-high in the *batch1* but negative in *batch2*. It should be noted that for length and SI, the model converged but did not provided errors. Phenotypic correlations between weight and length were high and positive and moderate and positive between LCDV DNA particles and SI. In *batch1*, the phenotypic correlations between biometric and susceptibility traits were close to zero while in *batch2* were low and negative.

GENERAL DISCUSSION

9.1 Feed and immersion challenges with Lymphocystis Disease Virus (LCDV) reveals specific mechanisms for horizontal transmission and immune response in Senegalese sole post-larvae

Understanding the transmission route used by LCDV to invade fish is critical to establish control and prevention measures in aquaculture facilities. Previous studies in gilthead sea bream demonstrated that both vertical and horizontal transmission routes (through the live preys) play a key role in LCDV epidemiology (Cano *et al.* 2009b; Cano *et al.* 2013; Borrego *et al.* 2017b). However, it is important to demonstrate if other horizontal transmission ways behind the LCD spreading exist as well as their main pathological consequences. The results of the chapter 3 demonstrates that LCDV infects Senegalese sole post-larvae both by immersion in contaminated water and through the feeding using LCDV-enriched artemia metanauplii pointing out these two via as essential in the horizontal transmission of this virus. Moreover, our data indicate that transmission route determine specific tissue distribution patterns, histopathological lesions and time-course response of defensive genes. Immersion challenge resulted in the highest viral load at the beginning of LCDV infection trial although the infection rates and the estimated number of viral DNA copies were kept at low levels at the end of the trial in both experimental infections. These results agree with the chapter 4, in which intraperitoneally infected Senegalese sole juveniles rapidly cleared LCDV from peripheral blood as well as from different organs (Carballo *et al.* 2017). However, infected fish still presented a low level of intracellular viral multiplication associated with the persistence of LCDV, a trait not observed in this study probably due to the temporal framework in the study.

Histological analysis confirmed the integrity of the skin barrier in post-larvae from the negative control groups, as expected. However post-larvae infected by immersion showed significant histopathological lesions in the skin, muscle and gills at 2 dpi that were even more evident at 7 dpi. The hypertrophy of mucous cells in

the skin and gut indicated that LCDV triggered a defensive response in the host by modulating mucus production. The increase of mucous cells and their sialic acid glycoproteic content were also reported in LCDV-infected *S. aurata* (Sarasquete *et al.* 1998) and it seems to be a key mechanism that interferes viral receptor binding and bacterial invasion (Zimmer *et al.* 1992; van der Marel *et al.* 2010; Hanson *et al.* 2011). This hypothesis is supported by previous observations in carp in which the removal of the skin mucous layer and the induction of epidermal lesions appear to play a major role in herpesvirus infection (Raj *et al.* 2011). It is noteworthy that gill lamellae were also highly affected by LCDV waterborne infection. Architecture of this tissue accompanied by severe inflammation is also affected by herpesvirus infection in carp (Hanson *et al.* 2011). These results demonstrate that a specific defensive response was activated in both LCDV horizontal transmission routes with the skin and gills as the main portals to LCDV entry in the waterborne infections.

The tissue remodeling observed in peripheral organs matches with the distribution of LCDV genome mainly in external mucosa (skin and gut) but also in the head kidney. The identification of LCDV-hybridization signal surrounding vasculature clearly points out the bloodstream as the main dissemination via for LCDV after immersion challenge. This mechanism agrees with the result of the chapter 4 (Carballo *et al.* 2017) that also detected a rapid spreading of LCDV from the peritoneal cavity through the bloodstream previous to the establishment of a systemic infection in sole juveniles. Unlike the immersion exposure, the vehiculation of LCDV through the feed confined the viral signal to the intestinal *lamina propria* and hepatic parenchyma indicating a tight restriction to virus dissemination. In sea bream larvae infected by feeding on LCDV-positive live preys viral antigens and genomes were firstly located in the digestive tract (Cano *et al.* 2013) but were detected in the skin after 48 h. All these data support the horizontal transmission of LCDV in Senegalese sole through contaminated water and feed,

although the former route leads to a wider virus spread and tissue damages presumably as a part of the defensive response.

Immune organs in Senegalese sole develop very early in the pelagic stage (Castro Cunha *et al.* 2003) and a wide set of innate immune genes are highly expressed in pre-metamorphosis larvae while adaptive genes seem to appear later after metamorphosis (Ponce *et al.* 2011; Salas-Leiton *et al.* 2012; Ferraresso *et al.* 2016). Our study demonstrates a highly coordinated response of interferon-related genes, chemokines, cytokines, lysozyme, complement and T-cell markers in response to LCDV infection, confirming that young post-larvae (31 dph) were able to activate a specific defensive response although with temporal and intensity differences depending on the infection route. Delivery of viral particles through artemia triggered the faster and more intense response. This response was similar to that reported in LCDV-injected sole juveniles that display tissue-specific responses depending on the amount of viral DNA quantified in each tissue (Carballo *et al.* 2017). We hypothesize that the weaker and delayed expression response observed in the immersion-infected fish could be due to a low concentration of LCDV particles in water able to circumvent an intense immune response and reach blood vessels to disseminate throughout the organism. In contrast, artemia concentrated LCDV in the gut allowing a quick viral recognition and a potent and localized immune response that limit virus dissemination and pathogenesis.

Expression profiles associated with LCD in gilthead sea bream with pronounced lesions indicated a down-regulation of antiviral genes such as *ifn* and *irf3* and other involved in cellular immunity in the skin and head kidney of LCDV-positive fish (Cordero *et al.* 2016). In contrast, in flounder (*P. olivaceus*) LCDV triggers the expression of *irf2*, *irf3*, *irf5*, *irf7 irf8* and *irf9* in immune and non-immune organs (Hu *et al.* 2010; 2011; 2012; 2013; 2014; Wu *et al.* 2018) but down-regulates *isg15* and *mx* expression in the gills (Wu *et al.* 2018). In Senegalese sole post-larvae,

eight genes encoding different *irf* genes were up-regulated as well as the *mx*, an expression profile similar to that found when LCDV was i.p. injected in sole juveniles (Carballo *et al.* 2017). This response of the interferon pathway could explain the resistance of soles against LCDV since the overexpression of *mx* is essential to prevent the *in vitro* cytopathic effects of LCDV (Fernandez-Trujillo *et al.* 2013) and for the establishment of an antiviral state *in vivo* (Fernandez-Trujillo *et al.* 2008). It is also noteworthy the activation of an acute-phase inflammatory response mediated by cytokines (*il1b* and *tnfa*), chemokines *cxc10* and cyclooxygenase *cox2* that increase vascular permeability and enhance the recruitment of inflammatory cells causing tissue remodeling and concertedly blocking LCDV replication (Gruys *et al.* 2005; Kalinski 2012). Although some viruses use the chaperone Hsp90 for nucleic acid replication (Geller *et al.* 2012), the lack of *mcp* expression indicates that *hsp90* mRNA levels could be modulated to regulate cellular homeostasis after virus infection.

9.2 Gene expression profiles associated with Lymphocystis Disease Virus (LCDV) in experimentally infected Senegalese sole (*Solea senegalensis*)

LCD is an important viral disease that provokes significant economic losses in aquaculture due to delayed growth and skin lesions that hamper fish commercialization (Borrego *et al.* 2017b). The LCDV was identified some years ago in soles with clinical signs in skin and fins (Alonso *et al.* 2005), however, limited information about the course of infection, pathogenesis and immune response in this species is available. The intensification of sole culture in recirculation facilities makes even more necessary to understand the mechanisms used by this virus to disseminate and the host immune response in order to establish efficient control measures and to identify suitable markers for breeding programs.

In the chaper 4, the LCDV was injected to juvenile soles and viral loads were monitored for 15 d. LCDV DNA was detected in the blood of infected fish but only at 1 and 2 dpi, indicating that the virus spreads rapidly from the peritoneal cavity through the bloodstream to reach target organs such as kidney, gut and liver, and establishes in this way a systemic infection (at least until 15 dpi). These data agree with LCDV infections in turbot in which the virus vehicled by leukocytes spread rapidly in the fish and can be detected in heart, peripheral blood cells, and head kidney (Sheng *et al.* 2015). Our data also indicate that LCDV is rapidly cleared from peripheral blood in spite of it remains detectable in target organs thorough all the experiment. Moreover, the detection of *mcp* transcripts between 5-15 dpi and the decrease in viral load indicate that the immune response triggered by LCDV in the infected animals could interfere virus replication and/or assembly. As consequence, these specimens become asymptomatic carriers, one of the major problems to control the disease as reported in gilthead sea bream (Cano *et al.* 2009a; Valverde *et al.* 2016b).

LCDV DNA was consistently detected in three internal organs (kidney, gut, and liver), and in skin/fin pools of one individual at 15 dpi. Kidney appeared as the main target organ, with the highest amounts of viral DNA at 2 dpi that decrease as infection progressed. Moreover, *mcp* mRNAs were detected in the four tissues indicated above between 5-7 dpi. *In vitro* infection studies demonstrated LCDV cytoplasmic inclusions and cytopathic effects on sea bream adherent kidney leukocytes and SAF-1 cells (Garcia-Rosado *et al.* 2002; Alonso *et al.* 2005). Moreover, viral DNA and proteins were detected in cells of the reticuloendothelial system of a wide range of tissues including skin, gills, liver, intestine and spleen in sea bream and yellow perch (Cano *et al.* 2009a; Palmer *et al.* 2012). Interestingly, the comparison between lymphocystis diseased and recovered sea breams showed that DNA was more intensely detected than proteins in the latter specimens suggesting a low level of intracellular multiplication linked to the persistence of LCDV in such

animals (Cano *et al.* 2009a). These data agree with the temporal differences between DNA abundance and expression of viral genes found in this chapter.

The rapid clearance of LCDV from blood and the reduction of viral DNA copies from tissues indicated that a robust immune response could be limiting virus replication. Transcriptomic analysis in kidney and intestine confirmed the activation of a wide set of transcripts related to the innate and adaptive immune responses. The injection of LCDV rapidly triggered the expression of some antiviral-related transcripts including the *mx* and seven IRFs (*irf1*, *irf2*, *irf3*, *irf7*, *irf8*, *irf9*, *irf10*). The Mx proteins are IFN-inducible proteins that are usually considered as suitable markers to monitor IFN-mediated responses, as well as to evaluate the efficacy and long-term protection of vaccines (Kim *et al.* 2000). These antiviral proteins interfere virus assembly by regulating transcription of viral proteins (Lin *et al.* 2006; Wu *et al.* 2010). An *in vitro* study demonstrated that two Mx paralogs from gilthead sea bream exerted an anti-LCDV activity decreasing the cytopathic effects in cultured cells (Fernandez-Trujillo *et al.* 2013). *In vivo* studies in sole demonstrated a strong induction of *mx* expression after stimulation with the synthetic dsRNA poly(I:C) that correlated with the protection against solevirus infection (Fernandez-Trujillo *et al.* 2008). In our study, a high activation of *mx* was detected in both organs analysed that, unlike IRFs, increased progressively over time. A similar response was also found in kidney of Japanese flounder specimens after challenging with synthetic dsRNA poly I:C and LCDV-C (genotype II) (Hu *et al.* 2010; 2011). Interestingly, Mx response peaked at a later stage and with a stronger inducibility than IRFs in gill and kidney (Hu *et al.* 2010; 2011), which support different roles of these antiviral factors against LCDV infections.

As indicated above, a set of 6 IRF-encoding transcripts (*irf1*, *irf3*, *irf7*, *irf8*, *irf9*, *irf10*) was activated after LCDV infection in both kidney and intestine and *irf2* in kidney. IRFs are transcriptional regulators of the type I interferon system (IFN) that can modulate both innate and adaptive immune responses (Honda *et al.* 2006;

Mancino & Natoli 2016). The IRF1, IRF3 and IRF7 act as positive regulators of type I IFN gene transcription through different regulatory pathways such as the RNA-mediated mitochondrial antiviral signalling protein pathway, and some Toll-like receptors including TLR3 and TLR4 through the TIR domain-containing adaptor protein pathway and MyD88 (Honda & Taniguchi 2006; Feng *et al.* 2016). In addition, the IRF9 participates in the IFN signalling pathway to trigger the transcription of hundreds of genes including the own IRFs through STAT-dependent mechanisms (Ivashkiv & Donlin 2014). This tight connection with the IFN-mediated response converts the IRFs in key molecules to respond rapidly to viral stimuli. An up-regulation of *irf1*, *irf* 3, *irf* 4, *irf* 7 and *irf* 8 were found in turbot after VHSV challenge or DNA vaccination (Pereiro *et al.* 2014). Moreover, *irf4a*, *irf4b*, *irf7*, *irf8* and *irf10* were activated after poly(I:C) injection in cod (Inkpen *et al.* 2015). In flounder, the *irf3*, *irf5*, *irf7 irf8* and *irf9* were induced in immune and non-immune organs by poly(I:C) and after LCDV-C challenge (Hu *et al.* 2010; 2011; 2012; 2013; 2014). All these data support our observation that a coordinated response of IRFs is essential to trigger properly the defensive IFN-mediated response to cope with the viral insult.

However, it is also noteworthy that the time-course of IRFs induction was different in kidney and intestine with a faster response in the former (all transcripts peaked at 1 dpi) than in the latter (maximum expression of *irf3*, *irf8* and *irf9* in the intestine was detected at 2 dpi). Previous experiments that characterized the response of different IRFs in Japanese flounder demonstrated that induction by poly(I:C) was faster and more intense than by LCDV-C due to its ability to rapidly activate the host immune response as a pathogen-associated molecular pattern (PAMP) (Hu *et al.* 2010; 2011; 2012; 2013; 2014). In these studies, the *irf7* showed the induction peak in the kidney at 4 days after viral challenge (Hu *et al.* 2010; 2011), whereas *irf3*, *irf8* and *irf9* peaked earlier between 12-48 h after challenge (Hu *et al.* 2013; 2014). In our study, the induction of IRFs was fast (within 24-48h) with no

significant effect at 5 dpi. The delay in the response found in the intestine might be associated with the highest viral load found in kidney that would provide enough PAMPs to rapidly trigger an immune response as previously suggested by Holopainen *et al.* (2012) and Avunje *et al.* (2011).

In addition to the induction of IFN-related genes, LCDV activated the expression of a wide set of cytokines (including ILs and chemokines) and their receptors. The coordinated activation of pro-inflammatory cytokines (*il1b*, *il6, il8, il12* and *tnfa*) represents a conserved mechanism of the immune system to enhance the clearance of viruses (Mogensen & Paludan 2001; Tafalla *et al.* 2005; McFadden *et al.* 2009; Rathinam & Fitzgerald 2010; Zheng *et al.* 2010). These cytokines are mainly produced by macrophages and monocytes through the NF-kB signalling pathway (Mogensen & Paludan 2001) triggering an acute-phase response characterized by increased vascular permeability and recruitment of inflammatory cells (Gruys *et al.* 2005) to concertedly build a barrier to pathogen replication through an intracellular antiviral state (that synergize with type I IFN) as well as modulating the adaptive immune response (Biron 1998; McFadden *et al.* 2009; Rathinam & Fitzgerald 2010). A fail in the induction of this consistent pro-inflammatory response was related to the susceptibility of salmonids to IPNV (Reyes-Cerpa *et al.* 2012; 2014). The high induction of IL-1β expression after LCDV challenge highlights a major role of this pleiotropic cytokine. IL-1β -derived peptides confer resistance to VHSV (Peddie *et al.* 2003), enhance production of other cytokines (such as IL-12 and IL-6) and the phagocytic and lysozyme activity of macrophages, activate the adaptive immune response (Rathinam & Fitzgerald 2010; Zou & Secombes 2016) and initiate, in collaboration with *tnfa*, the signalling pathway leading to apoptosis, a major mechanism preventing viral replication and dissemination through the removal of infected cells as previously shown in LCDV-C *in vitro* infections (Hu *et al.* 2004).

Additionally, macrophages also release chemokines, prostaglandins, and

complement as part of the inflammation response to a viral challenge. Chemokines expression (CXC-type, CC-type and IL-8) is triggered by IL-1β and interferons (Chen *et al.* 2013; Zou & Secombes 2016) to enhance the trafficking of neutrophils, macrophages and lymphocytes (Harun *et al.* 2008; Chen *et al.* 2013). The induction *il8*, *cc-ck3*, *cxc10*, *cxc13*, *cc19* and *cc20* observed in this study, with some differences between organs, supports tissue-specific responses devoted to increase leukocytes recruitment. The induction of *cd4* (a marker for helper T cells) in both organs, as well as *cd8a* and *cd8b* (a marker for cytotoxic T cells) in intestine at 2 dpi could be associated with the activation of the adaptive immune response since these organs contain different types of antigen presenting cells and lymphocytes (Reyes-Cerpa *et al.* 2014).

The transcriptional up-regulation of some other genes such as the antimicrobial peptide *hamp*, the prostaglandin synthesis-related *cox2*, g-type lysozymes (*lysg*) and some complement fractions (*c2*, *c4-1* and *c4-2*) indicates that a wide host defensive strategy is triggered by LCDV. The hepcidin peptides exert an antiviral activity by interfering capsid protein assembly (Wang *et al.* 2010; Rajanbabu & Chen 2011). This gene is transcriptionally activated in the liver of LCDV-infected turbot as part of the regulatory pathway mediated by the transcription factor STAT3 (Wang *et al.* 2011). The *cox-2* is responsible for the synthesis of prostaglandins (such as prostaglandin E) and its expression is regulated by viral stimuli (Symensma *et al.* 2003; Scapigliati *et al.* 2010; Kirkby *et al.* 2013) and some cytokines such as TNF-α and IL1β (Molina-Holgado *et al.* 2000; Roca *et al.* 2008) to cooperate in early stages of inflammation with local vasodilatation and attraction of neutrophils, macrophages and mast cells (Kalinski 2012). In addition, the lysozymes are highly responsive to viral insults modulating non-specific cellular and humoral defence mechanisms (Siwicki *et al.* 1998; Mai & Wang 2010; Ponce *et al.* 2011; Wei *et al.* 2014). All these data, joined to the induction of *c2* and *c4* fractions as part of to the classical and lectin complement pathways

(Nesargikar *et al.* 2012), reflect as a whole a common strategy of the innate immune system to respond globally and co-ordinately to a pathogen attack.

In conclusion, the time-course detection of LCDV DNA and mRNA in infected soles suggests that the virus rapidly moves into the bloodstream and spreads to several organs where it begins replication. Nevertheless, the wide immune response triggered by the host seems to limit the virus replication and the animals become asymptomatic carriers. The early activation of a wide set of IFN-related genes such as *mx* and IRFs, pro-inflammatory ILs and their receptors, *tnfa*, chemokines, lysozymes, antimicrobial peptides, complement fractions as well as T-cell markers indicated a highly protective response. Although this response was quite similar in kidney and intestine, some small differences in the intensity and time-course were observed that could be due to a higher amount of viral DNA found in kidney and/or to the different lymphohematopoietic structure of these organs.

9.3 Microalgal extracts induce a trained immune that modifies the responses to bioactive compounds and after a challenge with LCDV

Early training of innate immunity is becoming a new field to enhance immune system responses and fish survival in aquaculture. There are increasing evidences that fish larvae have a high genome plasticity as an adaptive mechanism in response to surrounding environmental conditions. Previous studies have demonstrated that temperature has persistent effects on myogenesis and somatic growth, stress responses (Fokos *et al.* 2017; 2017a; Mateus *et al.* 2017b) and sex differentiation (Navarro-Martin *et al.* 2011). More recently, a non-specific memory referred to as trained immunity has been demonstrated in fish (Petit & Wiegertjes 2016; Garcia-Valtanen *et al.* 2017; Petit *et al.* 2019b). The early training immunity has been proposed as a smart strategy to get long-lasting effects on immune defensive

responses that could be functional until adult ages improving larval rearing performances (Rojo-Cebreros *et al.* 2018). This study benefited of previous data on thermal imprinting in sole that demonstrated that a sensitive window to the environmental conditions just when larvae release from the egg chorion (Firmino *et al.* 2017; Carballo *et al.* 2018b). A crude extract of *N. gaditana* was selected as priming stimuli due to its high content of bioactive compounds including polysaccharides, pigments and lipids and antioxidant capacity (Letsiou *et al.* 2017). This microalga is frequently used in marine hatcheries due to its nutritional value and when used in green water for larval rearing that have demonstrated increased survival and optimal management of microorganism communities in the tank (Moretti *et al.* 1999; Palmer *et al.* 2007). Our study demonstrates for first time that a short exposure of larvae in lecithothrophic stages before mouth to the crude extracts of this microalga has long term effects on growth (data not shown) and immune system responses after the supply of bioactive compounds and a viral challenge indicating effective epigenetic reprograming. The results obtain on chapter 5 open a field to the use and application on microalgae not explored until now.

Under our experimental setting, the oxygen availability in the trays appeared as a major constraint for larval metabolism and survival. In the control group SW, the post-larvae mortality was almost negligible, however a high mortality was observed in the groups administrated the yeast β-glucans and the microalgal extracts indicating an enhanced metabolic activity and oxygen demands that were even higher in the Nanno group. Previous data of our group demonstrated yeast β-glucans and MAe acted as immunomodulators in juvenile soles with the former acting locally in the gut modulating the immune response and microbiomes and the latter exerting a systemic anti-inflammatory response (Carballo *et al.* 2019b). Furthermore, the MAe extract provokes a sustained and potent inflammatory response when injected (Carballo *et al.* 2018a). Interestingly, the effects observed in the Nanno-trained group supports the "metabolic

reprogramming" reported in reprogrammed larvae that in turn results in higher growth rates compared to the control. The metabolic shift from oxidative phosphorylation toward glycolysis and the activation of glutaminolysis, and the cholesterol synthesis pathway are indispensable for the induction of trained immunity (Arts *et al.* 2016; Petit *et al.* 2019b) indicating that the priming activity of *N. gaditana* extracts modified the metabolic pathways in post-larvae.

The total lysozyme and antiprotease activities are two components of the humoral defences against bacteria that attack the cell membranes or restrict the use of nutrients, respectively (Saurabh & Sahoo 2008; Priyadarshini *et al.* 2017). These activities are highly modulated by nutrition, stress, infection or pollution. An increase of serum lysozyme levels and antiprotease activities in response to bacterial infections or after the administration of immunostimulants has been associated with an enhanced disease resistance (Saurabh & Sahoo 2008; Priyadarshini *et al.* 2017). Recently, thermal imprinting was demonstrated to prime the innate immune system in zebrafish with modified expression of lysozymes (Zhang *et al.* 2018a). In our study, higher levels of lysozyme and antiprotease activities were detected in Nanno-trained larvae indicating a persistent effect to enhance innate immune system. Moreover, the MAe but not yeast β -glucan increased both activities rapidly at 6h. In a previous study of our group using juveniles orally administrated these bioactive compounds, we did not observe any effect of insoluble β-glucan on serum lysozyme activity due to its major action in the gut (Carballo *et al.* 2019b). However, the lysozyme activity decreased at 48h after MAe administration supporting our hypothesis that this change was part of temporal recovery response after a non-detected activation according to the kinetics observed when injected (Carballo *et al.* 2018a). The high decrease in activity at 24h could be associated with an acute stress episode due to hypoxia as indicated above since stressful situations reduce humoral defences and lysozyme levels (Jeney *et al.* 1997).

In addition to antibacterial activities, the reprogramming treatments with the *N. gaditana* extracts enhanced the steady-state mRNA levels of chemokine *cxc10* and the antiviral *Mx*. Moreover, Nanno-trained larvae also modulated the expression profiles in response to the LCDV challenge enhancing the activation of antiviral (*irf3*, *irf7*, and *mx*) and interfering the activation of pro-inflammatory cytokine *il1b*. These results agree with the antiviral alert state in $rag^{-/-}$ zebrafish mutants in the absence of adaptive immunity that overexpress apoptotic functions, immune-related multigene families, and interferon-related genes (Garcia-Valtanen *et al.* 2017). Moreover, β-glucans, and particularly the soluble laminarin, have been proven as a major inducer of trained immunity in fish heightening phagocytosis and increasing expression of the inflammatory cytokines and viral resistance (Medina-Gali *et al.* 2018; Petit *et al.* 2019a). Our crude extract is a complex mixture containing all cell content and it is not possible to relate the effects to a specific molecule but our data underline the high potential for reprogramming antiviral defences and proinflammatory cytokines and hence it could represent a novel method to control microbial diseases in fish. Although no significant differences in the number of LCDV DNA copies were observed for reprogramming treatments and the bioactive compounds, it should be noted LCDV is a good model to evaluate the antiviral defensive response but it requires more time than used in our experiment to invade and multiplicate in the cells and conclude about virus replication blocking (Carballo *et al.* 2017; 2019a).

Dietary supply or injection of β-glucans increases the expression and production of pro-inflammatory cytokines and stimulate phagocytic, cytotoxic, and antimicrobial activities although with some differences depending on β-glucan structure and solubility (Meena *et al.* 2013; Vetvicka *et al.* 2013). In this chapter, we also demonstrate that both MAe and yeast β-glucans can modify steady-state levels of innate immune genes as well as the response intensity to LCDV.

The administration of both bioactive compounds activates a quick

immunomodulatory response at 6h, when no mortality was recorded, stimulating the expression of pro-inflammatory cytokines and antiviral genes (*mx* and *irf7* in MAe and the *tnfa* in both MAe and Y). The heightened response observed for MAe indicates a higher systemic response than yeast β-glucans as suggested in Carballo *et al.* (2019b) and support the strong induction of the pro-inflammatory cytokines and other innate immune related genes when intraperitoneally injected in juveniles (Carballo *et al.* 2018a). The induction observed at 6h was followed by a decrease in expression levels of most of the genes in post-larvae fed MAe and yeast β-glucans at 24h that could be explained by the hypoxic acute stress (Salas-Leiton *et al.* 2010; 2012). However, it should be noted that post-larvae from Y group maintained low expression levels in the non-stimulated control of the challenge trial and the expression profiles appeared well differentiated from the SW group (Fig. 6) indicating a long-lasting effects of β-glucans administration. The down-regulation of cytokines and antiviral genes were associated with heightened responses to LCDV that coincides with the enhancement of immune system against pathogens but preventing an acute harmful inflammatory response (Falco *et al.* 2012; 2014).

The LCDV is useful to investigate the immune regulatory pathways due to the low mortality rates and the triggering of a quick and wide systemic defensive response that involved several antiviral pathways, cellular markers and inflammation-related genes able to cope with the viral insult, as a shown in the chapter 4 (Carballo *et al.* 2017). As expected, the LCDV challenge triggered the expression of most of the genes analysed (Carballo *et al.* 2017; 2019a) but the PCA analysis clearly demonstrated an effect of reprogramming and bioactive compounds that differentiated the expression profiles of antiviral genes *irf7*, *irf3* and *mx* response from those of pro-inflammatory cytokine *il1b*, c-lectin and lymphocytes markers *cd4* and *cd8a*. The β-glucans heightened the response of antiviral genes to LCDV in non-reprogrammed larvae as previously demonstrated for Spring Viraemia of Carp Virus (SVCV) and GCHV (Kim *et al.* 2009; Medina-Gali

et al. 2018). However, this antiviral response was abrogated in the Nanno-trained group that responded to virus even lower than post-larvae no administrated with the β-glucans. This effect was not observed in the pro-inflammatory cytokine *il1b*, c-lectin and lymphocytes markers heightened the response to LCDV in post-larvae fed β-glucans regardless the reprogramming group. These results demonstrate the activity of the *N. gaditana* extracts to prime immune cells and modify the steady-state levels and the response of antiviral genes to LCDV depending on the administration of yeast β-glucans points out to targeted modification of interferon-mediated pathways. Previous studies have demonstrated that innate immune system can be trained, through epigenetic modifications, toward a specific response depending on the molecule used to prime the innate immune system (Quinn *et al.* 2019). Whereas β-glucans enhance the production of pro-inflammatory immune responses, helminth products suppressing innate pro-inflammatory cytokines (Petit & Wiegertjes 2016; Petit *et al.* 2019b; Quinn *et al.* 2019). Further research will be necessary to identify the molecules responsible for trained immunity in the *N. gaditana* extract using fractioning and how they interact to the antiviral signalling of β-glucans.

In summary, this study demonstrates how a crude extract of *N. gaditana* can be used for early training of innate immune system in sole larvae. The higher growth and mortality suggested a metabolic reprogramming with a higher metabolism and oxygen demands that was also accompanied of higher enzymatic activities, the modification of steady-expression levels for innate immune genes and the enhancement of defensive response against LCDV. The orally administration of a microalgal extract and yeast β-glucans rapidly increased the expression of cytokines and antiviral genes. However, the steady-state were low but clearly differentiated from the non-supplied control in longer times enhancing the responses to LCDV. The reduced antiviral response of Nanno-trained post-larvae stimulated with β-glucans after the LCDV challenge clearly points out to actions

mediated different regulatory pathways. All these results provide evidences of the use of microalgae to reprogram larval plasticity promoting long-lasting immune system responses and improvement of disease resistance and growth performance. The methodology used represents an innovative method that can transform and benefit the current operational methods used in fish hatcheries.

9.4 Antioxidant capacity and immunomodulatory effects of a chrysolaminarin-enriched extract in Senegalese sole

The advances in microalgae biomass production at an industrial scale have brought to the market novel bioproducts that can be feasible exploited as it is the case of chrysolaminarin. The antioxidant, prebiotic and immunostimulant activity of β-(1,3;1,6)-glucans from different sources is well-recognized and hence, these polysaccharides have been proposed as potential functional dietary supplements or as vaccine adjuvants to enhance immune response in aquaculture (Meena *et al.* 2013; Petit & Wiegertjes 2016). However, the antioxidant capacity and immunomodulatory effects of these β-glucans in fish are still unexplored. In the present study the antioxidant capacity, cytotoxicity and immune response of a chrysolaminarin-enriched extract from the diatom *P. tricornutum* have been determined using the flatfish Senegalese sole as a model. These new data represent an initial study to develop new applications to functional extracts from microalgal biomass.

Previous studies on β-glucans have demonstrated their antioxidant and reactive oxygen species scavenger activity (Machová & Bystricky 2013; Du & Xu 2014; Xia *et al.* 2014; Liu *et al.* 2017). In the result obtain in chapter 6, our chrysolaminarin-enriched extract from *P. tricornutum* also showed antioxidant activity with higher TAC than particulate yeast β-glucan in the ORAC (~14-folds) and FRAP (~4-folds) assays but lower in the DPPH scavenging method. We should

note that although chrysolaminarin was a major component in our crude extract, we cannot fully discard a contribution to TAC of other minor cellular components. In fact, Kanmani *et al.* (2011) reported that crude exopolysaccharide extracts had higher reducing power and hydroxyl radical scavenging activity than purified exopolysaccharide as consequence of secondary metabolites in the extract. Anyway, the contrasting results in the three TAC assays between the microalgal extract and yeast β-glucan could be explained by two main factors: (i) the distinct structure, composition and solubility of β-glucans (Lo *et al.* 2011); and (ii) the specific thermodynamic, kinetic and chemical characteristics of each TAC assay and the oxidizing power of each TAC reagent against a given antioxidant (Rubio *et al.* 2016). The chrysolaminarin has a lower molecular weight (MW; ~10 kDa) and lower degree of polymerization (DP; 28-33) than yeast β-glucan (branch-on-branch, high MW (>200 kDa) and high DP (>100) (Zekovic *et al.* 2005; Barsanti *et al.* 2011; Caballero *et al.* 2016). Such differences in size, branching and conformation play a key role in water-solubility, a limiting factor in the FRAP assay (Apak *et al.* 2007) and hydroxyl radical scavenging activity (Kofuji *et al.* 2012). A previous study in the microalgae *Odontella aurita* demonstrated that chrysolaminarin had a stronger antioxidant activity for hydroxyl radical scavenging than for DPPH radicals (Xia *et al.* 2014) indicating that structural differences are important for a better neutralization the peroxyl radicals in ORAC and total reducing power in FRAP. Moreover, those molecules with lower antioxidant values in the ORAC relative to the DPPH assay as observed in yeast β-glucan have been proposed to act both as antioxidants and powerful pro-oxidants and this makes chrysolaminarin β-glucan even more interesting for the food and cosmetic industry (Roy *et al.* 2010).

Some β-glucans have been reported to exhibit anti-proliferative and antitumoral activities. For example, laminarin impairs the viability of human lung fibroblasts at concentrations higher than 0.004% with high inhibition achieved at concentrations higher than 0.02% w/v (Liu *et al.* 2017). However, when used at an

appropriate dose in *in vitro* cell assays, laminarin has an antioxidant action that protects against reactive oxygen species (Liu *et al.* 2017). Similarly, β-glucans from cereals exert cytotoxic actions against cancerous cells at concentrations lower than 0.02% w/v (Choromanska *et al.* 2018). The data from the present study indicate that chrysolaminarin-enriched extract at concentrations higher than 0.01% w/v affected cell viability of human dermal fibroblasts as has previously been shown for other β-glucans. More studies will be necessary to investigate the specific cancer-protective actions of this microalgal extract. Intriguingly, i.p. injection of this extract to soles induced a 29.4% mortality. This was unexpected since the dose used (1 mg/fish; 0.052mg/g) was close to the range previously used in other fish species (0.1-1mg/fish; 0.01-0.033 mg/g fish) (Fujiki *et al.* 2000; Selvaraj *et al.* 2005; Misra *et al.* 2006; Lovoll *et al.* 2007). The absence of mortality after the second exposure to chrysolaminarin tends to preclude the presence of adulterating toxic substances such as endotoxins. As the main differences between the present and previous studies was the vehicle used for injection (coconut oil instead of phosphate-buffered saline for a slow delivery), we hypothesize that the prolonged release of chrysolaminarin triggered a sustained and potent inflammatory response (see below), that in turn resulted in a non-adaptive stress response, a failure in homeostatic response and mortality. The exact mechanisms by which *in vivo* chrysolaminarin caused mortality will require further studies.

The β-glucans from different sources are well-known as enhancers of non-specific immunity in fish through the activation of macrophages and the production of pro-inflammatory cytokines. The i.p. injection of yeast β-glucan triggered the expression of *il1b* in carp head kidney macrophages after 24 and 48 h (Selvaraj *et al.* 2005). Moreover, laminarin i.p. injection activated the expression of *il1b* in salmonids using both *in vitro* (head kidney macrophages) and *in vivo* (in kidney and spleen after 48 h) approaches (Lovoll *et al.* 2007; Fredriksen *et al.* 2011). The β(1,3) scleroglucan activated expression of *il1b* peritoneal cells of carp at 2 dpi due to

inflammatory leukocyte migration (Fujiki *et al.* 2000). The polysaccharides from the herb *Astragalus* containing β-glucans also increased *il1b* mRNA abundance in the head kidney of common carp (*Cyprinus carpio*) (Yuan *et al.* 2008). The result showed in chapter 6 demonstrates that i.p. injection of the chrysolaminarin-enriched extract in sole elicited a similar response to laminarin in other fish and rapidly activated the expression of the pro-inflammatory cytokine *il1b* (at 2 dpi) in the three organs analysed. This cytokine acts as a mediator of β-glucan actions and triggers a generalized downstream response through the NF-κB and MAPK signalling pathways to produce cytokines and activate the migration and phagocytic activities of macrophages (Zou & Secombes 2016). It should be noted that magnitude of the *il1b* activation was higher in spleen and intestine than in kidney that also supports previous observations that reported the spleen as a major target for β-glucan actions with larger and more intense responses (Lovoll *et al.* 2007; Fredriksen *et al.* 2011; Douxfils *et al.* 2017). The lack of response of the pro-inflammatory cytokine *tnfa* could be due to a dose or time-point effect. A previous study indicated that the activation of *tnfa* was delayed with respect to *il1b* after β-glucan treatments in trout head kidney leukocytes (Chettri *et al.* 2011) and also showed dose-dependent effects as demonstrated by *in vitro* and *in vivo* trials assays with organ-specific response (Yuan *et al.* 2008; Chettri *et al.* 2011; Fredriksen *et al.* 2011; Douxfils *et al.* 2017).

In addition to *il1b*, the microalgal crude extract also stimulated the expression of chaperone *hsp90aa* in kidney and spleen and the antimicrobial peptide *hamp1* in the three tissues although with a high variable response among specimens. The expression of *hsp90* and *il1b* is up-regulated in a mutant zebrafish that lacks an adaptive immune response (Garcia-Valtanen *et al.* 2017). The co-expression was associated with the role of Hsp90 in ensuring the correct folding of several kinases and intermediates of the NF-κB signalling pathway and hence modulating NF-κB action and pro-inflammatory cytokine production in macrophages (Joly *et al.* 2010; Ambade *et al.* 2012; Thangjam *et al.* 2016). The modification of hepcidin expression

in soles injected with the microalgal extract may be related to its stimulation by pro-inflammatory cytokines such as IL-6 (Andrews 2004) and to the inhibitory effect on cytokine production through interfering the NF-κB pathway (Rajanbabu *et al.* 2010). Interestingly, a similar activation pattern of pro-inflammatory cytokines (*il1b*, *il6*, and *tnfa*) and *hamp1* was also observed in kidney and intestine of juvenile soles after infection with LCDV, as previously showed in the chapter 4 of the present PhD thesis (Carballo *et al.* 2017), indicating that this microalgal extract promotes the up-regulation of genes representative of an acute innate response against a pathogen.

In contrast to the fast activation of the inflammatory response at 2 dpi, genes related to the response to virus, *ifn1*, *irf1*, *irf3*, *irf8*, *irf9* and *mx*, and the chemokine *cxc10* were down-regulated in the kidney and/or spleen at 5 dpi and the sugar receptor *clec* in kidney (1.5-fold lower) at 2 dpi. The stabilization of mortality after 5-6 dpi observed in this chapter also supports the acute response as the primary cause for the expression patterns observed. In this regards, chrysolaminarin-enriched extract reinjection at 7 dpi did not induce further mortality and did not activate a pro-inflammatory response. Instead, a decrease of *hsp90aa* and *irf3* mRNA levels were measured as indicative of some resistance of sole to consequent injections of chrysolaminarin. A previous study in *Labeo rohita* fingerlings identified that only three out four injections of β-glucans and at a moderate concentration specifically maintained enhanced phagocytic cell functions (Misra *et al.* 2006). All these data suggest that the β-glucan exposure rapidly activated an acute inflammatory response but in the absence of a pathogen down-regulation of transcripts to restore the steady-state levels occurred. Clearly it will be relevant in the future to assess how β-glucan supplementation via diet changes the efficacy of the immune response to pathogens.

9.5 Yeast β-glucans and microalgal extracts modulate the immune response and gut microbiome in Senegalese sole (*Solea senegalensis*)

Research into prebiotics and immunostimulants is a fast-developing field in aquaculture as it is a sustainable way to enhance fish health with less regulatory restrictions in relation to food safety than other methods such as probiotics. The β-glucans are among the polysaccharides with high potential as a feed supplement in fish production because they can act as both (a) modulators of microbiota-host interactions; and (b) recruit and activate macrophages by binding to surface receptors (Ringø *et al.* 2012; Meena *et al.* 2013; Song *et al.* 2014). An important consideration when using β-glucans as a prebiotic is the effect of source organism and the preparation method (both influence the conformation and chemical properties) on their specific immunomodulatory actions. In the present study, a particulate β-glucan from yeast and a MAe enriched in polysaccharides were evaluated using a novel and optimized oral intubation approach in a flatfish, the Senegalese sole. This intubation approach was chosen to reduce the interference from multiple feed components and to reveal more clearly the specific actions of the administered substances (Kiron *et al.* 2016). A comprehensive study of the effects of prebiotics on the gut microbiome and modulation of regulatory pathways of the innate immune system was performed. Moreover, lysozyme and protease inhibitor activities, markers of the host anti-bacterial and anti-inflammatory response to pathogenic bacteria (Saurabh & Sahoo 2008; Magnadottir 2010), were also characterized.

Our results demonstrated that the tested yeast β-glucans and MAe had a different effect on the microbiota composition and the expression of innate immune genes in both the intestine and spleen. These data support the notion that solubility is a key factor for β-glucan bioactivity and that they may act through different signalling pathways (Goodridge *et al.* 2011; Qi *et al.* 2011) with the particulate β-glucans having a major local effect on the gut and its microbiota. In mammals,

particulate yeast β-glucans act as dectin-1 agonists and activate neutrophils, dendritic cells (DCs) and macrophages via two independent signalling pathways, Syk and Raf-1, which converge at the level of NF-*k*B (Goodridge *et al.* 2011; Qi *et al.* 2011). Activation via dectin-1 triggers the production and release of proinflammatory cytokines (IL1β, IL6 and TNF-α), phagocytosis, production of reactive oxygen species (ROS) and T-cell differentiation to control adaptive immunity (Gringhuis *et al.* 2009; Kankkunen *et al.* 2010). In fish, particulate β-glucans up-regulate the expression of *il1b, il6* and *il11* in carp macrophages and they have been proposed as good markers of macrophage activation (Pietretti *et al.* 2013). The activation of *il1b* has also been reported in Atlantic salmon orally intubated to supply MacroGard (Kiron *et al.* 2016). In the experiments developed in the chapter 7, yeast β-glucans triggered a fast and transient induction of *il1b* in the intestine (but no change in *tnfa* and *cxc10a* genes were observed) and a shift in the microbiota composition, particularly the abundance of *Vibrio*, a major component of the fish intestine microbiome (Llewellyn *et al.* 2014; Egerton *et al.* 2018). The results of the present study are in agreement with previous data in carp that reported a local stimulatory action of yeast β-glucans in the intestine (Pionnier *et al.* 2014) and a specific up-regulation of cytokine production indicative of glucan-mediated activation of macrophages (Pietretti *et al.* 2013). Although with our experimental design it was not possible to establish a robust regulatory pathway model involving the pro-inflammatory cytokine *il1b*, the opposing response of the antiviral defence *irf3* gene is similar to the response of juvenile sole after intraperitoneally injection of *P. tricornutum* extracts (Carballo *et al.* 2018a). These data suggest there is cross-talk between the type I interferon and IL-1 cytokine pathways to modulate the inflammatory responses and bacterial populations (Mayer-Barber & Yan 2017).

In contrast to the short-term response reported for yeast β-glucans, oral delivery of MAe was associated with a more systemic response with a reduction in blood lysozyme activity and the down-regulation of *tnfa* and *cxc* mRNAs in the

intestine and spleen and *il1b* and g-type lysozyme transcripts in spleen. These results contrast with the rapid inflammatory response observed when MAe was injected intraperitoneally (i.p.) (Carballo *et al.* 2018a). In the latter case induction of *il1b* in kidney, spleen and intestine was rapid and followed by the absence of a response to subsequent i.p. exposure to the same extracts. Such route-specific differences in the immunomodulatory response suggests a role for the microbiota and/or intestinal enzymes in the shift of MAe activity. In rainbow trout, dietary β-glucans differentially regulated the response of vaccinated trout after a microbial challenge and caused a down-regulation of pro-inflammatory, acute phase and lysozyme related genes in the head kidney (Skov *et al.* 2012). In carp, dietary β-glucans also reduced the expression of inflammation-related cytokines in the gut, but not in the kidney, after a challenge with *A. salmonicida* (Falco *et al.* 2012). In the rainbow trout, dietary β-glucans decreased the expression of genes involved in the acute inflammatory response after injection of bacterial lipopolysaccharide (LPS) in the spleen (Djordjevic *et al.* 2009). These data indicate that the regulation of immune-regulatory genes by β-glucans is dependent on the presence or absence of a microbial stimulus (Petit & Wiegertjes 2016) and based on our data, we propose that the gut microbiota may play a role in this differential response. We should note that due to the complexity of our MA extract it was not possible to associate the observed effects to specific components of the extract, particularly since one of the likely contaminants, laminarin has been shown to act as a Dectin-1 antagonist or agonist depending on its form eg. soluble or aggregated (Smith *et al.* 2018). Nonetheless, our results support an immunomodulatory and anti-inflammatory action for MAe as has previously been reported for crude polysaccharide extracts of *P. tricornutum* (Guzman *et al.* 2003).

In the present study of Senegalese sole supplied with Y and MAe there was an apparent decrease in the global microbial richness and diversity of the intestine, which included both allochthonous microbiota of the intestinal content and the

autochthonous microbiota of the intestine itself. The significant reduction in bacteria from the *Vibrio* genus, the most represented taxonomic group in the Senegalese sole microbiome (Martin-Antonio *et al.* 2007), was confirmed by qPCR in the Y and MAe groups. Modulation of the gut microbiota by β-glucans has also been reported in carp fed diets supplemented with insoluble yeast β-glucans and the number of OTUs and the species richness of the allochthonous microbiota was reduced (Kuhlwein *et al.* 2013). In seabass (*Dicentrarchus labrax*) β-glucans caused a transient reduction in the most abundant groups of microorganisms in the intestine due to a shift in the relative abundance of OTUs in the autochthonous microbial community (Carda-Dieguez *et al.* 2014). Dietary supplementation with laminarin extracts also had an inhibitory effect on the counts of *Escherichia coli* in the faeces in piglets (McDonnell *et al.* 2010; O'Doherty *et al.* 2010). The more intense reduction in *Vibrio* caused by yeast β-glucan is compatible with a mainly local action of insoluble β-glucans on the intestine. Considering the high impact of *Vibrio* on sole disease outbreaks (Morais *et al.* 2016), the present results indicate β-glucans from yeast or microalgae are promising candidate prebiotics for the health of the intestine in sole. Intriguingly, the *Shewanella* genus that is considered a probiotic in sole (Lobo *et al.* 2014) and which increases when sole juveniles are fed polychaeta (Martin-Antonio *et al.* 2007), was absent in the Y group. The failure to detect the *Shewanella* genus reveals there is a need for more studies to understand the factors that determine the gut microbiome and its modulation by pre-biotics. This knowledge will be essential for the application of pre-biotics to modify fish performance and to confer disease protection.

The supply of whole microalgae cells (MA treatment) decreased the relative abundance of *Vibrio* but in contrast to the Y and MAe groups, it also caused a slight increase in bacterial diversity. Microalgae are routinely used as a feed source for fish larvae (Hemaiswarya *et al.* 2011; Sørensen *et al.* 2016) and experimental diets using whole-cell microalgae as a supplement for fish larval rearing also

demonstrated a greater level of microbial diversity (Lyons *et al.* 2017). The nutritional value of the microalgae presumably favours enrichment of the intestinal microbial community with organisms that can utilize nutrients from microalgae. The use of the diatom *P. tricornutum* as a dietary supplement has been shown to enhance immune parameters such as, haemolytic complement activity and phagocytic capacity in the gilthead sea bream (Cerezuela *et al.* 2012). We hypothesize that the up-regulation of *il1b* in the spleen of sole treated with MA for 7 days could be a result of the time needed for the shift in the microbiota and the associated delivery of metabolites that have an immunostimulant effect.

In summary, the results showed in chapter 7 of the present PhD thesis demonstrate that oral administration of insoluble β-glucans had a major action on the intestine and was associated with rapid up-regulation of *il1b* followed by a significant decrease in intestinal *Vibrio* abundance. In contrast, administration of soluble MAe enriched in polysaccharides had a limited effect on the intestine and caused only a slight reduction in the *Vibrio* load. The moderate response of the gut to MAe exposure coincided with a transient down-regulation of pro-inflammatory cytokines and g-type lysozyme transcripts in the spleen and lysozyme activity in the blood serum. The oral supply of whole microalgae had the biggest effect on the intestinal microbial diversity presumably due to their nutrient content and this treatment was also associated with a delayed activation of *il1b*. The results obtained in chapter 7 will form the basis for the design of new β-glucan enriched diets to control *Vibrio* populations in the gut, one of the major challenges for sole aquaculture.

9.6 Heritability estimates and genetic correlation for growth traits and LCDV susceptibility in the gilthead sea bream (*Sparus aurata*)

Selective breeding for disease resistance is considered as a sustainable approach to support aquaculture growth. Previous studies in fish demonstrated that heritabilities for disease resistance traits oscillate from moderate to high and hence they can be incorporated to breeding programs to minimize fish losses and enhance fish welfare (Ødegård *et al.* 2011). In sea bream, genetic selection programs have focused mainly on growth, morphology and carcass quality traits (Navarro *et al.* 2009; Garcia-Celdran *et al.* 2015a; 2015b; Lee-Montero *et al.* 2015). Up to date, only heritabilities for fish survival after challenging with the pathogenic bacteria *P. damselae* subsp *piscicida* (Pdph) were estimated ranging from 0.12-0.28 (Antonello *et al.* 2009; Palaiokostas *et al.* 2016). In the case of LCDV, previous studies in *P. olivaceus* demonstrated that marker-assisted selection programs were successful to control the LCDV-C (genotype II) disease outbreaks (Fuji *et al.* 2007). In spite of the high incidence of LCDV in sea bream hatcheries, no report about the genetic variance for resistance is still available in part due to the difficulty to experimentally reproduce the disease, highly dependent on environmental conditions and fish immunological status. In the chapter 8, two fish batches generated by mass spawning from three broodstocks were produced in a commercial hatchery in which LCDV outbreaks were previously reported. In both fish batches, the same environmental conditions under standard production procedures were carried except for grading operations. A cross-sectional model was followed and fish was sampled for phenotyping and genotyping just when typical LCDV skin lesions were evident assuming that LCDV infections occurred at least three weeks earlier (Kvitt *et al.* 2008).

As LCDV outbreaks are benign infections with low mortality rates (Paperna *et al.* 1982; Smail & Munro 2001; Kvitt *et al.* 2008; Colorni & Padrós 2011), the measurement of traits associated to disease susceptibility should be carried out by quantifying the degree of clinical signs such as body surface covered by lesions and

their intensity. In our study, no mortality was observed at the sampling time although all animals had the typical LCDV lesions (Fig. 41). To quantify the infection degree an image analysis was carried out identifying a high variability in the body distribution and intensity of the lesions. Moreover, the amounts of LCDV DNA copies were calculated to determine the correlation with the severity of clinical signs. The qPCR analysis confirmed that all animals were positive to viral MCP protein (Valverde *et al.* 2016b), as expected by the lesions, although with a huge range of variation in viral loads. Moreover, the high correlation (>90%) between LCDV DNA copies and the four SI categories confirmed this index is a good indicator of viral replication. It should be noted that although the liver is not the target organ for LCDV viral replication, this virus is able to replicate on it before spreading in integumentary system (Kvitt *et al.* 2008; Carballo *et al.* 2017; Valverde *et al.* 2017a). The selection of this organ appears also as a key point to precisely quantify DNA copies to prevent cross-contaminations between skin lesions in highly infected fish populations.

The reconstructed familial structure revealed a high variance in the offspring contribution, a feature previously reported for mass-spawning in photoperiod-controlled sea bream broodstocks (Brown & Gordon 2005; Antonello *et al.* 2009). In the results of this chapter, only 59% breeders contributed progeny with a higher contribution of female breeders that it fits to the broodstock structure established at the beginning of the breeding period. The most striking was the strong bias for offspring contribution between F2 and the control broodstocks in spite of containing a similar number of breeders. Although the weight of breeders (average 1,875±240 vs 731±144 for F2 and control, respectively) could be a major factor behind the differences in egg production, the quadratic relationship reported for parental weights and progeny production (Brown & Gordon 2005) not fully support this hypothesis. We cannot exclude that selective breeding for growth in F2 could also indirectly improve relative fecundity, a hypothesis that needs to be tested.

Heritability estimates for the hepatic number of LCDV DNA copies was almost negligible in both batches (0.04 and 0.08) but it showed a high genetic correlation with SI (>0.99). Nevertheless, the heritability in the liability scale for binary SI was estimated to be 0.32-0.33 and 0.22-0.24 for *batch1* and *batch2*, respectively, indicating that this index could be a useful trait to evaluate the genetic susceptibility to LCDV. The heritabilities were moderate but similar to those reported for nodavirus resistance on the liability scale in the European sea bass (0.26±0.11) (Doan *et al.* 2017) or against Pdph in sea bream (0.12-0.28) (Antonello *et al.* 2009; Palaiokostas *et al.* 2016) supporting the idea that selective breeding for LCDV susceptibility is feasible.

Previous reports indicated that heritabilities for furcal length in juvenile sea bream specimens are moderate (h^2=0.31±0.07 for fish of 6.6 cm in length and age 130 dph (Navarro *et al.* 2009) and h^2=0.38±0.08 for fish of ~2.3 cm in length and age 110 dph (Antonello *et al.* 2009)). For weight, Navarro *et al.* (2009) showed that heritability at age 130 dph was 0.28±0.07. Although the fish weight and length values in the present study are closer to those reported by Navarro *et al*. (2009), our heritability estimates are still a bit lower for both traits (0.18 and 0.14 for *batch1* for weight and length, respectively and very close to zero in *batch2*). These lower genetic estimates could be due to the energy reallocation mediated by LCDV from somatic growth to virus replication and fibroblast hyperplasia in the integumentary tissues. Moreover, the heritability differences between batches with different age, weight and SI suggest that bigger fish can mobilize energy towards the immune system response to fight against the LCDV infection masking the genetic effects on growth. Supporting this hypothesis are the genetic correlations between growth traits (weight and length) and the SI in both batches: positive and high in *batch1* but negative in *batch2*. One major constraint in this study is the lack of longitudinal information to span whole infection period but the sampling of two aged-batches with contrary genetic correlations indicate that susceptibility is highly dependent on fish age. Resistance to viral diseases is generally negative correlated with weight

(Henryon *et al.* 2002; Doan *et al.* 2017). In sea bream, the resistance to Pdph was positive correlated to fork length although the authors could not explain if the association was due to the survival time or the weight itself (Antonello *et al.* 2009). In our study, a high variation in weight was found within each batch and the differences in genetic correlation seems to be more associated to development and a putative enhancement of immunocompetence than size itself that allow fish to better deal with this benign infection. According to this hypothesis a mixed selection index that combines length and SI could be useful for selective breeding of superior animals preserving growth potential but limiting the viral replication and phenotypic lesions.

CONCLUSIONS

1. LCDV is horizontally transmitted in Senegalese sole post-larvae through both rearing seawater and infected live preys. In both routes, a wide defensive response was triggered although with temporal and intensity differences. However, histopathological changes and LCDV distribution and loads were route-specific with severe lesions in skin and gills indicating these organs as the main entry of this virus into the host.

2. LCDV rapidly moves into the bloodstream when intraperitoneally injected in sole juveniles spreading rapidly to target organs such as kidney, gut and liver, appearing the kidney as the organ with the highest viral concentration The wide defensive response triggered in the host that include antiviral-specific genes, pro-inflammatory cytokines, chemokines and several other genes related to the innate and adaptive immune defence limits virus replication, reducing progressively the viral loads but with animals remaining as asymptomatic carriers.

3. A crude extract of *Nannochloropsis gaditana* whole-cells was effective in reprogramming larval plasticity. A long-lasting effect on growth performance, oxygen demands and immune system responses was demonstrated. The modification the steady-state levels of biochemical activities and gene expression patterns as well as treatment-specific defensive response against LCDV envises a novel application of microalgae in trained immunity.

4. The microalgae chrysolaminarin-enriched extract (MAe) from the diatom *Phaeodactylum tricornutum* has a potent antioxidant capacity and antiproliferative effect in cells higher than particulate yeast β-glucans.

Intraperitoneal injection in juvenile soles produces a moderate mortality and activates a fast, transient and potent inflammatory response with organ-specific expression patterns. The lack of response after reinjection indicated that soles developed a resistance state demonstrating the suitability of this enriched extract as a novel and potent source of β-glucans suitable for immunostimulation.

5. Orally administration of microalgae chrysolaminarin-enriched extract (MAe) to juvenile soles had a well differentiated response compared to particulate yeast-β-glucans or when intraperitoneal injected. MAe activated a transient systemic anti-inflammatory response with the down-regulation of pro-inflammatory cytokine expression, lysozyme activity in blood serum and a moderate reduction of *Vibrio* loads. In contrast, the administration of insoluble yeast β-glucans acted mainly locally in the gut modulating the immune response and controlling the *Vibrio* abundance. These results indicate that both bioactive molecules could be used as prebiotics able to modify the microbiomes and modulate the immune system.

6. A phenotyping methodology to quantify LCDV infections was developed. LCDV DNA particles in the liver were highly correlated with severity infection categories. Using this novel approach, the first genetic estimates for LCDV susceptibility in gilthead sea bream was obtained indicating a moderate heritability in the liability scale although estimates were highly dependent on the age. The data obtained demonstrate the adequacy of genetic programs to effectively reduce the susceptibilty of gilthead sea breams to LCDV.

RESUMEN

1. INTRODUCCIÓN

1.1 Estado del sector de la acuicultura de dorada (*Sparus aurata*) y lenguado senegalés (*Solea senegalensis*)

La dorada y el lenguado senegalés son dos especies de gran importancia económica en el sur de Europa, aunque la producción de dorada se extiende a toda la cuenca mediterránea. mientras que la de lenguado es principalmente en España y Portugal. El estado actual del desarrollo de la acuicultura en ambas especies es completamente diferente en términos de volumen de producción, tecnologías de cultivo, retos tecnológicos y cuellos de botella (Manchado *et al.* 2016).

La dorada es la primera especie marina por volumen de producción en Europa (95.390 toneladas y 435,1 M€). La producción total de esta especie, incluyendo a Turquía (el principal productor en la región mediterránea) se incrementó un 10,7% (~246.839 T) en 2018 con respecto a 2017 y se espera que continúe creciendo en 2019. Mientras Turquía produce un 33,6% de la producción total en el Mediterráneo, España ocupa la cuarta posición con solamente el 6% de la producción (APROMAR 2019). A diferencia de la dorada, la producción de lenguado sigue siendo escasa (Dinis *et al.* 1999; Morais *et al.* 2016; APROMAR 2018), siendo los principales países productores España, Islandia, Francia y Portugal. Las cifras de producción de esta especie aumentaron de 200 toneladas a principios de esta década a las 1.616 toneladas en 2017 y, aunque se registró una disminución de 3,9% en 2018, se espera una rápida expansión en 2019 (APROMAR 2018).

Para el cultivo de estas dos especies se emplean distintas tecnologías, que están adaptadas a su biología y comportamiento contribuyendo de esta manera a una óptima salud y bienestar (Palstra & Planas 2011; Oca & Masaló 2019). La dorada se cultiva en jaulas marinas y tanques interiores de forma intensiva y en estanques de tierra en extensivo o semi-intensivo (Basurco *et al.* 2011), mientras que el lenguado se cultiva en sistemas intensivos en tanques poco profundos tanto en

sistema abierto como principalmente en recirculación (RAS) con controles de los parámetros ambientales (Morais *et al.* 2016).

La acuicultura de la dorada comenzó en los años 1980, existiendo en la actualidad protocolos bien definidos para manipular los reproductores y su desove, así como para la cría larvaria (Basurco *et al.* 2011). Esta especie es muy robusta y con una alta plasticidad, capaz de adaptarse a diferentes ambientes, cambios de dieta y resistente a enfermedades que explican, al menos parcialmente, su éxito en la acuicultura (Manchado *et al.* 2016). La acuicultura industrial para el lenguado senegalés comenzó mucho más tarde, y el incremento en la producción de esta especie se debe, en gran medida, a la implantación de los RAS (Dinis *et al.* 1999; Morais *et al.* 2016; APROMAR 2018), junto a los avances en el cultivo larvario y fases post-larvarias (Cerda & Manchado 2013). No obstante, la reproducción y el control de enfermedades siguen siendo los principales problemas inherentes al cultivo de esta especie (Manchado *et al.* 2016).

A pesar de todos los progresos tecnológicos, aún existen importantes retos y cuellos de botella en la acuicultura de estas dos especies marinas en tres campos esenciales como son: a) Nutrición: Todavía se necesita optimizar las dietas para cada especie en las distintas etapas de desarrollo (EATiP 2014; Manchado *et al.* 2016), así como la utilización de nuevas materias primas de menor impacto ambiental y el desarrollo de aditivos funcionales, como probióticos, prebióticos e inmunoestimulantes (Encarnação 2016). b) Genética: La implementación de programas de selección, como los iniciados en dorada (Garcia-Celdran *et al.* 2015a; Lee-Montero *et al.* 2015; 2016), requiere la creación de estructuras que soporten los programas a largo plazo (EATiP 2014). En el caso del lenguado, a pesar de los primeros pasos en mejora genética (Manchado *et al.* 2019), el principal problema a resolver sigue siendo el control de la reproducción en cautividad (Manchado *et al.* 2016). c) Salud animal: Se requiere reducir la incidencia de las enfermedades infecciosas para reducir las pérdidas económicas associadas a estas patologías y

crear estándares de bienestar animal en las explotaciones piscícolas.

Para la dorada y el lenguado, las principales enfermedades infecciosas son las provocadas por bacterias, principalmente las vibriosis producidas por *Vibrio sp*. y *Photobacterium damselae* subsp. *piscicida* (Toranzo *et al.* 2005; Colorni & Padrós 2011; Morais *et al.* 2016). Asimismo, las enfermedades parasitarias representan un problema emergente en la acuicultura de estas dos especies (Colorni & Padrós 2011; Borrego *et al.* 2017a). Finalmente, entre las enfermedades infecciosas, las de origen vírico representan un grupo especial por su gran impacto económico, debido a las pérdidas directas de producción, sobrecostes derivados por la pérdida de productividad, los costes de eliminación de los restos animales durante los brotes y las limitaciones legales a las exportaciones (Whittington & Chong 2007; Rigos & Katharios 2010).

Entre las infecciones virales que pueden afectar a la dorada y el lenguado, se encuentran las producidas por betanodavirus (Virus de la Necrosis Nerviosa Viral, VNNV) que afecta principalmente al lenguado (Padros *et al.* 2019), aunque la dorada parece ser también susceptible (Cherif *et al.* 2009); el Virus de la Necrosis Pancreática Infecciosa (IPNV) y el Virus de la Septicemia Hemorrágica Viral (VHSV) en el lenguado, aunque el primero no parece tener un papel claro como patógeno primario y en el segundo caso no se han registrado brotes naturales (Rodriguez *et al.* 1997; Lopez-Vazquez *et al.* 2011; 2017; Padros *et al.* 2019); además se ha descrito un aquareovirus en estadíos larvarios de doradas (Bandin *et al.* 1995).

El Virus de la Enfermedad de Linfocistis (LCDV), que se considera la infección viral más importante que afecta a la dorada (Borrego *et al.* 2017b), y secundariamente al lenguado senegalés (Alonso *et al.* 2005; Cano *et al.* 2010).

1.2 Virus de la enfermedad de linfocistis

El LCDV es un virus icosaédrico, perteneciente a la familia *Iridoviridae*

(Jancovich *et al.* 2012), cuyo material genético está constituido por una molécula de ADN bicatenario (bc) lineal, con redundancia terminal y repeticiones invertidas, altamente metilada y con un contenido en G+C del 30% (Goorha & Murti 1982). El virión está formado por una membrana interna lipoproteica, con un alto contenido en fosfolípidos, y una cápside proteica, constituida fundamentalmente por la proteína principal de la cápside (MCP) y en la que aparecen estructuras filamentosas de función desconocida (Devauchelle 1985; Flugel 1985; Liu *et al.* 2016b). En función de las secuencias de la MCP, el LCDV se ha clasificado en nueve genotipos distintos, de los que solamente tres de ellos han sido identificados como especies distintas, como es el caso de la especie LCDV-Sa, asociada al genotipo VII al que pertenecen los aislados víricos de dorada y lenguado (Borrego *et al.* 2017b) y que se ha estudiado en esta tesis doctoral.

El LCDV es el agente causal de la enfermedad de linfocistis (LCD). Esta enfermedad infecciosa ha sido descrita en más de 140 especies diferentes de peces teleósteos, tanto marinos como dulceacuícolas, y está ampliamente distribuida por todo el mundo (Borrego *et al.* 2017b). La LCD se caracteriza por la aparición de lesiones proliferativas en la piel correspondientes a células fibroblásticas hipertrofiadas denominadas linfocistes o células linfoquísticas (Paperna *et al.* 1982; Samalecos 1986). Estas lesiones son de color blanquecino a grisáceo, que pueden aparecer aisladas o, con mayor frecuencia, agrupadas en racimos y localizadas en la superficie del cuerpo y las aletas, pudiendo llegar a cubrir todo el cuerpo del animal (Sarasquete *et al.* 1998; Borrego *et al.* 2017b).

Normalmente, la LCD no provoca mortalidades importantes, aunque animales con infecciones severas pueden llegar a morir, especialmente en individuos juveniles (Colorni & Padrós 2011). Sin embargo, los animales con LCD son más susceptibles a infecciones bacterianas secundarias, parasitismos o episodios de canibalismo, incrementando las tasas de mortalidad asociadas a la enfermedad (Williams *et al.* 2005; Colorni & Padrós 2011; Dezfuli *et al.* 2012;

Haddad-Boubaker *et al.* 2013). Además, la elevada morbilidad, cercana al 100%, provoca un retraso significativo en las tasas de crecimiento, que acarrea importantes pérdidas económicas en la acuicultura de las especies afectadas (Nishida *et al.* 1998; Iwamoto *et al.* 2002).

En la dorada se ha estudiado el curso de la infección viral, tanto los mecanismos de propagación, persistencia y tropismo del virus, utilizando diversas técnicas moleculares para la detección del virus (Cano *et al.* 2009b; 2013; Valverde *et al.* 2016b; 2017b), así como la caracterización de la respuesta inmune en doradas infectadas de forma natural (Cordero *et al.* 2016). Por otra parte, en el lenguado, existe escasa información sobre los mecanismos de infección y propagación del virus. De igual forma, se desconoce la respuesta inmune frente a la infección, por lo que es necesario estudiar los mecanismos implicados, así como caracterizar la respuesta inmune del lenguado frente a LCDV. En este sentido, la biotecnología ofrece nuevas y potentes herramientas para su aplicación en la acuicultura, como es el caso de la base de datos "SoleaDB" (Benzekri *et al.* 2014), que contiene una gran información genómica, permitiendo a su vez el desarrollo de herramientas de alto rendimiento para un rápido avance en el conocimiento de la respuesta inmunológica del lenguado.

1.3 El sistema inmune innato en teleósteos

El crecimiento de la acuicultura requiere un mejor conocimiento del sistema inmune de los peces con el fin de reforzar la defensa inmune innata de los peces, mediante la optimización de las condiciones de cultivo, la selección de reproductores y el desarrollo y mejora de las medidas profilácticas, tales como la vacunación y el uso de probióticos y prebióticos e inmunoestimulantes (Magnadottir 2010; Secombes & Wang 2012).

El sistema inmune de los peces, como el de vertebrados superiores, es

"completo", es decir, está compuesto por el sistema inmune innato y el sistema inmune adaptativo (Magnadottir 2006; Secombes & Wang 2012) que se expondrán a continuación.

1.3.1 Sistema inmune innato

El sistema inmune innato se considera la primera barrera para hacer frente a la invasión de patógenos. Este sistema reconoce motivos conservados en las superficies de los patógenos llamados patrones moleculares asociados a los patógenos (PAMPs). Estos patrones moleculares incluyen componentes de la pared celular bacteriana, como el lipopolisacárido (LPS) y el peptidoglucano (PGN), ácidos nucleicos presentes en virus y bacterias, incluido el ARN viral de doble cadena, y varios polisacáridos, como β-glucanos o mananos (Medzhitov & Janeway 2002).

El sistema inmune innato se puede dividir en tres componentes principales: la barrera epitelial/mucosa, los componentes celulares y los humorales (Magnadottir 2010).

Las barreras epiteliales y mucosas de la piel, las branquias y el tracto digestivo son muy importantes para hacer frente a las enfermedades, proporcionando una protección física y mecánica contra los ataques microbianos (Magnadottir 2006; 2010; Raj *et al.* 2011; Gomez *et al.* 2013; Merrifield & Rodiles 2015). Junto a estas barreras físicas se puede encontrar el tejido linfoide asociado a mucosas (MALT), en el que se encuentra abundantes leucocitos (Haugarvoll *et al.* 2008; Fuglem *et al.* 2010), y que se clasifica según su localización en: tejido linfoide asociado al intestino (GALT), tejido linfoide asociado a la piel (SALT), tejido linfoide asociado a las branquias (GIALT) y tejido linfoide asociado a la nasofaringe (NALT) recientemente descubierto (Salinas 2015). Otra barrera importante son los microbiomas, que también juegan un papel crucial en la maduración del sistema inmune de los peces (Wu *et al.* 2012) y que compite con microorganismos patógenos

para la colonización de los tejidos, y por tanto, evitar la infección (Llewellyn *et al.* 2014; Talwar *et al.* 2018).

Los componentes celulares del sistema inmune innato son las células fagocíticas (monocitos y macrófagos), que desempeñan funciones fundamentales en la protección del hospedador y la homeostasis, la fagocitosis y la producción y liberación de citocinas proinflamatorias, producción de óxido nítrico y actividad de estallido respiratorio (Grayfer *et al.* 2014; Hodgkinson *et al.* 2015); otro componente celular son los granulocitos (neutrófilos), que inician el estallido respiratorio y activan a los macrófagos para la producción de especies reactivas de oxígeno (ROS), además tienen un papel importante en la fase de recuperación de los niveles basales (Havixbeck *et al.* 2016); y las células citotóxicas no específicas (células NCC), hómologas de los linfocitos NK de mamíferos que están involucradas en la citotoxicidad celular no específica (CMC) (Shen *et al.* 2002; Nakanishi *et al.* 2011; Secombes & Wang 2012).

Finalmente, el componente humoral del sistema inmune innato esta constituido por diferentes receptores/proteínas (PRR/P) entre los que se incluyen: la transferrina, un quelante de hierro que afecta al crecimiento bacteriano (Trites & Barreda 2017); los receptores tipo-Toll (TLR), capaces de reconocer los distintos PAMP, tanto víricos como bacterianos (Pietretti & Wiegertjes 2014); los inhibidores de proteasas, la lisozima y el sistema del complemento que están presentes en el suero y otros fluidos corporales y que se ha demostrado en dorada y lenguado como esenciales en la respuesta frente a microorganismos patógenos (Prieto-Alamo *et al.* 2009; Salas-Leiton *et al.* 2010; Mauri *et al.* 2011; Ponce *et al.* 2011; Khosravi *et al.* 2015; Nunez-Diaz *et al.* 2016; Guardiola *et al.* 2019). Las aglutininas y precipitinas como las lectinas y las pentaxinas, que pueden unirse específicamente a glucoproteínas y glucolípidos presentes en las membranas de los patógenos (Magnadottir 2006; da Silva Lino *et al.* 2014); y las citocinas como las pro-inflamatorias TNF e IL1β, quimiocinas, que atraen células inmunológicas al foco inflamatorio y el interferón

(IFN) (Magnadottir 2010). El IFN inicia una cascada de activación intracelular que conlleva la expresión de los genes estimulados por interferón (ISGs), como la Mx con actividad antiviral frente a varios virus incluido LCDV en dorada y lenguado (Fernandez-Trujillo *et al.* 2008; Alvarez-Torres *et al.* 2013; Labella *et al.* 2018), además, también se incluyen diversos factores reguladores del interferón (IRFs) que tienen un papel central en la regulación de la ruta del IFN.

1.3.2 Sistema inmune adaptativo

El sistema inmunitario adaptativo, como en el innato, está formado por componentes celulares y humorales, como los linfocitos B y T, las inmunoglobulinas (Ig), el complejo principal de histocompatiblidad, así como diversas citocinas (Laing & Hansen 2011; Secombes & Wang 2012; Wang & Secombes 2013).

Los linfocitos B se caracterizan por poseer un receptor constituido por una molécula de Ig en su membrana celular y cuya función principal es la producción de las Igs (Parra *et al.* 2016; Scapigliati *et al.* 2018; Diaz-Rosales *et al.* 2019). Los linfocitos T se caracterizan por expresar el receptor de células T (TCR) en su superficie (Secombes & Wang 2012; Scapigliati *et al.* 2018), existiendo varios subtipos (Tc, Th o Treg) según su función (Laing & Hansen 2011; Nakanishi *et al.* 2011; Takizawa *et al.* 2016; Kasheta *et al.* 2017).

En cuanto a los factores humorales, las Igs son los más importantes en la inmunidad adaptativa. En los peces, existen tres isotipos de Igs: IgM, IgD e IgT/Z (Edholm *et al.* 2011; Zhang *et al.* 2011; Ramirez-Gomez *et al.* 2012). Además de las Igs, las moléculas de los MHC de clase I y MHC clase II tienen un papel primordial en la presentación antigénica (Wilson 2017). Las citocinas también desempeñan un papel importante en la inmunidad adaptativa, como los miembros de la familia de citocinas γc), el factor de crecimiento tumoral-β (TGF-β) y otras interleucinas (Wang & Secombes 2013; Zhu *et al.* 2013).

1.4 Estrategias para el control de enfermedades en acuicultura

El desarrollo de modelos sostenibles para la producción acuícola deben ir acompañados de avances en el control y prevención de enfermedades infecciosas como la provocada por el LCDV. En este sentido, y debido a la ausencia de vacunas eficientes frente a este virus, las principales estrategias para combatir el LCDV se basan en la monitorización y eliminación de los portadores asintomáticos, el uso de inmunoestimulantes y la mejora genética selectiva para linajes de resistencia.

1.4.1 Monitorización y eliminación de portadores asintomáticos

El control virológico de portadores asintomáticos de distintos lotes de peces ha demostrado ser una estrategia muy efectiva para prevenir brotes de LCDV, detectando y sacrificando los portadores asintomáticos, que son considerados como la principal ruta de introducción del virus en las instalaciones (Borrego *et al.* 2017b). Para el control de los portadores de LCDV se han desarrollado metodologías de diagnóstico molecular muy sensibles que permiten detectar el genotipo VII que afecta a doradas y lenguados en las piscifactorías europeas y del área meditarránea (Cano *et al.* 2007; Valverde *et al.* 2016b; 2017a).

1.4.2 Uso de compuestos inmunomoduladores

Otra estrategia para el control de la LCD es el uso de sustancias inmunoestimulantes por la alimentación, que limiten la multiplicación del virus como por ejemplo extractos de plantas, hongos y algas con función prebiótica capaces de mejorar la salud y prevenir brotes de enfermedades microbianas (Akhter *et al.* 2015; Douxfils *et al.* 2017), aunque su uso en la acuicultura todavía es limitado y su mecanismo de acción está todavía siendo estudiada (Dimitroglou *et al.* 2011).

Los prebióticos son normalmente moléculas no digeribles, generalmente poli- y oligosacáridos, que modulan selectivamente el microbioma intestinal al promover el crecimiento de poblaciones microbianas comensales y evitar la colonización y crecimiento de microorganismos patógenos (Dimitroglou *et al.* 2011; Akhter *et al.* 2015). Los β-glucanos se han usado como prebióticos debido a su acción

como moduladores de microbiomas que se unen a los receptores PAMP para desencadenar una respuesta inmune innata (Meena *et al.* 2013; Song *et al.* 2014). Estos compuestos comprenden un grupo heterogéneo de polisacáridos (D-glucosa unidos por enlaces (1,3)-β, (1,4)-β o (1,6)-β) con ramificación β-(1,4) o β-(1,6) que forman parte de la pared celular de organismos procarióticos y eucarióticos o son materiales de reserva energética en bacterias, hongos, algas y plantas. La unión de los β-glucanos a sus receptores desencadena una cascada de respuesta inmune innata y adaptativa, como la fagocitosis, el estallido oxidativo y la producción de citocinas y quimiocinas en DC y macrófagos (Brown *et al.* 2003).

Los β-glucanos poseen un alto interés biotecnológico y biomédico, debido a sus actividades como sustancias antitumorales, antiinflamatorias, antiobesidad, antialérgicas, antiosteoporóticas e inmunomoduladoras (Bashir & Choi 2017). Estos polisacáridos se pueden emplear en acuicultura como suplementos alimentarios y para enriquecer la alimentación viva (artemias y rotíferos) (Ringø *et al.* 2012). Se ha demostrado que poseen funciones inmunoestimulantes y prebióticas, pudiendo mejorar el crecimiento de los peces, su supervivencia y la respuesta inmune, así como la resistencia a microorganismos patógenos (Ringø *et al.* 2012; Meena *et al.* 2013). Además, trabajos recientes demuestran el papel de los β-glucanos en la reprogramación epigenética de células mieloides de peces (Saeed *et al.* 2014; Netea *et al.* 2016; Petit & Wiegertjes 2016; Petit *et al.* 2019b). La reprogramación del sistema inmune innato, que permite adaptar su función después de una exposición y generar una memoria duradera, ofrece un enfoque atractivo en el cultivo intensivo de larvas de peces, donde el sistema inmune adaptativo no está completamente desarrollado, mejorando la resistencia a enfermedades virales y bacterianas (Zhang *et al.* 2019).

En acuicultura, la fuente más común de β-glucanos es la levadura de cerveza (*Saccharomyces cerevisiae*), como el Macrogard® y Yestimun®, un β-glucano comercial insoluble pero altamente purificado (Stier *et al.* 2014). Sin embargo, el incremento

en la producción de microalgas abre la posibilidad de que estos microorganismos eucaróticos se puedan considerar como una nueva fuente de estos polisacáridos funcionales. Los β-glucanos de las microalgas, o crisolaminarina, son polisacáridos cortos y solubles sintetizados por varias microalgas marinas, como *Phaeodactylum tricornutum* y *Nannocloropsis* (Sadovskaya *et al.* 2014; Gugi *et al.* 2015; Rojo-Cebreros *et al.* 2017) y, aunque se utilizan varias especies de microalgas para la alimentación de los peces (Hemaiswarya *et al.* 2011), no existe suficiente información sobre su bioactividad en el cultivo de peces.

1.4.3 Mejora genética selectiva para linajes de resistencia.

El empleo de programas de selección genética enfocados a la resistencia o menor susceptibilidad a enfermedades infecciosas es considerada como la estrategia más sostenible para reducir y minimizar el impacto de las mismas en la acuicultura, aunque requiere que exista variabilidad genética en las poblaciones piscícoas a seleccionar (EATiP 2014). Trabajos previos en *Paralichthys olivaceus* han demostrado la posibilidad de seleccionar líneas de resistencia a la LCD donde se identificó un locus principal asociado con la resistencia contra el genotipo II de LCDV (Fuji *et al.* 2006) y se usó para el diseño de programas de reproducción asistida por marcadores y la construcción de reproductores resistentes a virus (Fuji *et al.* 2007).

En dorada, la mayoría de los programas genéticos en curso se centran principalmente en la mejora del crecimiento, la morfología y la calidad de la canal (Garcia-Celdran *et al.* 2015a; 2015b; 2015c; Lee-Montero *et al.* 2015; Navarro *et al.* 2016), y, sólo se ha evaluado resistencia a la bacteria *P. damselae* subsp. *piscicida*(Pdph) (Antonello *et al.* 2009; Palaiokostas *et al.* 2016). En esta tesis doctoral se ha evaluado la resistencia genética de familias de dorada frente a la LCD, dentro del plan de selección genética desarrollado a nivel nacional para la mejora de la producción de dorada PROGENSA (www.progensa.eu).

2. OBJETIVOS

En la presente tesis doctoral se han planteado 4 objetivos principales:

1. El estudio de la infección por LCDV en post-larvas de lenguado senegalés y la relación con la expresión de genes de inmunidad. Este objetivo se ha desarrollado en el capítulo 3 de la presente tesis: "La exposición de LCDV en post-larvas de lenguado senegalés mediante alimentación e inmersión revela mecanismos específicos para la transmisión horizontal del virus y una respuesta inmune específica".
2. El estudio del curso de la infección por LCDV en juveniles de lenguado senegalés y la relación con la expresión de genes de inmunidad, ha sido desarrollado en el capítulo 4 de la presente tesis: "Perfiles de expresión de genes asociados con LCDV en lenguado senegalés (*Solea senegalensis*) infectados experimentalmente".
3. La evaluación del efecto de sustancias bioactivas de microalgas para estimular la respuesta defensiva frente a linfocistis, se ha dividido en dos subobjetivos:
    a. Caracterización de la respuesta *in vivo* inducida por extractos de microalgas en post-larvas de lenguado: desarrollado en el capítulo 5 "Extractos de microalgas inducen la reprogramación inmunológica y modifica las respuestas a compuestos bioactivos y a infecciones por LCDV".
    b. Caracterización de la respuesta *in vivo* inducida por extractos de microalgas en juveniles de lenguado: desarrollado en el capítulo 6 "Capacidad antioxidante y efecto inmunomodulador del extracto enriquecido en crisolaminarina en lenguado senegalés" y capítulo 7 "β-glucanos de levadura y un extracto de microalgas modulan la respuesta inmune y el microbioma intestinal en lenguado senegalés (*Solea senegalensis*)".

4. La evaluación genética de la resistencia a la infección por linfocistis en dorada. Este objetivo ha sido desarrollado en el capítulo 8 de la presente tesis: "Evaluación genética de la resistencia frente a la infección por LCDV en dorada".

3. La exposición del LCDV en post-larvas de lenguado senegalés mediante alimentación e inmersión revela mecanismos específicos para la transmisión horizontal del virus y una respuesta inmune específica.

En este capítulo se investigó la transmisión horizontal del LCDV en post-larvas de lenguado senegalés a través del agua y el alimento contaminados (usando artemias como vehículo) y los perfiles de expresión de genes inmunes asociados.

Todas las muestras analizadas fueron positivas para la detección del genoma de LCDV en 1 día después de la exposición (1 dpe) con los niveles virales más altos en muestras inoculadas a través de la ruta de inmersión. Sin embargo, el porcentaje de animales positivos para LCDV y el número de copias de ADN viral disminuyeron progresivamente a 2 y 7 dpe. El análisis histológico identificó cambios estructurales en la piel, el músculo y las branquias de las post-larvas de lenguado inoculadas con LCDV vía inmersión. Además, la hibridación *in situ* confirmó una amplia distribución de LCDV en la piel, el intestino, los vasos circundantes en el músculo y el riñón cefálico, mientras que en la exposición a través de la alimentación, las señales de hibridación se restringieron al hígado y la lámina propria de intestino. El análisis de expresión utilizando un conjunto de 22 genes relacionados con el sistema inmune innato demostró diferencias temporales claras en la respuesta a LCDV, así como en función de la ruta de infección. La mayoría de los genes de defensa antiviral, las citocinas pro-inflamatorias, el complemento *c3*, la lisozima de tipo g y los marcadores de células T *cd4* y *cd8a* se indujeron rápidamente en las post-larvas infectadas con alimentación, y se mantuvieron activadas a 2 dpe. Sin embargo, en las post-larvas infectadas por inmersión, la inducción de la mayoría de los genes defensivos se retrasó y una menor intensidad a 2 dpe. Todos estos datos demuestran que LCDV puede infectar horizontalmente las post-larvas de lenguado senegalés a través del agua o el

alimento, aunque con diferentes patrones de daños histopatológicos, distribución de virus y perfiles de expresión específicos de la ruta.

4. Perfiles de expresión de genes asociados con LCDV en lenguado senegalés (*Solea senegalensis*) infectados experimentalmente

En este capítulo, se determinó la patogénesis del LCDV y los patrones de expresión de genes inmunes asociados con esta infección viral en el lenguado senegalés tras inoculación intraperitoneal en juveniles. Los resultados indicaron que el LCDV se diseminaba rápidamente desde la cavidad peritoneal a través del torrente sanguíneo para llegar a los órganos diana como el riñón, el intestino, el hígado y la piel/aleta. El riñón fue el órgano que presentó la mayor carga viral, reduciendo su título progresivamente a lo largo del experimento, a pesar de que se pudo detectar la transcripción del gen principal de la proteína de la cápside viral. La inoculación de LCDV activó la expresión de un amplio número de genes en riñón e intestino, aunque con algunas diferencias en la temporalidad y de intensidad de la respuesta. Este conjunto de genes diferencialmente expresado incluía genes de la respuesta antiviral (*mx* y los factores relacionados interferón *irf1, irf2, irf3, irf7, irf8, irf9, irf10*), citocinas (*il1b, il6, il8, il12* y *tnfa*) y sus receptores (*il1r, il8r , il10r, il15ra, il17r*), quimiocinas (tipo CXC, tipo CC e IL-8), prostaglandinas (*cox-2*), lisozimas de tipo g, hepcidina, factores del complemento (*c2, c4-1* y *c4-2*) y los marcadores linfocitarios *cd4*, *cd8a* y *cd8b*. El perfil de expresión observado indica que el hospedador era capaz de desencadenar una respuesta defensiva sistémica, que incluye inflamación, capaz de hacer frente a la infección vírica.

5. Extractos de microalgas inducen la reprogramación inmunológica y modifica las respuestas a compuestos bioactivos e infecciones por LCDV

El uso de inmunoestimulantes como aditivos de piensos y la inducción de la memoria inmunitaria innata recientemente descubierta son dos formas complementarias para aumentar las respuestas defensivas y la protección contra los patógenos en los peces. En el capítulo 5 de esta tesis se estudió la respuesta *in vivo* inducida por extractos de microalgas en post-larvas de lenguado senegalés. En concreto, se investigó el uso de un extracto crudo de células completas *Nannochloropsis gaditana* (Nanno) para modificar la plasticidad de las larvas en etapas tempranas y la reprogramación del sistema inmune innato en lenguado senegalés. Para ello, la respuesta imune de las post-larvas tratadas con los extractos de Nanno se ensayó por la administración de dos compuestos bioactivos, β-glucano de levadura (Y) y un extracto de microalgas derivado de la diatomea *Phaeodactylum tricornutum* (MAe), y tras una exposición con el LCDV. Las larvas reprogramadas con Nanno mostraron un mayor peso seco y longitud que el grupo control a los 21 días de la eclosión (dpe). A los 32 dias de edad, las post-larvas fueron alimentadas con dos dosis de los compuestos bioactivos Y y MAe , vehiculados a través de presas vivas (artemias). Las post-larvas alimentadas con los tratamientos bioactivos Y y MAe presentaron una mayor mortalidad que el grupo control (SW), así como las larvas reprogramadas con Nanno respecto a sus controles, indicando la existencia de una reprogramación metabólica y la modificación de la demanda de oxígeno. Por otra parte, las actividades enzimáticas para la lisozima y las antiproteasas totales en las post-larvas enteras indicaron niveles más altos de actividades en las post-larvas tratadas con Nanno y las alimentadas con MAe en comparación con sus grupos de control correspondientes a las 6 h. Los perfiles expresión indicaron que las post-larvas tratadas con Nanno tenían niveles más altos de ARNm de los genes *cxc10* y *mx* que el control sin tratar. Los genes *il1b* e *irf7* también modificaron los

niveles de expresión, aunque en este caso también mostraron interacción significativa con el tiempo. Con respecto a los compuestos bioactivos, MAe aumentó la expresión de *il1b* y *mx* aunque con diferencias temporales. A las 24 h, se observó una disminución general de los niveles de expresión de los nueve genes analizados, debido probablemente a condiciones estresantes asociadas a la hipoxia.

Las larvas supervivientes de los grupos control e Y fueron inoculadas con LCDV a las 72 h. No existieron diferencias en el número de copias de ADN viral entre los grupos reprogramados y de compuestos bioactivos, aunque el número de copias reducía con el tiempo. Los perfiles de expresión en el control (no infectado) separaron claramente las larvas pre-alimentadas con Y de su grupo control lo que indica un efecto duradero de los β-glucanos en la expresión de los genes estudiados. Además, los perfiles de expresión en el grupo infectado con el LCDV indicaron que las post-larvas activaban una respuesta defensiva amplia, aunque modulada por la reprogramación y los tratamientos con compuestos bioactivos. La expresión de los genes antivirales *irf7*, i*rf3* y *mx* aumentó después de a inoculación con LCDV en las post-larvas del grupo control, pero no en las del grupo Y, tratadas con Nanno. Además, los β-glucanos aumentaron la expresión de genes anti-virales en las post-larvas no reprogramadas, lo que indica una interacción en la regulación de genes antivirales entre los β-glucanos y los tratamientos de reprogramación. La activación de la expresión de las citocinas proinflamatorias *il1b* y *tnfa*, la quimiocina *cxc10* y los marcadores de linfocitos *cd4* y *cd8a* fue más intensa en post-larvas del grupo Y tras la inoculación con LCDV, independientemente del tratamiento de reprogramación. Todos estos datos demuestran la utilidad del extracto crudo de microalgas para reprogramar las larvas y producir una respuesta duradera que mejora el crecimiento y modifica los niveles basales de los genes del sistema inmune innato y de la respuesta al LCDV. Además, la administración a través de la alimentación del extracto de diatomeas MAe y β-glucanos demostró la capacidad de estos prebióticos para modular el sistema inmune en post-larvas y aumentar la

respuesta defensiva al LCDV.

6. Capacidad antioxidante y efecto inmunomodulador del extracto enriquecido en crisolaminarina en lenguado senegalés

Las microalgas son una fuente importante de moléculas bioactivas, incluyendo a los β-glucanos, que pueden usarse como inmunoestimulantes en la acuicultura. En este capítulo se evaluó la capacidad antioxidante, la citotoxicidad y la actividad inmunomoduladora del extracto enriquecido en crisolaminarina obtenido de la diatomea *Phaeodactylum tricornutum* empleado en el capítulo anterior.

El extracto de microalgas mostró una mayor actividad antioxidante total con respecto al de levadura de acuerdo con los ensayos ORAC y FRAP y una menor actividad de eliminación de DPPH. Además, la prueba de citotoxicidad indicó que las concentraciones de extracto de microalgas superiores al 0,01% p/v podrían afectar la viabilidad celular de los fibroblastos dérmicos humanos.

Para evaluar la actividad inmunomoduladora del extracto enriquecido en crisolaminarina, los lenguados juveniles se inyectaron intraperitonealmente con el extracto de microalgas suspendido en aceite de coco (1 mg / pez) seguido de una reinyección a los 7 días. Como control negativo, se inyectó un grupo con la solución de suspensión (aceite de coco). La mortalidad acumulada de los peces inyectados con el extracto enriquecido en crisolaminarina fue del 29,4% después de 6 días y no se registró mortalidad después de la reinyección del extracto. La expresión de los quince genes relacionados con el sistema inmune innato analizados en riñón, bazo e intestino, indicaron respuestas temporales y órgano-específicas. Además, se observó una intensa y rápida inducción (2 días después de la inyección, dpi) de la *il1b* proinflamatoria y del péptido antimicrobiano *hamp1* en los tres órganos inmunológicos, la *hsp90aa* en el riñón y el bazo, *irf3* en el intestino y *c3* en el bazo,

lo que indica una potente respuesta inflamatoria. Tras 5 dpi, los niveles de expresión de estos genes activados descendieron hasta niveles basales, incluyendo el descenso de la expresión del receptor de c-lectina, así como algunos genes relacionados con interferón (*ifn1, irf1, irf3, irf8, irf9* y *mx*) en riñón y *cxc10* en bazo. Todo esto indicó que los lenguados eran capaces de activar una respuesta homeostática frente a la exposición con β-glucano. La reinyección con el extracto enriquecido en crisolaminarina no activó una nueva respuesta inflamatoria, pero redujo los niveles de ARNm de *hsp90aa* e *irf3*, lo que indica que los lenguados desarrollaron cierta resistencia a los β-glucanos. En general, estos resultados revelan que este extracto enriquecido es una nueva y potente fuente de β-glucanos con capacidad antioxidante e inmunomoduladora adecuada para la inmunoestimulación en acuicultura.

7. Los β-glucanos de levadura y un extracto de microalgas modulan la respuesta inmune y el microbioma intestinal en lenguado senegalés

En el capítulo 7 de la presente tesis doctoral, se continuó con el estudio de la respuesta *in vivo* inducida por extractos de microalgas en lenguados juveniles iniciado en el capítulo anterior. Como se ha descrito anteriormente, la necesidad de controlar la aparición de enfermedades infecciosas es un obstáculo a salvar para alcanzar la sostenibilidad de la acuicultura de peces. Las tendencias actuales incluyen el uso profiláctico de sustancias inmunoestimulantes y prebióticas, como algunos polisacáridos. En este capítulo se investigó cómo el β-glucano de levadura (Y), los extractos enriquecidos en polisacáridos de microalgas (MAe) y las células completas de la diatomea *Phaeodactylum tricornutum* (MA) modulaban el microbioma intestinal y estimulaban el sistema inmune en el lenguado senegalés mediante administración oral por medio de intubación. En este ensayo, se

muestrearon la sangre, el intestino y el bazo de los peces a las 3h, 24h, 48h y 7 días después del tratamiento.

La respuesta a corto plazo (dentro de las 48 h posteriores al tratamiento) consistió en la regulación positiva de la expresión de *il1b* e *irf7* en el intestino del grupo tratado con Y. En cambio, la administración de MAe disminuyó la expresión de *tnfa* y la quimiocina *cxc10* en el intestino y el bazo. Mientras que ambos tratamientos disminuyeron la expresión de *irf3* con respecto al grupo control. Con respecto a las actividades enzimáticas, la actividad de la lisozima en plasma disminuyó a las 48 h solo en los lenguados tratados con MAe. La respuesta a medio plazo consistió en una regulación positiva de los niveles de ARNm de los genes *clec* e *irf7* en el intestino de los grupos Y, MAe y MA y de *il1b* en el bazo del grupo MA, en comparación con el grupo control.

El análisis de microbioma utilizando la secuenciación del gen 16S rDNA indicó que el género más abundante era *Vibrio* (> 95%). Todos los tratamientos disminuyeron la proporción relativa de *Vibrio* en el microbioma, mientras que la diversidad disminuyó en los grupos Y y MAe y aumentó en el caso del grupo MA. La PCR cuantitativa confirmó que la carga de bacterias del género *Vibrio* disminuyó significativamente, siendo esta disminución más pronunciada en los peces tratados con Y.

Estos datos indican que los β-glucanos de levadura insoluble administrados por vía oral actuaron localmente en el intestino modulando la respuesta inmune y controlando la abundancia de *Vibrio*. Por el contrario, el MAe redujo ligeramente la carga de *Vibrio* en el intestino y provocó una respuesta antiinflamatoria sistémica transitoria. Los resultados indican que estos polisacáridos son una fuente prometedora de prebióticos para la industria acuícola del lenguado.

8. Evaluación genética de la resistencia frente a la infección por LCDV en dorada

La LCD, como se ha descrito anteriormente, es una patología viral que representa un grave problema económico para los cultivos de dorada (*S. aurata*), debido al importante retraso en las tasas de crecimiento y la aparición de lesiones cutáneas típicas de esta enfermedad. En este capítulo, se determinaron las estimaciones genéticas de la susceptibilidad a la enfermedad provocada por el LCDV y el crecimiento en juveniles de dorada. Para ello, se construyeron dos lotes de peces (denominados lote1 y lote2) a partir puestas masales de tres grupos de reproductores (uno no seleccionado y dos seleccionados para el crecimiento). Estos dos lotes se cultivaron en condiciones industriales en una piscifactoría desde larvas hasta que apareció un brote natural de la enfermedad (LCD). En el momento del muestreo (n = 500 individuo para cada lote), todos los animales presentaban las típicas lesiones provocadas por el LCDV en la piel. Para cuantificar el grado de infección, se pesaron y fotografiaron los individuos para realizar el análisis de imágenes y la cuantificación de las lesiones (superficie cubierta e intensidad). Las copias de ADN de virus se cuantificaron en el hígado mediante qPCR.

El lote1 tuvo una mayor superficie cubierta por lesiones y de mayor intensidad que el lote2. Según el índice de gravedad (SI), el 60% de los peces se consideraba severo o muy severo en el lote1 mientras que sólo el 40% en el lote2. La región caudal del cuerpo fue la región con menor afectación de la enfermedad en ambos lotes. El promedio de copias de ADN de LCDV en el hígado fue mayor en el lote1 y el lote2 y se correlacionaron positivamente con las categorías SI (r^2 = 0,90-0,94). Los animales se genotiparon usando la PCR multiplex SMsa-1 y SMsa-2, siendo las tasas de asignación superiores al 93% para un reproductor y el 84% para una pareja única. El número total de familias fue de 150 y 128 para el lote 1 y el lote 2, respectivamente, con un alto sesgo en la contribución de la descendencia por

familia y reproductores. Las heredabilidades para el peso y la longitud fueron 0,18 y 0,14 en el lote1 y 0,06 y 0,05 en el lote2, respectivamente. La heredabilidad para el número de copias de ADN viral fue baja en ambos lotes (0,04 y 0,08 para el lote1 y el lote2, respectivamente). Las heredabilidades para el SI fueron 0,32/0,33 y 0,21/0,24 para el lote1 y el lote2, usando el modelo de umbral (débil/moderado versus severo/muy severo) en la escala subyacente o con una aproximación bayesiana, respectivamente. Las correlaciones genéticas fueron muy altas y positivas entre los rasgos de crecimiento (peso y longitud) y los rasgos de la enfermedad (número de copias de ADN de LCDV y SI) en ambos lotes. En cambio, las correlaciones genéticas entre el crecimiento y las características de la enfermedad fueron moderadas-altas y positivas en el lote1 pero negativas en el lote2. Estos resultados indican que la selección genética en juveniles de dorada para el crecimiento de los peces y su susceptibilidad a LCDV es factible, aunque las estimaciones dependen primordialmente de la edad. La información proporcionada es relevante para diseñar programas de selección en dorada.

BIBLIOGRAPHY

Akhter N., Wu B., Memon A.M. & Mohsin M. (2015) Probiotics and prebiotics associated with aquaculture: A review. Fish Shellfish Immunol 45, 733-741.

Alonso M.C., Cano I., Castro D., Perez-Prieto S.I. & Borrego J.J. (2004) Development of an in situ hybridisation procedure for the detection of sole aquabirnavirus in infected fish cell cultures. J Virol Methods 116, 133-138.

Alonso M.C., Cano I., Garcia-Rosado E., Castro D., Lamas J., Barja J.L., Borrego J.J. & Bergmann S.M. (2005) Isolation of lymphocystis disease virus from sole, *Solea senegalensis* Kaup, and blackspot sea bream, *Pagellus bogaraveo* (Brunnich). J Fish Dis 28, 221-228.

Alvarez-Torres D., Garcia-Rosado E., Fernandez-Trujillo M.A., Bejar J., Alvarez M.C., Borrego J.J. & Alonso M.C. (2013) Antiviral specificity of the *Solea senegalensis* Mx protein constitutively expressed in CHSE-214 cells. Mar Biotechnol 15, 125-132.

Ambade A., Catalano D., Lim A. & Mandrekar P. (2012) Inhibition of heat shock protein (molecular weight 90 kDa) attenuates proinflammatory cytokines and prevents lipopolysaccharide-induced liver injury in mice. Hepatology 55, 1585-1595.

Andrews N.C. (2004) Anemia of inflammation: the cytokine-hepcidin link. J Clin Invest 113, 1251-1253.

Antonello J., Massault C., Franch R., Haley C., Pellizzari C., Bovo G., Patarnello T., de Koning D.J. & Bargelloni L. (2009) Estimates of heritability and genetic correlation for body length and resistance to fish pasteurellosis in the gilthead sea bream (*Sparus aurata* L.). Aquaculture 298, 29-35.

Apak R., Guclu K., Demirata B., Ozyurek M., Celik S.E., Bektasoglu B., Berker K.I. & Ozyurt D. (2007) Comparative evaluation of various total antioxidant capacity assays applied to phenolic compounds with the CUPRAC assay. Molecules 12, 1496-1547.

APROMAR (2018) *La Acuicultura en España*, Cadiz, España.

APROMAR (2019) *La Acuicultura en España*, Cadiz, España.

Arason G.J. (1996) Lectins as defence molecules in vertebrates and invertebrates. Fish Shellfish Immunol 6, 277-289.

Arijo S., Rico R., Chabrillon M., Diaz-Rosales P., Martínez-Manzanares E., Balebona M.C., Magariños B., Toranzo A.E. & Moriñigo M.A. (2005) Effectiveness of a divalent vaccine

for sole, *Solea senegalensis* (Kaup), against *Vibrio harveyii* and *Photobacterium damselae* subsp *piscicida*. J. Fish Dis 28, 33–38.

Armesto P., Campinho M.A., Rodriguez-Rua A., Cousin X., Power D.M., Manchado M. & Infante C. (2014) Molecular characterization and transcriptional regulation of the Na^+/K^+ ATPase alpha subunit isoforms during development and salinity challenge in a teleost fish, the Senegalese sole (*Solea senegalensis*). Comp Biochem Physiol B Biochem Mol Biol 175, 23-38.

Arts R.J., Novakovic B., Ter Horst R., Carvalho A., Bekkering S., Lachmandas E., Rodrigues F., Silvestre R., Cheng S.C., Wang S.Y., Habibi E., Goncalves L.G., Mesquita I., Cunha C., van Laarhoven A., van de Veerdonk F.L., Williams D.L., van der Meer J.W., Logie C., O'Neill L.A., Dinarello C.A., Riksen N.P., van Crevel R., Clish C., Notebaart R.A., Joosten L.A., Stunnenberg H.G., Xavier R.J. & Netea M.G. (2016) Glutaminolysis and fumarate accumulation integrate immunometabolic and epigenetic programs in trained immunity. Cell Metab 24, 807-819.

Avunje S., Kim W.S., Park C.S., Oh M.J. & Jung S.J. (2011) Toll-like receptors and interferon associated immune factors in viral haemorrhagic septicaemia virus-infected olive flounder (*Paralichthys olivaceus*). Fish Shellfish Immunol 31, 407-414.

Bahri S. (2012) Protozoan and myxozoan infections in wild gilthead seabream (*Sparus aurata* L.) from North Lake of Tunis, Tunisia. Acta Parasitol 57, 114-121.

Bandin I., Rivas C., Noya M., Cutrin J.M., Barja J.L. & Dopazo C.P. (1995) Isolation of a new aquareovirus from gilthead sea bream cultured in Galicia (N.W. Spain). Bull Eur Ass Fish Pathol 15, 157-159.

Barsanti L., Passarelli V., Evangelista V., Frassanito A.M. & Gualtieri P. (2011) Chemistry, physico-chemistry and applications linked to biological activities of beta-glucans. Nat Prod Rep 28, 457-466.

Bashir K.M.I. & Choi J.S. (2017) Clinical and physiological perspectives of beta-glucans: the past, present, and future. Int J Mol Sci 18, 1906.

Basurco B., Lovatelli A. & García B. (2011) Current status of *Sparidae* aquaculture. In: *Sparidae: Biology and Aquaculture of Gilthead Sea Bream and Other Species* (ed. by P.M. A. & M.C.

C.), pp. 1-50. Blackwell Publishing Ltd., Oxford, United Kindom.

Benzekri H., Armesto P., Cousin X., Rovira M., Crespo D., Merlo M.A., Mazurais D., Bautista R., Guerrero-Fernandez D., Fernandez-Pozo N., Ponce M., Infante C., Zambonino J.L., Nidelet S., Gut M., Rebordinos L., Planas J.V., Begout M.L., Claros M.G. & Manchado M. (2014) *De novo* assembly, characterization and functional annotation of Senegalese sole (*Solea senegalensis*) and common sole (*Solea solea*) transcriptomes: integration in a database and design of a microarray. BMC Genomics 15, 952.

Benzie I.F. & Strain J.J. (1996) The ferric reducing ability of plasma (FRAP) as a measure of "antioxidant power": the FRAP assay. Anal Biochem 239, 70-76.

Berbel C., Aparicio M., Crespo A., Carballo C., Guerrero-Cozar I., Martín N. & Manchado M. (2018) Improvement of gilthead seabream and sole production in Andalucia. IFAPA, Cádiz, España.

Bierlich K.C., Miller C., DeForce E., Friedlaender A.S., Johnston D.W. & Apprill A. (2018) Temporal and regional variability in the skin microbiome of humpback whales along the Western Antarctic Peninsula. Appl Environ Microbiol 84.

Biron C.A. (1998) Role of early cytokines, including alpha and beta interferons (IFN-alpha/beta), in innate and adaptive immune responses to viral infections. Semin Immunol 10, 383-390.

Borrego J.J., Labella A.M., Castro D., Ortiz-Delgado J.B. & Sarasquete C. (2017a) Updated of the pathologies affecting cultured gilthead seabream, *Sparus aurata*. Ann Aquac Res 4, 1033.

Borrego J.J., Valverde E.J., Labella A.M. & Castro D. (2017b) Lymphocystis Disease Virus: its importance in aquaculture. Rev Aquacult 9, 179-193.

Boschi I., Randelli E., Buonocore F., Casani D., Bernini C., Fausto A.M. & Scapigliati G. (2011) Transcription of T cell-related genes in teleost fish, and the European sea bass (*Dicentrarchus labrax*) as a model. Fish Shellfish Immunol 31, 655-662.

Botes A., Peyrot B.M., Olivier A.J., Burger W.P. & Bellstedt D.U. (2005) Identification of three novel *mycoplasma* species from ostriches in South Africa. Vet Microbiol 111, 159-169.

Bovo G. & Florio D. (2008) Viral diseases of cultured fish. In: *Fish Diseases* (ed. by J.C. Eiras, H. Segner, T. Wahli & B.G. Kapoor), pp. 185–238. Science Publishers, Enfield, NH, USA.

Bowser P.R., Wooster G.A. & Getchell R.G. (1999) Transmission of walleye dermal sarcoma and

lymphocystis via waterborne exposure. J Aquat Anim Health 11, 158-161.

Bozarth A., Maier U.G. & Zauner S. (2009) Diatoms in biotechnology: modern tools and applications. Appl Microbiol Biotechnol 82, 195-201.

Brown G.D., Herre J., Williams D.L., Willment J.A., Marshall A.S. & Gordon S. (2003) Dectin-1 mediates the biological effects of beta-glucans. J Exp Med 197, 1119-1124.

Brown G.D. & Gordon S. (2005) Immune recognition of fungal beta-glucans. Cell Microbiol 7, 471-479.

Caballero M.A., Jallet D., Shi L., Rithner C., Zhang Y. & Peers G. (2016) Quantification of chrysolaminarin from the model diatom *Phaeodactylum tricornutum*. Algal Res 20, 180-188.

Cano I., Ferro P., Alonso M.C., Bergmann S.M., Romer-Oberdorfer A., Garcia-Rosado E., Castro D. & Borrego J.J. (2007) Development of molecular techniques for detection of lymphocystis disease virus in different marine fish species. J Appl Microbiol 102, 32-40.

Cano I., Ferro P., Alonso M.C., Sarasquete C., Garcia-Rosado E., Borrego J.J. & Castro D. (2009a) Application of *in situ* detection techniques to determine the systemic condition of lymphocystis disease virus infection in cultured gilt-head seabream, *Sparus aurata* L. J Fish Dis 32, 143-150.

Cano I., Lopez-Jimena B., Garcia-Rosado E., Ortiz-Delgado J.B., Alonso M.C., Borrego J.J., Sarasquete C. & Castro D. (2009b) Detection and persistence of lymphocystis disease virus in *Artemia* sp. Aquaculture 291, 230–236.

Cano I., Valverde E.J., Lopez-Jimena B., Alonso M.C., Garcia-Rosado E., Sarasquete C., Borrego J.J. & Castro D. (2010) A new genotype of *Lymphocystivirus* isolated from cultured gilthead seabream, *Sparus aurata* L., and Senegalese sole, *Solea senegalensis* (Kaup). J Fish Dis 33, 695-700.

Cano I., Valverde E.J., Garcia-Rosado E., Alonso M.C., Lopez-Jimena B., Ortiz-Delgado J.B., Borrego J.J., Sarasquete C. & Castro D. (2013) Transmission of lymphocystis disease virus to cultured gilthead seabream, *Sparus aurata* L., larvae. J Fish Dis 36, 569-576.

Caraux G. & Pinloche S. (2005) PermutMatrix: a graphical environment to arrange gene expression profiles in optimal linear order. Bioinformatics 21, 1280-1281.

Carballo C., Castro D., Borrego J.J. & Manchado M. (2017) Gene expression profiles associated with lymphocystis disease virus (LCDV) in experimentally infected Senegalese sole (*Solea senegalensis*). Fish Shellfish Immunol 66, 129-139.

Carballo C., Chronopoulou E.G., Letsiou S., Maya C., Labrou N.E., Infante C., Power D.M. & Manchado M. (2018a) Antioxidant capacity and immunomodulatory effects of a chrysolaminarin-enriched extract in Senegalese sole. Fish Shellfish Immunol 82, 1-8.

Carballo C., Firmino J., Anjos L., Santos S., Power D.M. & Manchado M. (2018b) Short- and long-term effects on growth and expression patterns in response to incubation temperatures in Senegalese sole. Aquaculture 495, 222-231.

Carballo C., Ortiz-Delgado J.B., Berbel C., Castro D., Borrego J.J., Sarasquete C. & Manchado M. (2019a) Feed and immersion challenges with lymphocystis disease virus (LCDV) reveals specific mechanisms for horizontal transmission and immune response in Senegalese sole post-larvae. Fish Shellfish Immunol 89, 710-718.

Carballo C., Pinto P.I.S., Mateus A.P., Berbel C., Guerreiro C.C., Martinez-Blanch J.F., Codoner F.M., Mantecon L., Power D.M. & Manchado M. (2019b) Yeast beta-glucans and microalgal extracts modulate the immune response and gut microbiome in Senegalese sole (*Solea senegalensis*). Fish Shellfish Immunol 92, 31-39.

Carda-Dieguez M., Mira A. & Fouz B. (2014) Pyrosequencing survey of intestinal microbiota diversity in cultured sea bass (*Dicentrarchus labrax*) fed functional diets. FEMS Microbiol Ecol 87, 451-459.

Castro Cunha M., Rodrigues P., Soares F., Makridis P., Skjermo J. & Dinis M. (2003) Development of the immune system and use of immunostimulants in Senegalese sole (*Solea senegalensis*). In: *The Big Fish Bang Proceedings of the 26th Annual Larval Fish Conference* (eds. by H. Browman & A. Skiftesvik), pp. 189-191. Institute of Marine Research, Bergen, Norway.

Cerda J., Mercade J., Lozano J.J., Manchado M., Tingaud-Sequeira A., Astola A., Infante C., Halm S., Vinas J., Castellana B., Asensio E., Canavate P., Martinez-Rodriguez G., Piferrer F., Planas J.V., Prat F., Yufera M., Durany O., Subirada F., Rosell E. & Maes T. (2008) Genomic resources for a commercial flatfish, the Senegalese sole (*Solea senegalensis*): EST sequencing, oligo microarray design, and development of the Soleamold bioinformatic

platform. BMC Genomics 9, 508.

Cerda J. & Manchado M. (2013) Advances in genomics for flatfish aquaculture. Genes Nutr 8, 5-17.

Cerezuela R., Guardiola F.A., Meseguer J. & Esteban M.A. (2012) Enrichment of gilthead seabream (*Sparus aurata* L.) diet with microalgae: effects on the immune system. Fish Physiol Biochem 38, 1729-1739.

Charoonnart P., Purton S. & Saksmerprome V. (2018) Applications of microalgal biotechnology for disease control in aquaculture. Biology (Basel) 7, pii: E24.

Chen J., Xu Q., Wang T., Collet B., Corripio-Miyar Y., Bird S., Xie P., Nie P., Secombes C.J. & Zou J. (2013) Phylogenetic analysis of vertebrate CXC chemokines reveals novel lineage specific groups in teleost fish. Dev Comp Immunol 41, 137-152.

Chen T.T., Tan L.R., Hu N., Dong Z.Q., Hu Z.G., Jiang Y.M., Chen P., Pan M.H. & Lu C. (2018) C-lysozyme contributes to antiviral immunity in *Bombyx mori* against nucleopolyhedrovirus infection. J Insect Physiol 108, 54-60.

Cherif N., Thiery R., Castric J., Biacchesi S., Bremont M., Thabti F., Limem L. & Hammami R. (2009) Viral encephalopathy and retinopathy of *Dicentrarchus labrax* and *Sparus aurata* farmed in Tunisia. Vet Res Commun 33, 345-353.

Chettri J.K., Raida M.K., Holten-Andersen L., Kania P.W. & Buchmann K. (2011) PAMP induced expression of immune relevant genes in head kidney leukocytes of rainbow trout (*Oncorhynchus mykiss*). Dev Comp Immunol 35, 476-482.

Chinchar V.G., Hick P., Ince I.A., Jancovich J.K., Marschang R., Qin Q., Subramaniam K., Waltzek T.B., Whittington R., Williams T., Zhang Q.Y. & Ictv Report C. (2017a) ICTV virus taxonomy profile: *Iridoviridae*. J Gen Virol 98, 890-891.

Chinchar V.G., Waltzek T.B. & Subramaniam K. (2017b) Ranaviruses and other members of the family Iridoviridae: Their place in the virosphere. Virology 511, 259-271.

Chiovitti A., Molino P., Crawford S.A., Teng R., Spurck T. & Wetherbee R. (2004) The glucans extracted with warm water from diatoms are mainly derived from intracellular chysolaminaran and not extracellular polysaccharides. Eur J Phycol 39, 117-128.

Choromanska A., Kulbacka J., Harasym J., Oledzki R., Szewczyk A. & Saczko J. (2018) High- and low-molecular weight oat beta-glucan reveals antitumor activity in human epithelial lung

cancer. Pathol Oncol Res 24, 583-592.

Codoner F.M., Ramirez-Bosca A., Climent E., Carrion-Gutierrez M., Guerrero M., Perez-Orquin J.M., Horga de la Parte J., Genoves S., Ramon D., Navarro-Lopez V. & Chenoll E. (2018) Gut microbial composition in patients with psoriasis. Sci Rep 8, 3812.

Colorni A. & Padrós F. (2011) Diseases and health management. In: *Sparidae: Biology and Aquaculture of Gilthead Sea Bream and Other Species* (ed. by M. Pavlidis & C.C. Mylonas), pp. 321-357. Blackwell Publishing Ltd., Oxford, United Kindom.

Constenla M., Padrós F. & Palenzuela O. (2014) *Endolimax piscium* sp. nov. (Amoebozoa), causative agent of systemic granulomatous disease of cultured sole, *Solea senegalensis* Kaup. J Fish Dis 37, 229-240.

Constenla M., Padrós F., Villanueva-Gonzalez A., Del Pozo R. & Palenzuela O. (2018) Horizontal transmission of *Endolimax piscium*, causative agent of systemic amoebiasis in Senegalese sole *Solea senegalensis*. Dis Aquat Organ 130, 235-240.

Cordero H., Cuesta A., Meseguer J. & Esteban M.A. (2016) Characterization of the gilthead seabream (*Sparus aurata* L.) immune response under a natural lymphocystis disease virus outbreak. J Fish Dis 39, 1467-1476.

da Silva Lino M.A., Bezerra R.F., da Silva C.D.C., Carvalho E.V.M.M. & Coelho L.C.B.B. (2014) Fish lectins: a brief review. In: Advances in Zoology Research (ed. by O.P. Jenkins), pp. 95-114. Nova Science Publishers.

Daboussi F., Leduc S., Marechal A., Dubois G., Guyot V., Perez-Michaut C., Amato A., Falciatore A., Juillerat A., Beurdeley M., Voytas D.F., Cavarec L. & Duchateau P. (2014) Genome engineering empowers the diatom *Phaeodactylum tricornutum* for biotechnology. Nat Commun 5, 3831.

de Jesus Raposo M.F., de Morais A.M. & de Morais R.M. (2015) Marine polysaccharides from algae with potential biomedical applications. Mar Drugs 13, 2967-3028.

De Swaef E., Demeestere K., Boon N., Van den Broeck W., Haesebrouck F. & Decostere A. (2017) Development of a reliable experimental set-up for Dover sole larvae *Solea solea* L. and exploring the possibility of implementing this housing system in a gnotobiotic model. Res Vet Sci 115, 418-424.

De Swaef E., Vercauteren M., Duchateau L., Haesebrouck F. & Decostere A. (2018) Experimental infection model for vibriosis in Dover sole (*Solea solea*) larvae as an aid in studying its pathogenesis and alternative treatments. Vet Res 49, 24.

Dempster E.R. & Lerner I.M. (1950) Heritability of threshold characters. Genetics 35, 212-236.

Devauchelle G., Stoltz, D.B., Darcy-Tripier, F. (1985) Comparative ultrastructure of *iridoviridae*. Curr Top Microbiol Immunol 116, 1–21.

Dezfuli B.S., Lui A., Giari L., Castaldelli G., Mulero V. & Noga E.J. (2012) Infiltration and activation of acidophilic granulocytes in skin lesions of gilthead seabream, *Sparus aurata*, naturally infected with lymphocystis disease virus. Dev Comp Immunol 36, 174-182.

Diaz-Rosales P., Munoz-Atienza E. & Tafalla C. (2019) Role of teleost B cells in viral immunity. Fish Shellfish Immunol 86, 135-142.

Dimitroglou A., Merrifield D.L., Carnevali O., Picchietti S., Avella M., Daniels C., Guroy D. & Davies S.J. (2011) Microbial manipulations to improve fish health and production -a Mediterranean perspective. Fish Shellfish Immunol 30, 1-16.

Dinis M.T., Ribeiro L., Soares F. & Sarasquete C. (1999) A review on the cultivation potential of *Solea senegalensis* in Spain and in Portugal. Aquaculture 176, 27-38.

Djordjevic B., Skugor S., Jorgensen S.M., Overland M., Mydland L.T. & Krasnov A. (2009) Modulation of splenic immune responses to bacterial lipopolysaccharide in rainbow trout (*Oncorhynchus mykiss*) fed lentinan, a beta-glucan from mushroom *Lentinula edodes*. Fish Shellfish Immunol 26, 201-209.

Doan Q.K., Vandeputte M., Chatain B., Haffray P., Vergnet A., Breuil G. & Allal F. (2017) Genetic variation of resistance to Viral Nervous Necrosis and genetic correlations with production traits in wild populations of the European sea bass (*Dicentrarchus labrax*). Aquaculture 478, 1-8.

Douxfils J., Fierro-Castro C., Mandiki S.N., Emile W., Tort L. & Kestemont P. (2017) Dietary beta-glucans differentially modulate immune and stress-related gene expression in lymphoid organs from healthy and *Aeromonas hydrophila*-infected rainbow trout (*Oncorhynchus mykiss*). Fish Shellfish Immunol 63, 285-296.

Du B. & Xu B. (2014) Oxygen radical absorbance capacity (ORAC) and ferric reducing antioxidant

power (FRAP) of β-glucans from different sources with various molecular weight. Bioact Carbohydr Dietary Fibre 3, 11-16.

Du B., Lin C., Bian Z. & Xu B. (2015) An insight into anti-inflammatory effects of fungal beta-glucans. Trends Food Sci Technol 41, 49-59.

Dubois M., Gilles K.A., Hamilton J.K., Rebers P.A. & Smith F. (1956) Colorimetric method for determination of sugars and related substances. Anal Chem 28, 350-356.

EATiP (2014) Performance of the sea bass and sea bream sector in the Mediterranean, Minutes of a Workshop held within Aquaculture Europe. In: *European Aquaculture Society and the European Aquaculture Technology & Innovation Platform*, San Sebastián, Spain.

Eaton H.E., Metcalf J., Penny E., Tcherepanov V., Upton C. & Brunetti C.R. (2007) Comparative genomic analysis of the family *Iridoviridae*: re-annotating and defining the core set of iridovirus genes. Virol J 4, 11.

Edholm E.S., Bengten E. & Wilson M. (2011) Insights into the function of IgD. Dev Comp Immunol 35, 1309-1316.

Egerton S., Culloty S., Whooley J., Stanton C. & Ross R.P. (2018) The gut microbiota of marine fish. Front Microbiol 9, 873.

Ellis A.E. (1990a) Lysozyme assays In: *Techniques in fish immunology* (ed. by J.S. Stolen, F.T. Fletcher, D.P. Anderson & B.S. Roberson), pp. 101-103. SOS Publications, Fair Haven, NJ.

Ellis A.E. (1990b) Serum antiproteases in fish. In: *Techniques in fish immunology* (ed. by J.S.F. Stolen, F.T.; Anderson, D.P.; Roberson, B.S.), pp. 95-99. SOS Publications, Fair Haven, NJ.

Ellis A.E. (2001) Innate host defense mechanisms of fish against viruses and bacteria. Dev Comp Immunol 25, 827-839.

Encarnação P. (2016) Functional feed additives in aquaculture feeds. In: *Aquafeed Formulation* (ed. by S.F. Nantes), pp. 217-237. Academic Ptess, Kidlington, Oxford

Estensoro I., Redondo M.J., Alvarez-Pellitero P. & Sitja-Bobadilla A. (2010) Novel horizontal transmission route for *Enteromyxum leei (*Myxozoa) by anal intubation of gilthead sea bream *Sparus aurata*. Dis Aquat Organ 92, 51-58.

Evans D.L. & Jaso-Friedmann L. (1992) Nonspecific cytotoxic cells as effectors of immunity in fish. Annual Review of Fish Diseases 2, 109-121.

Falco A., Frost P., Miest J., Pionnier N., Irnazarow I. & Hoole D. (2012) Reduced inflammatory response to *Aeromonas salmonicida* infection in common carp (*Cyprinus carpio* L.) fed with beta-glucan supplements. Fish Shellfish Immunol 32, 1051-1057.

Falco A., Miest J.J., Pionnier N., Pietretti D., Forlenza M., Wiegertjes G.F. & Hoole D. (2014) beta-Glucan-supplemented diets increase poly(I:C)-induced gene expression of Mx, possibly via Tlr3-mediated recognition mechanism in common carp (*Cyprinus carpio*). Fish Shellfish Immunol 36, 494-502.

FAO (2005-2019a) Food and Agriculture Organization of the United Nations. Cultured Aquatic Species Information Programme. *Solea* spp. (*S. solea, S. senegalensis*). URL http://www.fao.org/fishery/culturedspecies/Solea_spp/en.

FAO (2005-2019b) Food and Agriculture Organization of the United Nations. Cultured Aquatic Species Information Programme. *Sparus aurata*. URL http://www.fao.org/fishery/species/2384/en.

FAO (2016) *The State of World Fisheries and Aquaculture 2016. Contributing to food security and nutrition for all*, Rome.

FAO (2018) *The State of World Fisheries and Aquaculture 2018 - Meeting the sustainable development goals*, Rome.

Fearon D.T. & Locksley R.M. (1996) The instructive role of innate immunity in the acquired immune response. Science 272, 50-53.

Feng H., Zhang Q.M., Zhang Y.B., Li Z., Zhang J., Xiong Y.W., Wu M. & Gui J.F. (2016) Zebrafish IRF1, IRF3, and IRF7 differentially regulate IFNPhi1 and IFNPhi3 expression through assembly of homo- or heteroprotein complexes. J Immunol 197, 1893-1904.

Fernández-Díaz C., Yúfera M., Cañavate J.P., Moyano F.J., Alarcón F.J. & Díaz M. (2001) Growth and physiological changes during metamorphosis of Senegal sole reared in the laboratory. J Fish Biol 58, 1-13.

Fernandez-Trujillo A., Ferro P., Garcia-Rosado E., Infante C., Alonso M.C., Bejar J., Borrego J.J. & Manchado M. (2008) Poly I:C induces Mx transcription and promotes an antiviral state against sole aquabirnavirus in the flatfish Senegalese sole (*Solea senegalensis* Kaup). Fish Shellfish Immunol 24, 279-285.

Fernandez-Trujillo M.A., Garcia-Rosado E., Alonso M.C., Borrego J.J., Alvarez M.C. & Bejar J. (2011) Differential antiviral activity of Mx1, Mx2 and Mx3 proteins from gilthead seabream (*Sparus* aurata) against Infectious Pancreatic Necrosis Virus (IPNV). Mol Immunol 49, 107-114.

Fernandez-Trujillo M.A., Garcia-Rosado E., Alonso M.C., Castro D., Alvarez M.C. & Bejar J. (2013) Mx1, Mx2 and Mx3 proteins from the gilthead seabream (*Sparus aurata*) show *in vitro* antiviral activity against RNA and DNA viruses. Mol Immunol 56, 630-636.

Ferraresso S., Bonaldo A., Parma L., Buonocore F., Scapigliati G., Gatta P.P. & Bargelloni L. (2016) Ontogenetic onset of immune-relevant genes in the common sole (*Solea solea*). Fish Shellfish Immunol 57, 278-292.

Ferreira M., Cortina-Burgueño A., Freire I. & Otero A. (2018) Effect of nutritional status and concentration of *Nannochloropsis gaditana* as enrichment diet for the marine rotifer *Brachionus* sp. Aquaculture 491, 351-357.

Firmino J., Carballo C., Armesto P., Campinho M.A., Power D.M. & Manchado M. (2017) Phylogeny, expression patterns and regulation of DNA Methyltransferases in early development of the flatfish, *Solea senegalensis*. BMC Dev Biol 17, 11.

Fischer U., Utke K., Somamoto T., Kollner B., Ototake M. & Nakanishi T. (2006) Cytotoxic activities of fish leucocytes. Fish Shellfish Immunol 20, 209-226.

Flugel R.M. (1985) Lymphocystis disease virus. Curr Top Microbiol Immunol 116, 133-150.

Fokos S., Pavlidis M., Yiotis T., Tsalafouta A., Papandroulakis N. & Dermon C.R. (2017) Early life low intensity stress experience modifies acute stress effects on juvenile brain cell proliferation of European sea bass (*D. Labrax*). Behav Brain Res 317, 109-121.

Fortin O., Aguilar-Uscanga B., Vu K.D., Salmieri S. & Lacroix M. (2018) Cancer chemopreventive, antiproliferative, and superoxide anion scavenging properties of *Kluyveromyces marxianus* and *Saccharomyces cerevisiae* var. *boulardii* cell wall components. Nutr Cancer 70, 83-96.

Fredriksen B.N., Saevareid K., McAuley L., Lane M.E., Bogwald J. & Dalmo R.A. (2011) Early immune responses in Atlantic salmon (*Salmo salar* L.) after immunization with PLGA nanoparticles loaded with a model antigen and beta-glucan. Vaccine 29, 8338-8349.

Fuglem B., Jirillo E., Bjerkas I., Kiyono H., Nochi T., Yuki Y., Raida M., Fischer U. & Koppang

E.O. (2010) Antigen-sampling cells in the salmonid intestinal epithelium. Dev Comp Immunol 34, 768-774.

Fuji K., Kobayashi K., Hasegawa O., Coimbra R., Sakamoto R. & Okamoto N. (2006) Identification of a single major genetic locus controlling the resistance to lymphocystis disease in Japanese flounder (*Paralichthys olivaceus*). Aquaculture 254, 203-210.

Fuji K., Hasegawa O., Honda K., Kumasaka K., Sakamoto T. & Okamoto N. (2007) Marker-assisted breeding of a lymphocystis disease-resistant Japanese flounder (*Paralichthys olivaceus*). Aquaculture 272, 291–295.

Fujiki K., Shin D.H., Nakao M. & Yano T. (2000) Molecular cloning and expression analysis of carp (*Cyprinus carpio*) interleukin-1 beta, high affinity immunoglobulin E Fc receptor gamma subunit and serum amyloid A. Fish Shellfish Immunol 10, 229-242.

Gao B., Chen A., Zhang W., Li A. & Zhang C. (2017) Co-production of lipids, eicosapentaenoic acid, fucoxanthin, and chrysolaminarin by *Phaeodactylum tricornutum* cultured in a flat-plate photobioreactor under varying nitrogen conditions. J Ocean Univ China 16, 916-924.

Garcia-Celdran M., Ramis G., Manchado M., Estévez A., Afonso J.M. & Armero E. (2015a) Estimates of heritabilities and genetic correlations of carcass quality traits in a reared gilthead sea bream (*Sparus aurata* L.) population sourced from three broodstocks along the Spanish coasts. Aquaculture 446, 175-180.

Garcia-Celdran M., Ramis G., Manchado M., Estevez A., Afonso J.M., Maria-Dolores E., Peñalver J. & Armero E. (2015b) Estimates of heritabilities and genetic correlations of growth and external skeletal deformities at different ages in a reared gilthead sea bream (*Sparus aurata* L.) population sourced from three broodstocks along the Spanish coasts. Aquaculture 445, 33-41.

Garcia-Celdran M., Ramis G., Manchado M., Estévez A., Navarro A. & Armero E. (2015c) Estimates of heritabilities and genetic correlations of raw flesh quality traits in a reared gilthead sea bream (*Sparus aurata* L.) population sourced from broodstocks along the Spanish coasts. Aquaculture 446, 181-186.

Garcia-Celdran M., Cutáková Z., Ramis G., Estévez A., Manchado M., Navarro A., Maria-Dolores E., Peñalver J., Sanchez J.A. & Armero E. (2016) Estimates of heritabilities and genetic

correlations of skeletal deformities and uninflated swimbladder in a reared gilthead sea bream (*Sparus aurata* L.) juvenile population sourced from three broodstocks along the Spanish coasts. Aquaculture 464, 601-608.

Garcia-Rosado E., Castro D., Cano I., Perez-Prieto S.I. & Borrego J.J. (2002) Serological techniques for detection of lymphocystis virus in fish. Aquat Living Resour 15, 179-185.

Garcia-Valtanen P., Martinez-Lopez A., Lopez-Munoz A., Bello-Perez M., Medina-Gali R.M., Ortega-Villaizan M.D., Varela M., Figueras A., Mulero V., Novoa B., Estepa A. & Coll J. (2017) Zebra Fish lacking adaptive immunity acquire an antiviral alert state characterized by ppregulated gene expression of apoptosis, multigene families, and Interferon-telated genes. Front Immunol 8, 121.

Geller R., Taguwa S. & Frydman J. (2012) Broad action of Hsp90 as a host chaperone required for viral replication. Biochim Biophys Acta 1823, 698-706.

Gillespie K.M., Chae J.M. & Ainsworth E.A. (2007) Rapid measurement of total antioxidant capacity in plants. Nat Protoc 2, 867-870.

Goetz F.W., Planas J.V. & MacKenzie S. (2004) Tumor necrosis factors. Dev Comp Immunol 28, 487-497.

Gomez D., Sunyer J.O. & Salinas I. (2013) The mucosal immune system of fish: the evolution of tolerating commensals while fighting pathogens. Fish Shellfish Immunol 35, 1729-1739.

Goodridge H.S., Reyes C.N., Becker C.A., Katsumoto T.R., Ma J., Wolf A.J., Bose N., Chan A.S., Magee A.S., Danielson M.E., Weiss A., Vasilakos J.P. & Underhill D.M. (2011) Activation of the innate immune receptor Dectin-1 upon formation of a 'phagocytic synapse'. Nature 472, 471-475.

Goorha R. & Murti K.G. (1982) The genome of frog virus 3, an animal DNA virus, is circularly permuted and terminally redundant. Proc Natl Acad Sci USA 79, 248–252.

Grayfer L., Hodgkinson J.W. & Belosevic M. (2014) Antimicrobial responses of teleost phagocytes and innate immune evasion strategies of intracellular bacteria. Dev Comp Immunol 43, 223-242.

Grayfer L., Kerimoglu B., Yaparla A., Hodgkinson J.W., Xie J. & Belosevic M. (2018) Mechanisms of fish macrophage antimicrobial immunity. Front Immunol 9, 1105.

Gringhuis S.I., den Dunnen J., Litjens M., van der Vlist M., Wevers B., Bruijns S.C. & Geijtenbeek T.B. (2009) Dectin-1 directs T helper cell differentiation by controlling noncanonical NF-kappaB activation through Raf-1 and Syk. Nat Immunol 10, 203-213.

Gruys E., Toussaint M.J., Niewold T.A. & Koopmans S.J. (2005) Acute phase reaction and acute phase proteins. J Zhejiang Univ Sci B 6, 1045-1056.

Guardiola F.A., Mabrok M., Machado M., Azeredo R., Afonso A., Esteban M.A. & Costas B. (2019) Mucosal and systemic immune responses in Senegalese sole (*Solea senegalensis* Kaup) bath challenged with *Tenacibaculum maritimum*: A time-course study. Fish Shellfish Immunol 87, 744-754.

Gugi B., Le Costaouec T., Burel C., Lerouge P., Helbert W. & Bardor M. (2015) Diatom-specific oligosaccharide and polysaccharide structures help to unravel biosynthetic capabilities in diatoms. Mar Drugs 13, 5993-6018.

Guzman S., Gato A., Lamela M., Freire-Garabal M. & Calleja J.M. (2003) Anti-inflammatory and immunomodulatory activities of polysaccharide from *Chlorella stigmatophora* and *Phaeodactylum tricornutum*. Phytother Res 17, 665-670.

Haddad-Boubaker S., Bouzgarou N., Fakhfakh E., Khayech M., Mohamed S.B., Megdicn A. & Chéhida N.B. (2013) Detection and genetic characterization of Lymphocystis Disease Virus (LCDV) isolated during disease outbreaks in cultured gilt-head seabream *Sparus aurata* inTunisia. Fish Pathol 48, 101–104.

Hadfield J.D. (2010) MCMC methods for multi-response generalized linear mixed models: the MCMCglmm R package. J Stat Soft 33, 1-22.

Hamed I. (2016) The evolution and versatility of microalgal biotechnology: A Review. Compr Rev Food Sci Food Saf 6, 1104-1123.

Hanif A., Bakopoulos V. & Dimitriadis G.J. (2004) Maternal transfer of humoral specific and non-specific immune parameters to sea bream (*Sparus aurata*) larvae. Fish Shellfish Immunol 17, 411-435.

Hansen J.D. & Zapata A.G. (1998) Lymphocyte development in fish and amphibians. Immunol Rev 166, 199-220.

Hanson L., Dishon A. & Kotler M. (2011) Herpesviruses that infect fish. Viruses 3, 2160-2191.

Harikrishnan R., Balasundaram C. & Heo M.S. (2010a) Effect of probiotics enriched diet on *Paralichthys olivaceus i*nfected with lymphocystis disease virus (LCDV). Fish Shellfish Immunol 29, 868-874.

Harikrishnan R., Heo J., Balasundaram C., Kim M.C., Kim J.S., Han Y.J. & Heo M.S. (2010b) Effect of *Punica granatum* solvent extracts on immune system and disease resistance in *Paralichthys olivaceus* against lymphocystis disease virus (LDV). Fish Shellfish Immunol 29, 668-673.

Harun N.O., Zou J., Zhang Y.A., Nie P. & Secombes C.J. (2008) The biological effects of rainbow trout (*Oncorhynchus mykiss*) recombinant interleukin-8. Dev Comp Immunol 32, 673-681.

Haugarvoll E., Bjerkas I., Nowak B.F., Hordvik I. & Koppang E.O. (2008) Identification and characterization of a novel intraepithelial lymphoid tissue in the gills of Atlantic salmon. J Anat 213, 202-209.

Havixbeck J.J., Rieger A.M., Wong M.E., Hodgkinson J.W. & Barreda D.R. (2016) Neutrophil contributions to the induction and regulation of the acute inflammatory response in teleost fish. J Leukoc Biol 99, 241-252.

Hemaiswarya S., Raja R., Ravi Kumar R., Ganesan V. & Anbazhagan C. (2011) Microalgae: a sustainable feed source for aquaculture. World J Microbiol Biotechnol 27, 1737-1746.

Henryon M., Jokumsen A., Berg P., Lund I., Pedersen P.B., Olesen N.J. & Slierendrecht W.J. (2002) Genetic variation for growth rate, feed conversion efficiency, and disease resistance exists within a farmed population of rainbow trout. Aquaculture 209, 59–76.

Hodgkinson J.W., Grayfer L. & Belosevic M. (2015) Biology of bony fish macrophages. Biology 4, 881-906.

Hogan R.J., Stuge T.B., Clem L.W., Miller N.W. & Chinchar V.G. (1996) Anti-viral cytotoxic cells in the channel catfish (Ictalurus punctatus). Developmental & Comparative Immunology 20, 115-127.

Holopainen R., Tapiovaara H. & Honkanen J. (2012) Expression analysis of immune response genes in fish epithelial cells following ranavirus infection. Fish Shellfish Immunol 32, 1095-1105.

Honda K., Takaoka A. & Taniguchi T. (2006) Type I interferon gene induction by the interferon regulatory factor family of transcription factors. Immunity 25, 349-360.

Honda K. & Taniguchi T. (2006) IRFs: master regulators of signalling by Toll-like receptors and cytosolic pattern-recognition receptors. Nat Rev Immunol 6, 644-658.

Hossain M., Kim S.R., Kitamura S.I., Kim D.W., Jung S.J., Nishizawa T., Yoshimizu M. & Oh M.J. (2009) Lymphocystis disease virus persists in the epidermal tissues of olive flounder, *Paralichthys olivaceus* (Temminch & Schlegel), at low temperatures. J Fish Dis 32, 699-703.

Houston R.D., Haley C.S., Hamilton A., Guy D.R., Tinch A.E., Taggart J.B., McAndrew B.J. & Bishop S.C. (2008) Major quantitative trait loci affect resistance to infectious pancreatic necrosis in Atlantic salmon (*Salmo salar*). Genetics 178, 1109-1115.

Houston R.D., Haley C.S., Hamilton A., Guy D.R., Mota-Velasco J.C., Gheyas A.A., Tinch A.E., Taggart J.B., Bron J.E., Starkey W.G., McAndrew B.J., Verner-Jeffreys D.W., Paley R.K., Rimmer G.S., Tew I.J. & Bishop S.C. (2010) The susceptibility of Atlantic salmon fry to freshwater infectious pancreatic necrosis is largely explained by a major QTL. Heredity 105, 318-327.

Hu G., Yin X., Xia J., Dong X., Zhang J. & Liu Q. (2010) Molecular cloning and characterization of interferon regulatory factor 7 (IRF-7) in Japanese flounder, *Paralichthys olivaceus*. Fish Shellfish Immunol 29, 963-971.

Hu G., Yin X., Lou H., Xia J., Dong X., Zhang J. & Liu Q. (2011) Interferon regulatory factor 3 (IRF-3) in Japanese flounder, *Paralichthys olivaceus*: sequencing, limited tissue distribution, inducible expression and induction of fish type I interferon promoter. Dev Comp Immunol 35, 164-173.

Hu G., Chen X., Gong Q., Liu Q., Zhang S. & Dong X. (2013) Structural and expression studies of interferon regulatory factor 8 in Japanese flounder, *Paralichthys olivaceus*. Fish Shellfish Immunol 35, 1016-1024.

Hu G.B., Cong R.S., Fan T.J. & Mei X.G. (2004) Induction of apoptosis in a flounder gill cell line by lymphocystis disease virus infection. J Fish Dis 27, 657-662.

Hu G.B., Lou H.M., Dong X.Z., Liu Q.M. & Zhang S.C. (2012) Characteristics of the interferon regulatory factor 5 (IRF5) and its expression in response to LCDV and poly I:C challenges in Japanese flounder, *Paralichthys olivaceus*. Dev Comp Immunol 38, 377-382.

Hu G.B., Zhao M.Y., Lin J.Y., Liu Q.M. & Zhang S.C. (2014) Molecular cloning and characterization of interferon regulatory factor 9 (IRF9) in Japanese flounder, *Paralichthys olivaceus*. Fish Shellfish Immunol 39, 138-144.

Infante C., Matsuoka M.P., Asensio E., Canavate J.P., Reith M. & Manchado M. (2008) Selection of housekeeping genes for gene expression studies in larvae from flatfish using real-time PCR. BMC Mol Biol 9, 28.

Inkpen S.M., Hori T.S., Gamperl A.K., Nash G.W. & Rise M.L. (2015) Characterization and expression analyses of five interferon regulatory factor transcripts (Irf4a, Irf4b, Irf7, Irf8, Irf10) in Atlantic cod (*Gadus morhua*). Fish Shellfish Immunol 44, 365-381.

Ivashkiv L.B. & Donlin L.T. (2014) Regulation of type I interferon responses. Nat Rev Immunol 14, 36-49.

Iwakiri S., Song J.Y., Nakayama K., Oh M.J., Ishida M. & Kitamura S. (2014) Host responses of Japanese flounder *Paralichthys olivaceus* with lymphocystis cell formation. Fish Shellfish Immunol 38, 406-411.

Iwamoto R., Hasegawa O., LaPatra S. & Yoshimizu M. (2002) Isolation and characterization of the Japanese flounder (*Paralichthys olivaceus*) lymphocystis disease virus. J Aquat Anim Health 14, 114-123.

Jancovich J.K., Chinchar V.G., Hyatt A., Miyazaki T., Williams T. & Zhang Q.Y. (2012) Family *Iridoviridae*. In: *Virus Taxonomy: Ninth Report of the International Committee on Taxonomy of Viruses* (ed. by A.M.Q. King, M.J. Adams, E.B. Carstens & E.J. Lefkowitz), pp. 193-210, Elsevier, San Diego, USA.

Jancovich J.K., Qin Q., Zhang Q.-Y. & Chinchar V.G. (2015) Ranavirus replication: molecular, cellular, and immunological events. In: *Ranaviruses: Lethal Pathogens of Ectothermic Vertebrates.* (ed. by M.J. Gray & V.G. Chinchar), pp. 71–104. Springer International Publishing, Switzerland.

Jeney G., Galeotti M., Volpatti D., Jeney Z. & Anderson D. (1997) Prevention of stress in rainbow trout (*Oncorhynchus mykiss*) fed diets containing different doses of glucan. Aquaculture 154, 1-15.

Jin Y., Li P. & Wang F. (2018) beta-glucans as potential immunoadjuvants: A review on the

adjuvanticity, structure-activity relationship and receptor recognition properties. Vaccine 36, 5235-5244.

Joly A.L., Wettstein G., Mignot G., Ghiringhelli F. & Garrido C. (2010) Dual role of heat shock proteins as regulators of apoptosis and innate immunity. J Innate Immun 2, 238-247.

Kalinski P. (2012) Regulation of immune responses by prostaglandin E2. J Immunol 188, 21-28.

Kankkunen P., Teirila L., Rintahaka J., Alenius H., Wolff H. & Matikainen S. (2010) (1,3)-beta-glucans activate both dectin-1 and NLRP3 inflammasome in human macrophages. J Immunol 184, 6335-6342.

Kanmani P., Satish kumar R., Yuvaraj N., Paari K.A., Pattukumar V. & Arul V. (2011) Production and purification of a novel exopolysaccharide from lactic acid bacterium *Streptococcus phocae* PI80 and its functional characteristics activity in vitro. Bioresour Technol 102, 4827-4833.

Kasheta M., Painter C.A., Moore F.E., Lobbardi R., Bryll A., Freiman E., Stachura D., Rogers A.B., Houvras Y., Langenau D.M. & Ceol C.J. (2017) Identification and characterization of T reg-like cells in zebrafish. J Exp Med 214, 3519-3530.

Khosravi S., Rahimnejad S., Herault M., Fournier V., Lee C.R., Dio Bui H.T., Jeong J.B. & Lee K.J. (2015) Effects of protein hydrolysates supplementation in low fish meal diets on growth performance, innate immunity and disease resistance of red sea bream *Pagrus major*. Fish Shellfish Immunol 45, 858-868.

Kim C.H., Johnson M.C., Drennan J.D., Simon B.E., Thomann E. & Leong J.A. (2000) DNA vaccines encoding viral glycoproteins induce nonspecific immunity and Mx protein synthesis in fish. J Virol 74, 7048-7054.

Kim Y.S., Ke F. & Zhang Q.Y. (2009) Effect of beta-glucan on activity of antioxidant enzymes and Mx gene expression in virus infected grass carp. Fish Shellfish Immunol 27, 336-340.

Kirkby N.S., Zaiss A.K., Wright W.R., Jiao J., Chan M.V., Warner T.D., Herschman H.R. & Mitchell J.A. (2013) Differential COX-2 induction by viral and bacterial PAMPs: Consequences for cytokine and interferon responses and implications for anti-viral COX-2 directed therapies. Biochem Biophys Res Commun 438, 249-256.

Kiron V., Kulkarni A., Dahle D., Vasanth G., Lokesh J. & Elvebo O. (2016) Recognition of purified

beta 1,3/1,6 glucan and molecular signalling in the intestine of Atlantic salmon. Dev Comp Immunol 56, 57-66.

Klindworth A., Pruesse E., Schweer T., Peplies J., Quast C., Horn M. & Glockner F.O. (2013) Evaluation of general 16S ribosomal RNA gene PCR primers for classical and next-generation sequencing-based diversity studies. Nucleic Acids Res 41, e1.

Kofuji K., Aoki A., Tsubaki K., Konishi M., Isobe T. & Murata Y. (2012) Antioxidant Activity of beta-Glucan. ISRN Pharm 2012, 125864.

Kuhlwein H., Emery M.J., Rawling M.D., Harper G.M., Merrifield D.L. & Davies S.J. (2013) Effects of a dietary beta-(1,3)(1,6)-D-glucan supplementation on intestinal microbial communities and intestinal ultrastructure of mirror carp (*Cyprinus carpio* L.). J Appl Microbiol 115, 1091-1106.

Kvitt H., Heinisch G. & Diamant A. (2008) Detection and phylogeny of *Lymphocystivirus* in sea bream *Sparus aurata* based on the DNA polymerase gene and major capsid protein sequences. Aquaculture 275, 58-63.

Labella A.M., Garcia-Rosado E., Bandin I., Dopazo C.P., Castro D., Alonso M.C. & Borrego J.J. (2018) Transcriptomic profiles of Senegalese sole infected with Nervous Necrosis Virus reassortants presenting different degree of virulence. Front Immunol 9, 1626.

Labella A.M., Leiva-Rebollo R., Alejo A., Castro D. & Borrego J.J. (2019) Lymphocystis disease virus (LCDV-Sa), polyomavirus 1 (SaPyV1) and papillomavirus 1 (SaPV1) in samples of Mediterranean gilthead seabream. Dis Aquat Organ 132, 151-156.

Laing K.J. & Secombes C.J. (2004) Chemokines. Dev Comp Immunol 28, 443-460.

Laing K.J. & Hansen J.D. (2011) Fish T cells: recent advances through genomics. Dev Comp Immunol 35, 1282-1295.

Larsen A., Tao Z., Bullard S.A. & Arias C.R. (2013) Diversity of the skin microbiota of fishes: evidence for host species specificity. FEMS Microbiol Ecol 85, 483-494.

Lê S., Josse J. & Husson F. (2008) FactoMineR: An R Package for Multivariate Analysis. J Stat Soft 25, 1-18.

Lee-Montero I., Navarro A., Borrell Y., Garcia-Celdran M., Martin N., Negrin-Baez D., Blanco G., Armero E., Berbel C., Zamorano M.J., Sanchez J.J., Estevez A., Ramis G., Manchado M. &

Afonso J.M. (2013) Development of the first standardised panel of two new microsatellite multiplex PCRs for gilthead seabream (*Sparus aurata* L.). Anim Genet 44, 533-546.

Lee-Montero I., Navarro A., Negrin-Baez D., Zamorano M.J., Borrell Pichs Y.J., Berbel C., Sanchez J.A., Garcia-Celdran M., Manchado M., Estevez A., Armero E. & Afonso J.M. (2015) Genetic parameters and genotype-environment interactions for skeleton deformities and growth traits at different ages on gilthead seabream (*Sparus aurata* L.) in four Spanish regions. Anim Genet 46, 164-174.

Leiva-Rebollo R. (2019) Patogénesis y profilaxis de la infección por el virus de la enfermedad de linfocistis (LCDV-Sa) en doradas cultivadas (Sparus aurata L.). In: *Departamento de Microbiología*. Universidad de Málaga, Málaga.

Letsiou S., Kalliampakou K., Gardikis K., Mantecon L., Infante C., Chatzikonstantinou M., Labrou N.E. & Flemetakis E. (2017) Skin protective effects of *Nannochloropsis gaditana* extract on H_2O_2-stressed human dermal fibroblasts. Front Mar Sci 4, 221.

Libran-Perez M., Costa M.M., Figueras A. & Novoa B. (2018) beta-glucan administration induces metabolic changes and differential survival rates after bacterial or viral infection in turbot (*Scophthalmus maximus*). Fish Shellfish Immunol 82, 173-182.

Lin C.H., Christopher John J.A., Lin C.H. & Chang C.Y. (2006) Inhibition of nervous necrosis virus propagation by fish Mx proteins. Biochem Biophys Res Commun 351, 534-539.

Liu P., Wang L., Wan Z.Y., Ye B.Q., Huang S., Wong S.M. & Yue G.H. (2016a) Mapping QTL for resistance against viral nervous necrosis disease in asian seabass. Mar Biotechnol 18, 107-116.

Liu X., Liu H., Zhai Y., Li Y., Zhu X. & Zhang W. (2017) Laminarin protects against hydrogen peroxide-induced oxidative damage in MRC-5 cells possibly via regulating NRF2. PeerJ 5, e3642.

Liu Y., Tran B.N., Wang F., Ounjai P., Wu J. & Hew C.L. (2016b) Visualization of assembly intermediates and budding vacuoles of Singapore grouper iridovirus in grouper embryonic cells. Sci. Rep. 6, 18696. Sci Rep 6, 18696.

Livak K.J. & Schmittgen T.D. (2001) Analysis of relative gene expression data using real-time quantitative PCR and the 2(-Delta Delta C(T)) Method. Methods 25, 402-408.

Llewellyn M.S., Boutin S., Hoseinifar S.H. & Derome N. (2014) Teleost microbiomes: the state of the art in their characterization, manipulation and importance in aquaculture and fisheries. Front Microbiol 5, 207.

Lo T.C.-T., Chang C.A., Chiuc K.-H., Tsayd P.-K. & Jena J.-F. (2011) Correlation evaluation of antioxidant properties on the monosaccharide components and glycosyl linkages of polysaccharide with different measuring methods. Carbohydr Polym 86, 320-327.

Lobo C., Moreno-Ventas X., Tapia-Paniagua S., Rodriguez C., Morinigo M.A. & de La Banda I.G. (2014) Dietary probiotic supplementation (*Shewanella putrefaciens* Pdp11) modulates gut microbiota and promotes growth and condition in Senegalese sole larviculture. Fish Physiol Biochem 40, 295-309.

Lopez-Bueno A., Mavian C., Labella A.M., Castro D., Borrego J.J., Alcami A. & Alejo A. (2016) Concurrence of iridovirus, polyomavirus, and a unique member of a new group of fish papillomaviruses in lymphocystis disease-affected gilthead sea bream. J Virol 90, 8768-8779.

Lopez-Munoz A., Roca F.J., Meseguer J. & Mulero V. (2009) New insights into the evolution of IFNs: zebrafish group II IFNs induce a rapid and transient expression of IFN-dependent genes and display powerful antiviral activities. J Immunol 182, 3440-3449.

Lopez-Vazquez C., Conde M., Dopazo C.P., Barja J.L. & Bandin I. (2011) Susceptibility of juvenile sole *Solea senegalensis* to marine isolates of Viral Haemorrhagic Septicaemia Virus from wild and farmed fish. Dis Aquat Organ 93, 111-116.

Lopez-Vazquez C., Alonso M.C., Dopazo C.P. & Bandin I. (2017) *In vivo* study of Viral Haemorrhagic Septicaemia Virus and Infectious Pancreatic Necrosis Virus coexistence in *Senegalese sole* (*Solea senegalensis*). J Fish Dis 40, 1129-1139.

Lovoll M., Fischer U., Mathisen G.S., Bogwald J., Ototake M. & Dalmo R.A. (2007) The C3 subtypes are differentially regulated after immunostimulation in rainbow trout, but head kidney macrophages do not contribute to C3 transcription. Vet Immunol Immunopathol 117, 284-295.

Lyons P.P., Turnbull J.F., Dawson K.A. & Crumlish M. (2017) Effects of low-level dietary microalgae supplementation on the distal intestinal microbiome of farmed rainbow trout

Oncorhynchus mykiss (Walbaum). Aquacult Res 48, 2438-2452.

Machová E. & Bystricky S. (2013) Antioxidant capacities of mannans and glucans are related to their susceptibility of free radical degradation. Int J Biol Macromol 61, 308-311.

Magnadottir B. (2006) Innate immunity of fish (overview). Fish Shellfish Immunol 20, 137-151.

Magnadottir B. (2010) Immunological control of fish diseases. Mar Biotechnol 12, 361-379.

Mai W.J. & Wang W.N. (2010) Protection of blue shrimp (*Litopenaeus stylirostris*) against the White Spot Syndrome Virus (WSSV) when injected with shrimp lysozyme. Fish Shellfish Immunol 28, 727-733.

Manchado M., Salas-Leiton E., Infante C., Ponce M., Asensio E., Crespo A., Zuasti E. & Canavate J.P. (2008) Molecular characterization, gene expression and transcriptional regulation of cytosolic HSP90 genes in the flatfish Senegalese sole (*Solea senegalensis* Kaup). Gene 416, 77-84.

Manchado M., Planas J.V., Cousin X., Rebordinos L. & Claros M.G. (2016) Current status in other finfish species: Description of current genomic resources for the gilthead seabream (*Sparus aurata*) and soles (*Solea senegalensis* and *Solea solea*). In: *Genomics in Aquaculture* (ed. by S.A. MacKenzie & S. Jentoft), pp. 195-221. Elsevier, Cambridge, MA, USA.

Manchado M., Planas J.V., Cousin X., Rebordinos L. & Claros M.G. (2019) Genetic and genomic characterization of soles. In: *The Biology of Sole* (ed. by J. Munoz-Cueto, E. Mañanós-Sánchez & F. Sánchez-Vázquez), pp. 375-394. CDC Press., Boca Raton.

Mancino A. & Natoli G. (2016) Specificity and function of IRF family transcription factors: insights from genomics. J Interferon Cytokine Res 36, 462-469.

Martin-Antonio B., Manchado M., Infante C., Zerolo R., Labella A., Alonso C. & Borrego J.J. (2007) Intestinal microbiota variation in Senegalese sole (*Solea senegalensis*) under different feeding regimes. Aquac Res 38, 1213-1222.

Mateus A.P., Costa R., Gisbert E., Pinto P.I.S., Andree K.B., Estevez A. & Power D.M. (2017a) Thermal imprinting modifies bone homeostasis in cold-challenged sea bream (*Sparus aurata*). J Exp Biol 220, 3442-3454.

Mateus A.P., Costa R.A., Cardoso J.C.R., Andree K.B., Estevez A., Gisbert E. & Power D.M. (2017b) Thermal imprinting modifies adult stress and innate immune responsiveness in the

teleost sea bream. J Endocrinol 233, 381-394.

Mauri I., Romero A., Acerete L., Mackenzie S., Roher N., Callol A., Cano I., Alvarez M.C. & Tort L. (2011) Changes in complement responses in gilthead seabream (*Sparus aurata*) and European seabass (*Dicentrarchus labrax*) under crowding stress, plus viral and bacterial challenges. Fish Shellfish Immunol 30, 182-188.

Mayer-Barber K.D. & Yan B. (2017) Clash of the cytokine titans: counter-regulation of interleukin-1 and type I interferon-mediated inflammatory responses. Cell Mol Immunol 14, 22-35.

McDonnell P., Figat S. & O'Doherty J.V. (2010) The effect of dietary laminarin and fucoidan in the diet of the weanling piglet on performance, selected faecal microbial populations and volatile fatty acid concentrations. Animal 4, 579-585.

McFadden G., Mohamed M.R., Rahman M.M. & Bartee E. (2009) Cytokine determinants of viral tropism. Nat Rev Immunol 9, 645-655.

McIntosh M., Stone B.A. & Stanisich V.A. (2005) Curdlan and other bacterial (1-->3)-beta-D-glucans. Appl Microbiol Biotechnol 68, 163-173.

McLoughlin R.F., Berthon B.S., Jensen M.E., Baines K.J. & Wood L.G. (2017) Short-chain fatty acids, prebiotics, synbiotics, and systemic inflammation: a systematic review and meta-analysis. Am J Clin Nutr 106, 930-945.

Medina-Gali R.M., Ortega-Villaizan M.D.M., Mercado L., Novoa B., Coll J. & Perez L. (2018) Beta-glucan enhances the response to SVCV infection in zebrafish. Dev Comp Immunol 84, 307-314.

Medzhitov R. & Janeway C.A., Jr. (2002) Decoding the patterns of self and nonself by the innate immune system. Science 296, 298-300.

Meena D.K., Das P., Kumar S., Mandal S.C., Prusty A.K., Singh S.K., Akhtar M.S., Behera B.K., Kumar K., Pal A.K. & Mukherjee S.C. (2013) Beta-glucan: an ideal immunostimulant in aquaculture (a review). Fish Physiol Biochem 39, 431-457.

Merrifield D.L. & Rodiles A. (2015) The fish microbiome and its interactions with mucosal tissues. In: *Mucosal Health in Aquaculture* (ed. by B.H. Beck & E. Peatman), pp. 273-295. Academic Press, Oxford, UK.

Miest J.J., Arndt C., Adamek M., Steinhagen D. & Reusch T.B. (2016) Dietary beta-glucan

(MacroGard(R)) enhances survival of first feeding turbot (*Scophthalmus maximus*) larvae by altering immunity, metabolism and microbiota. Fish Shellfish Immunol 48, 94-104.

Misra C.K., Das B.K., Mukherjee S.C. & Pattnaik P. (2006) Effect of multiple injections of beta-glucan on non-specific immune response and disease resistance in *Labeo rohita* fingerlings. Fish Shellfish Immunol 20, 305-319.

Mitra M., Patidar S.K., George B., Shah F. & Mishra S. (2015) A euryhaline Nannochloropsis gaditana with potential for nutraceutical (EPA) and biodiesel production. Algal Res 8, 161-167.

Moen T., Torgersen J., Santi N., Davidson W.S., Baranski M., Odegard J., Kjoglum S., Velle B., Kent M., Lubieniecki K.P., Isdal E. & Lien S. (2015) Epithelial cadherin determines resistance to Infectious Pancreatic Necrosis Virus in atlantic salmon. Genetics 200, 1313-1326.

Mogensen T.H. & Paludan S.R. (2001) Molecular pathways in virus-induced cytokine production. Microbiol Mol Biol Rev 65, 131-150.

Molina-Holgado E., Ortiz S., Molina-Holgado F. & Guaza C. (2000) Induction of COX-2 and PGE(2) biosynthesis by IL-1beta is mediated by PKC and mitogen-activated protein kinases in murine astrocytes. Br J Pharmacol 131, 152-159.

Molyneux P. (2004) The use of the stable free radical diphenylpicrylhydrazyl (DPPH) for estimating antioxidant activity. Songklanakarin J Sci Technol 26, 211-219.

Montero D., Benitez-Dorta V., Caballero M.J., Ponce M., Torrecillas S., Izquierdo M., Zamorano M.J. & Manchado M. (2015) Dietary vegetable oils: effects on the expression of immune-related genes in Senegalese sole (*Solea senegalensis*) intestine. Fish Shellfish Immunol 44, 100-108.

Morais S., Aragão C., Cabrita E., Conceição L.E.C., Constenla M., Costas B., Dias J., Duncan N., Engrola S., Estevez A., Gisbert E., Mañanós E., Valente L.M.P., Yúfera M. & Dinis M. (2016) New developments and biological insights into the farming of *Solea senegalensis* reinforcing its aquaculture potential. Rev Aquacult 6, 1-37.

Moretti A., Pedini Fernandez-Criado M.P., Cittolin G. & Guidastri R. (1999) *Manual on hatchery production of seabass and gilthead seabream*. FAO, Rome.

Morrison D.J. & Preston T. (2016) Formation of short chain fatty acids by the gut microbiota and their impact on human metabolism. Gut Microbes 7, 189-200.

Mutsafi Y., Fridmann-Sirkis Y., Milrot E., Hevroni L. & Minsky A. (2014) Infection cycles of large DNA viruses: emerging themes and underlying questions. Virology 466-467, 3-14.

Myklestad S.M. & Granum E. (2009) Biology of (1,3)-beta-glucans and related glucans in protozoans and chromistans. In: *Chemistry, biochemistry, and biology of 1-3 beta glucans and related polysaccharides* (ed. by A. Bacic, G.B. Fincher & B.A. Stone). Academic Press, San Diego.

Nakanishi T., Toda H., Shibasaki Y. & Somamoto T. (2011) Cytotoxic T cells in teleost fish. Dev Comp Immunol 35, 1317-1323.

Nakao M., Mutsuro J., Obo R., Fujiki K., Nonaka M. & Yano T. (2000) Molecular cloning and protein analysis of divergent forms of the complement component C3 from a bony fish, the common carp (*Cyprinus carpio*): presence of variants lacking the catalytic histidine. Eur J Immunol 30, 858-866.

Nakao M., Tsujikura M., Ichiki S., Vo T.K. & Somamoto T. (2011) The complement system in teleost fish: progress of post-homolog-hunting researches. Dev Comp Immunol 35, 1296-1308.

Navarro A., Zamorano M.J., Hildebrandt S., Ginés R., Aguilera C. & Afonso J.M. (2009) Estimates of heritabilities and genetic correlations for growth and carcass traits in gilthead seabream (*Sparus auratus* L.), under industrial conditions. Aquaculture 289, 225-230.

Navarro A., Lee-Montero I., Santana D., Henríquez P., Ferrer M.A., Morales A., Soula M., Badilla R., Negrin-Baez D., Zamorano M.J. & Afonso J.M. (2016) IMAFISH_ML: A fully-automated image analysis software for assessing fish morphometric traits on gilthead seabream (*Sparus aurata* L.), meagre (*Argyrosomus regius*) and red porgy (*Pagrus pagrus*). Comput Electron Agr. 121, 66-73.

Navarro-Martin L., Vinas J., Ribas L., Diaz N., Gutierrez A., Di Croce L. & Piferrer F. (2011) DNA methylation of the gonadal aromatase (cyp19a) promoter is involved in temperature-dependent sex ratio shifts in the European sea bass. PLoS Genet 7, e1002447.

Nesargikar P.N., Spiller B. & Chavez R. (2012) The complement system: history, pathways, cascade

and inhibitors. Eur J Microbiol Immunol 2, 103-111.

Netea M.G., Joosten L.A., Latz E., Mills K.H., Natoli G., Stunnenberg H.G., O'Neill L.A. & Xavier R.J. (2016) Trained immunity: A program of innate immune memory in health and disease. Science 352, aaf1098.

Nishida H., Yoshimizu M. & Ezura Y. (1998) Detection of antibody against lymphocystis disease virus in Japanese flounder by enzyme-linked immunosorbent assay. Fish Pathol 33, 207-211.

Noss I., Doekes G., Thorne P.S., Heederik D.J. & Wouters I.M. (2013) Comparison of the potency of a variety of beta-glucans to induce cytokine production in human whole blood. Innate Immun 19, 10-19.

Novak M. & Vetvicka V. (2008) Beta-glucans, history, and the present: immunomodulatory aspects and mechanisms of action. J Immunotoxicol 5, 47-57.

Nunez-Diaz J.A., Fumanal M., Mancera J.M., Morinigo M.A. & Balebona M.C. (2016) Two routes of infection with *Photobacterium damselae* subsp. *piscicida* are effective in the modulation of the transcription of immune related genes in *Solea senegalensis*. Vet Immunol Immunopathol 179, 8-17.

O'Doherty J.V., Dillon S., Figat S., Callan J.J. & Sweeney T. (2010) The effects of lactose inclusion and seaweed extract derived from *Laminaria* spp. on performance, digestibility of diet components and microbial populations in newly weaned pigs. Anim Feed Sci Tech 157, 173-180.

Oca J. & Masaló I. (2019) Engineering of sole culture facilities. In: *The Biology of Sole* (ed. by J. Munoz-Cueto, E. Mañanós-Sánchez & F. Sánchez-Vázquez), pp. 23-35. CRC Press., Boca Raton.

Ødegård J., Baranski M., Gjerde B. & Gjedrem T. (2011) Methodology for genetic evaluation of disease resistance in aquaculture species: Challenges and future prospects. Aquacult Res 42, 103-114.

Ortiz-Delgado J., Simes D., Gavaia P., Sarasquete C. & Cancela M. (2005) Osteocalcin and matrix GLA protein in developing teleost teeth: identification of sites of mRNA and protein accumulation at single cell resolution. Histochem Cell Biol 124, 123-130.

Ortiz-Delgado J., Fernández I., Sarasquete C. & Gisbert E. (2014) Normal and histopathological organization of opercular bone and vertebrae in gilthead seabream *Sparus aurata*. Aquat Biol 21, 67-84.

Osorio F. & Reis e Sousa C. (2011) Myeloid C-type lectin receptors in pathogen recognition and host defense. Immunity 34, 651-664.

Padros F., Constenla M. & Zarza C. (2019) Pathology and diseases control. In: *The Biology of Sole* (ed. by J. Munoz-Cueto, E. Mañanós-Sánchez & J. Sánchez-Vázquez), pp. 326-353. CRC Press, Boca Raton.

Palaiokostas C., Ferraresso S., Franch R., Houston R.D. & Bargelloni L. (2016) Genomic prediction of resistance to pasteurellosis in gilthead sea bream (*Sparus aurata*) Using 2b-RAD Sequencing. G3 6, 3693-3700.

Palmer L.J., Hogan N.S. & van den Heuvel M.R. (2012) Phylogenetic analysis and molecular methods for the detection of lymphocystis disease virus from yellow perch, *Perca flavescens* (Mitchell). J Fish Dis 35, 661-670.

Palmer P.J., Burke M.J., Palmer C.J. & Burke J.B. (2007) Developments in controlled green-water larval culture technologies for estuarine fishes in Queensland, Australia and elsewhere. Aquaculture 272, 1-21.

Palstra A.P. & Planas J.V. (2011) Fish under exercise. Fish Physiol Biochem 37, 259-272.

Paperna I. & Baudin-Laurencin F. (1979) Parasitic infections of sea bass, *Dicentrarchus labrax*, and gilthead sea bream, *Sparus aurata*, in mariculture facilities in France. Aquaculture 16, 173-175.

Paperna I., Sabnat I. & Colorni A. (1982) An outbreak of lymphocystis in *Sparus aurata* L. in the Gulf of Aqaba, Red Sea. J Fish Dis 5, 433-437.

Parma L., Candela M., Soverini M., Turroni S., Consolandi C., Brigidi P., Mandrioli L., Sirri R., Fontanillas R., Gatta P.P. & Bonaldo A. (2016) Next-generation sequencing characterization of the gut bacterial community of gilthead sea bream (*Sparus aurata*, L.) fed low fishmeal based diets with increasing soybean meal levels. Anim Feed Sci Techno 222, 204-216.

Parra D., Korytar T., Takizawa F. & Sunyer J.O. (2016) B cells and their role in the teleost gut. Dev Comp Immunol 64, 150-166.

Peddie S., McLauchlan P.E., Ellis A.E. & Secombes C.J. (2003) Effect of intraperitoneally administered IL-1beta-derived peptides on resistance to viral haemorrhagic septicaemia in rainbow trout *Oncorhynchus mykiss*. Dis Aquat Organ. 56, 195-200.

Pereiro P., Dios S., Boltana S., Coll J., Estepa A., Mackenzie S., Novoa B. & Figueras A. (2014) Transcriptome profiles associated to VHSV infection or DNA vaccination in turbot (*Scophthalmus maximus*). PLoS One 9, e104509.

Pereiro P., Figueras A. & Novoa B. (2019) Insights into teleost interferon-gamma biology: An update. Fish Shellfish Immunol 90, 150-164.

Petit J. & Wiegertjes G.F. (2016) Long-lived effects of administering beta-glucans: Indications for trained immunity in fish. Dev Comp Immunol 64, 93-102.

Petit J., Bailey E.C., Wheeler R.T., de Oliveira C.A.F., Forlenza M. & Wiegertjes G.F. (2019a) Studies into beta-glucan recognition in fish suggests a key role for the c-type lectin pathway. Front Immunol 10, 280.

Petit J., Embregts C.W.E., Forlenza M. & Wiegertjes G.F. (2019b) Evidence of trained immunity in a fish: conserved features in carp macrophages. J Immunol 203, 216-224.

Pietretti D., Vera-Jimenez N.I., Hoole D. & Wiegertjes G.F. (2013) Oxidative burst and nitric oxide responses in carp macrophages induced by zymosan, MacroGard((R)) and selective dectin-1 agonists suggest recognition by multiple pattern recognition receptors. Fish Shellfish Immunol 35, 847-857.

Pietretti D. & Wiegertjes G.F. (2014) Ligand specificities of Toll-like receptors in fish: indications from infection studies. Dev Comp Immunol 43, 205-222.

Pinto P.I.S., Andrade A.R., Estevao M.D., Alvarado M.V., Felip A. & Power D.M. (2018) Duplicated membrane estrogen receptors in the European sea bass (*Dicentrarchus labrax*): Phylogeny, expression and regulation throughout the reproductive cycle. J Steroid Biochem Mol Biol 178, 234-242.

Pinto P.I.S., Guerreiro C.C., Costa R.A., Martinez-Blanch J.F., Carballo C., Codoner F.M., Manchado M. & Power D.M. (2019) Understanding pseudo-albinism in sole (*Solea senegalensis*): a transcriptomics and metagenomics approach. Sci Rep 9, 13604.

Pionnier N., Falco A., Miest J.J., Shrive A.K. & Hoole D. (2014) Feeding common carp *Cyprinus*

carpio with beta-glucan supplemented diet stimulates C-reactive protein and complement immune acute phase responses following PAMPs injection. Fish Shellfish Immunol 39, 285-295.

Ponce M., Salas-Leiton E., Garcia-Cegarra A., Boglino A., Coste O., Infante C., Gisbert E., Rebordinos L. & Manchado M. (2011) Genomic characterization, phylogeny and gene regulation of g-type lysozyme in sole (*Solea senegalensis*). Fish Shellfish Immunol 31, 925-937.

Poynter S., Lisser G., Monjo A. & DeWitte-Orr S. (2015) Sensors of infection: viral nucleic acid PRRs in fish. Biology 4, 460-493.

Press C.M., Dannevig B.H. & Landsverk T. (1994) Immune and enzyme histochemical phenotypes of lymphoid and nonlymphoid cells within the spleen and head kidney of Atlantic salmon (*Salmo salar* L.). Fish Shellfish Immunol 4, 79-93.

Prieto-Alamo M.J., Abril N., Osuna-Jimenez I. & Pueyo C. (2009) *Solea senegalensis* genes responding to lipopolysaccharide and copper sulphate challenges: large-scale identification by suppression subtractive hybridization and absolute quantification of transcriptional profiles by real-time RT-PCR. Aquat Toxicol 91, 312-319.

Priyadarshini S.K., Subramani P.A. & Michael R.D. (2017) Modulation of the innate immune responses in the striped snakehead murrel, *Channa striata* upon experimental infection with live and heat killed *Aeromonas hydrophila*. Open Vet J 7, 157-164.

Qi C., Cai Y., Gunn L., Ding C., Li B., Kloecker G., Qian K., Vasilakos J., Saijo S., Iwakura Y., Yannelli J.R. & Yan J. (2011) Differential pathways regulating innate and adaptive antitumor immune responses by particulate and soluble yeast-derived beta-glucans. Blood 117, 6825-6836.

Quinn S.M., Cunningham K., Raverdeau M., Walsh R.J., Curham L., Malara A. & Mills K.H.G. (2019) Anti-inflammatory trained immunity mediated by helminth products attenuates the induction of T cell-mediated autoimmune disease. Front Immunol 10, 1109.

Raj V.S., Fournier G., Rakus K., Ronsmans M., Ouyang P., Michel B., Delforges C., Costes B., Farnir F., Leroy B., Wattiez R., Melard C., Mast J., Lieffrig F. & Vanderplasschen A. (2011) Skin mucus of *Cyprinus carpio* inhibits cyprinid herpesvirus 3 binding to epidermal cells.

Vet Res 42, 92.

Rajanbabu V., Pan C.Y., Lee S.C., Lin W.J., Lin C.C., Li C.L. & Chen J.Y. (2010) Tilapia hepcidin 2-3 peptide modulates lipopolysaccharide-induced cytokines and inhibits tumor necrosis factor-alpha through cyclooxygenase-2 and phosphodiesterase 4D. J Biol Chem 285, 30577-30586.

Rajanbabu V. & Chen J.Y. (2011) Antiviral function of tilapia hepcidin 1-5 and its modulation of immune-related gene expressions against infectious pancreatic necrosis virus (IPNV) in Chinook salmon embryo (CHSE)-214 cells. Fish Shellfish Immunol 30, 39-44.

Ramirez-Gomez F., Greene W., Rego K., Hansen J.D., Costa G., Kataria P. & Bromage E.S. (2012) Discovery and characterization of secretory IgD in rainbow trout: secretory IgD is produced through a novel splicing mechanism. J Immunol 188, 1341-1349.

Rathinam V.A. & Fitzgerald K.A. (2010) Inflammasomes and anti-viral immunity. J Clin Immunol 30, 632-637.

Rauta P.R., Nayak B. & Das S. (2012) Immune system and immune responses in fish and their role in comparative immunity study: A model for higher organisms. Immunol Lett 148, 23-33.

Reyes-Cerpa S., Reyes-Lopez F.E., Toro-Ascuy D., Ibanez J., Maisey K., Sandino A.M. & Imarai M. (2012) IPNV modulation of pro and anti-inflammatory cytokine expression in Atlantic salmon might help the establishment of infection and persistence. Fish Shellfish Immunol 32, 291-300.

Reyes-Cerpa S., Reyes-Lopez F., Toro-Ascuy D., Montero R., Maisey K., Acuna-Castillo C., Sunyer J.O., Parra D., Sandino A.M. & Imarai M. (2014) Induction of anti-inflammatory cytokine expression by IPNV in persistent infection. Fish Shellfish Immunol 41, 172-182.

Rigos G. & Katharios P. (2010) Pathological obstacles of newly-introduced fish species in Mediterranean mariculture: a review. Rev Fish Biol Fish 20, 47-70.

Rimoldi S., Gliozheni E., Ascione C., Gini E. & Terova G. (2018) Effect of a specific composition of short- and medium-chain fatty acid 1-monoglycerides on growth performances and gut microbiota of gilthead sea bream (*Sparus aurata*). PeerJ 6, e5355.

Ringø E., Olsen R., Gifstad T., Dalmo R., Amlund H., Hemre G.I. & Bakke A.M. (2010) Prebiotics in aquaculture: a review. Aquacult Nutr 16, 117-136.

Ringø E., Olsen R., Vecino J., Wadsworth S. & Song S. (2012) Use of immunostimulants and nucleotides in aquaculture: a review. J Marine Sci Res Development 2, 104-125.

Roca F.J., Mulero I., Lopez-Munoz A., Sepulcre M.P., Renshaw S.A., Meseguer J. & Mulero V. (2008) Evolution of the inflammatory response in vertebrates: fish TNF-alpha is a powerful activator of endothelial cells but hardly activates phagocytes. J Immunol 181, 5071-5081.

Rodriguez S., Vila P., Sarasquete M.C., Rodriguez R.B., Gutierrez M.C. & Perez-Prieto S.I. (1997) Isolation and preliminary characterization of a birnavirus from *Solea senegalensis* in Southwest Spain. J Aquat Anim Hlth 9, 295-300.

Rojo-Cebreros A.H., Ibarra-Castro L., Martínez-Brown J.M., Velasco-Blanco G., Martínez-Téllez M.A., Medina-Jasso M.A., Nieves-Soto M. & Quintana-Zavala D. (2017) Potential of *Nannochloropsis* in beta glucan production. In: *Nannochloropsis: Biology, Biotechnological, Potential and Challenges* (ed. by M. Jan & P. Kazik). Nova Science Publishers, Inc, Hauppauge, New York.

Rojo-Cebreros A.H., Ibarra-Castro L. & Martinez-Brown J.M. (2018) Immunostimulation and trained immunity in marine fish larvae. Fish Shellfish Immunol 80, 15-21.

Roman-Padilla J., Rodriguez-Rua A., Claros M.G., Hachero-Cruzado I. & Manchado M. (2016a) Genomic characterization and expression analysis of four apolipoprotein A-IV paralogs in Senegalese sole (*Solea senegalensis* Kaup). Comp Biochem Physiol B Biochem Mol Biol 191, 84-98.

Roman-Padilla J., Rodriguez-Rua A., Manchado M. & Hachero-Cruzado I. (2016b) Molecular characterization and developmental expression patterns of apolipoprotein A-I in Senegalese sole (*Solea senegalensis* Kaup). Gene Expr Patterns 21, 7-18.

Rombout J.H., Abelli L., Picchietti S., Scapigliati G. & Kiron V. (2011) Teleost intestinal immunology. Fish Shellfish Immunol 31, 616-626.

Roy M.K., Koide M., Rao T.P., Okubo T., Ogasawara Y. & Juneja L.R. (2010) ORAC and DPPH assay comparison to assess antioxidant capacity of tea infusions: relationship between total polyphenol and individual catechin content. Int J Food Sci Nutr 61, 109-124.

Rubio C.P., Hernandez-Ruiz J., Martinez-Subiela S., Tvarijonaviciute A. & Ceron J.J. (2016) Spectrophotometric assays for total antioxidant capacity (TAC) in dog serum: an update.

BMC Vet Res 12, 166.

Sadovskaya I., Souissi A., Souissi S., Grard T., Lencel P., Greene C.M., Duin S., Dmitrenok P.S., Chizhov A.O., Shashkov A.S. & Usov A.I. (2014) Chemical structure and biological activity of a highly branched (1 --> 3,1 --> 6)-beta-D-glucan from *Isochrysis galbana*. Carbohydr Polym 111, 139-148.

Saeed S., Quintin J., Kerstens H.H., Rao N.A., Aghajanirefah A., Matarese F., Cheng S.C., Ratter J., Berentsen K., van der Ent M.A., Sharifi N., Janssen-Megens E.M., Ter Huurne M., Mandoli A., van Schaik T., Ng A., Burden F., Downes K., Frontini M., Kumar V., Giamarellos-Bourboulis E.J., Ouwehand W.H., van der Meer J.W., Joosten L.A., Wijmenga C., Martens J.H., Xavier R.J., Logie C., Netea M.G. & Stunnenberg H.G. (2014) Epigenetic programming of monocyte-to-macrophage differentiation and trained innate immunity. Science 345, 1251086.

Salas-Leiton E., Anguis V., Martin-Antonio B., Crespo D., Planas J.V., Infante C., Canavate J.P. & Manchado M. (2010) Effects of stocking density and feed ration on growth and gene expression in the Senegalese sole (*Solea senegalensis*): potential effects on the immune response. Fish Shellfish Immunol 28, 296-302.

Salas-Leiton E., Coste O., Asensio E., Infante C., Cañavate J.P. & Manchado M. (2012) Dexamethasone modulates expression of genes involved in the innate immune system, growth and stress and increases susceptibility to bacterial disease in Senegalese sole (*Solea senegalensis* Kaup, 1858). Fish Shellfish Immunol 32, 769-778.

Salazar-Mather T.P. & Hokeness K.L. (2006) Cytokine and chemokine networks: pathways to antiviral defense. Curr Top Microbiol Immunol 303, 29-46.

Salinas I. (2015) The mucosal immune system of teleost fish. Biology (Basel) 4, 525-539.

Samalecos C. (1986) Biochemical and structural studies of fish lymphocystis disease virions isolated from skin tumours of *Pleuronectes*. J Virol Methods 13, 197-205.

Sarasquete C., Gonzalez de Canales M.L., Arellano J., Perez-Prieto S., Garcia-Rosado E. & Borrego J.J. (1998) Histochemical study of lymphocystis disease in skin of gilthead seabream, *Sparus aurata* L. Histol Histopathol 13, 37-45.

Saurabh S. & Sahoo P.K. (2008) Lysozyme: an important defence molecule of fish innate immune

system. Aquaculture Res 39, 223-239.

Scapigliati G., Buonocore F., Randelli E., Casani D., Meloni S., Zarletti G., Tiberi M., Pietretti D., Boschi I., Manchado M., Martin-Antonio B., Jimenez-Cantizano R., Bovo G., Borghesan F., Lorenzen N., Einer-Jensen K., Adams S., Thompson K., Alonso C., Bejar J., Cano I., Borrego J.J. & Alvarez M.C. (2010) Cellular and molecular immune responses of the sea bass (*Dicentrarchus labrax*) experimentally infected with betanodavirus. Fish Shellfish Immunol 28, 303-311.

Scapigliati G., Fausto A.M. & Picchietti S. (2018) Fish Lymphocytes: An evolutionary equivalent of mammalian innate-like lymphocytes? Front Immunol 9, 971.

Schindelin J., Arganda-Carreras I., Frise E., Kaynig V., Longair M., Pietzsch T., Preibisch S., Rueden C., Saalfeld S., Schmid B., Tinevez J.Y., White D.J., Hartenstein V., Eliceiri K., Tomancak P. & Cardona A. (2012) Fiji: an open-source platform for biological-image analysis. Nat Methods 9, 676-682.

Schmittgen T.D. & Livak K.J. (2008) Analyzing real-time PCR data by the comparative C(T) method. Nat Protoc 3, 1101-1108.

Secombes C.J. & Wang T. (2012) The innate and adaptive immune system of fish. In: *Infectious Disease in Aquaculture* (ed. by B. Austin), pp. 3-68. Woodhead Publishing.

Selvaraj V., Sampath K. & Sekar V. (2005) Administration of yeast glucan enhances survival and some non-specific and specific immune parameters in carp (*Cyprinus carpio*) infected with *Aeromonas hydrophila*. Fish Shellfish Immunol 19, 293-306.

Sfacteria A., Brines M. & Blank U. (2015) The mast cell plays a central role in the immune system of teleost fish. Mol Immunol 63, 3-8.

Shen L., Stuge T.B., Zhou H., Khayat M., Barker K.S., Quiniou S.M.A., Wilson M., Bengtén E., Chinchar V.G., Clem L.W. & Miller N.W. (2002) Channel catfish cytotoxic cells: a mini-review. Developmental & Comparative Immunology 26, 141-149.

Shen L., Stuge T.B., Bengtén E., Wilson M., Chinchar V.G., Naftel J.P., Bernanke J.M., Clem L.W. & Miller N.W. (2004) Identification and characterization of clonal NK-like cells from channel catfish (*Ictalurus punctatus*). Developmental & Comparative Immunology 28, 139-152.

Sheng X., Wu R., Tang X., Xing J. & Zhan W. (2015) Tissue localization of Lymphocystis Disease Virus (LCDV) receptor-27.8 kDa and its expression kinetics induced by the viral infection in turbot (*Scophthalmus maximus*). Int J Mol Sci 16, 26506-26519.

Sheng X.Z., Zhan W.B., Xu S. & Cheng S. (2007) Histopathological observation of lymphocystis disease and lymphocystis disease virus (LCDV) detection in cultured diseased *Sebastes schlegeli*. J Ocean U China 6, 378-382.

Silva Y., Moreirinha C., Pereira C., Costa L., Rocha R., Cunha A., Gomes N., Calado R. & Almeida A. (2016) Biological control of *Aeromonas salmonicida* infection in juvenile Senegalese sole (*Solea senegalensis*) with phage AS-A. Aquaculture 450, 225-233.

Siwicki A.K., Morand M., Klein P. & Kiczka W. (1998) Treatment of infectious pancreatic necrosis virus (IPNV) disease using dimerized lysozyme (KLP-602). J Appl Ichthyol 14, 229–232.

Skov J., Kania P.W., Holten-Andersen L., Fouz B. & Buchmann K. (2012) Immunomodulatory effects of dietary beta-1,3-glucan from *Euglena gracilis* in rainbow trout (*Oncorhynchus mykiss*) immersion vaccinated against *Yersinia ruckeri*. Fish Shellfish Immunol 33, 111-120.

Smail D.A. & Munro A.L.S. (2001) The virology of teleosts. In: *Fish Pathology* (ed. by R.J. Roberts), pp. 169–253. W.B. Saunders, Edinburgh.

Smith A.J., Graves B., Child R., Rice P.J., Ma Z., Lowman D.W., Ensley H.E., Ryter K.T., Evans J.T. & Williams D.L. (2018) Immunoregulatory activity of the natural product laminarin varies widely as a result of its physical properties. J Immunol 200, 788-799.

Smith S.A. (1998) Biosecurity and fish health monitoring for aquaculture facilities. In: *Proceedings of the Second International Conference on Recirculating Aquaculture* (eds. by G.S. Libey & M.B. Timmons), pp. 22-24, Virginia Sea Grant.

Song S.K., Beck B.R., Kim D., Park J., Kim J., Kim H.D. & Ringo E. (2014) Prebiotics as immunostimulants in aquaculture: a review. Fish Shellfish Immunol 40, 40-48.

Sørensen M., Berge G.M., Reitan K.I. & Ruyter B. (2016) Microalga *Phaeodactylum tricornutum* in feed for Atlantic salmon (*Salmo salar*) - effect on nutrient digestibility, growth and utilization of feed. Aquaculture 460, 116-123.

Souto S., Olveira J.G., Alonso M.C., Dopazo C.P. & Bandin I. (2018) Betanodavirus infection in

bath-challenged *Solea senegalensis* juveniles: A comparative analysis of RGNNV, SJNNV and reassortant strains. J Fish Dis 41, 1571-1578.

Stier H., Ebbeskotte V. & Gruenwald J. (2014) Immune-modulatory effects of dietary yeast beta-1,3/1,6-D-glucan. Nutr J 13, 38.

Suarez C., Andres G., Kolovou A., Hoppe S., Salas M.L., Walther P. & Krijnse Locker J. (2015) African swine fever virus assembles a single membrane derived from rupture of the endoplasmic reticulum. Cell Microbiol 17, 1683-1698.

Sun C., Hu L., Liu S., Hu G. & Zhang S. (2013) Antiviral activity of phosvitin from zebrafish *Danio rerio*. Dev Comp Immunol 40, 28-34.

Sunyer J.O., Tort L. & Lambris J.D. (1997) Diversity of the third form of complement, C3, in fish: functional characterization of five forms of C3 in the diploid fish *Sparus aurata*. Biochem J 326, 877-881.

Sych G., Frost P. & Irnazarow I. (2013) Influence of β-Glucan (MACROGARD®) on innate immunity of carp fry B Vet I Pulawy 52, 219-223.

Symensma T.L., Martinez-Guzman D., Jia Q., Bortz E., Wu T.T., Rudra-Ganguly N., Cole S., Herschman H. & Sun R. (2003) COX-2 induction during murine gammaherpesvirus 68 infection leads to enhancement of viral gene expression. J Virol 77, 12753-12763.

Synytsya A. & Novak M. (2014) Structural analysis of glucans. Ann Transl Med 2, 17.

Tacchi L., Musharrafieh R., Larragoite E.T., Crossey K., Erhardt E.B., Martin S.A.M., LaPatra S.E. & Salinas I. (2014) Nasal immunity is an ancient arm of the mucosal immune system of vertebrates. Nat Commun 5, 5205.

Tafalla C., Coll J. & Secombes C.J. (2005) Expression of genes related to the early immune response in rainbow trout (*Oncorhynchus mykiss*) after viral haemorrhagic septicemia virus (VHSV) infection. Dev Comp Immunol 29, 615-626.

Tafalla C., Leal E., Yamaguchi T. & Fischer U. (2016) T cell immunity in the teleost digestive tract. Dev Comp Immunol 64, 167-177.

Takizawa F., Magadan S., Parra D., Xu Z., Korytar T., Boudinot P. & Sunyer J.O. (2016) Novel teleost CD4-bearing cell populations provide insights into the evolutionary origins and primordial roles of CD4+ lymphocytes and CD4+ macrophages. J Immunol 196, 4522-4535.

Tall A., Teillon A., Boisset C., Delesmont R., Touron-Bodilis A. & Hervio-Heath D. (2012) Real-time PCR optimization to identify environmental *Vibrio* spp. strains. J Appl Microbiol 113, 361-372.

Talwar C., Nagar S., Lal R. & Negi R.K. (2018) Fish gut microbiome: current approaches and future perspectives. Indian J Microbiol 58, 397-414.

Tapia-Paniagua S.T., Fumanal M., Anguis V., Fernandez-Diaz C., Alarcon F.J., Morinigo M.A. & Balebona M.C. (2019) Modulation of intestinal microbiota in *Solea senegalensis* fed low dietary level of *Ulva ohnoi*. Front Microbiol 10, 171.

Terlizzi A., Tedesco P. & Patarnello P. (2012) Spread of pathogens from marine cage aquaculture. A potential threat for wild fish assemblages under protection regimes? In: *Health and Environment in Aquaculture* (ed. by E. Carvalho), pp. 403-414. InTech, Rijeka.

Thangjam G.S., Birmpas C., Barabutis N., Gregory B.W., Clemens M.A., Newton J.R., Fulton D. & Catravas J.D. (2016) Hsp90 inhibition suppresses NF-kappaB transcriptional activation via Sirt-2 in human lung microvascular endothelial cells. Am J Physiol Lung Cell Mol Physiol 310, L964-974.

Tian J.Y., Xie H.X., Zhang Y.A., Xu Z., Yao W.J. & Nie P. (2009) Ontogeny of IgM-producing cells in the mandarin fish *Siniperca chuatsi* identified by *in situ* hybridisation. Vet Immunol Immunopathol 132, 146-152.

Tidona C.A., Schnitzler P., Kehm R. & Darai G. (1998) Is the major capsid protein of iridoviruses a suitable target for the study of viral evolution? Virus Genes 16, 59–66.

Toranzo A.E., Magariños B. & Romalde J.L. (2005) A review of the main bacterial fish diseases in mariculture systems. Aquaculture 246, 37-61.

Trites M.J. & Barreda D.R. (2017) Contributions of transferrin to acute inflammation in the goldfish, *C. auratus*. Dev Comp Immunol 67, 300-309.

Uribe C., Folch H., Enríquez R. & Moran G. (2011) Innate and adaptive immunity in teleost fish: a review. Veterinární medicína 56, 486-503.

Vadstein O., Bergh Ø., Gatesoupe F.-J., Galindo-Villegas J., Mulero V., Picchietti S., Scapigliati G., Makridis P., Olsen Y., Dierckens K., Defoirdt T., Boon N., De Schryver P. & Bossier P. (2013) Microbiology and immunology of fish larvae. Rev Aquacult 5, S1-S25.

Vallejos-Vidal E., Reyes-Lopez F., Teles M. & MacKenzie S. (2016) The response of fish to immunostimulant diets. Fish Shellfish Immunol 56, 34-69.

Valverde E.J., Borrego J.J. & Castro D. (2016a) Evaluation of an integrated cell culture RT-PCR assay to detect and quantify infectious lymphocystis disease virus. J Virol Methods 238, 62-65.

Valverde E.J., Cano I., Labella A., Borrego J.J. & Castro D. (2016b) Application of a new real-time polymerase chain reaction assay for surveillance studies of lymphocystis disease virus in farmed gilthead seabream. BMC Vet Res 12, 71.

Valverde E.J., Borrego J.J., Sarasquete M.C., Ortiz-Delgado J.B. & Castro D. (2017a) Target organs for lymphocystis disease virus replication in gilthead seabream (*Sparus aurata*). Vet Res 48, 21.

Valverde E.J., Cano I., Castro D., Paley R.K. & Borrego J.J. (2017b) Rapid and sensitive detection of Lymphocystis Disease Virus genotype VII by loop-mediated isothermal amplification. Food Environ Virol 9, 114-122.

van der Heijden C., Noz M.P., Joosten L.A.B., Netea M.G., Riksen N.P. & Keating S.T. (2018) Epigenetics and trained immunity. Antioxid Redox Signal 29, 1023-1040.

van der Marel M., Caspari N., Neuhaus H., Meyer W., Enss M.L. & Steinhagen D. (2010) Changes in skin mucus of common carp, *Cyprinus carpio* L., after exposure to water with a high bacterial load. J Fish Dis 33, 431-439.

Vandeputte M., Mauger S. & Dupont-Nivet M. (2006) An evaluation of allowing for mismatches as a way to manage genotyping errors in parentage assignment by exclusion. Mol Ecol Notes 6, 265-267.

Vannucci L., Krizan J., Sima P., Stakheev D., Caja F., Rajsiglova L., Horak V. & Saieh M. (2013) Immunostimulatory properties and antitumor activities of glucans (Review). Int J Oncol 43, 357-364.

Vetvicka V. & Vetvickova J. (2010) beta1,3-Glucan: Silver Bullet or Hot Air? Open Glycoscience 3, 1-6.

Vetvicka V., Vannucci L. & Sima P. (2013) The effects of beta-glucan on fish immunity. N Am J Med Sci 5, 580-588.

Vinolo M.A., Rodrigues H.G., Nachbar R.T. & Curi R. (2011) Regulation of inflammation by short chain fatty acids. Nutrients 3, 858-876.

Walport M.J. (2001) Complement. First of two parts. N Engl J Med 344, 1058-1066.

Wang N., Yang C.G., Sun Z.Z., Wang X.L. & Chen S.L. (2011) Signal transducer and activator of transcription 3 (STAT3) homologue in turbot (*Scophthalmus maximus*): molecular characterization and expression analysis. Fish Shellfish Immunol 30, 255-262.

Wang N., Wang X.L., Yang C.G. & Chen S.L. (2013) Molecular cloning, subcelluar location and expression profile of signal transducer and activator of transcription 2 (STAT2) from turbot, *Scophthalmus maximus*. Fish Shellfish Immunol 35, 1200-1208.

Wang T. & Secombes C.J. (2013) The cytokine networks of adaptive immunity in fish. Fish Shellfish Immunol 35, 1703-1718.

Wang Y.D., Kung C.W. & Chen J.Y. (2010) Antiviral activity by fish antimicrobial peptides of epinecidin-1 and hepcidin 1-5 against nervous necrosis virus in medaka. Peptides 31, 1026-1033.

Wei S., Huang Y., Huang X., Cai J., Wei J., Li P., Ouyang Z. & Qin Q. (2014) Molecular cloning and characterization of a new G-type lysozyme gene (*Ec-lysG*) in orange-spotted grouper, *Epinephelus coioides*. Dev Comp Immunol 46, 401-412.

Whittington R.J. & Chong R. (2007) Global trade in ornamental fish from an Australian perspective: the case for revised import risk analysis and management strategies. Prev Vet Med 81, 92-116.

Williams T. (1996) The iridoviruses. Adv Virus Res 46, 345-412.

Williams T., Barbosa-Solomieu V. & Chinchar V.G. (2005) A decade of advances in iridovirus research. Adv Virus Res 65, 173-248.

Wilson A.B. (2017) MHC and adaptive immunity in teleost fishes. Immunogenetics 69, 521-528.

Wolf K. (1988) Lymphocystis disease. In: *Fish Viruses and Fish Viral Diseases* (ed. by K. Wolf), pp. 268-291. Cornell University Press, Ithaca, NY.

Wu R., Sheng X., Tang X., Xing J. & Zhan W. (2018) Transcriptome analysis of flounder (*Paralichthys olivaceus*) gill in response to lymphocystis disease virus (LCDV) infection: Novel insights into fish defense mechanisms. Int J Mol Sci 19, 160.

Wu S., Wang G., Angert E.R., Wang W., Li W. & Zou H. (2012) Composition, diversity, and origin of the bacterial community in grass carp intestine. PLoS One 7, e30440.

Wu Y.C., Lu Y.F. & Chi S.C. (2010) Anti-viral mechanism of barramundi Mx against betanodavirus involves the inhibition of viral RNA synthesis through the interference of RdRp. Fish Shellfish Immunol 28, 467-475.

Xia S., Gao B., Li A., Xiong J., Ao Z. & Zhang C. (2014) Preliminary characterization, antioxidant properties and production of chrysolaminarin from marine diatom *Odontella aurita*. Mar Drugs 12, 4883-4897.

Yoder J.A. & Litman G.W. (2011) The phylogenetic origins of natural killer receptors and recognition: relationships, possibilities, and realities. Immunogenetics 63, 123-141.

Yoshida S.H., Stuge T.B., Miller N.W. & Clem L.W. (1995) Phylogeny of lymphocyte heterogeneity: Cytotoxic activity of channel catfish peripheral blood leukocytes directed against allogeneic targets. Dev Comp Immunol 19, 71-77.

Yuan C., Pan X., Gong Y., Xia A., Wu G., Tang J. & Han X. (2008) Effects of *Astragalus* polysaccharides (APS) on the expression of immune response genes in head kidney, gill and spleen of the common carp, *Cyprinus carpio* L. Int Immunopharmacol 8, 51-58.

Zapata A., Diez B., Cejalvo T., Gutierrez-de Frias C. & Cortes A. (2006) Ontogeny of the immune system of fish. Fish Shellfish Immunol 20, 126-136.

Zekovic D.B., Kwiatkowski S., Vrvic M.M., Jakovljevic D. & Moran C.A. (2005) Natural and modified (1-->3)-beta-D-glucans in health promotion and disease alleviation. Crit Rev Biotechnol 25, 205-230.

Zhang Q., Kopp M., Babiak I. & Fernandes J.M.O. (2018a) Low incubation temperature during early development negatively affects survival and related innate immune processes in zebrafish larvae exposed to lipopolysaccharide. Sci Rep 8, 4142.

Zhang S., Wang Z. & Wang H. (2013) Maternal immunity in fish. Dev Comp Immunol 39, 72-78.

Zhang S. & Cui P. (2014) Complement system in zebrafish. Dev Comp Immunol 46, 3-10.

Zhang W., Wang F., Gao B., Huang L. & Zhang C. (2018b) An integrated biorefinery process: Stepwise extraction of fucoxanthin, eicosapentaenoic acid and chrysolaminarin from the same *Phaeodactylum tricornutum* biomass. Algal Res 32, 193-200.

Zhang Y.A., Salinas I. & Sunyer J.O. (2011) Recent findings on the structure and function of teleost IgT. Fish Shellfish Immunol 31, 627-634.

Zhang Z., Chi H. & Dalmo R.A. (2019) Trained innate immunity of fish is a viable approach in larval aquaculture. Front Immunol 10, 42.

Zheng F.R., Sun X.Q. & Xing M.Q. (2010) Immune response of DNA vaccine against lymphocystis disease virus and expression analysis of immune-related genes after vaccination. Aquacult Res 41, 1444-1451.

Zhu L.Y., Nie L., Zhu G., Xiang L.X. & Shao J.Z. (2013) Advances in research of fish immune-relevant genes: a comparative overview of innate and adaptive immunity in teleosts. Dev Comp Immunol 39, 39-62.

Zimmer G., Reuter G. & Schauer R. (1992) Use of influenza C virus for detection of 9-O-acetylated sialic acids on immobilized glycoconjugates by esterase activity. Eur J Biochem 204, 209-215.

Zou J., Tafalla C., Truckle J. & Secombes C.J. (2007) Identification of a second group of type I IFNs in fish sheds light on IFN evolution in vertebrates. J Immunol 179, 3859-3871.

Zou J. & Secombes C.J. (2016) The function of fish cytokines. Biology 5, 23.

COMPENDIO DE PUBLICACIONES

Fish and Shellfish Immunology 89 (2019) 710–718

Contents lists available at ScienceDirect

Fish and Shellfish Immunology

journal homepage: www.elsevier.com/locate/fsi

Full length article

Feed and immersion challenges with lymphocystis disease virus (LCDV) reveals specific mechanisms for horizontal transmission and immune response in senegalese sole post-larvae

Carlos Carballo[a], Juan B. Ortiz-Delgado[b], Concha Berbel[a], Dolores Castro[c], Juan J. Borrego[c], Carmen Sarasquete[b], Manuel Manchado[a,*]

[a] IFAPA Centro El Toruño, Junta de Andalucía, Camino Tiro Pichón s/n, 11500, El Puerto de Santa María, Cádiz, Spain
[b] Instituto de Ciencias Marinas de Andalucía-ICMAN, CSIC-Campus Universitario Río San Pedro, Puerto Real, 11510, Cádiz, Spain
[c] Universidad de Málaga, Departamento de Microbiología, Campus Teatinos, 29071, Málaga, Spain

ARTICLE INFO

Keywords:
LCDV
Horizontal transmission
Immune gene expression
Senegalese sole

ABSTRACT

The horizontal transmission of lymphocystis disease virus (LCDV) through contaminated water and feed (using artemia as vehicle) and the associated immune gene expression profiles in Senegalese sole post-larvae were investigated. All specimens analyzed were positive for LCDV DNA detection at 1-day post-challenge (1 dpc) with the highest viral levels in specimens infected through the immersion route. However, the percentage of LCDV-positive animals and number of viral DNA copies dropped progressively at 2 and 7 dpc. The histological analysis identified structural changes in the skin, muscle and gills of sole post-larvae LCDV-challenged by immersion. *In situ* hybridization confirmed a wide distribution of LCDV in the skin, gut, surrounding vessels in trunk muscle and head kidney in the immersion route, while the signals were restricted to the liver and *lamina propria* in the feeding treatment. Expression analysis using a set of 22 genes related to innate immune defense system demonstrated clear differences in the time-course response to LCDV as function of the infection route. Most antiviral defense genes, the proinflammatory cytokines, the complement c3, g-type lysozyme and T-cell markers *cd4* and *cd8a* were rapidly induced in the feeding-infected post-larvae, and they were remained activated at 2 dpc. In contrast, in the immersion-infected post-larvae the induction of most defensive genes was delayed, with a low intensity at 2 dpc. All these data demonstrate that LCDV can horizontally infect Senegalese sole post-larvae through the water or feed although with different patterns of histopathological disorders, virus distribution and route-specific expression profiles.

1. Introduction

The lymphocystis disease (LCD) is a viral pathology that affects more than one hundred fish species worldwide both in freshwater and marine environments (reviewed in Ref. [1]). The causative agent is the lymphocystis disease virus (LCDV) that belongs to the genus *Lymphocystivirus*, family *Iridoviridae*, and exhibits a marked tropism towards dermal fibroblasts. The typical lesions, known as lymphocysts, have a nodular aspect that in massive infections can spread and cover most of the skin body surface including fins [2]. In the Mediterranean basin and European South Atlantic coasts, LCDV infections are mainly identified in hatcheries producing gilthead seabream (*Sparus aurata*) appearing as self-limiting episodes with a high morbidity and low mortality, unless secondary infections or exacerbated cannibalism occur [3]. In most cases, the infected animals remain as asymptomatic carriers and only develop the disease under stress conditions. Experimental infections showed a long incubation time (~one month) before first detection of the characteristic lesions [1,4]. The integumentary lesions fully disappear in a few weeks, depending on the environmental temperature, and the recovered animals remain as asymptomatic carriers that convert the LCD in a chronic and recurrent problem in aquaculture hatcheries. Although LCDV has been detected in a wide range of fish species including the Senegalese sole (*Solea senegalensis*), the reported outbreaks of LCD in this species are still scarce [5,6].

The high rates of LCDV prevalence have been associated with both vertical and horizontal viral transmission [7]. Embryos from infected brooders were demonstrated to carry the LCDV on the egg surface [7]. However, the horizontal transmission by direct contact with infected

* Corresponding author. IFAPA Centro *El Toruño*Camino Tiro de Pichón s/n, 11500, El Puerto de Santa María (Cádiz), Spain.
E-mail address: manuel.manchado@juntadeandalucia.es (M. Manchado).

https://doi.org/10.1016/j.fsi.2019.04.049
Received 7 December 2018; Received in revised form 5 March 2019; Accepted 13 April 2019
Available online 15 April 2019

Fish & Shellfish Immunology 66 (2017) 129–139

Contents lists available at ScienceDirect

Fish & Shellfish Immunology

journal homepage: www.elsevier.com/locate/fsi

Full length article

Gene expression profiles associated with lymphocystis disease virus (LCDV) in experimentally infected Senegalese sole (*Solea senegalensis*)

Carlos Carballo [a], Dolores Castro [b], Juan J. Borrego [b], Manuel Manchado [a, *]

[a] IFAPA Centro El Toruño, Junta de Andalucía, Camino Tiro Pichón s/n, 11500 El Puerto de Santa María, Cádiz, Spain
[b] Universidad de Málaga, Departamento de Microbiología, Campus Universitario Teatinos, 29071 Málaga, Spain

ARTICLE INFO

Article history:
Received 20 February 2017
Received in revised form
28 April 2017
Accepted 30 April 2017
Available online 3 May 2017

Keywords:
Immune gene expression
Senegalese sole
LCDV
Pathogenesis

ABSTRACT

In the present study, the pathogenesis of lymphocystis disease virus (LCDV) and the immune gene expression patterns associated with this viral infection were determined in the flatfish Senegalese sole. The results indicate that LCDV spreads rapidly from the peritoneal cavity through the bloodstream to reach target organs such as kidney, gut, liver, and skin/fin. The viral load was highest in kidney and reduced progressively thorough the experiment in spite of the viral major capsid protein gene was transcribed. The LCDV injection activated a similar set of differentially expressed transcripts in kidney and intestine although with some differences in the intensity and time-course response. This set included antiviral-related transcripts (including the *mx* and interferon-related factors *irf1*, *irf2*, *irf3*, *irf7*, *irf8*, *irf9*, *irf10*), cytokines (*il1b*, *il6*, *il8*, *il12* and *tnfa*) and their receptors (*il1r*, *il8r*, *il10r*, *il15ra*, *il17r*), chemokines (CXC-type, CC-type and IL-8), prostaglandins (*cox-2*), g-type lysozymes, hepcidin, complement fractions (*c2*, *c4-1* and *c4-2*) and the antigen differentiation factors *cd4*, *cd8a*, and *cd8b*. The expression profile observed indicated that the host triggered a systemic defensive response including inflammation able to cope with the viral challenge.

1. Introduction

Fish farming requires adequate management and control measures to cope with disease outbreaks specially for those of viral aetiology due to the lack of effective therapies [1]. The lymphocystis disease (LCD) is a worldwide disease reported in several fish species both in wild and cultured populations [2]. In the Mediterranean aquaculture, LCD is mainly observed in gilthead seabream (*Sparus aurata*) and secondary in other species such as Senegalese sole (*Solea senegalensis*) [3,4]. The typical sign of LCD is the presence of small pearl-like nodules (known as lymphocysts) on the skin and fins, which may occur singly or more generally grouped in raspberry-like clusters of tumorous appearance [5]. Mortality rates are normally low and the recovered fish remain as asymptomatic hosts without clinical signs that could shed viral particles into the environment to infect new fish [3,4]. In spite of this low mortality, the LCD imposes important economic losses to the aquaculture industry since animals with the typical lesions appear unsightly and cannot be commercialized [2]. Moreover, LCD outbreaks increase the susceptibility to secondary bacterial infections, cannibalism and/or parasitic infestations that negatively influence fish performance and indirectly mortality [6].

The lymphocystis disease virus (LCDV) belongs to genus *Lymphocystivirus*, family *Iridoviridae*. According to the polymorphisms in the gene encoding for the major capsid protein (MCP), the LCDV isolates are classified into nine different genotypes, from which the genotype VII is routinely found in gilthead seabream and Senegalese sole [2,4]. Previous studies have demonstrated that this virus, after contacting the host, spreads rapidly to several internal organs through the leukocytes to replicate in fibroblasts, hepatocytes and macrophages [7–9]. This rapid viral dissemination activates a systemic defensive response that comprises some interferon regulatory factors (IRFs) (including *irf3*, *irf5*, *irf7*, *irf8* and *irf9*) and *mx* [10–14], the signal transducer and activator of transcription (STAT) 2 and STAT3, and the hepcidin [15,16]. This early response seems essential to cope with virus infection as demonstrated by *in vitro* studies with clonal populations of transfected CHSE-214 cells that stably express Mx proteins [17]. Once the virus bypasses these defence mechanisms, the number of viral copies increases and the typical lymphocystis lesion arises [18]. In Japanese flounder, the lymphocyst formation implies changes in the expression of genes related to apoptosis inhibition, cell cycle arrest and alterations of collagen fibres with the proliferation of macrophages, granulocytes and epithelioid cells in the dermis [8,18,19].

* Corresponding author.
E-mail address: manuel.manchado@juntadeandalucia.es (M. Manchado).

http://dx.doi.org/10.1016/j.fsi.2017.04.028
1050-4648/

Fish and Shellfish Immunology 82 (2018) 1–8

Contents lists available at ScienceDirect

Fish and Shellfish Immunology

journal homepage: www.elsevier.com/locate/fsi

Full length article

Antioxidant capacity and immunomodulatory effects of a chrysolaminarin-enriched extract in Senegalese sole

Carlos Carballo[a], Evangelia G. Chronopoulou[b], Sofia Letsiou[c], Claudia Maya[d], Nikolaos E. Labrou[b], Carlos Infante[d], Deborah M. Power[e], Manuel Manchado[a,*]

[a] IFAPA Centro El Toruño, Junta de Andalucía, Camino Tiro Pichón s/n, 11500, El Puerto de Santa María, Spain
[b] Laboratory of Enzyme Technology, Department of Biotechnology, School of Food, Biotechnology and Development, Agricultural University of Athens, Athens, Greece
[c] Laboratory of Biochemistry, Scientific Affairs Department, APIVITA S.A., Athens, Greece
[d] Fitoplanton Marino S.L., 11500, El Puerto de Santa María, Spain
[e] Comparative Molecular Endocrinology Group, Marine Science Center (CCMAR), Universidade do Algarve, 8005-139, Faro, Portugal

ARTICLE INFO

Keywords:
Microalgae
Glucans
Antioxidant capacity
Gene expression
Senegalese sole

ABSTRACT

The microalgae are an important source of bioactive molecules including β-glucans that can be used as immunostimulants in aquaculture. In the present study, the antioxidant capacity, cytotoxicity and immunomodulatory activity of a chrysolaminarin-enriched extract obtained from the diatom *Phaeodactylum tricornutum* was evaluated. The extract showed a higher total antioxidant activity as determined by ORAC and FRAP assays and a lower DPPH scavenging activity than particulate yeast-β-glucan. The cytotoxicity test indicated that extract concentrations higher than 0.01% w/v could impair cell viability of human dermal fibroblasts. To evaluate the immunomodulatory activity, juvenile soles were intraperitoneally injected with the chrysolaminarin-enriched extract suspended in coconut oil (1 mg/fish) followed by a reinjection at 7 days. A sham group injected with the carrier solution was maintained as a negative control. Cumulated mortality of fish injected with the chrysolaminarin-enriched extract was 29.4% after six days and no mortality was recorded after extract reinjection. Expression analyses of fifteen genes related to the innate immune system in kidney, spleen and intestine showed temporal and organ-specific responses. A rapid (2 days post-injection; dpi) and strong induction of the pro-inflammatory *il1b* and the antimicrobial peptide *hamp1* in the three immunological organs, the *hsp90aa* in kidney and spleen, *irf3* in intestine and *c3* in spleen was observed indicating a potent inflammatory response. The recovery of steady-state levels for all activated genes at 5 dpi, and the down-regulation of c-lectin receptor as well as some interferon-related genes (*ifn1*, *irf1*, *irf3*, *irf8*, *irf9* and *mx*) in kidney and *cxc10* in spleen indicated that the soles were able to activate a homeostatic response against the β-glucan insult. The reinjection of the chrysolaminarin-enriched extract did not activate a new inflammatory response but reduced the mRNA levels of *hsp90aa* and *irf3* indicating that soles developed some resistance to β-glucans. Overall, these results reveal this enriched extract as a novel and potent source of β-glucans with antioxidant and immunomodulatory capacity suitable for immunostimulation in aquaculture.

1. Introduction

The β-glucans are considered as potent immunosaccharides able to enhance the immune response and prevent disease outbreaks [1,2]. These bioactive molecules activate the production of pro- and anti-inflammatory cytokines, which in turn modulate humoral and cellular immunity through different pathways conferring antimicrobial, anti-tumor and anti-proliferative properties [3–5]. Moreover, β-glucans exhibit antioxidant, anti-diabetic, and anti-obesity effects [3,6] and the broad spectrum of applications in biotechnology and biomedicine fields makes them of high biotechnological and biomedical interest. In aquaculture, β-glucans are mainly used as immunostimulants and prebiotics and are administered by injection or as a dietary supplement able to enhance fish growth, survival and the immune response and also improve resistance to several different pathogens [2,7]. Moreover, recent findings that reported a role of β-glucans on trained immunity by epigenetic reprogramming of monocyte-to-macrophage differentiation [8–10] have even increased the interest on these polysaccharides.

The β-glucans are widely distributed in the nature and can be obtained from different sources such as bacteria, algae, fungi and plants.

* Corresponding author. IFAPA Centro *El Toruño*, Camino Tiro de Pichón s/n, 11500, El Puerto de Santa María, Cádiz, Spain.
E-mail address: manuel.manchado@juntadeandalucia.es (M. Manchado).

https://doi.org/10.1016/j.fsi.2018.07.052
Received 23 February 2018; Received in revised form 20 July 2018; Accepted 27 July 2018
Available online 29 July 2018
1050-4648/

Fish and Shellfish Immunology 92 (2019) 31–39

Contents lists available at ScienceDirect

Fish and Shellfish Immunology

journal homepage: www.elsevier.com/locate/fsi

Full length article

Yeast β-glucans and microalgal extracts modulate the immune response and gut microbiome in Senegalese sole (*Solea senegalensis*)

Carlos Carballo[a,f], Patricia I.S. Pinto[b], Ana Patricia Mateus[b,c], Concha Berbel[a], Cláudia C. Guerreiro[b], Juan F. Martinez-Blanch[d], Francisco M. Codoñer[d], Lalia Mantecon[e], Deborah M. Power[b,**], Manuel Manchado[a,*]

[a] IFAPA Centro El Toruño, Junta de Andalucía, Camino Tiro Pichón s/n, 11500 El Puerto de Santa María, Cádiz, Spain
[b] Centre of Marine Sciences (CCMAR), Universidade do Algarve, Campus de Gambelas, 8005-139, Faro, Portugal
[c] Escola Superior de Saúde da Universidade do Algarve, Campus de Gambelas, 8005-139, Faro, Portugal
[d] LifeSequencing, Parc Cientific Universidad De Valencia, Edif. 2, C/ Catedrático Agustín Escardino Benlloch, 9, 46980, Paterna, Spain
[e] Fitoplancton Marino, Dársena Comercial S/N (Muelle Pesquero), 11500, El Puerto de Santa María, Cádiz, Spain
[f] Universidad de Málaga, Departamento de Microbiologia, Campus de Teatinos, 29071, Malaga, Spain

ARTICLE INFO

Keywords:
Beta-glucans
Immune response
Microalgae
Microbiota
Senegalese sole

ABSTRACT

One bottleneck to sustainability of fish aquaculture is the control of infectious diseases. Current trends include the preventive application of immunostimulants and prebiotics such as polysaccharides. The present study investigated how yeast β-glucan (Y), microalgal polysaccharide-enriched extracts (MAe) and whole *Phaeodactylum tricornutum* cells (MA) modulated the gut microbiome and stimulated the immune system in Senegalese sole (*Solea senegalensis*) when administered by oral intubation. Blood, intestine and spleen samples were taken at 3 h, 24 h, 48 h and 7 days after treatment. The short-term response (within 48 h after treatment) consisted of up-regulation of *il1b* and *irf7* expression in the gut of the Y treated group. In contrast, administration of MAe decreased expression of *tnfa* and the chemokine *cxc10* in the gut and spleen. Both treatments down-regulated the expression of *irf3* with respect to the control group. Lysozyme activity in plasma decreased at 48 h only in the MAe-treated soles. Medium-term response consisted of the up-regulation of *clec* and *irf7* expression in the gut of the Y, MAe and MA groups and of *il1b* mRNAs in the spleen of the MA group compared to the control group. Microbiome analysis using 16S rDNA gene sequencing indicated that the intestine microbiome was dominated by bacteria of the *Vibrio* genus (> 95%). All the treatments decreased the relative proportion of *Vibrio* in the microbiome and Y and MAe decreased and MA increased diversity. Quantitative PCR confirmed the load of bacteria of the *Vibrio* genus was significantly decreased and this was most pronounced in Y treated fish. These data indicate that orally administrated insoluble yeast β-glucans acted locally in the gut modulating the immune response and controlling the *Vibrio* abundance. In contrast, the MAe slightly reduced the *Vibrio* load in the intestine and caused a transient systemic anti-inflammatory response. The results indicate that these polysaccharides are a promising source of prebiotics for the sole aquaculture industry.

1. Introduction

Prebiotics are important feed supplements in aquaculture due to their capacity to enhance health and prevent disease outbreaks. These ingredients are normally non-digestible molecules that selectively modulate the intestinal microbiome by promoting indigenous microbial populations and preventing pathogen proliferation [1,2]. Carbohydrates (poly- and oligosaccharides) such as mannan-, fructo- and galacto-oligosaccharides, inulin or β-glucans are widely recognized for their prebiotic activity. All these non-digestible sugars are fermented in the gut resulting in the enhanced production of short chain fatty acids (SCFA), mainly formate, acetate, propionate and butyrate [3,4]. These secondary metabolites modulate the production and release of cytokines and chemokines and leukocyte recruitment producing beneficial effects on diabetes, colon cancer, obesity and systemic inflammation in mammals [4,5]. In spite of the potential benefits of prebiotics for animal health, their use in aquaculture is still limited and their actions are far from understood [1].

* Corresponding author. IFAPA Centro *El Toruño*, Camino Tiro de Pichón s/n, 11500, El Puerto de Santa María, Cádiz, Spain.
** Corresponding author. Universidade do Algarve, Campus de Gambelas, 8005-139, Faro, Portugal.
E-mail addresses: dpower@ualg.pt (D.M. Power), manuel.manchado@juntadeandalucia.es (M. Manchado).

https://doi.org/10.1016/j.fsi.2019.05.044
Received 27 March 2019; Received in revised form 15 May 2019; Accepted 20 May 2019
Available online 23 May 2019

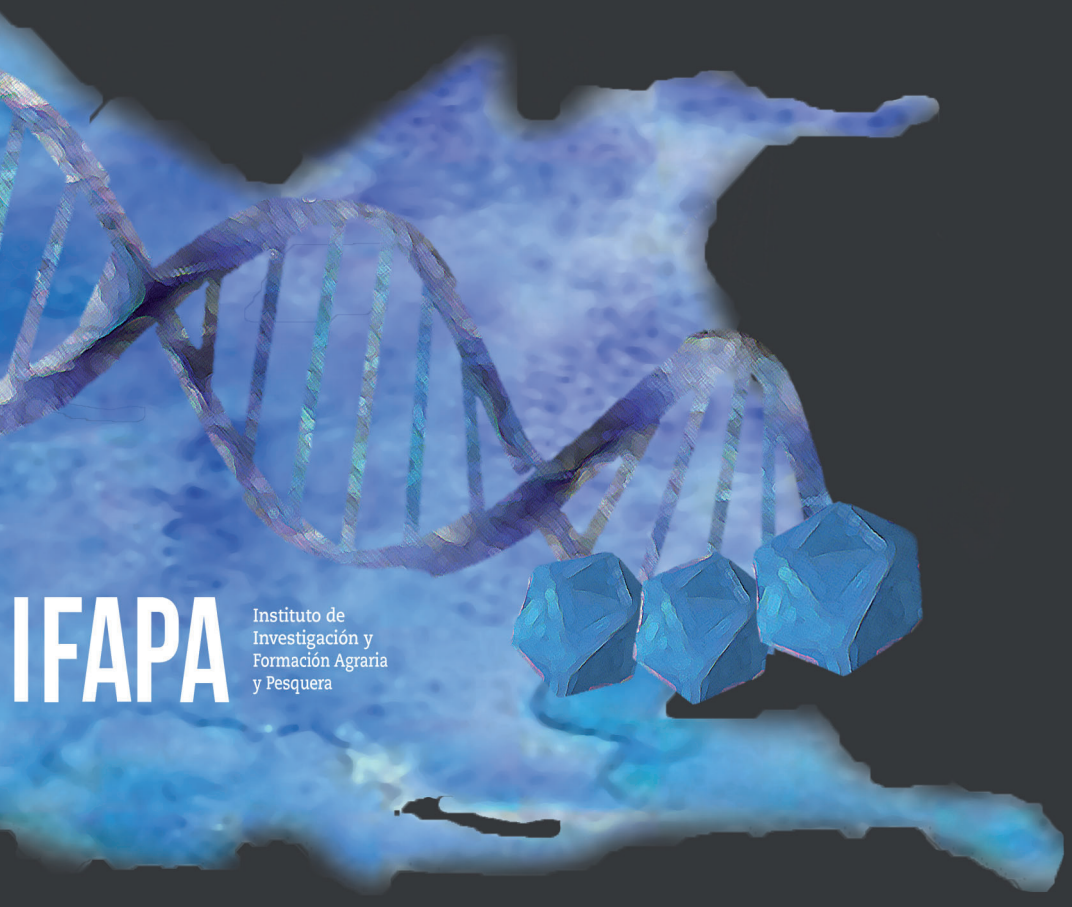

IFAPA

Instituto de Investigación y Formación Agraria y Pesquera

UNIVERSIDAD DE MÁLAGA

JUNTA DE ANDALUCIA

Instituto de Investigación y Formación Agraria y Pesquera

CONSEJERÍA DE AGRICULTURA, PESCA Y DESARROLLO RURAL

GOBIERNO DE ESPAÑA

MINISTERIO DE CIENCIA, INNOVACIÓN Y UNIVERSIDADES

INIA Instituto Nacional de Investigación y Tecnología Agraria y Alimentaria

ma UNIVERSIDAD DE MÁLAGA